Brachypodium distachyon as a genetic model pathosystem to study resistance against fungal pathogens of small grain cereals

ANTOINE PERALDI

A thesis submitted to the University of East Anglia

for the degree of Doctor of Philosophy

Department of Disease and Stress Biology

John Innes Centre

September 2012

ABSTRACT

Fusarium head blight (FHB) and other Fusarium diseases of wheat and other small-grain cereals cause yield reduction and grain contamination with harmful mycotoxins, mainly deoxynivalenol (DON). Little is known about the mechanistic basis of resistance to Fusarium in cereals due to the large, polyploid and unsequenced genome of wheat. Host ethylene (ET) signalling was previously shown to be a factor of susceptibility to FHB. Chapter 2 uses wheat EMS mutant lines characterized for altered senescence to test for a relationship between ET-sensitivity, senescence and resistance to FHB. Candidate mutant lines displaying high level of resistance to FHB were identified and resistance was associated with delayed senescence, reduced ET-sensitivity, or developmental delay. *Brachypodium distachyon* (Bd) has the potential to serve as a model pathosystem relevant to small-grain cereals. Chapter 3 provides evidence of compatibility between Bd and the main causal agents of FHB and shows that symptom development mirrors closely that in wheat. Natural variation in disease resistance exists among Bd accessions and a novel route for initial infection is suggested. Bd is also compatible with other important pathogens of small-grain cereals causing ramularia, eyespot and take-all diseases. In Chapter 4, a preliminary study of Bd T-DNA mutant lines altered in phytohormone biosynthesis or response investigates alteration of Fusarium resistance. Mutation of the main brassinosteroid (BR) receptor (BRI1) was characterized and validated. Other mutants defective in auxin or ET responsiveness and jasmonic acid (JA) biosynthesis were investigated. Results suggest that JA and BRI1 promote disease susceptibility. Finally, Chapter 5 uses a chemical and genetic approach to investigate the mechanisms of DON phytotoxicity using the Bd root system. Effects induced by the mycotoxin are compared with BRs, inhibitors of protein synthesis and compounds altering BR biosynthesis or signalling. Results suggest that DON may disrupt host BR homeostasis to promote disease susceptibility.

ACKNOWLEDGEMENTS

I am particularly grateful to my supervisor, Dr Paul Nicholson for his confidence, academic guidance, enthusiasm and encouragements throughout the project. I would also like to thank Paul for always being willing and available to discuss about the project and help with long and tedious field trials and SPADmeter measurements.

I would like to sincerely thank a number of people in the Nicholson group; Mr Andy Steed, Dr Robert Saville, Dr Chritopher Burt and Ms Martha Thomsett; not only for their technical assistance, but also for their friendship. I am particularly grateful to Chritopher Burt for his statistical advice throughout. I am also very grateful to all the students and casual workers I have met and helped me during this project: Ms Helene Lagraulet, Mr Jim Barnes, Mr Dean Cole, Dr Giovanni Beccari, Mr Andrea Ridolfini, Ms Jie Li and Ms Lucie Griffe. I must also thank Dr Philippe Vain, Dr Vera Thole, Ms Barbara Worland for providing the Brachypodium mutant lines but also for being among the kindest people I have met at the JIC. I would also like to thank Mr. Grant Calder for his training and advices in microscopy and tissue-staining techniques, Dr Graham McGrann for his passion for science, Mr Henry Creissen for his sense of humour, Mr Simon Orford, as well as Mr Simon Saucet and Dr Naveed Ishaque, my dearest friends. Also at JIC, I would like to thank my supervisory team; Dr. Simon Griffiths and Dr. Adrian Turner for many helpful conversations about the project.

On a different note, I would like to thank my parents, Ms Mireille Prono and Dr Michel Peraldi, for everything they have done for me, and especially my father for inspiring me. And finally, I will always be grateful to Ms Sara Fernandez-Careaga, for her love, understanding and support over the past four years.

This project was funded by BBSRC which I shall thank too.

For performing or assisting in experiments presented in this work, I must specifically thank: Dr Giovanni Beccari for the ACC-sensitivity tests and CLSM images of Bd infected roots, Mr Andrea Ridolfini for numerous SPADmeter measurements and FHB disease scores, Dr Chritopher Burt and Ms Lucie Griffe for the eyespot infections, Dr Graham McGrann for the ramularia infections and Ms Jie Li and Mr Jim Barnes for peeling thousands of Brachypodium seeds and for their help with the T-DNA work.

Philippe Boubille

19th May 1982 ~ 24th June 2004

ABBREVIATIONS

ABA	abscisic acid	HR	hypersensitive response
ACC	1-amino-cyclopropane-1-carboxylic acid	IAA	indole-3-acetic acid
		JA	jasmonic acid
At	*Arabidopsis thaliana*	L	litre
AUDPC	area under disease progress curve	kb	kilobase
		kg	kilogram
BSMV	barley stripe mosaic virus	kV	kilovolt
BMH	base of macro-hair	LRR	leucine-rich repeat
BIK	bikinin	MAS	marker assisted selection
Bd	*Brachypodium distachyon*	m	meter
BRZ	brassinazole	MeJA	methylester jasmonate
BR	brassinosteroid	µ	micro
CLSM	confocal laser scanning microscope	mL	millilitre
		mg	milligram
CHX	cycloheximide	min	minute
CK	cytokinin	M	molar
DIS	dark-induced senescence	MB	mung bean
dpg	days post germination	nm	nanometre
dpi	days post inoculation	NIL	near isogenic line
°C	degrees Celcius	NO	nitric oxide
DON	deoxynivalenol	NIV	nivalenol
DLA	detached leaf assay	nt	nucleotide
DAS	diacetoxyscirpenol	Oa	*Oculimacula acuformis*
DMSO	dimethyl sulfoxide	Oy	*Oculimacula yallundae*
DHL	double haploid line	Os	*Oryza sativa*
eBL	epibrassinolide	PDA	potato dextrose agar
ELISA	enzyme-linked immunoabsorbant assay	PDB	potato dextrose broth
		PCD	programmed cell death
ET	ethylene	PSI	protein synthesis inhibitor
EMS	ethyl methanesulfonate	SA	salicylic acid
EST	expressed sequence tag	QTL	quantitative trait loci
FS	fast-senescing	Rcc	*Ramularia collo-cygni*
Fc	*Fusarium culmorum*	ROS	reactive oxygen species
Fg	*Fusarium graminearum*	RH	relative humidity
FHB	Fusarium head blight	SEM	scanning electron micrograph
Gg	*Gaeumannomyces graminis*		
GLM	generalized linear model	s	second
GA	gibberellic acid	SAG	senescence-associated gene
g	grams	SU	SPADmeter unit
GS	growth stage	SG	stay green
He	hemizygous	SDW	sterile distilled water
Ho	homozygous	TGW	thousand grain weight
h	hour	T-DNA	transfer DNA
hpi	hours post inoculation	WT	wild-type

CONTENTS

LIST OF TABLES

LIST OF FIGURES

Chapter 1

General Introduction

Approximately 17 plant species provide 90% of mankind's food supply, of which cereal grains supply far and away the greatest percentage (Simopoulos, 1999). Cereal grain production is a fundamental component of human societies and its development. It is widely recognized that, combined with animal domestication, agriculture enabled the emergence and development of human civilizations, 10 to 12,000 years ago, in the Fertile Crescent.

However, cereal crop production is limited by a plethora of factors that can be divided into abiotic and biotic stresses. Pathogen infections can damage both yield and quality, but one of the fundamental difficulties in managing disease resistance is the constant adaptation of the disease causing agents to new means of resistance. In addition, an ever growing human population, predicted to reach 9 billion by 2050, poses a difficult challenge for farmers, breeders and scientists in order to match production with the global needs.

This work is dedicated to the study of the genetic basis of plant resistance to biotic stresses, with a particular focus on the threat posed by fungal pathogens to cereal production. A particular attention will be paid to one of the major fungal diseases of small grain cereals in order to assess the current state of research and tools available. This will set the basis for the assessment of a model plant pathosystem aimed to improve the means by which research in disease resistance is approached.

1.1 Fusarium head blight

Fusarium species are facultative fungal pathogens, belonging to the ascomycota phylum, able to cause various diseases on most cultivated plant genera, including all members of *Gramineae* (Parry *et al.*, 1995). *Fusarium* infections can develop on all plant parts and at all stages, causing various wilts, rots and molds (Miedaner, 1997). Fusarium head blight (FHB), also named Fusarium ear blight or head scab, is a disease that can affect all small-grain cereals but seems more commonly found on wheat (*Triticum aestivum*) and barley (*Hordeum vulgare*). This disease is described as the infection of the host floral tissues and occurs in humid and semi-humid areas of the world where small grain cereals are grown

(Parry *et al.*, 1995). FHB disease is a significant threat to small grain cereal production as it compromises both yield and grain quality. The combined direct and secondary economic losses due to FHB for all crops were estimated at $7.7 billion over the period 1993 to 2001, in the US only (Nganje *et al.*, 2004). Major FHB epidemics that have occurred in the last two decades have established its main causal agent as a major global pathogen of cereals (Kazan *et al.*, 2012).

1.1.1 Causal agents and host range

FHB of wheat, considered the most damaging of *Fusarium* diseases worldwide, has been linked with up to 17 different species (see Table 1), from which *F. graminearum* (Fg) and *F. culmorum* (Fc) are the most common and pathogenic (Gosman, 2001; Parry *et al.*, 1995). The different FHB-causing species of *Fusarium* share complex ecological relationship as they can be found co-existing in the same infected plant tissues (Parry *et al.*, 1995; Xu and Nicholson, 2009). The geographic distribution and predominance of *Fusarium* pathogens is believed, to a large extent, to be determined by climatic factors, particularly temperature and moisture (Xu *et al*., 2008). In semi-arid climates, Fg is mainly found infecting roots, crowns, and basal portions of stems (Cook, 1980) whereas, in humid climates, the fungus causes seedling disease and commonly infects spikes and stems of wheat in the heading stage (Sutton, 1982). FHB is thought to become a more severe problem for farmers as the study of Ward *et al*. (2008) indicates a recent and significant shift in FHB pathogen composition toward a more toxigenic and potentially more vigorous strain in North America. Certain species of *Fusarium* (*F. solani* and *F. oxysporum*) can even be found in human pathologies of the cornea, and more commonly in immunocompromised patients (Dignani and Anaissie, 2004).

Table 1.1: List of reported FHB-causing pathogens (Parry *et al*., 1995).

F. graminearum	*F. tricinctum*	*F. sambucinum*
F. culmorum	*F. moniliforme*	*F. subgtutinans*
F. avenaceum	*F. oxysporum*	*F. semitectum*
F. poae	*F. lateritium*	*Microdochium nivale*
F. sporotrichioides	*F. protiferatum*	*Microdochium majus*
F. equiseti	*F. sambucinum*	
F. acuminatum	*F. crookwettense*	

1.1.2 Biology and life cycle

All FHB-causing species of *Fusarium* are necrotrophic pathogens capable of surviving saprophytically on crop debris (Parry *et al.*, 1995). The life cycle of Fg and Fc comprise a saprophytic and a pathogenic phase (Sutton, 1982). Most *Fusarium* species are not known to produce a teleomorph stage, i.e. Fc, and reproduce asexually by means of conidia existing in several forms (Gosman, 2001). However, Fg does have a sexual stage (teleomorph: *Gibberella zeae*) and therefore is able to produce ascospores in addition to asexually produced conidia (Parry *et al.*, 1995). Fg produces fruiting bodies, called perithecia, and ascospores released from these perithecia can infect cereal heads during flowering, especially under conducive climatic conditions (e.g. high humidity during flowering) (Kazan *et al.*, 2012). The primary source of inoculum can be soilborne, seedborne or airborne (Parry *et al.*, 1995; Paul *et al.*, 2004; Xu and Nicholson, 2009). However, ascospore-laden perithecia of *F. graminearum* developing on mature cereal crops as well as crop debris generally provide the primary inoculum of the disease (Guenther, 2005). Figure 1.1 illustrates the life cycle of Fg.

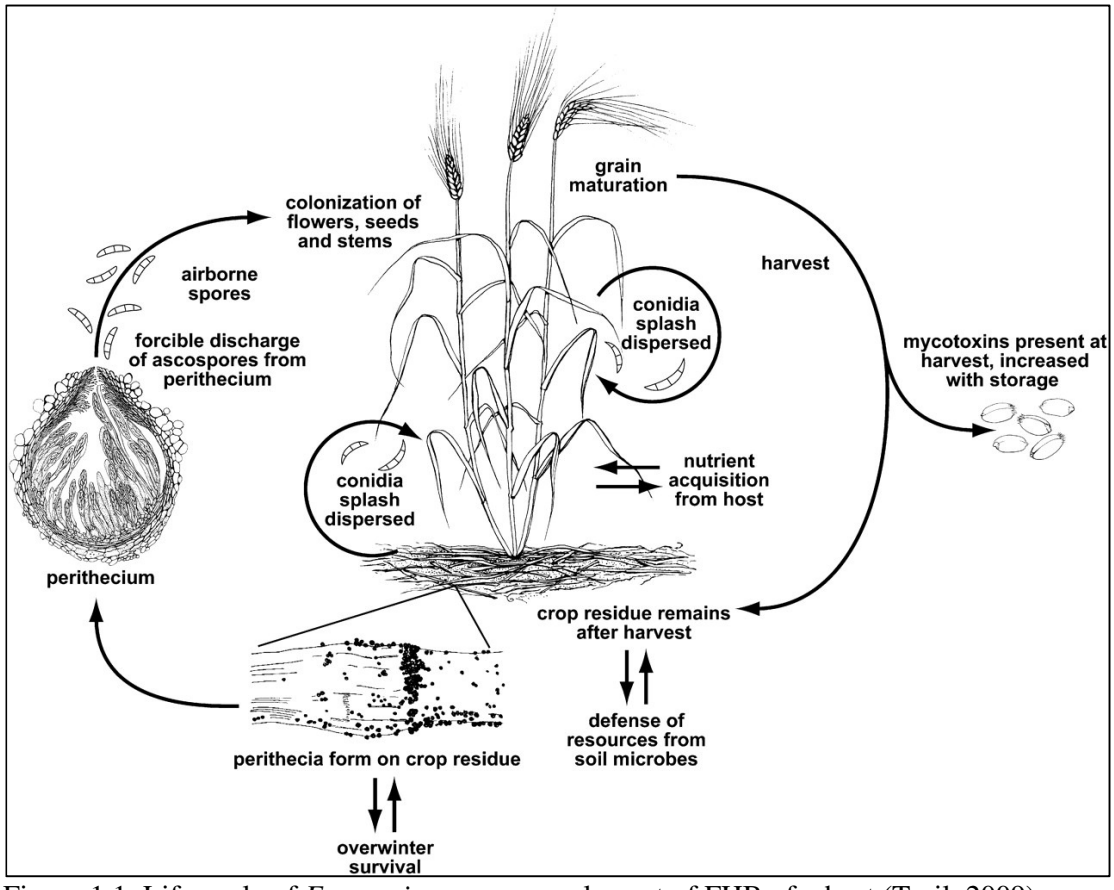

Figure 1.1: Life cycle of *F. graminearum*, causal agent of FHB of wheat (Trail, 2009).

1.1.3 Symptom development

FHB symptoms are generally similar in all small grain cereal crops (Parry *et al.*, 1995). Sutton (1982) reported that wheat spikes are not receptive (meaning susceptible) to Fg infection prior to anthesis, but susceptible from flowering to the soft dough stage, after which it rapidly declines. Hence, the risk of FHB infection of wheat ears is commonly viewed as most severe during anthesis (Parry *et al.*, 1995; Xu *et al.*, 2008). Typical symptoms start as small water-soaked brownish spots, first appearing at the base or middle of the glume, or on the rachis (Mathre, 1982). Premature death or bleaching of cereal spikelets is also a common symptom (Parry *et al.*, 1995, see Figure 1.2). Water soaking and discoloration then spread in all direction from the initial point of infection. Infected floral tissues can display a salmon-pink to red fungal growth along the edge of the glumes or at the base of the spikelet (Parry *et al.*, 1995).

Figure 1.2: Visual symptoms of FHB on heads of *T. aestivum* cv. Huntsman infected by point inoculation with 50 µL of *F.graminearum* conidia solution ($1x10^5$ conidia mL^{-1}). Left: Moderate symptoms (Picture provided by Steed A.), Right: Severe symptoms showing a completely bleached head (Gosman *et al.*, 2010).

1.1.4 Infection strategy

Germinating hyphae initially develop on the exterior surfaces of florets and glumes (Bushnell *et al.*, 2003) and often extend into the apical floret mouth or crevices between the palea and lemma (Lewandowski *et al.*, 2006) to reach the floret cavity. *Fusarium* hyphae do not directly penetrate the host epidermis but rather extend and branch in all directions, allowing access to stomata and other susceptible sites within the inflorescence

(Bushnell *et al.*, 2003). According to Kang and Buchenauer (2000), the inner surfaces of the palea, lemma and glumes are more easily invaded than the respective outer surfaces. Peculiar lobed structures have often been observed between the cuticule and epidermal cell walls on the surface of inoculated glumes (Pritsch *et al.*, 2000). Subcuticular growth is thought to allow fungal spread and probably leads to direct penetration of epidermal cells in the case of adaxial floret surfaces (Bushnell *et al.*, 2003). Subcuticular and intercellular growth is generally observed during the first 2 days after infection, in wheat and barley (Jansen *et al.*, 2005). Observation made by Brown and collegues (2010) confirmed that, at the cellular level, the intercellular hyphae of Fg always advanced through living host tissue. This short asymptomatic phase of infection has raised the idea that Fg may exhibit an initial biotrophic phase preceding host cells necrotization (Boddu *et al.*, 2006). However, biotrophic life-style is commonly characterized by specific structures closely associating fungal hyphae with living host cells, called haustoria, which to date have never been observed in Fg or Fc. Therefore, the classification of Fg as a hemibiotroph has been discussed but remains a matter of debate (Kazan *et al.*, 2012). The principal mode of fungal spread in wheat between adjacent florets and or between adjacent spikelets is through the vascular bundles in the rachis and rachilla (Ribichich *et al.*, 2000 as mentioned in Goswami and Kistler, 2004).

1.2 Other Fusarium diseases

Fusarium diseases occur on all vegetative and reproductive organs of plants and *Fusarium culmorum* and *F. graminearum* can cause seedling blight, crown rot, foot rot as well as head blight in wheat and rye (Miedaner, 1997).

1.2.1 Seedling blight

The symptoms associated with seedling blight in cereals range from pre-emergence death, post-emergence death and lesions on stems and leaves (Wisniewska and Busko, 2005). Seedlings surviving the disease have been reported to lack vigour, produce few tillers and frequently produce a single stem baring a small head (Parry *et al.*, 1995). Seedling blight caused by *F. culmorum* and *F. graminearum* is mainly seed-borne in the humid climates and leads to a reduced number of plants and increased secondary attack by pests due to thinned stands and delayed plant development (Miedaner, 1997). Seedling blight caused by *F. graminearum* Group 1 (now *Fusarium pseudograminearum*; see Aoki and O'Donnell,

1999) results, in contrast, from soilborne infection and occurs mostly in dry soils (Burgess *et al.,* 1981).

1.2.2 Root rot

Fusarium root rot causes browning and necrosis of roots. As a consequence, seedling vigour is reduced and infection of root and crown functions result in loss of stand, reduced yield and lower grain quality (Mergoum *et al.*, 1998). *Fusarium* root infection can also take place through the hypocotyl, from where the fungus can then colonize roots and shoots (Malalasekera *et al.*, 1973; Knudsen *et al.*, 1995). Recent results obtained by Beccari and collegues (2011) revealed that infection by Fc hyphae develops in the rhizodermal layer and cortex of wheat roots but not in the stele.

1.2.3 Foot rot

Epidemiologically distinct diseases have been recognized as stem base infections caused by *Fusarium* species (Gosman, 2001). Brown foot rot caused by Fc and Fg is mostly found in wet humid areas (Cook, 1981) and crown rot caused by *F. pseudograminearum* in dry weather and soils (Cook, 1968). *Fusarium* crown rot symptoms appear as brown necrotic discoloration and, following their appearance, can expand throughout the crown and infect the stems (Hare and Parry, 1996). Infection can cause 'whiteheads', possibly as a result of mycotoxin translocation or interference with translocation of water and nutrients to the head (Hogg *et al.*, 2007).

1.3 Mycotoxin production and grain contamination

Trichothecenes are the main class of mycotoxins produced by *Fusarium* species; a large family of non-volatile sesquiterpenoid secondary metabolites highly toxic at low concentrations to humans and animals. Deoxynivalenol (DON or vomitoxin), nivalenol (NIV) and T-2 toxin (Kimura *et al*., 2007) and other trichothecenes are known to act as translational inhibitors in eukaryotic ribosomes without inducing a defence response in *Arabidopsis thaliana* (At) cells (Masuda *et al*., 2007). Trichothecenes are not the only mycotoxins produced by *Fusarium,* others being fumonisins and zearalenone, but they are probably the most economically damaging and scientifically studied in small-grain cereals (Kimura *et al*., 2007). Although DON is not considered to be acutely toxic to farm animals,

it is considered to be a major cause of economic loss due to reduced performance (Morgavi and Riley, 2007).

1.3.1 Role of deoxynivalenol during host colonization

Trichothecenes are considered to be virulence factors of several *Fusarium* species (Lemmens *et al.*, 2005). Boesnisch and Schaffer (2011) used a Fg mutant strain constitutively expressing the dsRed reporter gene as well as the GFP coupled to the Tri5 (Thrichothecene biosynthetic gene) promoter to demonstrate that trichothecene biosynthesis is specifically induced in *Fusarium* infection structures. They observed that trichothecene biosynthesis is neither necessary for the development of infection structures nor for formation of primary symptoms on wheat. In the absence of trichothecene production, the fungus is blocked by the development of heavy cell wall thickenings in the rachis node of Nandu wheat, a defence mechanism which is inhibited by the amendment of mycotoxin. In barley, hyphae of both wild-type and the trichothecene knockout mutant are inhibited at the rachis node and rachilla, limiting infection of adjacent florets through the phloem and along the surface of the rachis (Jansen *et al.*, 2005). Lemmens and colleagues (2005) concluded from the results of their study that resistance to DON correlated with resistance to the spread of FHB symptoms in wheat ears.

1.3.2 Deoxynivalenol toxicity in plants

The production of DON by the fungus within its host has been correlated with the bleaching of infected wheat heads as this effect is also induced following injection of DON alone in this tissue (Lemmens *et al.*, 2005). Induction of programmed cell death (PCD) has been characterized in *Arabidopsis* following exposure to various trichothecenes (i.e. T-2 toxin, DON; Masuda *et al.*, 2007). The work of Desmond and colleagues (2008), demonstrated using a wheat leaf system that DON induces the production of reactive oxygen species, PCD as well as the production of antimicrobial host defences. Interestingly, authors noticed a concentration-dependent induction of defence gene transcripts, with larger effects of the accumulation of defence proteins at concentrations higher than those known to inhibit protein synthesis in wheat (Rocha *et al.*, 2005). Studies of the effect of DON in barley leaf sections from which the epidermal cell layer was striped revealed two opposing effects that are potentially relevant roles in FHB. Toxic concentrations of DON induced the bleaching of leaf tissues as expressed by loss in content of nearly all chlorophyll and carotenoid pigments. However, Non-toxic

concentrations of DON caused no injury but tended to prevent the gradual reduction in chlorophyll content of detached leaf segments. Therefore, authors suggested that DON-induced delay in senescence may be based on the activation of a response separate from that leading to PCD (Bushnell *et al.*, 2010).

1.4 Host resistance

A gene-for-gene resistance interaction has not been identified to date in FHB-resistance, and immunity to the disease has never been observed (Foroud and Eudes, 2009). The use of resistant wheat cultivars is thought to be the most effective strategy for protection against FHB due to the lack of control provided by crop management and agrochemical measures (Buerstmayr *et al*., 2009), the high variability in disease severity relying on environmental conditions, and an increase in severity of FHB epidemics in Northern America (Ward *et al*., 2008).

1.4.1 Components of host resistance

The mechanisms of resistance to FHB in wheat and its components are presented in the excellent review written by Ban (2000). It was first described by Schroeder and Christensen (1963) that two types of mechanisms were distinguishable: type I resistance operates against initial infection (fungal penetration) whereas type II resistance operates against the spread of the pathogen within the host (fungal invasion). Later, Miller and colleagues (1985) described a different mechanism of FHB resistance based on the plant's ability to degrade DON and/or other trichothecenes and was named type III resistance. This nomenclature was then completed by the description of a type IV resistance based on tolerance to high trichothecene concentrations (Wang & Miller, 1988) and finally a type V relying on resistance to kernel infection and tolerance (Mesterházy, 1995). The discrimination of type I and type II components of FHB resistance is widely accepted. However, resistance component relative to DON detoxification and tolerance is not generally accepted as Mesterházy and co-workers (2005) considered differently the type III resistance component as not only DON detoxification but also mechanisms inhibiting toxin production. Therefore, Mesterházy's classification, which seems to be more widely used, considers resistance components IV and V as resistance to kernel infection and tolerance to DON accumulation, respectively.

1.4.2 *Sources of resistance*

Generally found in winter wheat, reduced plant height loci are probably the most famous genes in wheat as they are referred to as the "green revolution" genes (Peng *et al*., 1999). *Rht* semi-dwarfing genes participated in the important reduction in height of wheat cultivars, increase in grain yield and in resistance to damage caused by wind and rain. *Rht1* (Gale and Marshall, 1976) and *Rht2* (Gale and Law, 1976) were the first genes to be described as responsible for a "reduced height" phenotype and were later re-named *Rht-B1b* (located on chromosome 4B) and *Rht-D1b* (located on chromosome 4D), respectively. *Rht* genes appear to be homologs of the *Arabidopsis GAI* (Gibberellin insensitive) gene, also found in other cereal species presenting reduced height phenotype (Peng *et al*., 1999). The *GAI* protein normally functions as a negative regulator of gibberellin (GA) signalling. GA is an essential plant hormone involved in important aspects of plant growth and development such as seed germination, hypocotyl and stem elongation, leaf expansion, pollen development and flower initiation (Richards *et al*., 2001). The wild-type *GAI* protein, which contains a DELLA domain (required for the interaction), acts as a repressor of the GA response. GA functions through removing the negative growth regulatory effect of *GAI* (*via* proteasome degradation) to promote growth (Hussein and Peng, 2003). The *gai* mutant contains an in-frame deletion of 17 amino acids in the DELLA domain which leads to a constitutive repression of plant growth. Several *Rht* loci have been identified within the wheat genome (Gale and Youssefian, 1985), some of which appear to be different alleles of the same locus (i.e. *Rht1* or *Rht-B1b* and *Rht3* or *Rht-B1c*). In a recent work by Srinivasachary and colleagues (2009) on winter wheat DHLs, *Rht-B1b* and *Rht-D1b* were observed to differ in their influence on FHB resistance. Authors found that under high disease pressure, both *Rht-B1b* and *Rht-D1b* significantly decreased type I resistance whereas *Rht-D1b* had no effect on type II resistance, *Rht-B1b* significantly increased type II resistance. The authors presented evidence that association with FHB resistance could be due to pleiotropy or linkage of deleterious genes to the *Rht-D1b* semi-dwarfing allele rather than differences in height *per se* (Buerstmayr *et al*. 2009). Buerstmayr *et al*. (2009) report a QTL for FHB resistance located near the *rht8/Rht8* semi-dwarfing gene locus on the chromosome 2DS which appeared to be closely linked to a multidrug resistance-related protein (MRP) gene. Handa and colleagues (2008) proposed that this QTL may be a gene complex consisting of morphological traits modulated by *rht8/Rht8* associated with type I resistance and specific gene(s) controlling type II resistance by detoxification of DON, like MRP. Finally, recent work by Saville and collegues (2012) used defined wheat Rht near-isogenic lines and barley *Sln1* (barley DELLA ortholog) gain and loss-of-function to

investigate the role played by DELLA in response to biotrophic and necrotrophic pathogen infection. Authors showed that gain-of-function mutant alleles in wheat and barley confer resistance to FHB as well as another necrotrophic fungus causing eyespot disease. Interestingly, a trade-off in resistance conferring susceptibility to biotrophic pathogens such as *Blumeria graminis* was observed which authors correlated with the role played by DELLA proteins in the regulation of reactive oxygen species production and the onset of PCD.

1.4.3 Genetic components of resistance to Fusarium

Despite a large genetic variation for FHB resistance available in the wheat gene pool, breeders have had a difficult task to combine high productivity and disease resistance because often the best regionally adapted and highly productive cultivars are susceptible to the disease (Buerstmayr *et al*., 2009). However, available resistance to FHB in wheat is quantitatively inherited with a continuous distribution among progeny (Anderson, 2007 and references within). Therefore, the method of choice to investigate FHB resistance has been to apply a quantitative trait loci (QTL) mapping approach (Buerstmayr *et al*., 2009). Results gathered during a decade of research in QTL mapping and marker-assisted selection (MAS) for FHB resistance in wheat were recently reviewed by Buerstmayr *et al*. (2009) who summarized 52 peer-reviewed studies, most of which concern hexaploid wheat. More than 100 QTLs were detected in wheat to date, although it is quite certain some are false positives, and are spanning on all chromosomes except the 7D. Buerstmayr and colleagues (2009) concluded that the most repeatable QTLs found in hexaploid spring wheat were located on chromosomes 3BS, 5AS and 6BS (named *Fhb1*, *Qfhs.ifa-5A* and *Fhb2*, respectively; See Table 1.2). Both *Fhb1* and *Fhb2* are resistant loci derived from the highly resistant Chinese cultivar "Sumai-3" and have now been identified as single Mendelian factors. Lemmens *et al*. (2005) first found that lines carrying the marker called *Qfhs.ndsu-3BS* (later renamed *Fhb1*; Liu *et al*., 2006) were able to convert DON into less phytotoxic DON-3-O-glucoside (type II resistance) and hypothesized it either encoded a DON-glucosyltransferase or modulated the expression or activity of such an enzyme. *Fhb2* was found to provide protection against fungal spread (type II resistance) but no putative function is attributed to this gene so far (Cuthbert *et al*., 2007). Finally, a locus named *Qfhs.ifa-5A* was associated with type I resistance as its presence in DHLs conferred less disease protection after single-floret inoculation (type II resistance) than spray inoculation (type I and II resistance). However, the chromosome location of *Qfhs.ifa-5A* is still

imprecise. Among other QTLs found, a proportion of loci detected were associated with plant height and flowering date. Hence, disease escape has long been considered to be potentially important in relation to resistance to FHB (Srinivasachary, 2009). Concerning plant height, it was postulated that conidia spread more easily to the heads of short varieties because of the reduced distance between leaf layers, supported by the findings that tall and short varieties expressed similar levels of FHB symptoms following artificial inoculation (Mesterházy, 1995).

Table 1.2: Most repeatable QTLs for FHB resistance in spring wheat.

Name	Chromosome location	Resistance component	Mapping precision	Putative function
Fhb1	3BS	Type II	Single Mendelian gene (1.2 cM precision)	DON-glucosyl transferase or modulator
Fhb2	6BS	Type II	Single Mendelian gene (2 cM precision)	Unknown
Qfhs.ifa-5A	5AS	Type I	imprecise	Unknown

1.4.4 Known mechanisms of FHB resistance

Knowledge on the genetic mechanisms able to mount effective defences against Fusarium diseases remains scarce (Buerstmayr *et al*., 2009). Most of the reports proposing a role for a genetic component in the resistance to Fusarium infection implicated phytohormones such as salicylic acid (SA), jasmonic acid (JA) and ethylene (ET) and support the view that these are core hormonal signalling-pathways regulating defence mechanisms against a broad range of pathogens with different life-styles (Glazebrook, 2005). Most investigations however are based on the At model system from which insight is difficult to translate to cereal crops due to the distant divergence of At with the core *Gramineae*. The most recent advances made in identification of the genetic components altering resistance to Fusarium will be presented in following chapters, where appropriate.

1.5 Disease control strategies

Different methods of control exist to reduce FHB epidemics as well as mycotoxin grain contamination including crop rotation, the use of resistant cultivars, biocontrol agents and

fungicide treatments. However, the control of FHB disease is at best inconsistent in the field (Parry *et al.*, 1995). It is known that plots where wheat had been repeatedly grown or in alternance with maize correlated with increased FHB incidence and decreased yield (Dill-Macky, 2000). Fungicide treatments are, at best, partially effective (Parry *et al.*, 1995) and several reports of fungicide-resistant strain of *Fusarium* species have been published (Parry *et al.*, 1995, Chen and Zhou, 2009). Studies investigating biocontrol strategies such as the use of antagonistic micro-organisms to protect against FHB epidemics are still scarce but some reports suggest a potentially very significant effect. Schisler and co-workers (2002) observed up to 95% reduction in FHB disease severity in glasshouse and 56% reduction in field trials using four tartaric acid-producing and three non-producing microbial strains isolated from wheat anthers. Biological control using endophytic bacterial strains has also been reported to prime resistance against vascular wilt of cotton caused by *Fusarium oxysporum* f. sp. *vasinfectum* (Chen *et al.*, 1995).

1.6 Aim of this work

This work aims to take a novel approach to study the genetic mechanisms of phytohormonal signalling involved in plant-pathogen interactions. To exemplify the inherent difficulty to conduct genetic research in cereal disease resistance, the first chapter will take a classic approach of phenotypic characterisation in the perspective of QTL detection. A mutant wheat population previously characterised will be used to study alterations in disease resistance, taking FHB as an example of a fungal disease of wheat and barley in relationship with other physiological mechanisms largely controlled by hormonal signalling. Then, the recently sequenced grass model *Brachypodium distachyon* will be used as an alternative pathosystem model to conduct functional genetic studies relevant for cereals. The Bd tool will be tested for compatibility with major necrotrophic fungal pathogens of small-grain cereals. The pathosystem model will be then used in chapter 4 to undertake a reverse genetic approach to investigate and characterise genes involved in phytohormone production, signalling or response also altering resistance to FHB. Finally, *Brachypodium* will be used as a functional model to conduct a chemical and genetic analysis of the phytohormone signalling elements involved in plant-pathogen interactions. The Bd root system will be used in chapter 5 to investigate the mechanisms of action of the fungal effector deoxynivalenol in plants.

Chapter 2

Characterisation of *Fusarium* resistance in a spring wheat EMS mutant population selected for altered senescence

2.1 Introduction

Despite numerous studies on the resistance to FHB in wheat and other small-grain cereals, and despite the identification of hundreds of QTL (Buerstmayr *et al.*, 2009) that confer various level of protection against this disease, very little is known about the genetic mechanisms allowing the host plant to mount a successful defence against *Fusarium* pathogens. However, it is currently well established that the balance of hormonal crosstalk strongly influences the outcome of plant-pathogen interactions (Robert-Seilaniantz *et al.*, 2011). Hormone homeostasis and responses are vital for normal immune responses (Mengiste *et al.*, 2012) and numerous studies have shown that mutation in genes involved in phytohormone biosynthesis, perception and/or signal transduction can greatly reduce or enhance disease resistance (Bari and Jones, 2009). Most of these studies use the plant genetic model *Arabidopsis* but reports of the involvement of phytohormones in cereal-pathogen interactions exist suggesting disruption of the host hormonal balance is a common infection strategy adopted by plant pathogens. A classic example is the production of gibberellic acid (GA) by *Fusarium fujikuroi* (teleomorph *Gibberella fujikuroi*), the causal agent of foolish seedling disease of rice, which induces abnormal growth of the host stem and promotes disease (Eckardt, 2002). The best example in relation to FHB to date comes from the work of Chen and co-workers (2009) who characterized the role played by ethylene (ET) signalling during host colonization by *Fusarium* pathogens. Therefore, current knowledge on the production, signalling and role of ET in plants will be reviewed. Also, the implication of ET signalling in the resistance against pathogens will be discussed, as well as the role that this phytohormone plays in various physiological programs that are known to influence plant-pathogen interactions.

2.1.1 *Ethylene signalling pathway in plants*

Ethylene, C_2H_4, is a volatile olefin hormone involved in numerous processes underlying plant physiology and pathology. Exposure to ET can produce a myriad of effects on plant growth, development, and physiology, most notably the ripening of fruits, inhibition of

stem and root elongation, promotion of seed germination and flowering, senescence of leaves and flowers, and sex determination (Ecker, 1995). Significantly, the biosynthesis of ET is stimulated prior to several developmentally programmed senescence processes and in response to environmental insults such as mechanical trauma and pathogen infection (Yang & Hoffman, 1984).

The biosynthesis of ET, taking place during the Yang cycle of methionine turnover, is now largely understood as a result of the biochemical analysis made in the 1980s by Yang and Hoffman (1984) and which led to the identification of the key enzymes involved in the production of ET. Briefly, as reviewed by Ecker (1995), the rate-limiting step is the conversion of S-adenosyl-L-methionine (SAM) into 1-amino-cyclopropane-1-carboxylic acid (ACC) catalysed by ACC synthase. ACC is then converted by ACC oxidase, an enzyme constitutively expressed in most plant tissues, into ET, carbon dioxide and cyanide. The genes encoding ACC synthase and ACC oxidase have been cloned and characterised in many plant species (Kende, 1993) including in cereals such as rice, maize and wheat. Finally, environmental stresses (physical, chemical and biological) and hormonal signals, such as auxin, cytokinin and ethylene itself stimulate the production of ACC synthase, as a means for autoregulation of ET production (Ecker, 1995).

According to Guo and Ecker (2004), the signalling pathway activated in response to ethylene is largely linear, from hormone perception at the endoplasmic reticulum membrane to transcriptional regulation in the nucleus. Knowledge on the genetic components of the ET signalling pathway comes from a combination of genetic and molecular analyses of many *Arabidopsis* mutants discovered during the past two decades. ET is detected by a family of membrane-associated receptors such as *ETHYLENE RECEPTOR* (*ETR*) *1* and *2*, *ETHYLENE RESPONSE SENSOR* (*ERS*) *1* and *2* and *ETHYLENE INSENSITIVE* (*EIN*) *4* (Guo and Ecker, 2004; Hua et al., 1998). The binding of ET has been predicted to inactivate its receptor (Hua and Meyerowitz, 1998). In the absence of ET, ET-receptors are thought to be in a functionally active form that constitutively activates a Raf-like serine/threonine kinase, *CONSTITUTIVE TRIPLE RESPONSE* (*CTR*) *1*, which is a negative regulator of the pathway (Kieber *et al*., 1993). Positive regulators such as *EIN2*, *EIN3, EIN5* and *EIN6* transduce the ET signal downstream of *CTR1*, although only the function of *EIN3* is fairly well understood (Guo and Ecker, 2004). *EIN3* is a transcription factor (TF) regulating the expression of genes such as the *ETHYLENE RESPONSE FACTOR* (*ERF*) *1* (Solano *et al.* 1998). *ERF1* is a protein belonging to a large family of APETALA2-domain-containing TFs specifically

binding to promoters containing a GCC-box (also named ERE for ET Response Element) present in many ethylene-inducible, defence-related genes (Hao *et al*., 1998). Then, a transcriptional cascade mediated by EIN3/EIN3-like and ERF proteins leads to the regulation of ET-controlled gene expression (Guo and Ecker, 2004). All ET responses are understood to require the same components, from the ET receptors to the EIN3/EIN3-like TFs. However, exogenous applications of ET or a constitutive increase in its synthesis do not always induce the same responses in different tissue types or at different developmental stages. As the vast majority of genetic and molecular studies on the components of the ET signalling pathways were performed on dicotyledonous plants (i.e. Arabidopsis, tomato and tobacco), little is known about the mechanisms regulating ET signalling in monocotyledonous plants and research on homologous genes in cereals is needed.

2.1.2 *ET at the crossroad of plant defence signalling*

The plant hormone ET has been implicated, alone or in cooperation with other hormones, in numerous defence response mechanisms such as the production of xylem occlusions, cell wall-strengthening hydroxyproline-rich glycoproteins, phytoalexins and PR proteins (Adie *et al*., 2007). ET is understood to be one of the key players in the determination of the most suitable host defence response as it can modulate responses to other plant hormones such as jasmonic acid (JA), salicylic acid (SA), auxin, abscisic acid and cytokinin but the mechanisms controlling the crosstalk between individual phytohormone signalling pathways are largely unknown (Guo and Ecker, 2004; Fujita *et al.*, 2006).

Exogenous application of SA, JA and/or ET has been repeatedly associated with enhancement of resistance to pathogen attacks and, inversely, blocking the response to either of these signals can render plants susceptible to certain pathogens or even insects (Ton *et al*. 2006). The activation of an SA-dependent signalling pathway has been long recognized to be associated with the local and systemic expression of Pathogenesis-Related (PR) proteins, some of which have been shown to possess anti-microbial activity, effective against biotrophic pathogens (Glazebrook 2005). In contrast, ET and JA-dependent signals have been associated to defence responses effective against necrotrophs and herbivorous insects, working antagonistically with the SA-dependent signalling (Pieterse *et al.*, 2001). It is generally accepted that ET cooperates with JA in the activation of defence against necrotrophic pathogens and that it antagonizes SA dependent resistance against biotrophic pathogens (Berrocal-Lobo *et al.*, 2002; Lorenzo & Solano, 2005). Extensive crosstalk has

been observed between SA- and ET/JA-dependent pathways, resulting mostly in antagonistic effects on one-another, although synergistic effects have also been reported (Mur *et al.*, 2006). Hence, a strict antagonistic view of SA and JA/ET signalling pathways is likely an oversimplified view because cooperative interactions between ET and SA pathways have been reported and ET has been implicated in the activation of defences against some biotrophic and hemibiotrophic pathogens (Adie *et al*., 2007). In contrast to dicotyledonous plant models, almost nothing is known about the role of ET signalling in defence responses of monocotyledonous species (Chen *et al*. 2009).

2.1.3 *Exploitation of the ET signalling pathway by pathogens as a strategy for host infection*

It was demonstrated by Beltrano *et al*. (1994) with exogenous application of the ET donor ethephon, as well as with the ET perception inhibitor silver thiosulfate, that ET promotes grain maturation and ear senescence in wheat. According to Díaz *et al*. (2002), this might predispose the tissue for development of disease caused by some, mostly necrotrophic, pathogens. In tomato, ET stimulates the development of necrosis (Lund *et al*. 1998) and in many cases the hypersensitive response (HR; Ciardi *et al*. 2001). It is suspected that necrotrophic pathogens may benefit from HR because they feed on dead plant cells (Díaz *et al*. 2002). It was reported that HR facilitates infection of Arabidopsis by necrotrophs such as *Botrytis cinerea* or *Sclerotinia sclerotiorum* (Govrin and Levine, 2000). Mayer *et al.* (2001) speculated that necrotrophic pathogens may be well adapted to deal with HR-based defence mechanisms that are active against biotrophs.

The best demonstration to date of translation of knowledge regarding Fusarium host interactions from dicotyledonous model to monocotyledonous crop species was provided by Chen and co-workers (2009) who investigated the role of ET in the infection of *Arabidopsis*, wheat (*T. aestivum*) and barley (*Hordeum vulgare*) by *F. graminearum*. Considered as a necrotroph, *F. graminearum* has been shown to grow for the first 48 hours without causing host cell necrosis (Kruger *et al*., 2002). However, it was observed in the closely related species *F. culmorum* that production of DON mycotoxin occurred as early as 36 hours after inoculation, while growing on the surface of tissues (Kang & Buchenauer, 1999). After this short period, *F. graminearum* induces cell death as soon as it enters into the cytosol of wheat and barley pericarp cells, causing FHB (Jansen *et al*., 2005). In addition, typical infection of wheat heads by *F. graminearum* leads to bleaching symptoms of upper spikelets suggesting that senescence mechanisms might be involved in the

development of FHB symptoms. Chen and co-workers (2009) hypothesized that ET may be playing a role in FHB. The result of their work demonstrated that Arabidopsis mutants with decreased ET signalling or perception were more resistant to *F. graminearum* than wild-type accessions, while mutants enhanced in ET production were more susceptible. Wheat plants impaired in expression of *EIN2* showed both reduced disease symptoms and DON contamination of grain. In wheat, barley and *Arabidopsis* leaf sections inoculated with conidia of *F. graminearum*, exposure to ET enhanced susceptibility whereas inhibition of ET perception or signalling lead to enhanced resistance. The authors concluded that *F. graminearum* may exploit ET signalling to colonize monocotyledonous and dicotyledonous species.

However, recent work by Gottwald and collegues (2012) reported contradicting results concerning the role played by ET signalling pathways in the resistance to FHB in a study comparing differential gene espression between resistant (Dream and Sumai-3) and susceptible (Lynx and Florence-Aurore) wheat cultivars. Authors observed the upregulation of several genes associated with ET-biosynthesis (ACC oxidase) or ET-response (GDSL-like lipase). It is important to note that those reports are based on different approaches in that Gottwald used a bioinformatic prediction approach to assign putative gene functions to wheat transcripts while Chen used a reverse genetic approach, enabling to work on genes with characterised functions. Also, Gottwald and collegues used different wheat cultivars than those used by Chen and collegues. Discussion about the potential explanation for such opposing views will be discussed later in the General Discussion section and focus on the impact of phytohormone cross-talk on disease resistance.

2.1.4 *Senescence*

Nooden defined, in 1988, senescence as the age-dependent deterioration process at the cellular, tissue, organ, or organismal level, leading to death or the end of the plant life-span. It is a complex process, leading eventually to the death of the photosynthetic and other vegetative organs, involving a well-orchestrated activation of genes encoding catabolic enzymes that gradually dismantle cellular components that mainly reside in the chloroplast. Basic metabolic activities are maintained until cell death to ensure the recycling of high molecular weight components and export of the degradation products and minerals to the phloem (Gregersen *et al.*, 2008). During this process, nutrients are re-mobilized from senescing tissues to sinks such as reproductive organs. Nearly a quarter of

a century following Nooden's definition of senescence, progress towards molecular and genetic understanding of senescence has been made, mostly from studies on the model system *Arabidopsis thaliana* (At). However, At is a very distantly related model with respect to small-grain cereals. Hence, knowledge transfer from a dicotyledonous model to monocotyledonous systems should be undertaken with extreme caution. Nevertheless, it is apparent that plants share a common programme for senescence, which can be modulated by a range of biotic and abiotic factors (Gregersen *et al.*, 2008).

2.1.5 *The leaf senescence model*

Leaf senescence is an organ-level senescence but is often intimately associated with cellular or organismal death. Annual plants undergo leaf senescence along with the organismal-level senescence when they reach the end of their temporal niche. Leaf senescence is often developmentally coordinated with senescence of other organs or whole plants, such as in the case of monocarpic plants (Lim *et al.*, 2007). This phenomenon is probably best illustrated at the grain-filling and maturation stage of cereals.

In cereals, senescence appears to be regulated at the level of the individual leaf. Nutrients are mobilised from the older leaves to the younger ones and eventually to the flag leaf, which contributes the majority of the nutrients and photoassimilates used for filling of the grain. In small-grain cereals like wheat, barley and rice, up to 90% of the nitrogen content from the vegetative plant parts can be mobilized to the grain, while in other plants such as maize, 35 to 55% of the grain nitrogen is derived from soil uptake after anthesis (Gregersen *et al.*, 2008). Up to 75% of the reduced nitrogen in photosynthetically active cells of cereal leaves is located in chloroplasts (Peoples & Dalling 1988), most of which is found in ribulose-1,5-bisphosphate carboxylase/oxygenase (Rubisco) (Hörtensteiner& Feller, 2002), an enzyme involved in the first major steps of carbon fixation in the Calvin cycle. The dismantling of the photosynthetic apparatus and decline in photosynthetic activity represent therefore the major event in senescence, providing most of the nitrogen that will be translocated to the grain (Gregersen *et al.*, 2008). In At, approximately 10% of genes are differentially expressed during leaf senescence (Guo *et al.*, 2004). Genes involved in photosynthesis are down-regulated while senescence-associated genes (SAGs) are up-regulated (Niu and Guo, 2012).

It is generally considered that cell death occurring during leaf senescence is a form of programmed cell death (PCD). Hence, cell death involved in leaf senescence is controlled

by many active genetic programs (Cao *et al.*, 2003), is dependent on age and influenced by endogenous and environmental factors, which is a common definition for mechanisms of PCD. First, mesophyll cells start entering the cell death process, then proceeding to other cell types. It appears that cell death does not occur coherently but starts with local patches of early-dying cells and then propagates across the whole-leaf area (Lim *et al.*, 2007).

2.1.6 *Role of ethylene in senescence*

Phytohormonal pathways appear to play a role at all stages of leaf senescence; including initiation, progression and terminal phase of senescence (Lim *et al.*, 2007). Among hormones influencing mechanisms of senescence, ET has long been known to hasten leaf senescence as well as fruit ripening and flower senescence (Abeles *et al.*, 1988). In many plant species, ET level increases during senescence, and, accordingly, the ET biosynthetic genes encoding ACC synthase, ACC oxidase and nitrilase are up-regulated in senescing leaves (van der Graaf *et al.*, 2006). Accordingly, Beltrano and colleagues (1994) observed a progressive increase in ET production in wheat ears, starting from pre-anthesis, to peak at the hard dough stage of the grains and falling to a minimum at the dormant seed stage. Also, researchers observed that exogenous treatment of wheat ears with ET donor hastened grain maturation as well as senescence of the ears, and that, conversely, ET quenching treatments resulted in opposite effects. Two *Arabidopsis* mutants deficient in ET perception and signal transduction (*etr1* and *ein2*, respectively) exhibit significant delay in leaf senescence. However, mutant plants constitutively overproducing ET do not exhibit earlier onset of leaf senescence, suggesting that ET alone is not sufficient to initiate leaf senescence (Lim *et al.*, 2007). Recent study by Niu and Guo (2012) investigated in At the interaction between ET signalling and nitric oxide (NO), known as an anti-senescence agent, comparing the effects of NO-deficiency and ET-signalling impairment in the *ein2nos1/noa1*double mutant. NO-deficient plants exhibit an early-senescence phenotype, but dark-induced senescence and chlorophyll loss can be rescued by exogenous NO supply. However, the mutation of EIN2 was found to suppress dark-induced early senescence in the double mutant, suggesting that EIN2 is involved in NO signalling in the regulation of leaf senescence. The authors concluded that EIN2 acts downstream of NO signalling and plays a critical role in maintaining the integrity of thylakoid membranes during dark-induced senescence, which strengthens the view that EIN2 is a critical factor in the regulation of leaf senescence.

2.1.7 *Scientific hypothesis*

Plants have evolved a variety of programmed cell death (PCD) mechanisms designed to regulate critical aspects of their development, throughout the life cycle, including senescence. The mechanisms involved in the hypersensitive response and chlorosis are forms of plant PCD which have been implicated in the effective resistance to pathogens displaying a biotrophic life-style (Glazebrook, 2005). It is commonly accepted that necrotrophic pathogens, which take up nutrients from dying cells, benefit from such mechanisms. Also, it has been previously demonstrated that some necrotrophic pathogens have evolved infection strategies relying on effectors specifically disrupting the host metabolism in order to trigger certain mechanisms of PCD (Bae *et al.*, 2006). Also, Fg has been shown to exploit ET-signalling in monocotyledonous and dicotyledonous plants in order to establish a host metabolic state favourable to fungal colonization. Therefore, it is tempting to hypothesize that some forms of FHB resistance may rely on altered mechanisms of senescence which may be, at least partially, regulated by ET-signalling. In this chapter a set of wheat mutants altered in senescence were characterised and examined to establish whether correlation could be observed between plants exhibiting accelerated (or early) senescence and/or hypersensitivity to ET with susceptibility to FHB or, conversely, whether there was a correlation between delayed senescence and/or reduced sensitivity to ET with resistance to FHB.

Seven thousand Paragon EMS mutant lines were generated at the John Innes Centre by Dr S. Griffiths and Mr S. Orford. Each line generated by chemical mutagenesis was characterised on the basis of altered senescence when compared to the Paragon control. A subset of 70 mutant lines was further tested in field conditions on the basis of visual scoring of the flag-leaf post-anthesis senescence. A final set of 30 EMS mutant lines differing in their rate of post-anthesis flag leaf senescence were provided for my investigation.

2.2 Material and Methods

2.2.1 *Plant material and growth conditions*

A total of 30 ethyl methanesulfonate (EMS)-mutagenized *T. aestivum* cv. Paragon lines were obtained from Dr Simon Griffiths (JIC, Norwich, UK) at M7 stage. This subset of mutant lines were selected, on the basis of visual scoring of flag leaf yellowing in the field, for altered senescence timing (advanced or delayed) when compared to the wild-type

Paragon control. Seeds of each EMS Paragon mutant line and Paragon control were germinated by placing them on dampened filter papers (Sartorius; grade 292) in round Petri dishes (Sterilin) and placed at 5°C in the dark for 6 days. Seeds were then moved to the bench, at 20°C in the dark for two days to obtain uniform germination. Plant material used for the detached leaf and dark-induced senescence tests was planted in Cereal mix compost (Petersfield growing mediums Ltd., Leicester, England) and grown in controlled environment chambers at 17°C (day) - 12°C (night), 70% RH under a 16 h/8 h light-dark cycle (300 μmol m^{-2} s^{-1}).

2.2.2 *ACC sensitivity assay*

Twelve pre-germinated seeds per line, with three replicates each, were placed in cylindrical plastic tubes (10 x 5 cm) and filled with 75 mL of 0.5% agar-agar medium for the controls and amended with 1 mM 1-aminocyclopropane-1-carboxylic acid (ACC, Sigma-Aldrich, CAS number: 22059-21-8) for the treatments. Seeds were left to grow at 22°C in the dark (RH 70%) without lid. After 6 days, etiolated seedlings were delicately removed with tweezers, laid flat and photographed (Olympus digital camera 4-15C, Olympus Tokyo, Japan). Images were then processed with Image-J software v.1.41 (Abramoff *et al.*, 2004) to measure shoot and root lengths of treated and untreated mutant lines for later comparison with respective treated and untreated controls.

2.2.3 *Dark-induced senescence tests*

Leaf number two of each EMS mutant line, as well as the Paragon control, were detached, placed on damped filter paper (Sartorius; grade 292) in plastic boxes, 25 cm in diameter, and kept in the dark for 4 days at RT. Chlorophyll contents in the leaf was measured using a chlorophyll meter (SPAD-502PLUS, Minolta, UK) which measures the light absorbance of the leaf blade in correlation with the chlorophyll content. The device displays SPAD units (SU) ranging from 0 to 60: values of 40 and above correlate with intense green foliage and values below 20 correlate with visual chlorosis. Data was recorded on three parts of the leaf blade (determined as base, middle and tip of the leaf) at the start of the experiment and 4 days after incubation in the dark. Each individual line was used, as well as a Paragon control leaf, in each of the 20 replicates present in two independent experiments, and in 12 replicates for a third repeat experiment. Out of the 30 mutant lines investigated, the seeds of 6 mutant lines (306A, 2457A, 2457B, 2521A, 3131A and 3266B)

consistently failed to germinate in the 3 repeat experiments and therefore data could not be obtained for these lines.

2.2.4 *Maintenance and preparation of Fusarium inoculum*

DON-producing isolates of Fg (UK1) and Fc (Fu42) from the culture collection of the John Innes Centre were cultured on solid medium containing V8 vegetable juice mixed with potato dextrose agar (PDA, Difco Laboratories, Detroit, MI, U.S.A.) at 20°C for 7 days. Sporulation was induced by culturing the fungus in mung bean (MB) liquid medium with shaking for 7 days at 25°C. To prepare MB liquid medium, 40g of mung beans, bought from the local market, were boiled for 10 min in 1 L of tap water, the solution filtered through sterilized muslin and autoclaved. The fungal conidial suspension was filtered through sterilized muslin to remove fungal mycelia and centrifuged at 3000g for 5 min (SIGMA centrifuge 4-15C). The pellet was washed once, conidial concentration was quantified using a haemocytometer (Hawksley, Lancing, UK) and conidia were re-suspended in sterile water (SDW) at a concentration of $1x10^6$ spores per mL and stored at -20°C until use (method adapted from Makandar *et al.*, 2006).

2.2.5 *Detached leaf bioassays*

Leaf 3 (L3) and leaf (L4) leaf of each EMS mutant line, as well as the Paragon control, were detached from seedlings at growth stage (GS) 14 (Zadoks *et al.*, 1974) and cut to 8 cm length and wounded in two positions, 2 cm apart and on opposite sides of the mid-rib by gentle compression with a glass Pasteur pipette on the adaxial surface. A total of six leaf sections were then placed in 10 x 10cm square plastic boxes containing 0.8% Agar-Agar medium, from which the central part was removed so that only the pre-cut ends of the leaf blades were in contact with the gel. Each line was individually tested in four replicates, each plastic box containing a control Paragon leaf and L3 and L4 leaves of mutant lines. A 10 μL drop of conidial suspension containing 1 x 10^6 of Fg UK1 conidia per mL, amended with 0.01% Tween 20 (Sigma-Aldrich, CAS number: 9005-64-5), was deposited on each wound previously made with a glass Pasteur pipette (1 mm in diameter). The inner surface of the plate lid was misted with SDW to maintain 100% RH and plastic boxes were incubated at 22°C in a 16h light photoperiod (300 μmol m^{-2} s^{-1}) for 6 days. For each replicate of each mutant line, L3 and L4 were separately placed in tubes containing 4 mL of SDW and thoroughly shaken for 1 min in order to harvest secondarily produced

conidia. Tubes were then centrifuged at 3000g for 5 min and the leaves gently removed. Conidial concentrations were determined using a haemocytometer.

2.2.6 *Spray and point inoculation tests in polytunnel*

A total of 40 plants of each investigated line were grown in an unheated glasshouse into P40 trays filled with peat and sand compost (1:1). When tillering was observed about one month after planting, plants were individually transferred into 1 L pots filled with Cereal mix and moved to a polytunnel, which had below-pot watering and manual venting systems (side panels). Plants were manually randomized into four, physically separated replicates. Three replicates were spray inoculated for assessment of combined type I and II resistance and one was point inoculated for assessment of type II resistance (GS 64, Zadoks *et al.*, 1974). Spray inoculation of Fc conidia of the Fu42 isolate (5×10^5 conidia/mL amended with 0.01% Tween) was performed using a handheld sprayer. Point inoculation was performed by injecting 10µL of a Fc conidial suspension (1×10^6 conidia ml^{-1}) into the floral cavity using a sterile syringe. Mutant lines investigated for spray and point inoculation tests were separated in two independent experiments in order to ensure the handling of a reasonable number of plants for each experiment. In the first experiment, three plant replicates were spray inoculated and one plant replicate point inoculated on the 9th of June 2010. Spray inoculated heads were scored for type I resistance, when the first symptoms were detected, on the following day, and scored for type I and II resistance 5, 9 and 12 days following spray inoculation, whereas point inoculated heads were scored 16 days following infection. In the second experiment, three plant replicates were sprayed and one replicate point inoculated on the 21st of June 2010. Spray inoculated heads were scored for type I resistance three days following spray inoculation, and type I and II resistance scores were performed 3, 8 and 14 days following infection. Type II scores of point inoculated heads were taken 18 days following infection. Due to an extremely reduced number of healthy plants available for the point inoculation experiment, type II resistance scores were excluded for the mutant lines 306A and 2939A.

2.2.7 *Spray inoculation test in field trial*

Investigation of FHB resistance of EMS Paragon mutants with regards to the wild type control was carried in the field during the 2011 growing season, from march to august (sowing date: 16-03-11). Lines were organized in randomized split-plots of 1 x 1 m, each containing six rows and replicated three times. Each of the three rows was sown with 5g of

mutant seeds and each of the three other rows with 5g of Paragon wild type control. Spray inoculation with Fc conidia of the Fu42 isolate (5 x 10^5 conidia mL^{-1} amended with 0.01% Tween) was performed using a backpack sprayer on the 14th, 17th and 24th of June 2011 when plants were at mid-anthesis. Type I and II scores were performed every week, for four weeks, 17 days following the first spray inoculation.

2.2.8 *Senescence rate in the field*

Flag leaves of 8 randomly chosen plants in each split-plot were measured (when available), as well as one randomly chosen flag leaf from Paragon control in the same split-plot, using the previously described chlorophyll meter around the mid region of the leaf. Measurements were taken on the 14th of June 2011, corresponding to mid-anthesis, growth GS 64, prior to spray inoculation, and on the 25th of July 2011 (approximately 41 days following mid-anthesis) and on the 9th of August 2011 (56 days following mid-anthesis).

2.2.9 *Quantification of mycotoxin contamination of grain*

Heads of a subset of Paragon EMS mutant lines that had exhibited reduced symptoms of FHB relative to Paragon were harvested at the end of the growing season (GS 90, Zadoks *et al.*, 1974) as well as heads of the Paragon control. These were frozen in liquid N_2 and ground to a fine powder. DON quantification was performed using an ELISA competitive immunoassay (AgraQuant®, ROmer Labs Singapore Pte Ltd) according to the manufacturer's recommendation.

2.2.10 *Statistical analysis*

Student T-tests were calculated using a generalized linear model (GLM) in Genstat, ninth edition (Copyright 2006, Lawes Agricultural Trust –Rothamsted Experimental Station-) to assess variability attributed to blocks and genotypes. Predicted average values for each investigated line were generated from data collected in the dark-induced senescence (DIS) test and DON quantification and a threshold p-value of 0.01 (confidence interval = 99%) was chosen. Results from the chlorophyll content assessment in the field, spray and point inoculations in polytunnel as well as the spray inoculation test in the field were analyzed using a student *t*-test test. The area under disease progress curve (AUDPC) was calculated according to Buerstmayr *et al.* (2000).

2.3 Results

2.3.1 *Plant phenotypes*

Plant phenotypes were consistently observed compared to the control when growing the EMS mutant lines in heated glasshouses, polytunnels and in the field. Six mutant lines, 1385A, 1385B, 2514A, 2516A, 2686A and 3266B displayed spontaneous chlorotic lesions on most leaves, including flag leaves (See Figure 2.1 for mutant foliar phenotypes; B-G, compared to the WT control; A). The extent of the foliar lesion varied among mutants displaying this phenotype and also varied according to the different environmental conditions. The phenotype displayed by the mutant line 2516A consisted of spontaneous chlorotic lesions generally centred around small dark-brown lesions which resembled necrotic spots (See Figure 2.1, E). Similar dark-brown lesions were observed on the stems of 2516A plants, and sometimes on the abaxial surface of leaves, which were not, however, associated with surrounding chlorosis (See Figure 2.1, H). It was observed that the extent of leaf area displaying spontaneous chlorotic lesions in these six mutant lines increased overtime. Two other mutants, lines 423AG and 2939A, consistently displayed a delay in development when compared with the wild type control. During the field experiment, retardation of the overall plant growth was particularly observed around anthesis stage, as these two mutant lines still had ears enclosed in the boot while WT control plants in the corresponding split-plot were fully emerged (See Figure 2.1, I-J). Additionally, it was noticed that flag leaves were visually larger than those of the wild type control, although no assessment of this parameter was undertaken. The impact of delayed ear emergence on the head inoculation experiments was significant in the field trial, but was marginal in the heated glasshouse and polytunnel environments.

Figure 2.1: Mutant phenotypes observed at anthesis stage in glasshouse, polytunnel and field trial compared to the Paragon wild type control: A) Paragon WT leaf. B-H: foliar and stem phenotypes; I & J) Developmental delay in flowering time, B) 1385A C) 1385B, D) 2514A, E) 2516A, F) 2686A, G) 3266A, H) 2516A, I) 423AG, J) 2939A. Yellow line indicates split-plot separation between mutant (bottom left) and Paragon WT control (top right) rows.

2.3.2 *Characterisation of the senescence properties of a selected subset of Paragon EMS mutant lines*

Paragon EMS mutant lines generated by Dr S. Griffith and Mr S. Orford (John Innes Center) were characterized for altered senescence pattern in the field. Ranking of individual lines was then achieved based on the "stay green effect" scoring system based on the visual scoring of post-anthesis discolouration of the flag leaves (See Annexe 1, Supplementary Figure 1). Assessment of the senescence characteristics of each mutant line was undertaken to confirm classification of individual lines into "delayed senescence" or "fast senescence" categories using relative measurements of chlorophyll contents *in vivo* and *in vitro*.

2.3.3 *Characterisation of dark-induced senescence*

A subset of 24 EMS mutant lines were selected for re-assessment of the chlorophyll content in L2 as measured by the light absorbance in leaves at the start of the experiment, prior to exposure to darkness. Paragon control leaves contained an average of 51.68 (s.e. = 0.2592) SPAD units (SU) at the start of the experiment. Variation in average chlorophyll content ranged from a minimum of 44.76 SU (s.e. = 0.6782) for the line 2145B to a maximum of 54.31 SU (s.e. = 0.6898) for the line 2316A (See Figure 2.2). The mutant lines 2316A and 2939A were found to contain significantly (p-value ≤ 0.01) higher levels of chlorophyll when compared to the WT control, 54.31 and 53.68 SU respectively. Mutant lines 2145B, 2516A, 1385A, 2056A, 423AG and 1385B were found to contain significantly (p-value ≤ 0.01) lower levels of chlorophyll compared to the WT control.

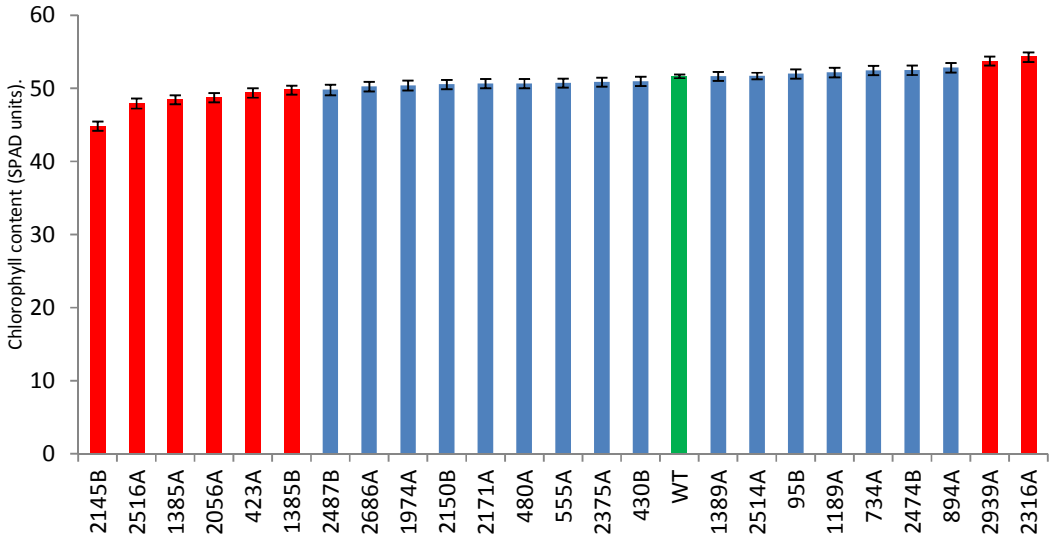

Figure 2.2: Predicted mean of the chlorophyll content of a subset of Paragon EMS mutant lines as measured by the light absorbance (SPADmeter reading), at the start of the experiment, prior exposure to darkness. Error bars show standard errors. Green colour bar indicates the wild-type Paragon control. Red colour bars indicate mutant line for which values significantly departed from the control (p-value ≤ 0.01). Blue bars indicate mutant lines for which average values did not significantly depart from the control.

Chlorophyll contents were measured 4 days following exposure to darkness in the same mutant and control leaves to allow direct comparison. Paragon control leaves contained an average of 28.86 SU (s.e. = 0.489) following 96 hours incubation in the dark. Variation in average chlorophyll content ranged from a minimum of 24.12 SU (s.e. = 0.6782) for the line 1385A to a maximum of 34.98 SU (s.e. = 0.6898) for the line 2939A (See Figure 2.3).

The mutant lines 2939A, 2474B, 1974A, 423AG and 555A were found to contain significantly (p-value ≤ 0.01) higher levels of chlorophyll when compared to the WT control. The line 1385A was the only mutant found to contain significantly (p-value ≤ 0.01) lower levels of chlorophyll when compared to the WT control.

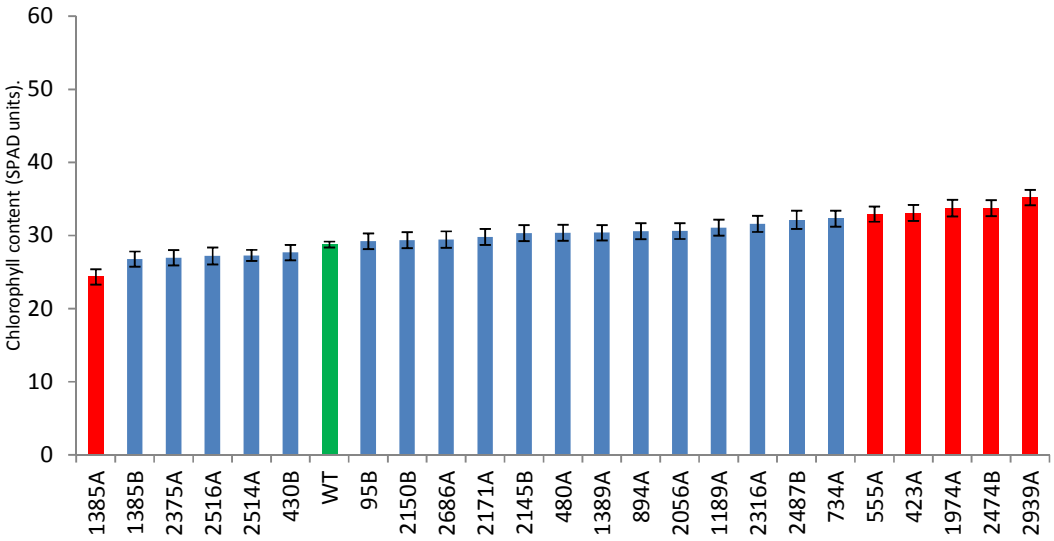

Figure 2.3: Predicted mean of the chlorophyll content of a subset of Paragon EMS mutant lines as measured by the light absorbance (SPADmeter reading), 4 days following exposure to darkness. Error bars show standard errors. Green colour bar indicates the wild-type Paragon control. Red colour bars indicate mutant line for which values significantly depart from the control (p-value ≤ 0.01). Blue bars indicate mutant lines for which average values did not significantly depart from the control.

Mean percentage chlorophyll loss were calculated for each individual line in order to assess the relative percentage chlorophyll loss compared to the wild type control. The control leaves of Paragon wild-type showed an average of 44.45% (s.e. = 0.859) of chlorophyll loss in four days of exposure to darkness (See Figure 2.4). Variation was observed ranging from a minimum of 31.06% (s.e. = 2.375) of chlorophyll loss as displayed by the line 1974A, to a maximum of 49.79% (s.e. = 2.177) of chlorophyll loss as displayed by the line 1385A. The line 1385A was found to be the only mutant to lose significantly (p-value ≤ 0.01) more chlorophyll content than the WT control while six mutant lines (1974A, 423AG, 2145B, 2474A, 2939A and 555A) exhibited significantly (p-value ≤ 0.01) less chlorophyll loss than the WT control.

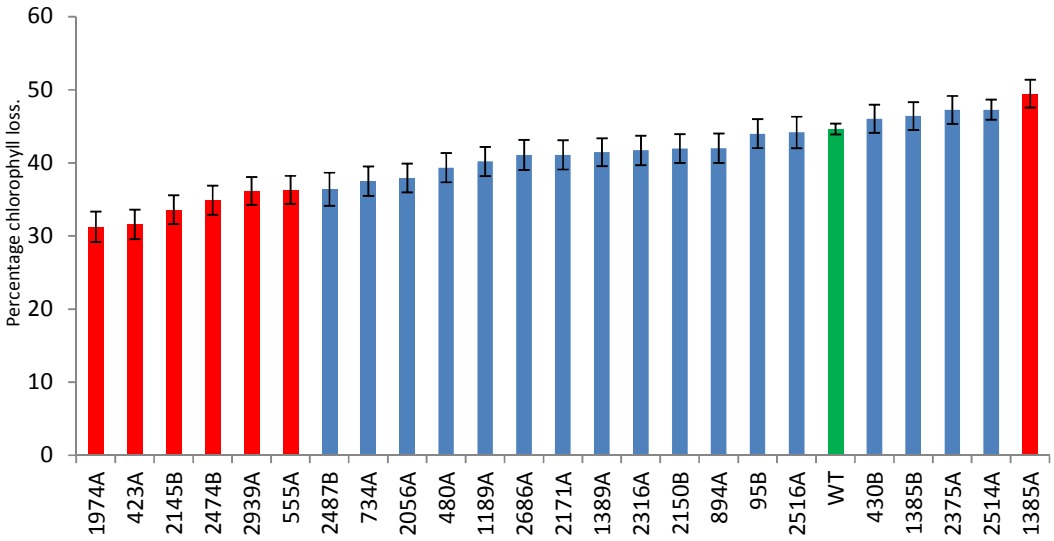

Figure 2.4: Predicted mean percentage of chlorophyll loss as measured by the light absorbance of detached leaf 2 of a subset of Paragon EMS mutant lines, in four days of exposure to darkness. Error bars show standard errors. Green colour bar indicates the wild-type Paragon control. Red colour bars indicate mutant line for which values significantly depart from the control (p-value ≤ 0.01). Blue bars indicate mutant lines for which average values did not significantly depart from the control.

2.3.4 *Characterisation of chlorophyll contents in flag leaves at mid-anthesis*

During the course of the 2011 field trial, chlorophyll content of the flag leaves of mutant and wild type control plants was measured at mid-anthesis stage (GS 64, Zadock *et al.*, 19). Flag leaves of the Paragon control plants displayed an average of 56.77 SU (s.e. = 0.783; See Figure 2.5). Variation in chlorophyll content was observed to range between a minimum of 25.82 SU (s.e. = 1.541) as displayed by the mutant line 1385A to a maximum of 59.18 SU (s.e. = 1.541) as displayed by the mutant line 894A. No mutant line was found to contain significantly greater levels of chlorophyll when compared to the WT control. However, eleven mutant lines (1385A, 1389B, 2514A, 2457B, 2686A, 3131A, 2457A, 3266B, 423AG, 2056A and 2516A) were observed to contain significantly (p-value ≤ 0.01) lower chlorophyll levels when compared with the WT control.

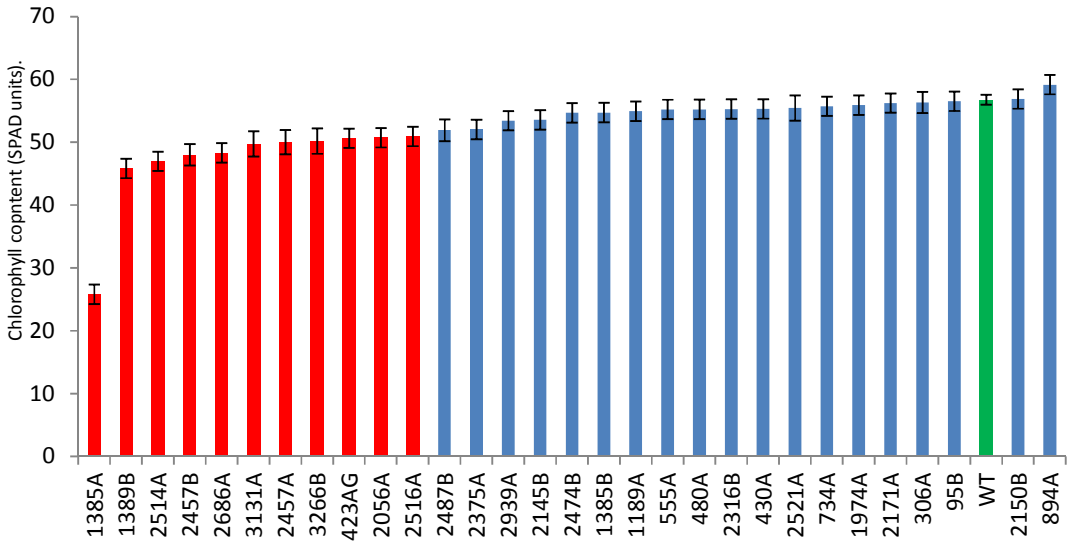

Figure 2.5: Predicted mean of chlorophyll content as measured by the light absorbance recorded in the flag leaves of a subset of Paragon EMS mutant lines grown in the field at mid-anthesis stage. Error bars show standard errors. Green colour bar indicates the wild-type Paragon control. Red colour bars indicate mutant line for which values significantly depart from the control (p-value ≤ 0.01). Blue bars indicate mutant lines for which average values did not significantly depart from the control.

2.3.5 *Characterisation of flag leaf senescence*

Assessment of the chlorophyll content in the flag leaves of field grown EMS mutant and wild type control lines was measured 41 days following mid-anthesis in order to assess the senescence characteristics of each line in the field. Flag leaves of the Paragon control line displayed an average of 41.24 SU (s.e. = 1.148). Variation in chlorophyll content was observed ranging between a minimum of 13.26 SU (s.e. = 2.479) as displayed by the mutant line 2516A to a maximum of 46.72 SU (s.e. = 2.96) as displayed by the mutant line 2521A (See Figure 2.6). No mutant line was observed to retain significantly (p-value $\leq$ 0.01) higher levels of chlorophyll when compared to the control. However, ten mutant lines (2516A, 2686A, 3266B, 430A, 2514A, 2056A, 1385A, 2150B, 1389B and 1385B) were observed to contain significantly (p-value ≤ 0.01) lower levels of chlorophyll when compared to the WT control.

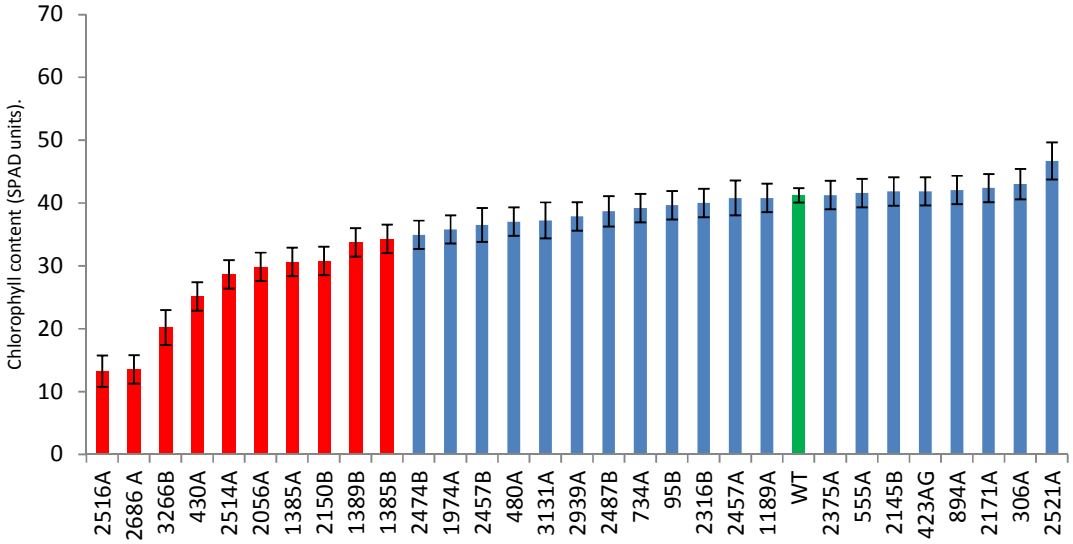

Figure 2.6: Predicted mean of chlorophyll content as measured by the light absorbance recorded in the flag leaves of a subset of Paragon EMS mutant lines grown in the field 41 days following mid-anthesis. Error bars show standard errors. Green colour bar indicates the wild-type Paragon control. Red colour bars indicate mutant line for which values significantly depart from the control (p-value ≤ 0.01). Blue bars indicate mutant lines for which average values did not significantly depart from the control.

The mean percentage of chlorophyll lost in flag leaves over the period of forty-one days following mid-anthesis was calculated for each EMS Paragon mutant line and the wild-type control. Flag leaves of the Paragon control line lost in average 27.35% (s.e. = 2.354) of their chlorophyll content (See Figure 2.7). Variation in percentage chlorophyll loss was observed to range from a minimum of 15.7% (s.e. = 6.069) as displayed by the mutant line 2521A, to a maximum of 74.01% (s.e. = 5.081) as displayed by the mutant line 2516A. No mutant line was found to retain significantly higher levels of chlorophyll compared to the wild-type control. However, six mutant lines (2056A, 2150B, 430A, 3266B, 2686A and 2516A) were found to lose significantly greater levels of chlorophyll when compared to the wild-type control. The results displayed by the mutant line 1385A were discarded from the bar chart as the average percentage change in chlorophyll content was found negative (corresponding to an average gain of 18.86% in chlorophyll content). This result was not judged relevant for reasons that will be explained in the following section.

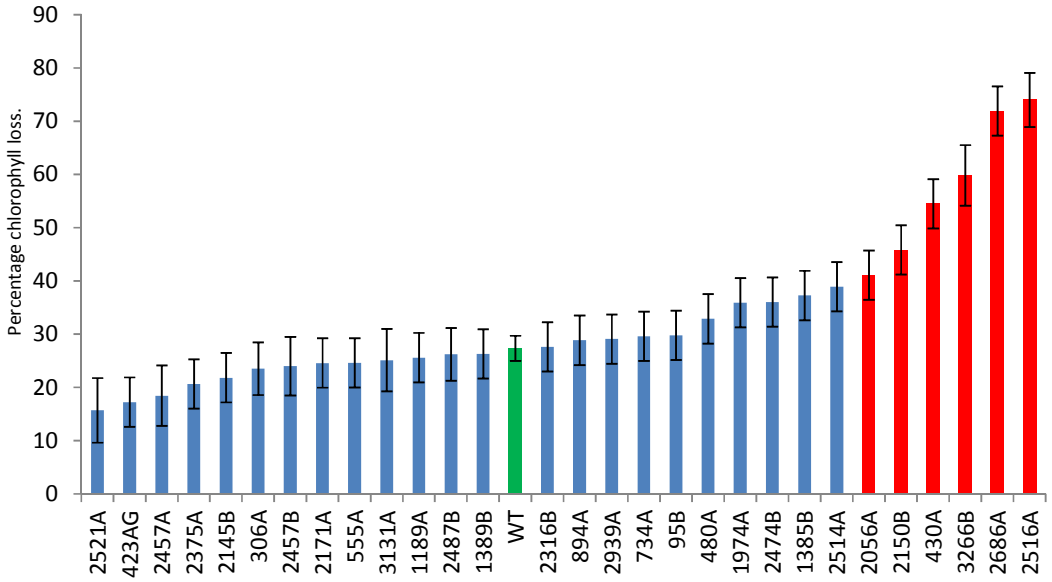

Figure 2.7: Predicted mean percentage of chlorophyll loss as measured by the light absorbance recorded in the flag leaves of a subset of Paragon EMS mutant lines grown in the field 41 days following mid-anthesis. Error bars show standard errors. Green colour bar indicates the wild-type Paragon control. Red colour bars indicate mutant line for which values significantly depart from the control (p-value $\leq$ 0.01). Blue bars indicate mutant lines for which average values did not significantly depart from the control.

At a late stage of the growing season, when flag leaves of Paragon wild-type plants and most mutant lines exhibited complete senescence, six mutant lines were visually observed to retain chlorophyll in the flag leaf compared to the corresponding split-plot control. Therefore, the final assessment of chlorophyll contents in the flag leaves of a sub-set of mutants as well as the control was performed, 56 days following mid-anthesis. Flag leaves of the Paragon control plants exhibited an average of 13.03 SU (s.e. = 0.938; See Figure 2.8), a SU value lower than 20, which visually correlates with a yellow colouration of the leaves. The mutant lines 423AG, 1189A, 2521A and 2939A had significantly (p-value $\leq$ 0.01) greater chlorophyll contents compared to the WT control leaves.

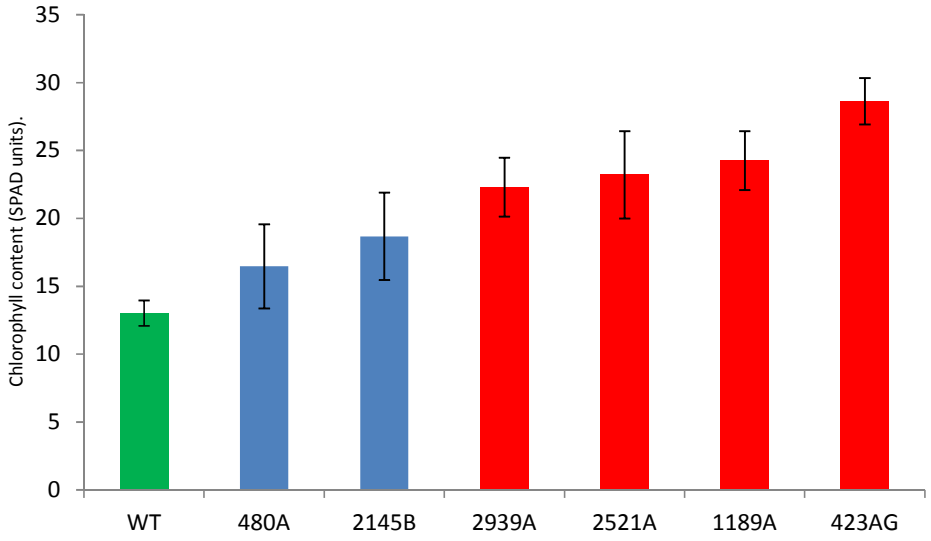

Figure 2.8: Predicted mean of chlorophyll content as measured by the light absorbance recorded in the flag leaves of six Paragon EMS mutant lines and the wild-type control grown in the field, 56 days following mid-anthesis. Error bars show standard errors. Green colour bar indicates the wild-type Paragon control. Red colour bars indicate mutant line for which leaves lost significantly less chlorophyll (p-value ≤ 0.01). Blue bars indicate mutant lines for which average values did not significantly depart from the control.

2.3.6 *Characterisation of ACC-sensitivity of a selected subset of EMS mutant lines*

The phytohormone ethylene (ET) is a volatile compound well-known to inhibit the growth of root and shoot tissues of etiolated seedlings. The production of ET in plants is mainly regulated by the conversion of ACC, the last precursor along the hormone biosynthesis pathway, catalyzed by the rate-limiting enzyme ACC-synthase (ACS). Therefore, exogenous exposure to ACC in seedlings grown in absence of light results in the production of ET *In Situ* and results in severe inhibition of growth. ACC was therefore chosen as a treatment to characterise the sensitivity to ET of a sub-set of EMS Paragon mutant lines.

To allow a detailed analysis of the ET-sensitivities of each individual EMS mutant line with respect to the control, data of the length of etiolated treated and control seedlings was separately analysed, and the ratio between treated over untreated seedling length was calculated for each individual line. In order to allow direct comparison across the two sets of experiments, measurements of the mutant seedling lengths were normalized according to the respective mean of control seedling length.

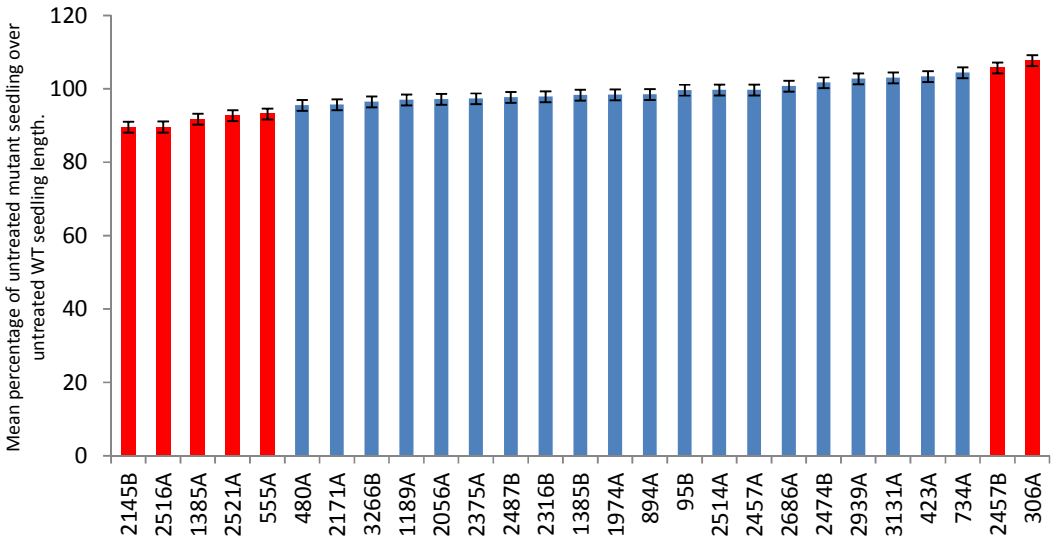

Figure 2.9: Predicted mean percentage of untreated etiolated mutant compared to the control seedlings length, as measured 6 days following incubation in the dark. Error bars show standard errors. Red colour bars indicate mutant line for which average seedling length was significantly (p-value ≤ 0.01) different from the Paragon wild type control. Blue bars indicate mutant lines for which average means did not significantly depart from the control.

Variation in the mean of untreated seedling length ranged from a minimum of 89.61% (s.e. 1.48) of the control as displayed by the mutant line 2145B to a maximum of 107.71% IU (s.e. = 1.48) of the control as displayed by the mutant line 306A (See Figure 2.9). The seedlings of mutant 306A and 2457B were significantly (p-value ≤ 0.01) longer than those of the WT control. The average length of untreated seedlings was significantly shorter for five mutant lines; 2145B, 2516A, 1385A, 2521A and 555A when compared to the WT.

Treatment with 1 mM ACC resulted in the reduction in growth of the root and shoot of etiolated seedlings. Variation in average seedling length ranged from a minimum of 89.27% (s.e. 1.571) of the control as displayed by the mutant line 2521A to a maximum of 116.7% (s.e. = 1.277) as displayed by the mutant line 2056A (See Figure 2.10). Average seedling length of the mutant lines 2521A, 2516A, 1385A, 2686A, 480A, 3266B and 1189A were significantly (p-value ≤ 0.01) reduced by ACC treatment when compared to the control. At the opposite end of the spectrum, four mutant lines (2056A, 2457A, 734A, 2457B, 2316B, 306A and 2939A) were significantly (p-value ≤ 0.01) longer following ACC treatment compared to the control.

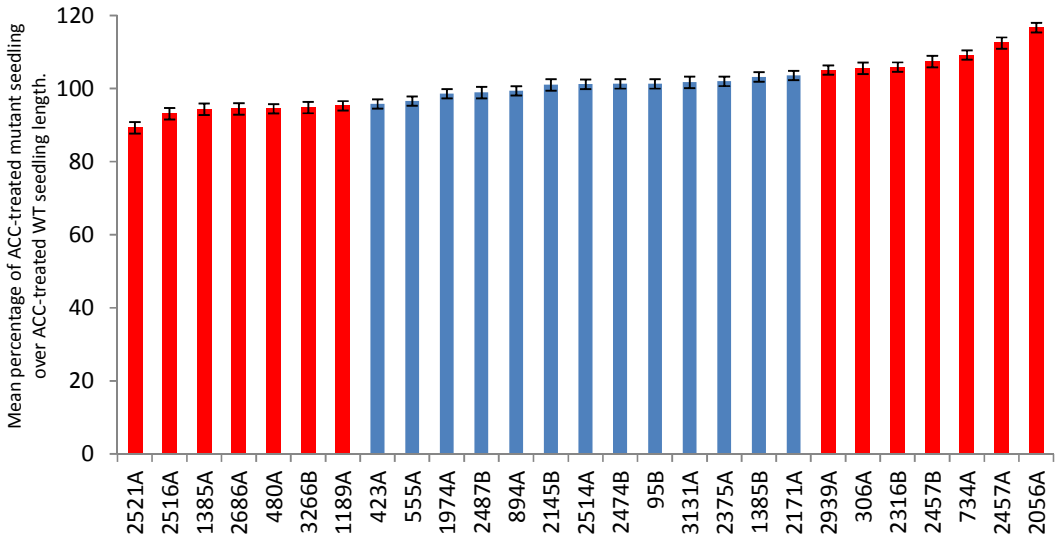

Figure 2.10: Predicted mean percentage of ACC-treated etiolated mutant compared to the control seedlings length, as measured by the Image-J software, 6 days following incubation in the dark. Error bars show standard errors. Red colour bars indicate mutant line for which average seedling length was significantly different from the control (p-value ≤ 0.01). Blue bars indicate mutant lines for which average values did not significantly depart from the control.

The ratio of the average length of ACC-treated seedling over untreated seedling was calculated to assess the ET sensitivity of each mutant line relative to the wild type control. Data were separated into two sets as the mutant lines were assessed in two separate experimental sets, and therefore had to be compared with their respective control values.

In the first experimental set, wild type Paragon seedlings displayed an average reduction in seedling length of 49.18% (s.e. = 0.7824) in response to ACC treatment compared to the untreated wild type seedlings (See Figure 2.11). The variation in percentage seedling length reduction caused by ACC treatment relative to the untreated seedling length was observed to range between a minimum of 46.06% (s.e. = 0.7824) as displayed by the mutant line 2686A to a maximum of 55.4% (s.e. = 0.7824) as displayed by the mutant line 2457A. A single mutant line (2686A) was found to have a significantly (p-value ≤ 0.01) reduced ratio of ACC-treated over untreated seedling length, indicative of an enhanced sensitivity to ACC, whereas two mutant lines (2457A and 2145B) were found to have a significantly (p-value ≤ 0.01) greater ratio, indicative of a reduced ET sensitivity.

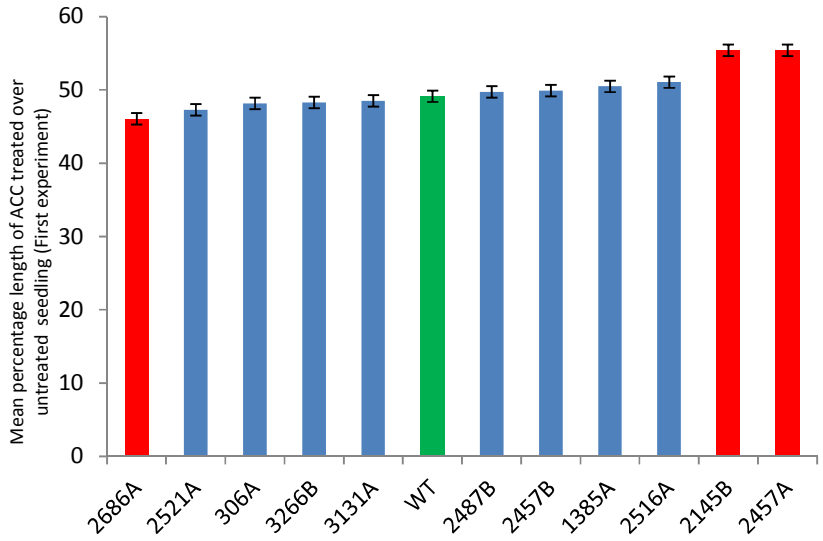

Figure 2.11: Predicted mean percentage of ACC treated over untreated etiolated seedlings from experiment 1, as measured 6 days following incubation in the dark. Error bars show standard errors. Green bar indicates the average value for the Paragon wild type control seedlings. Red colour bars indicate mutant line for which average seedling length was significantly different from the control (p-value ≤ 0.01). Blue bars indicate mutant lines for which average values did not significantly depart from the control.

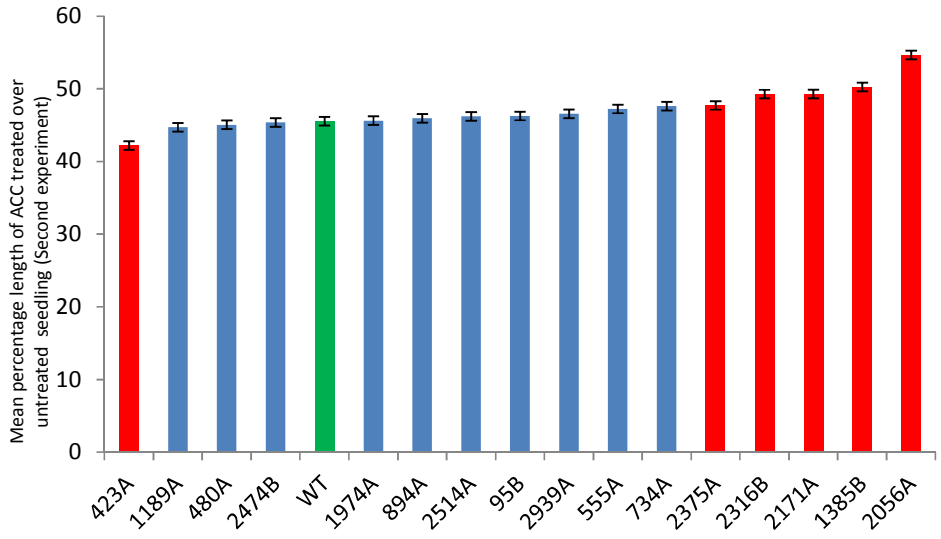

Figure 2.12: Predicted mean percentages of ACC treated over untreated etiolated seedlings from experiment 2, as measured 6 days following incubation in the dark. Error bars show standard errors. Green bar indicates the average value for the Paragon wild type control seedlings. Red colour bars indicate mutant line for which average seedling length was significantly different from the control (p-value ≤ 0.01). Blue bars indicate mutant lines for which average values did not significantly depart from the control.

In the second experimental set, wild type Paragon seedlings displayed an average reduction in seedling length of 45.55% (s.e. = 0.5829) in response to ACC treatment compared to the untreated wild type seedlings (See Figure 2.12). The variation in percentage reduction relative to the wild type response was observed to range between a minimum of 42.19% (s.e. = 0.5829) as displayed by the mutant line 423AG to a maximum of 54.67% (s.e. = 0.5829) as displayed by the line 2056A. Mutant seedlings of the line 423AG showed the only significant (p-value ≤ 0.01) reduction in ratio, indicating an enhanced sensitivity to ACC whereas five mutant lines (2056A, 2171A, 2316B, 1385B and 2375A) displayed a significantly (p-value ≤ 0.01) reduced sensitivity to ACC relative to the wild type control.

2.3.7 Characterisation of FHB resistance

2.3.8 *FHB resistance test in polytunnel*

Investigation of type I and type II resistance to FHB in the set of Paragon EMS mutant lines was performed in two separate polytunnel experiments in 2010. In order to have a reasonable number of plants to handle for each test, plants were processed two weeks apart from each other. Plants were divided into four replicate sets of five, three of which were spray inoculated and one point inoculated with Fu42 conidia. Therefore, the results obtained had to be analysed separately, and allow the statistical analysis to account for potential variation in the environmental conditions.

Area under disease progress curve (AUDPC) generated from three visual disease scores were generated to assess both type I and II resistance to FHB. A predicted mean AUDPC of 583.7 (s.e. = 32.92) was observed in the wild-type control heads (See Figure 2.13). Variation in AUDPC was observed to range, in the first experiment, from 442.2 (s.e. = 32.92), as displayed by the mutant line 2487B, to a maximum of 732.4 (s.e. = 31.46), as displayed by the mutant line 2457A. The line 2487B was the only mutant observed to display a significant (p-value ≤ 0.01) reduction in AUDPC compared to the control. However, four mutant lines (2514A, 2516A, 2686A and 2457A) were observed to have a significantly (p-value ≤ 0.01) greater AUDPC than the control.

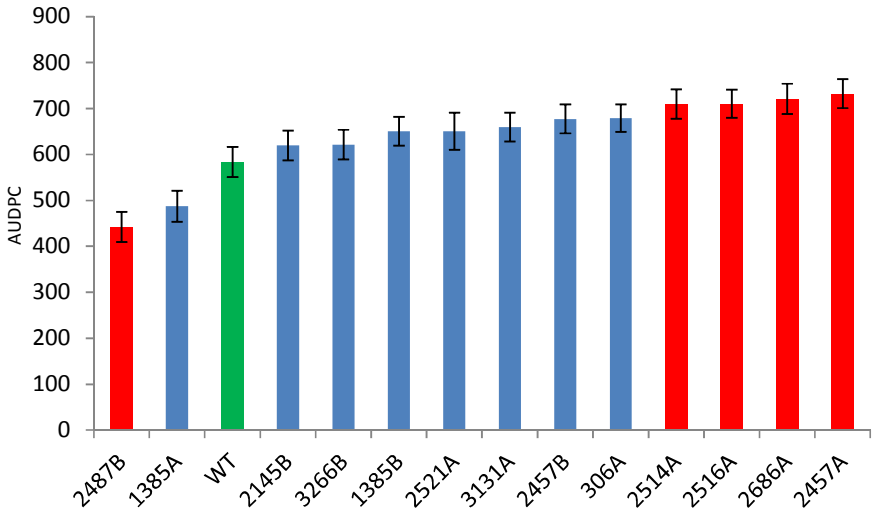

Figure 2.13: Predicted mean area under disease progress curve (AUDPC) following spray inoculation with Fu42 in a Polytunnel on Paragon EMS mutant lines from the first experiment. Error bars show standard errors. Green bar indicates the average value for the Paragon wild type control seedlings. Red colour bars indicate mutant line for which average seedling length was significantly different from the control (p-value ≤ 0.01). Blue bars indicate mutant lines for which average values did not significantly depart from the control.

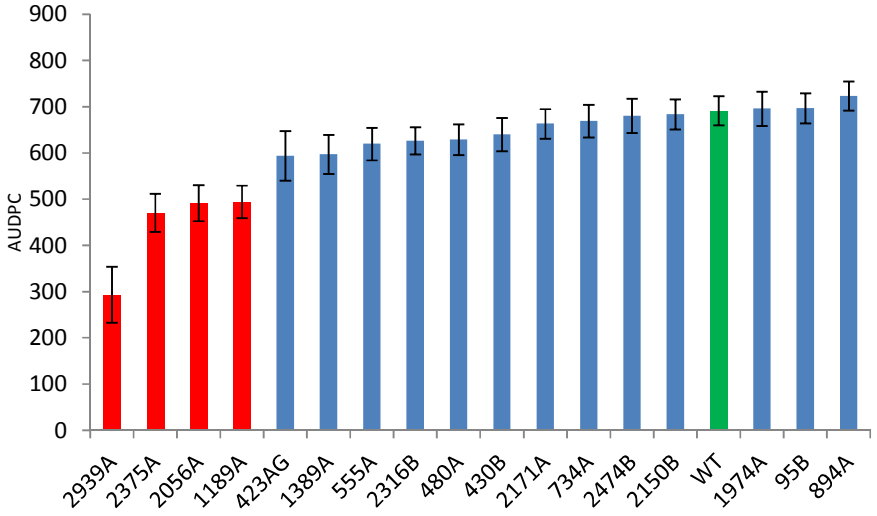

Figure 2.14: Predicted mean area under disease progress curve (AUDPC) following spray inoculation with Fu42 in a Polytunnel on Paragon EMS mutant lines from the second experiment. Error bars show standard errors. Green bar indicates the average value for the Paragon wild type control seedlings. Red colour bars indicate mutant line for which average seedling length was significantly different from the control (p-value ≤ 0.01). Blue bars indicate mutant lines for which average values did not significantly depart from the control.

In the second experiment, a predicted mean AUDPC of 691.6 (s.e. = 31.42) was observed in the wild-type control heads (see Figure 2.14). Variation in AUDPC was observed ranging from 293.5 (s.e. = 60.54), as displayed by the mutant line 2939A, to a maximum of

723.4 (s.e. = 31.35), as displayed by the mutant line 894A. Four mutant lines (2939A, 2375A, 2056A and 1189A) displayed a significantly (p-value ≤ 0.01) reduced AUDPC compared to the wild-type control. However, no mutant line was observed to display a significant increase in AUDPC compared to the wild-type control.

The first visual disease score, from each of the two experiments, were analysed separately in an effort to estimate the level of type I resistance. The first visible symptoms appearing on *Fusarium* spray inoculated heads are widely recognized as an indicator of type I resistance to FHB, relating to resistance mechanisms effective during the initial penetration attempt by the fungus.

Wild-type control plants from the first experiment displayed an average of 17.92% (s.e. = 5.092) FHB symptoms on the heads (see Figure 2.15), at the time of the first assessment following spray inoculation. Variation in percentage diseased head ranged from a minimum of 4.36% (s.e. = 5.172), as displayed by the mutant line 1385A, to a maximum of 53.01% (s.e. = 5.048), as displayed by the mutant line 2686A. No mutant line exhibited significantly less disease than the WT in the first experiment. However, five mutant lines (306A, 2457A, 2457B, 2514A and 2686A) displayed significantly (p-value ≤ 0.01) more disease symptoms than the wild-type control.

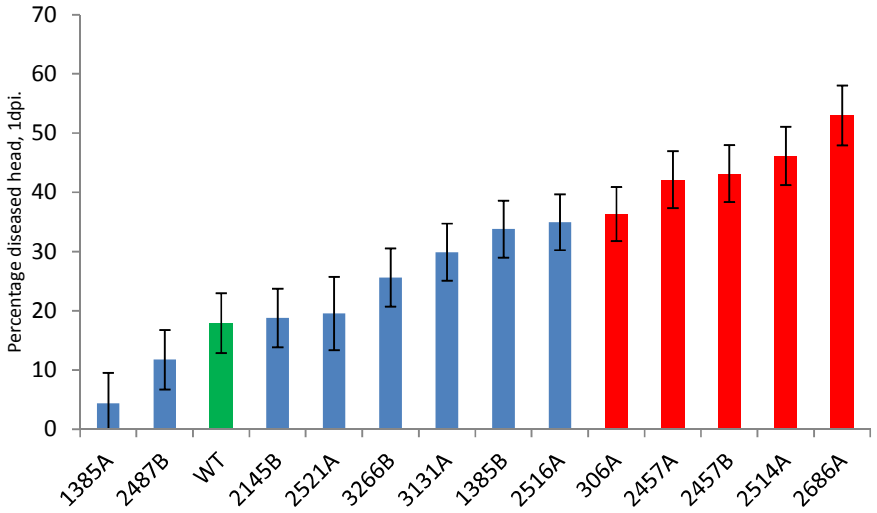

Figure 2.15: Predicted mean percentage diseased head, 1 day following spray inoculation with Fu42 in a Polytunnel on Paragon EMS mutant lines from the first experiment. Error bars show standard errors. Green bar indicates the average value for the Paragon wild type control seedlings. Red colour bars indicate mutant line for which average seedling length was significantly different from the control (p-value ≤ 0.01). Blue bars indicate mutant lines for which average values did not significantly depart from the control.

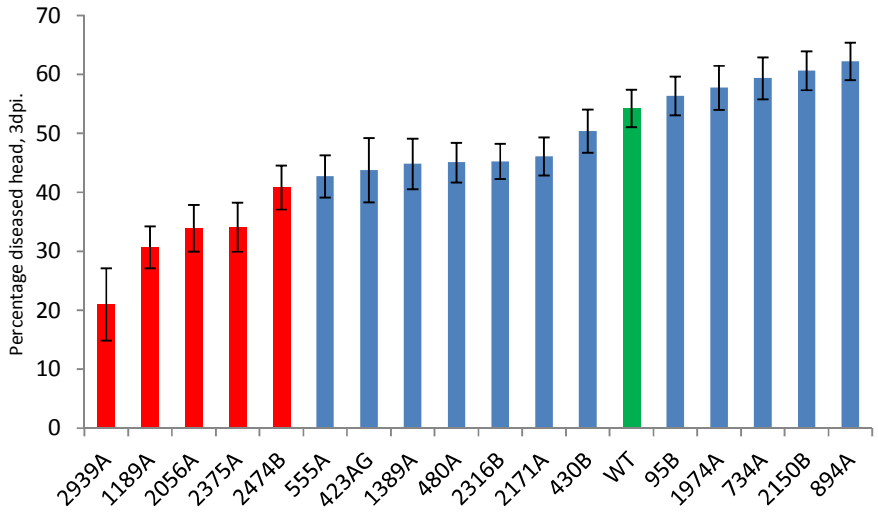

Figure 2.16: Predicted mean percentage diseased head, 3 day following spray inoculation with Fu42 in a Polytunnel on Paragon EMS mutant lines from the second experiment. Error bars show standard errors. Green bar indicates the average value for the Paragon wild type control seedlings. Red colour bars indicate mutant line for which average seedling length was significantly different from the control (p-value $\leq$ 0.01). Blue bars indicate mutant lines for which average values did not significantly depart from the control.

In the second experiment, wild-type control plants displayed an average of 54.26% (s.e. = 3.187) FHB symptoms on the heads (see Figure 2.16). Variation in percentage diseased head ranged from a minimum of 21.02% (s.e. = 6.14), as displayed by the mutant line 2939A, to a maximum of 62.22% (s.e. = 3.18), as displayed by the mutant line 894A. No mutant line displayed a significant increase in FHB symptoms. However, five mutant lines (2939A, 1189A, 2056A, 2375A and 2474B) were found to have significantly (p-value $\leq$ 0.01) reduced FHB symptoms when compared to the wild-type control.

Visual assessments of FHB disease symptoms developing from point inoculated spikelets are widely accepted as indicative of type II resistance, relating to resistance mechanisms effective against the spread of the fungus within the host tissues.

Wild-type control plants from the first experiment displayed an average of 23.86% (s.e. = 5.581) in head infection, twenty-one days following point inoculation (see Figure 2.17). Variation in percentage infected head were observed ranging from a minimum of 9.93% (s.e. = 7.383), as displayed by the mutant line 3131A, to a maximum of 38.51% (s.e. = 6.028), as displayed by the mutant line 2516A but no mutant lines differed significantly from the wild-type control value.

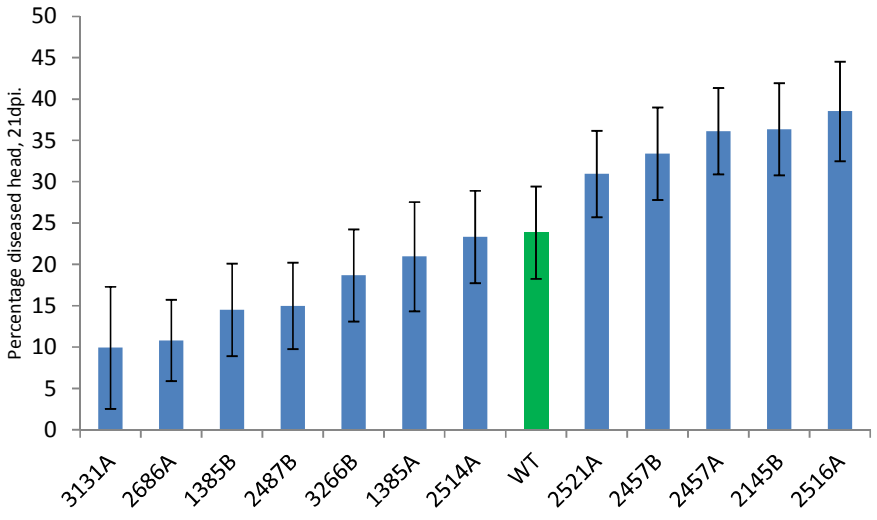

Figure 2.17: Predicted mean percentage diseased head, 21 day following point inoculation with Fu42 in a Polytunnel on Paragon EMS mutant lines from the first experiment. Error bars show standard errors. Green bar indicates the average value for the Paragon wild type control seedlings. Blue bars indicate mutant lines for which average values did not significantly depart from the control.

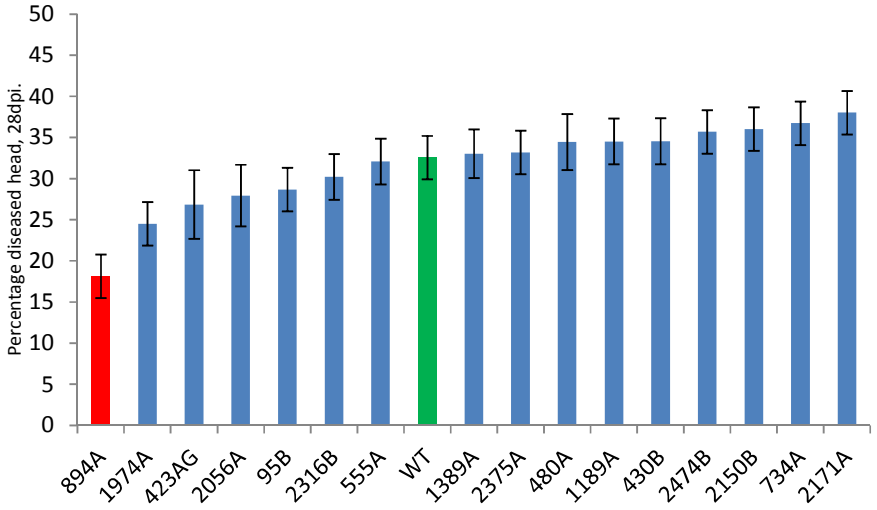

Figure 2.18: Predicted mean percentage diseased head, 28 days following point inoculation with Fu42 in a Polytunnel on Paragon EMS mutant lines from the second experiment. Error bars show standard errors. Green bar indicates the average value for the Paragon wild type control seedlings. Red colour bars indicate mutant line for which average seedling length was significantly different from the control (p-value ≤ 0.01). Blue bars indicate mutant lines for which average values did not significantly depart from the control.

In the second experiment, wild-type control plants displayed an average of 32.55% (s.e. = 2.643) in head infection, twenty-eight days following point inoculation (see Figure 2.18). Variation in percentage infected head were observed ranging from a minimum of 18.14% (s.e. = 2.643), as displayed by the mutant line 894A, to a maximum of 38.02% (s.e. = 2.643), as displayed by the mutant line 2171A. Only one mutant line, 894A, was observed with significantly (p-value $\leq$ 0.01) reduced symptoms when compared to the wild-type control.

2.3.9 *FHB resistance in field trial*

Investigation of the combined type I and type II resistance to FHB in the set of Paragon EMS mutant lines was also assessed in a field trial in 2011.

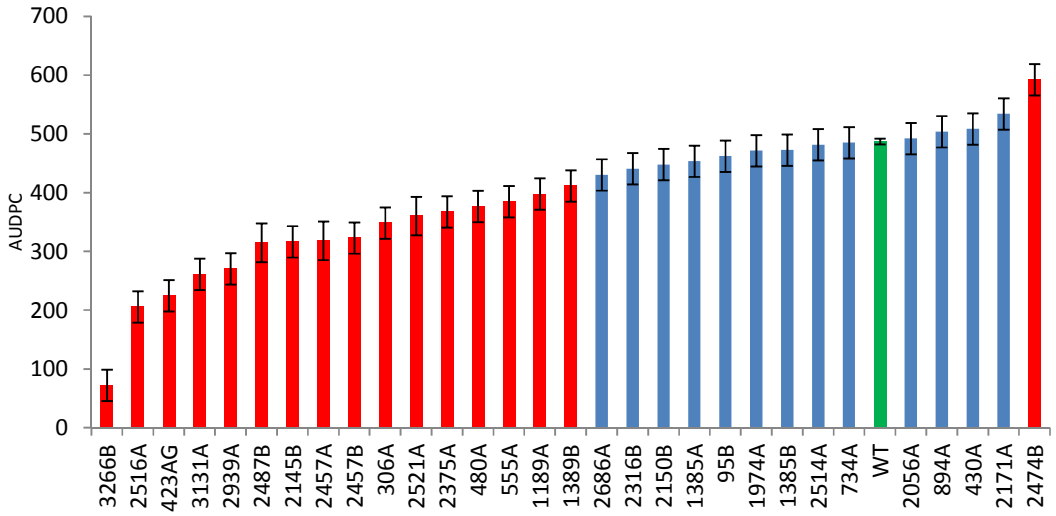

Figure 2.19: Predicted mean of area under disease progress curve (AUDPC) following spray inoculation with Fu42 in the field on a subset of Paragon EMS mutant lines. Error bars show standard errors. Green bar indicates the average value for the Paragon wild type control seedlings. Red colour bars indicate mutant line for which average seedling length was significantly different from the control (p-value $\leq$ 0.01). Blue bars indicate mutant lines for which average values did not significantly depart from the control.

Spray inoculated heads of field grown wild-type Paragon control plants displayed an average AUDPC of 487.2 (s.e. 4.92). Variation in mean AUDPC was observed ranging from a minimum of 72.3 (s.e. = 26.67), as displayed by the mutant line 3266B, to a maximum of 592.6 (s.e. = 26.67), as displayed by the mutant line 2474B (see Figure 2.19). Only one mutant line, 2474B, displayed a significantly (p-value $\leq$ 0.01) increased AUDPC

when compared to the wild-type controls. However, sixteen mutant lines (3266B, 2516A, 423AG, 3131A, 2939A, 2487B, 2145B, 2457A, 2457B, 306A, 2521A, 2375A, 480A, 555A, 1189A and 1389B displayed a significant (p-value ≤ 0.01) reduction in AUDPC as compared with the heads of the wild-type control plants.

2.3.10 *Deoxynivalenol grain contamination*

Whole heads of EMS mutant lines as well as of the wild type control were harvested at the end of the growing season. Selected mutant lines grown in the field trial that had shown significant effects on FHB were assessed for DON content. Whole heads of the Paragon wild type contained an average of 29.69 ppm of DON (s.e. = 2.309; see Figure 2.20), the lowest content observed in this experiment. The highest DON content was that of the line 555A which contained an average of 47.74 ppm of DON (s.e. = 3.265). The six mutant lines 555A, 2487B, 1189A, 423AG, 2514A and 2171A contained significantly (p-value ≤ 0.01) higher quantities of DON compared to the WT control.

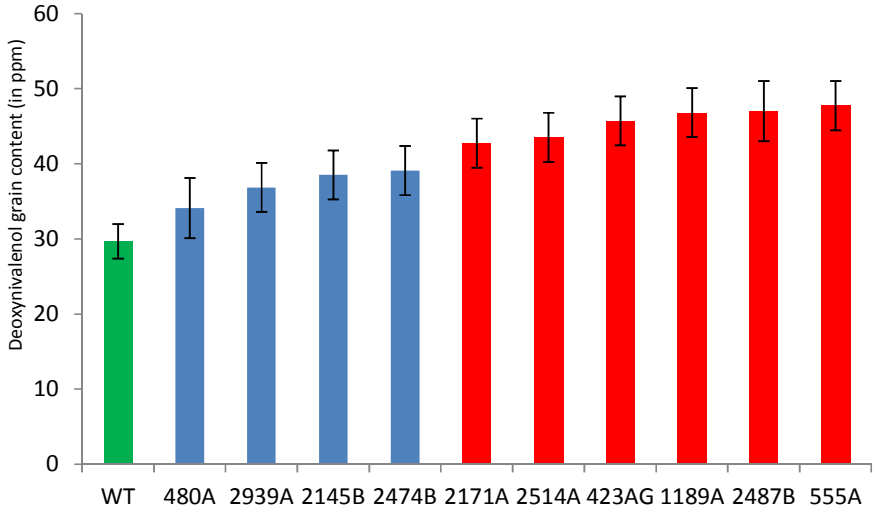

Figure 2.20: Predicted mean of Deoxynivalenol grain content at the end of the growing season in a selected subset of Paragon EMS mutant lines and wild-type control. Error bars show standard errors. Green bar indicates the average value for the Paragon wild type control heads. Red colour bars indicate mutant line for which mean value was significantly different from the control (p-value ≤ 0.01). Blue bars indicate mutant lines for which mean values did not significantly depart from the control.

2.3.11 *Assessment of resistance to Fusarium in the developmentally delayed mutant lines using a detached leaf assay*

A special interest was raised towards the developmentally delayed mutant lines 423AG and 2939A with regards to the high level of resistance observed during the FHB spray inoculation in both polytunnel and field experiments. Re-assessment of the resistance to *Fusarium* infection in these two lines was performed using the detached leaf test to examine the effect of the mutations in these lines on the resistance to *Fusarium* infection in a different tissue than the heads.

Detached leaves of the Paragon control produced an average 130,750 conidia per leaf (s.e. = 20,600; see Figure 2.21). The mutant line 2939A showed a significant (p-value ≤ 0.01) reduction in secondary spore production, with an average of 22,833 conidia per leaf (s.e. = 29,132) whereas the conidia produced on leaves of the line 423AG did not significantly differ from the WT control.

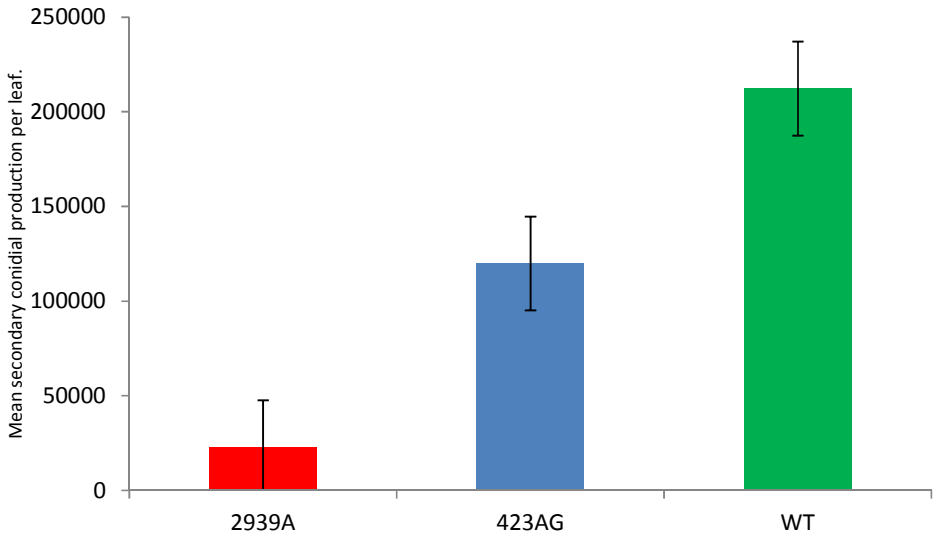

Figure 2.21: Secondary *Fusarium graminearum* (UK1) conidial production, 5 days following detached leaf infection on wound, of a subset of EMS Paragon mutant lines characterized by a developmental delay. Error bars show standard errors. Green bar indicates the average value for the Paragon wild type control seedlings. Red colour bars indicate mutant line for which average seedling length was significantly different from the control (p-value ≤ 0.01). Blue bars indicate mutant lines for which average values did not significantly depart from the control.

2.4 Discussion

Interpretation of the dataset presented in this chapter was complex as the experimental design aimed to investigate the relationship between alteration in two plant physiological mechanisms, senescence and sensitivity to the phytohormone ET, with alterations in the resistance to FHB in a spring wheat EMS mutant population. Each of these mechanisms are likely to be controlled by a myriad of genes, some of which remain to be identified, and are also understood to be influenced by multiple environmental factors. The scientific hypothesis aimed to test whether a delay in senescence and/or reduced sensitivity to ET correlates with an increased resistance to FHB, and conversely, whether accelerated senescence and/or increased sensitivity to ET can be correlated with an increased susceptibility to FHB. A summary of all performed experiments and results is presented in Appendix 1, Supplementary Table 1.

2.4.1 *Classification of EMS mutants as stay-green (SG) or fast-senescing (FS) lines*

Measurement of the chlorophyll content in leaves with a SPADmeter is highly correlated with nitrogen contents and is also indicative of photosynthetic efficiency (Percival *et al.*, 2008). The dark-induced senescence test, which is generally considered to mimic, at least partially, natural senescence, presents the advantage that its initiation is synchronized among all different genotypes (Niu *et al.*, 2012). However, plants grown in a field are subjected to a plethora of biotic and abiotic stresses, potentially greatly influencing senescence mechanism (Lim et al., 2007). Therefore, the classification of each mutant lines into WT-like, fast-senescing (FS) and slow-senescing (stay-green: SG) categories, was inferred from cross-analysis of the senescence characteristics measured in both laboratory and field conditions. However, it was observed that the DIS test was only able to detect characteristics indicating a delay in senescence, while measurements in the flag leaves of field grown plants primarily enabled the characterization of fast senescing lines. Nevertheless, measurements of the chlorophyll contents of flag leaves during the end of the growing season, 56 days following mid-anthesis, strongly supported the classification of these mutant lines delayed in senescence in the DIS tests. Results from the current study could be compared with those of Derkx and co-workers (2012), and this also supported the classification of mutant lines 555A and 2056A as stay green and 2514A as fast senescing mutants. Interestingly, six out of the nine mutant lines which displayed a significant

reduction in chlorophyll content measured in the field at post-anthesis also displayed a spontaneous apparition of chlorotic lesions (1385A, 1385B, 2514A, 2516A, 2686A and 3266B). This 'flecking' phenotype is understood to be a factor potentially interfering with measurements of the chlorophyll content, although its impact on the current dataset is not known. Overall, the dataset presented was able to characterise most mutant lines as displaying delayed, rather than accelerated, senescence. The reasons for this are unclear but perhaps the situation observed in the current dataset indicates that a high number of randomly distributed mutations along a given genome would impair the onset/development of senescence rather than accelerate this process.

2.4.2 *Mutant lines supporting a link between ET-sensitivity, senescence and resistance to FHB*

Paragon EMS lines 2686A, 2145B and 2056A were the only mutant candidates that displayed an alteration in senescence, ET-sensitivity and FHB resistance characteristics that might enable validation of the scientific hypothesis proposed. The mutant line 2686A displayed a significant increase in percentage chlorophyll lost in the field post-anthesis, an increase in ET-sensitivity and enhanced susceptibility to FHB in the polytunnel tests. The enhancement in FHB symptoms observed in line 2686A was correlated with the first visual score of the spray infection test, which would suggest an increase in type I susceptibility. Conversely, the mutant line 2145B displayed a significant reduction in percentage chlorophyll lost during the DIS test, a reduction in ET-sensitivity and enhanced resistance to FHB in the field although it did not differ from the wild type in either of the polytunnel experiments. The mutant line 2056A also supported the hypothesis as it was characterised by a significant reduction in percentage chlorophyll lost in the DIS test, a reduction in ET-sensitivity and enhanced resistance to FHB in the polytunnel tests. However, the line 2056A displayed a significant increase in percentage of chlorophyll lost post-anthesis in the field trial. Interestingly, however Derkx and co-workers (2012) studied the same EMS Paragon population and characterised the mutant line 2056A (re-named SG1 by authors) as stay green (SG) based on observation of increased chlorophyll content and retention of photosynthesis efficiency, both in controlled condition and in field experiments. This independent characterisation of line 2056A as delayed in the onset of senescence supports our results obtained in the DIS for this line and along with the other data provides material with which to further examine the relationship between FHB resistance, ET sensitivity and senescence.

2.4.3 *Mutant lines supporting a link between senescence and resistance to FHB, independently of ET-sensitivity*

Most Paragon EMS lines displaying significant results departing from the WT suggested an association between a delay in senescence and enhanced resistance to FHB, independently of an alteration in sensitivity to ET. Three mutant lines; 1189A, 2487B and 555A displayed a significant delay in senescence characteristics as well as resistance to FHB. Two of these lines, 1189A and 2487B, showed a significant resistance to FHB, in both the polytunnel and field conditions, and this was associated with a type I resistance for the line 1189A. Mutant lines 555A and 2487B both displayed a reduction in percentage chlorophyll lost in the DIS test but did not display results significantly departing from the WT in flag leaf senescence characteristics measured in the field. Line 555A was, however, independently characterized as a stay green line on the basis of chlorophyll retention and photosynthesis efficiency, by Derkx and co-workers (2012). Interestingly, the results displayed by line 1189A did not significantly depart from the WT in the DIS test, but displayed greenness retention in the field, late in the growing season. These lines may exemplify the diversity of mechanisms potentially affecting both the onset of senescence in a DIS test and in the flag leaf of plants grown in the field. The resistance to FHB displayed by the line 1189A in the field was supported by results from the polytunnel tests, suggesting a resistance to initial penetration of the fungus (type I). In contrast, resistance to FHB displayed by the lines 555A and 2487B could not be associated with either type I or type II resistance mechanism. The mutant line 2514A displayed, to a certain extent, results suggesting an association between accelerated senescence and susceptibility to Fusarium. This line had lower chlorophyll content, around and post mid-anthesis, in the field as well as enhanced susceptibility to Fusarium infection in the polytunnel tests, independently of an alteration in ET-sensitivity. However, no significant departure from the WT was observed in FHB resistance measured in the field, nor a significant result in percentage chlorophyll lost, although line 2514A was independently characterized as a fast senescing line on the basis of chlorophyll retention and photosynthesis efficiency, by Derkx and co-workers (2012). Surprisingly, DON contamination of grain was significantly greater in mutant lines 555A, 1189A and 2487B compared to the WT, but not in 2514A. This result is counter-intuitive since levels of DON contamination in the grain of FHB infected wheat plants generally correlate with the severity of floral symptoms expressed (Xu *et al.*, 2007). The reason for the contrast in FHB and DON levels is unknown. Notably, other phytohormones such as auxin, abscisic acid and cytokinin are known to influence the onset of senescence in plants (Lim *et al.*, 2007). Therefore, it would be important to further

characterize the FHB-resistant lines displaying a delay in senescence, independently of ET-signalling, for their respective sensitivity to these other phytohormones.

2.4.4 *Mutant lines displaying delayed development and supporting a link between senescence and resistance to FHB, independently of ET-sensitivity*

Both mutant lines 423AG and 2939A displayed a significant delay in senescence, confirmed in both the DIS test and in the field, based on greenness retention in the field compared to the WT, and a strong level of resistance to FHB. Noticeably, these two EMS mutant lines consistently displayed altered development, as observed by delayed flowering time, exemplified by the images taken in the field trial at mid-anthesis (see Figure 2.21:I-J). It is likely that the delay in senescence observed may be, at least partially, linked to the delay in development observed. Delay in flower emergence and, especially, anthesis timing are known to have a potentially great impact on the resistance to FHB in wheat (Xu *et al.*, 2007). However, spraying and disease scoring dates as well as AUDPC calculations all accounted for the developmental delay observed between lines 423AG and 2939A compared to the WT, as best as possible. Nevertheless, it was decided to further confirm the resistance to *Fusarium* in these two lines in a bioassay using a different tissue than the flowers. Results from the detached leaf assays (DLA) showed that the mutant line 2939A displayed a significant reduction in the production of Fg secondary conidia. In contrast, the enhanced resistance of line 423AG to FHB observed in the field was not observed in the polytunnel tests nor in the DLA. In addition, DON contamination in the grain of line 423AG was significantly higher than that of WT plants. Interestingly, the mutant line 423AG also displayed a significant increase in ET sensitivity. This line may exemplify the fact that both ET-dependent and ET-independent mechanisms may influence the onset of senescence in wheat. However, the strong resistance displayed by the line 2939A was shown to be independent of the sensitivity to ET but associated with a developmental delay. It would be extremely valuable to further characterize the line 2939A for its sensitivity to other phytohormones such as brassinosteroids (BR) and gibberellic acid (GA), which are known to be involved in the control of growth and developmental processes and have also been implicated in the modulation of immune responses (Belkhadir *et al.*, 2012, Saville *et al.*, 2012).

2.4.5 *Mutant lines supporting a link between ET-sensitivity and resistance to FHB, independently of senescence*

The mutant line 2375A was the only EMS line displaying a significant increase in resistance to FHB which was confirmed in both the polytunnel and field experiments. In contrast to most of the other mutant lines, resistance to FHB was associated with a reduced sensitivity to ET but not with an alteration in the senescence characteristics. This mutant line may exemplify that FHB resistance mechanisms, as well as mechanisms controlling senescence, may be influenced by both ET-dependent and ET-independent signals. However, further molecular characterization of the genetic mutations altering FHB resistance in the mutant line 2375A would be necessary to confirm the link between reduced ET-sensitivity and enhanced resistance to FHB. This would involve crossing to a WT parent and examining segregation of the different traits in the progeny to establish whether increased resistance was always associated with reduced sensitivity to ET.

2.4.6 *Impact of abnormal weather conditions during the 2010 and 2011 growing seasons*

Interpretation of the dataset was disturbed in some experiments by extreme environmental conditions that probably influenced both pathogen growth and host resistance mechanisms. Disease assessments in the polytunnel during the 2010 growing season suffered from atypically high temperatures, 3 degrees hotter than the average temperatures in Norfolk during the 30 previous years, which resulted in temperatures under the plastic polytunnel system reaching 40°C, which most certainly influenced plant development and host response to *Fusarium* infection. The impact of abnormally high temperatures is expected to have had a negative impact on the growth and virulence of *Fusarium* species, as temperatures above 40°C can considerably slow down the fungus growth. It was observed in other experiments performed in the same environment that the high temperatures compromised fungal development particularly as evidenced by the failure of fungus to spread from inoculated spikelets in point inoculation experiments (Dr P. Nicholson, personal communication). During the 2011 growing season, rainfall was about 20% of the average precipitations in Norfolk during the 30 previous years, and resulted in overall severe reduction in plant height, regardless of the genotype, due to semi-drought conditions. Also, during the field experiment, two out of the six rows per plot were variably affected by a problem at drilling leading to poor emergence of mutant lines in these rows. This resulted in the reduction of the number of mutant plants available for the disease test with data for mutant lines 2457A, 2457B, 2516A, 2521A, 3131A and 3266B being lost. Also, the overall reduction in mutant plant number available in the dataset

reduced the detection of significant differences in lines from the WT control due to large standard errors.

2.4.7 *Further analysis of FHB resistant lines*

Despite limitation factors due to unusual environmental conditions, EMS mutant lines 2375A and 2939A, displayed a significant and repeatable increase in resistance to FHB, either correlated with a delayed senescence or a reduced ET-sensitivity, but not both. Furthermore, the mutant line 2939A was the only FHB resistant mutant line included for the detection of DON contamination of the grain which did not display a significantly greater content than the WT. Therefore, these results do not enable to complete validation or refutation of the starting hypothesis. However, at least the two FHB resistant lines, 2375A and 2939A, should be further analyzed to identify the mutations responsible for an alteration in FHB resistance and to determine whether this trait segregates with those for reduced sensitivity to ET or altered senescence/development respectively. Comparison of the different gene transcripts expressed between mutants and the WT control should provide a genetic characterisation of the mutations altering FHB resistance, senescence or ET-sensitivity in these mutants. Such analysis could be performed via RNA sequencing, a technology that has become increasingly accessible as costs have been tremendously reduced over the past years. This method should enable researchers to identify the genomic locations of mutations conferring the observed phenotypes to the mutant, and correlate genetically the potential association between mechanisms of FHB resistance with ET-, senescence- or development-associated mechanisms.

2.4.8 *Limitations of the genetic approach in research on small-grain cereal diseases*

In conclusion, this chapter exemplifies the difficulties met by researchers when studying the genetic basis of plant-pathogen interactions applied to small-grain cereals. A classic methodology was employed to assess alteration of physiological traits (senescence and ET-sensitivity) and disease resistance, but exposure to extreme weather conditions has compromised some of the experiments. Also, the large plant stature and relatively long life cycle of cereals, compared to the genetic plant model *Arabidopsis thaliana*, renders any investigation time- and space-consuming, preventing the opportunity to use high-throughput assessment methods in controlled environment chambers. Polyploidy of the wheat genome impedes the use of chemically-induced and T-DNA mutagenesis

approaches because the presence of homoeologous genes can potentially mask mutant phenotypes. Limited information and access available to genomic sequences relating to most small-grain cereal species, with the exception of rice (*Oryza sativa*), which was the first monocotyledonous plant genome sequenced (IRGSP, 2005), slows down research dedicated to the study of the genetic mechanisms of cereal-pathogen interactions. Also, it has been proposed that the domestication of temperate cereal species by humans may have resulted in population bottlenecks and that perhaps only 10 to 20% of the genetic variation of the wild species remains in modern varieties (Langridge *et al.*, 2006). The resulting reduction in allelic diversity in modern germplasm is likely to participate to the limitations increasingly experienced by scientists and breeders to improve yield and other desirable traits of modern cereal varieties. Overall, it would seem extremely useful for scientists to employ a closely related plant model to allow for model-to-crop translation studies relevant for cereal crops. Such monocotyledonous plant model should have a small plant stature, rapid life cycle and, preferably, have a sequenced genome and genomic tools available. *Brachypodium distachyon* displays all these features and its potential to be used as a reference model will be discussed in the following chapter.

Chapter 3

Assessment of *Brachypodium distachyon* compatibility of interaction with major fungal pathogens of small-grain cereals

Data from this chapter has been included in the publication:

Peraldi A, Beccari G, Steed A, Nicholson P: *Brachypodium distachyon*: a new pathosystem to study Fusarium head blight and other *Fusarium* diseases of wheat. *BMC Plant Biology* 2011, 11:100.

3.1 Introduction

Several Fusarium species are globally important pathogens of wheat (*Triticum aestivum*). These fungi infect floral tissues as well as seedlings, stem bases and roots causing Fusarium head blight (FHB), seedling blight, crown rot and root rot, respectively (Bottalico, 1998; Desmond *et al.*, 2008). Of these, FHB is the one of greatest significance worldwide being one of the most destructive diseases of wheat, with economic and health impacts (Foroud and Eudes, 2009; Parry *et al.*, 1995). The predominant Fusarium species associated with FHB are *Fusarium graminearum* (Fg) (teleomorph: Gibberella zeae) and *Fusarium culmorum* (Fc) which are also the most economically relevant (Tóth *et al.*, 2005; Foroud and Eudes, 2009). FHB is of primary concern because Fg and Fc produce a number of secondary metabolites within infected grain that are toxic to human and animal consumers. The most prevalent Fusarium mycotoxins in wheat are trichothecenes such as deoxynivalenol (DON) and nivalenol (NIV) (Placinta *et al.*, 1999). Experiments using mutants of Fg unable to produce DON showed that this mycotoxin functions as a virulence factor in wheat, enhancing spread of the disease within heads but in contrast plays no discernable role in barley (Maier *et al.*, 2006). Studies on trichothecene toxicity indicate that DON inhibits protein synthesis by binding to the 60S ribosomal subunit, activating a cellular signalling pathway resulting in a form of programmed cell death (Pestka *et al.*, 2004; Rocha *et al.*, 2005). The phytotoxic effects of DON in wheat are chlorosis, necrosis and wilting, often leading to the bleaching of the whole head above the inoculation point (Lemmens *et al.*, 2005). The use of resistant wheat cultivars is considered to be the most effective strategy to prevent FHB epidemics and contamination of grain with trichothecenes (Buerstmayr *et al.*, 2009). FHB resistance in wheat has been broadly classified into two different types: resistance to initial penetration (type I) and resistance to pathogen spread within the head (type II) (Schroeder and Christensen, 1963). However,

other types of resistance have also been proposed; resistance to kernel infection (type III), tolerance against FHB and trichothecenes (type IV) (Mesterházy, 1995) and tolerance to trichothecene accumulation (type V) by two means: chemical modification of trichothecenes (type V-1) and inhibition of trichothecene synthesis (type V-2) (Boutigny *et al.*, 2008). Over a hundred quantitative trait loci (QTL) for FHB resistance in wheat have been reliably identified (Buerstmayr *et al.*, 2009), but to date, only four loci have been shown to exhibit Mendelian inheritance (Cuthbert *et al.*, 2006; Cuthbert *et al.*, 2007; Qi *et al.*, 2008; Xue *et al.*, 2010). *Fhb1*, derived from the resistant Chinese cultivar 'Sumai-3' is the only locus for which a molecular mechanism has been proposed. Wheat lines containing this QTL are able to convert DON into less phytotoxic DON-3-O-glucoside (type V-1) indicating that *Fhb1* is either encoding a DON-glucosyltransferase or a modulator of the expression or activity of such an enzyme (Lemmens *et al.*, 2005). Wheat is not readily amenable for undertaking genetic studies of complex traits because of its large allohexaploid genome (three ancestral genomes totalling about 17,000 Mbp) which greatly hinders the complete genetic characterization of FHB-resistance QTLs. Because of the inherent difficulties associated with wheat, a number of alternative hosts have been proposed as models with which to investigate host-pathogen interactions in FHB. Although its genome is not yet fully sequenced, barley (*Hordeum vulgare*) presents the advantage of having a diploid genome, whilst also being a monocotyledonous plant naturally infected by Fusarium spp. However, barley has an inherent FHB-type II resistance (Foroud and Eudes, 2009) which can be a hindrance for studying the mechanisms underlying FHB-resistance in wheat. Rice (*Oryza sativa*) was the first monocotyledonous plant to have its genome sequenced and is a natural host for Fusarium spp. However, certain characteristics of rice and its interaction with Fusarium fungi reduce its potential for modelling FHB of wheat: rice is a tropical plant adapted to an aquatic environment at an early stage of development and is predominantly infected by Fusarium spp. other than those that cause FHB of wheat (Amatulli *et al.*, 2010). Several researchers have used the best studied plant model available, Arabidopsis thaliana, because it is ideally suited to laboratory studies and there are extensive genetic and genomic resources available (Huala *et al.*, 2001). Floral and foliar bioassays have been reported for studies of the interaction between Fg and Fc with Arabidopsis (Urban *et al.*, 2002; Chen *et al.*, 2006). Such assays have demonstrated that NPR1 and EDS11 contribute to resistance of Arabidopsis against Fc (Cuzick *et al.*, 2008) and that over-expression of the GLK transcriptional activator confers resistance to Fg (Savitch *et al.*, 2007). However, to date, translation of findings on the genetic mechanisms involved in host resistance to *Fusarium* infection from Arabidopsis to cereal crops is

scarce. One example is Chen and co-workers (Chen *et al.*, 2009) who demonstrated that Fg exploits the ethylene (ET) signalling pathway to colonise Arabidopsis and showed that ET signalling also contributes to susceptibility of wheat to FHB. Despite the numerous advantages of using Arabidopsis as a model for FHB, it is not a natural host of Fusarium, and it displays different floral symptoms to those that occur on wheat (Urban *et al.*, 2002). Consequently, the identification of a model, genetically tractable, monocot system that is more closely related to wheat is highly desirable. *Brachypodium distachyon* (Bd) is a temperate monocotyledonous plant of the grass family which has been proposed as a new model species for comparative genomics in grasses (Draper *et al.*, 2001). The inbred line Bd21 has been recently sequenced to an 8 fold coverage (The Int. Brachy. Init., 2010). Several aspects of Bd make it a very attractive model for temperate small grain cereals, including wheat. Bd has one of the smallest genomes found in grasses (Huo *et al.*, 2009) comprising 5 chromosomes spanning over 272 Mbp in which about 25,000 protein-coding sequences are predicted (The Int. Brachy. Init., 2010). Bd diverged just prior to the clade of the 'core pooid' genera that contain the majority of the temperate cereals, including wheat, making it potentially useful for functional genomics (Draper *et al.*, 2001). There is extensive chromosomal synteny between Bd and other cereals with the strongest syntenic relationship being with wheat for which about 77% of Bd genes have strong Triticeae EST matches (Huo *et al.*, 2009). In addition, it is possible to obtain genetic/physical locations in the wheat genome directly using Bd markers as demonstrated in the fine mapping of the complex Ph1 locus region in wheat (Griffiths *et al.*, 2006). A further advantage of Bd is that it is a self-fertile, inbreeding annual with a rapid life cycle of around 8-10 weeks (Draper *et al.*, 2001) depending on the environmental growth conditions. In addition, this species is small in size (approximately 30 cm at maturity) and has undemanding growth requirements. Furthermore, resources are being developed to permit functional genetic studies to be undertaken in Bd. Several mutant collections exist including EMS and T-DNA insertional mutants (http://brachypodium.pw.usda.gov, BrachyTAG.org, Vain *et al.*, 2008), as well as a segregating population using Bd21 and Bd3-1 as parental lines [http://www.modelcrop.org].

The potential for Bd to form compatible interactions with other necrotrophic fungal pathogens of small-grain cereals will also be tested. The goal is to further assess the capacity of this host as a pathosystem model to study a wide range of cereal diseases and exploit all the advantages in terms of genetic and genomic resources available.

Take-all disease is an important root disease of wheat caused by the necrotrophic pathogen *Gaeumannomyces graminis* (Gg) var. *tritici*. The disease starts as a root rot and can cause stunting and nutrient deficiency symptoms in the aerial parts of the plant as it progresses upward towards the stem base (Cook, 2003). Disease symptoms appear as dark lesions on the roots (Guilleroux and Osbourn, 2004). *Ramularia collo-cygni* (Rcc) is the causal agent of Ramularia leaf spot disease of barley (Sachs *et al.*, 1998). Infection by Rcc induces necrotic spotting and premature leaf senescence, leading to loss of green leaf area in crops, and can result in substantial yield losses (Walters *et al.*, 2007). A characteristic feature of Rcc biology is the production of curved conidiophores, which resemble a swan's neck. It was demonstrated that pre-treatment of barley plants by growing under high light intensities prior to infection by *R. collo-cygni* maximizes the expression of leaf spot symptoms (Makepeace *et al.*, 2008). Eyespot disease is a stem base infection of wheat and other small-grain cereals caused by two species of fungi, *Oculimacula yallundae* (Oy) and *O. acuformis* (Oa) (Burt *et al.*, 2011). Symptoms are characterized by elliptical-shaped lesions forming on the leaf sheath and culms near the soil level, which dark centres (pupils) give rise to the name of the disease (Wei *et al.*, 2011). One of the most distinctive infection structures produced by the eyespot-causing fungi is the formation of multicellular aggregates on the host leaf sheath termed infection plaques. Branching and aggregation of hyphae provide the source of subsequent infection hyphae which penetrate the host cuticule and epidermal cell wall (Lucas *et al.*, 2000).

The current study aims to examine the potential of Bd as a model to study interactions with the main FHB-causing *Fusarium* species and test the compatibility of interaction with a range of other economically important fungal pathogens of small-grain cereals studied in the John Innes Centre. This work aims to establish a base for Bd as a model pathosystem for small-grain cereal diseases from which to undertake model to crop translational investigations.

3.2 Material and methods

3.2.1 *Maintenance and preparation of fungal inoculum*

Fusarium inoculum

DON-producing isolates of Fg (UK1 and S1) from the culture collection of the John Innes Centre were used throughout. A DON-producing constitutive GFP expressing isolate

(FcGFP1) of Fc (kindly provided by Dr F. Doohan, University College Dublin, Ireland) was used for confocal microscopy. Conidial inoculum was produced in mung bean (MB) liquid medium and prepared as described previously with shaking for 7 days at 25°C (Makandar *et al.*, 2006). To harvest conidia, the culture solution was filtered through sterilized muslin and centrifuged at 3000 g for 5 min. The pellet was washed once and re-suspended in sterile distilled water (SDW) at a concentration of 1×10^6 conidia ml^{-1} and stored at -20°C until use.

Eyespot inoculum

Inoculum of *Oculimacula yallundae* (Oy) and *O. acuformis* (Oa) species from the JIC culture collection were prepared on V8 agar (9 g of bactoagar, 50 ml of V8 vegetable juice in 450 ml of de-ionised water) in a 15°C growth cabinet for 21 days, according to the method described by Burt and co-workers (2011). For each species, a homogenized mixture of six different isolates was used for inoculations as described in Chapman *et al.*, 2008.

Ramularia inoculum

Ramularia inoculum was prepared according to the method described by Makepeace and coworkers (2008) except inoculum was grown in Potato dextrose broth (PDB) liquid culture prepared from a 5 mm agar plug of a 2-4 week old Rcc 094B culture on PDA. Liquid cultures were supplemented with 10 μg mL^{-1} streptomycin and incubated at 20°C for 13-14 days under constant agitation at 175 rpm (New Brunswick Scientific Co. Inc. Edison, New Jersey, USA) in the dark.

Take-all inoculum

Fungal colonies of Gg T5 isolate (JIC culture collection) were grown on PDA supplemented with 50 μM streptomycin and 50 μM carbenicillin and incubated at 20°C in the light (light intensity) for one to two weeks before use.

3.2.2 *Brachypodium lines and growth conditions*

Brachypodium distachyon inbred lines Bd21 and Bd3-1 (Vogel *et al.*, 2006) were used throughout. Bd seeds were germinated and incubated for 5 days in Petri dishes on damp filter paper in the dark at 5°C. Seed were then incubated in darkness at 15°C for 24 h before exposing to a 16 h/8 h light-dark cycle for 24 h at 20°C. Seeds were then planted in 8 × 8 × 10 cm pots filled with 50% peat and sand mixed with 50% John Innes number 2

loam compost, and placed in a climatically controlled chamber with a relative humidity (RH) of 70% at 22°C. Foliar tissue was obtained from plants grown under a 16 h/8 h light-dark cycle while plants were grown under a 20 h/4 h light-dark cycle to obtain floral tissues. For the Ramularia infection tests, 15 pots each containing one Bd21 and one Bd3-1 plant were grown at two different light intensity regimes; low light (150-200 μmol m^{-2} s^{-1}) and high light (400-450 μmol m^{-2} s^{-1}) for 2-3 weeks before spray inoculation. Two independent experiments were performed for the eyespot infection tests with one test carried out at 10°C and one at 15°C. A total of 30 pots each containing one Bd21 and one Bd3-1 plant were grown, for which six pots were left un-inoculated to serve as control and 12 pots were dedicated for each infection test with Oa and Oy.

3.2.3 *Brachypodium spray, point, coleoptile and root inoculations, incubation and symptom assessment*

Fusarium inoculation

Whole Bd21 plants were sprayed with FgUK1 conidial suspension (1×10^5 conidia ml^{-1}), amended with 0.05% Tween 20, using a handheld mister until run off. Sprayed plants were placed under a plastic cover and misted periodically with SDW to increase relative RH to about 90%, until 3 days post inoculation (dpi) when covers were removed and misting ceased. Disease symptoms were photographed using a Samsung NV7 digital camera. Floral point inoculations were performed by inserting a piece (2 × 8 mm) of filter paper (Sartorius; grade 292) between two adjacent florets. Conidial suspension (5 μl of 1×10^6 conidia ml^{-1}) of Fg UK1 was carefully applied to the filter paper. Following inoculation, plants were treated as for spray inoculation above. Floral symptom development was quantified by visual assessment and the number of infected florets was counted at 2, 4 and 8 dpi. Studies on infection of roots and coleoptiles were carried out on Bd seedlings germinated as described above and incubated for 5 days at 20°C under a 16 h/8 h lightdark cycle. Seedlings used for root infection were inoculated using a mycelium plug (5 mm dia) from the growing edge of a 14 day old colony grown on potato dextrose agar (PDA) at 20°C and with a PDA plug for the controls. Coleoptiles were inoculated by spraying 1 ml of conidial suspension (1×10^6 conidia ml^{-1}) per plate and with sterile water for the controls as an attempt to mimic crown rot infection of wheat. Bd21 and Bd3-1 flowers were harvested 21 days after spray inoculation with Fg S1 or Fc GFP1 conidial suspension (1×10^5 conidia ml^{-1}), frozen in liquid N_2 and ground to a fine powder. DON detection and

quantification was performed using an ELISA competitive immunoassay (AgraQuant®, Romer Labs Singapore Pte Ltd) according to the manufacturer's recommendation.

Take-all inoculation

Studies on infection of roots with Gg were carried out on Bd seedlings germinated as described above and grown on the surface of plates containing 0.8% agar-agar media inclined at about 60° angle for two days at 20°C under a 16 h/8 h light/dark cycle. Mycelium plugs of 5 mm in diameter taken from the growing edges of one to two week old colonies growing on PDA were deposited on the mid-part of each Bd root.

Ramularia inoculation

Three 200 mL cultures were combined in a blender to form a slurry containing smaller hyphal fragments. One drop (about 20 μL) of Tween 20 to 50 mL inoculum was added and plants sprayed evenly at a rate of 10 mL inoculum 50 plants^{-1} using an air brush sprayer (Clarke International, Epping, UK).

Eyespot inoculation

Plastic collars (3cm long and 0.5 mm internal diameter) were placed on the stem bases of one week old Bd21 and Bd3-1 plants. One week later, Oa and Oy fungal inoculum was mixed with a slurry of PDA, of which 2 mL was injected with a pipette into the collar. The architecture of Bd stem base differs from that of wheat and barley in that tillers only emerge from the base of the main stem at an early stage, but as the mesocotyl grows, tillering continues to occur overtime above successive nodes along the stem. Therefore, a simple visual disease scoring system was adapted from the method used in wheat (Scott and Hollins, 1974) to account for the architecture of Bd stem base. The incidence of the disease, was calculated as the number of symptomatic tillers divided by the total number of tillers. The severity of the disease was calculated as the number of symptomatic layers (leaf sheath and stem) divided by the number of infected tillers. A disease index was also calculated by multiplying the incidence score by the severity score.

3.2.4 *Inoculation, incubation and symptom assessment of detached leaves*

Leaves were removed from 21 days old plants, cut to 5 cm length and wounded in two positions 2 cm apart and on opposite sides of the mid-rib by gentle compression with a glass Pasteur pipette on the adaxial surface. Leaf sections were placed in 10 × 10 cm square plastic boxes containing 0.8% water agar and treated as reported previously for wheat and barley (Chen *et al.*, 2009). Each box contained eight leaf sections from different

plants. A droplet (10 µl) of conidial suspension (1 × 10^6 conidia ml-1), amended with 0.05% Tween 20, was deposited onto each wound site. In other experiments the conidial suspension was amended with DON (75 µM). Mock inoculation was performed similarly using SDW amended with 0.05% Tween 20 (10 µl). In separate experiments, unwounded leaves were similarly inoculated with Fg or treated by addition of DON (15, 75 and 150 µM amended with 0.01% Tween 20). The inner surface of the plate lid was misted with SDW to maintain 100% RH and plates were incubated at 22°C under a 16 h/8 h light-dark cycle. Disease symptoms were recorded every 24 h and lesion sizes were measured using IMAGE-J software (Abramoff *et al.*, 2004).

3.2.5 *Light microscopy*

Bd leaf sections and flowers were cleared in 70% ethanol at 70°C for one hour to remove chlorophyll. Samples were stained for 1 min in trypan blue or aniline blue (0.1%) in lactoglycerol (1:1:1, lactic acid: glycerol: H_2O) and rinsed in a 15 M solution of chloral hydrate. Samples were mounted in 40% glycerol, viewed with a Nikon Eclipse 800 microscope and photographed with a Pixera Pro ES 600 digital camera. Inoculated palea and lemma tissues were dissected, cleared of chlorophyll, stained with aniline blue and observed under a light microscope. Bd root samples infected with Gg and Bd leaf sheath infected with Oy were stored in lactoglycerol (1:1:1) for long term storage and, on the day of observation, were stained for 1 min in 0.1% aniline blue and mounted on microscope slides before observation under a Leica DM6000 light microscope.

3.2.6 *Confocal microscopy*

Horizontal cross sections (50 µm thickness) of roots (inoculated and non-inoculated) were dissected 24, 48, 72 and 96 h post inoculation (hpi) using a sectioning system (Vibratome 1000 plus) and placed between glass slides in SDW. Root sections were analysed under a confocal microscope (Leica DMR SP1) excited with a 488 nm Argon ion laser and detected at 505-555 nm. Autofluorescence of cell walls and chloroplasts was detected at 580-680 nm. Samples of take-all infected roots and eyespot infected leaf sheath were stained with Uvitex-2B (Polyscience Inc.). Root samples were kept in lactoglycerol (1:1:1, lactic acid: glycerol: H_2O) for long term storage. One day prior to microscope observation, samples were delicately transferred into small Petri dishes (Sterilin® Limited, 30mm diameter), containing sterile distilled water (SDW) and rinsed for 10 minutes on orbital

shaker three times. Samples were then incubated on an orbital shaker for 7 minutes in a 0.1 M Tris HCl solution amended with 0.01% Uvitex, with the pH adjusted to 5.8 (100 mL of 0.1 M Tric HCl pH 5.8 + 0.01 mg Uvitex). The Uvitex solution was discarded and samples were rinsed three times in SDW, for 10 min each on orbital shaker. SDW was then replaced by 25% glycerol for 20 minutes on orbital shaker and then stored in the dark in 40% glycerol overnight. On the day of microscope observation, samples were mounted on a microscope slide in 40% glycerol. Samples were observed using a Leica SP5 (II) confocal microscope. Samples were excited with a 405 nm laser diode and detected at 505-555 nm. Autofluorescence of cell walls was detected at 600-700 nm.

3.2.7 *Scanning electron microscopy*

Intact Bd leaf sections were mounted on an aluminium stub by using O.C.T. compound (BDH), plunged into liquid nitrogen slush, and then transferred onto the cryostage of an ALTO 2500 cryo-transfer system (Gatan) attached to a Zeiss Supra 55 VP FEG scanning electron microscope. Samples were then sputter-coated with platinum (90 s at 10 mA, -110°C), and imaged at 3 kV on the cryo-stage in the main chamber of the microscope at -130°C. An alternative fixation method was used to remove wax crystals from the surface of Bd leaves and allow observation of sub-cuticular structures. Leaf sections were fixed for approximately 4 hrs at 20°C in FAA (3.7% formaldehyde, 5% acetic acid, 50% ethanol) and subsequently dehydrated through an ethanol series. After critical point drying, tissues were coated with gold and examined in a Philips XL30 FEG microscope using an acceleration voltage of 3 kV.

3.2.8 *Statistical analysis*

The disease severity, conidial production, DON accumulation and lesion area data were analysed by generalised linear modelling (GLM) using the software package GENSTAT version 9.1 (Lawes Agricultural Trust, Rothamsted Experimental Station, UK). Individual treatments were compared with controls using the unpaired t-tests within the GLMs.

3.3 Results

3.3.1 *Floral infection*

FHB is the disease of greatest significance in wheat and, if Bd is to be useful as a model, it is imperative that it expresses symptoms similar to those of wheat. Spikes of Bd were spray inoculated to assess the susceptibility of Bd to Fg and Fc and to compare symptoms to those of FHB on wheat (Figure 3.1a,b). Optimum infection was achieved by placing plants into 8 h darkness immediately following inoculation (plants were inoculated at the start of the dark period). Similar to the situation for FHB of wheat, Bd spikes appeared to be most susceptible to infection by Fusarium spp at the period around mid-anthesis (Parry *et al.*, 1995; Xu *et al.*, 2008). Symptom development was markedly restricted when Bd spikes were inoculated either prior to or after mid-anthesis. Mycelial growth was detectable on the host surface from between 12 and 36 hpi and light brown, watersoaked lesions appeared proximally on the outer surface of the lemma, between 24 and 48 hpi (results not shown). From 48 h to 96 h, florets lost their green appearance and became bleached in a manner highly reminiscent of the bleaching symptoms exhibited by wheat heads with FHB (compare Figure 3.1a,b with Figure 3.1c,d). Following spray inoculation, whole spikelets became bleached and, between 96 and 144 hpi, necrotic symptoms spread down the rachis and into neighbouring spikelets above and below (Figure 3.1d). Disease continued to develop and between 7 and 14 days post inoculation (dpi), whole spikes became bleached and necrosis spread down into the peduncule (Figure 3.1e). If humidity was not maintained following inoculation, infection was reduced or even unsuccessful, leading to the total arrest of symptom development after 24 to 48 hours post inoculation (hpi), (results not shown). In contrast, maintaining high humidity for longer than 48 hpi resulted in the extensive growth of aerial mycelium which often covered the whole spike (Figure 3.1h). Although floral symptoms on Bd21 and Bd3-1 were similar following spray inoculation with either Fg or Fc (data not shown) disease generally developed more rapidly on Bd3-1 than on Bd21, particularly following inoculation with the Fg isolates. Point inoculation was carried out to determine whether, like wheat, Bd exhibits susceptibility to spread within the spikelet (type II susceptibility sensu; Schroeder and Christensen, 1963). Following point inoculation, bleaching of the floral tissues tended to spread from the inoculation site towards the upper end of the spikelet with less pronounced disease progression below the point of inoculation (Figure 3.1f: 2 dpi, 3.1g: 4 dpi). Contamination of wheat grain with DON is the most important aspect of FHB with respect to food safety. The ability of Fg to produce DON within Bd tissues was investigated following spray inoculation of Bd21

spikes with Fg. Very large amounts of DON were detected in infected spikes with concentrations up to 1815 mg/kg of fresh tissue when conditions were highly conducive to infection and fungal growth (Figure 3.1h). Detached Bd21 florets inoculated with Fg were studied 3dpi under a light microscope to investigate the early phase of infection in regards to pathogen penetration and early host response. Adaxial (lemma) and abaxial (palea) foliar tissues were dissected and observed individually. Extensive hyphal growth and branching was observed on the external surface of the lemma, anchoring and branching on voluminous macro-hairs (Figure 3.1i, arrows). Closer observation suggested that hyphae coiled around the base of macro-hairs (Figure 3.1j, arrow) and formed globose structures (Figure 3.1k, arrow) the presence of which was correlated with an amber-brown discolouration of the host tissue. At early stages of interaction, hyphae formed aggregated structures around the base of macro-hairs (BMH) with little or no discolouration of the host tissues (Figure 1m). However, at late stages of interaction, extensive hyphal growth around the BMH was correlated with intense discolouration and collapse of the host tissues (Figure 3.1n). Similar observations were made on the external surface of the palea where globose hyphal structures were associated with BMH and nearby cells of corrugated circular shape (Figure 3.1o,p) and strong amber-brown discolouration. Macro-hairs are absent from the internal surface of the palea. However, amber-brown discolouration and cell death was observed among these corrugated circular cells which we interpret to be developmentally arrested hair primordia (Figure 3.1l).

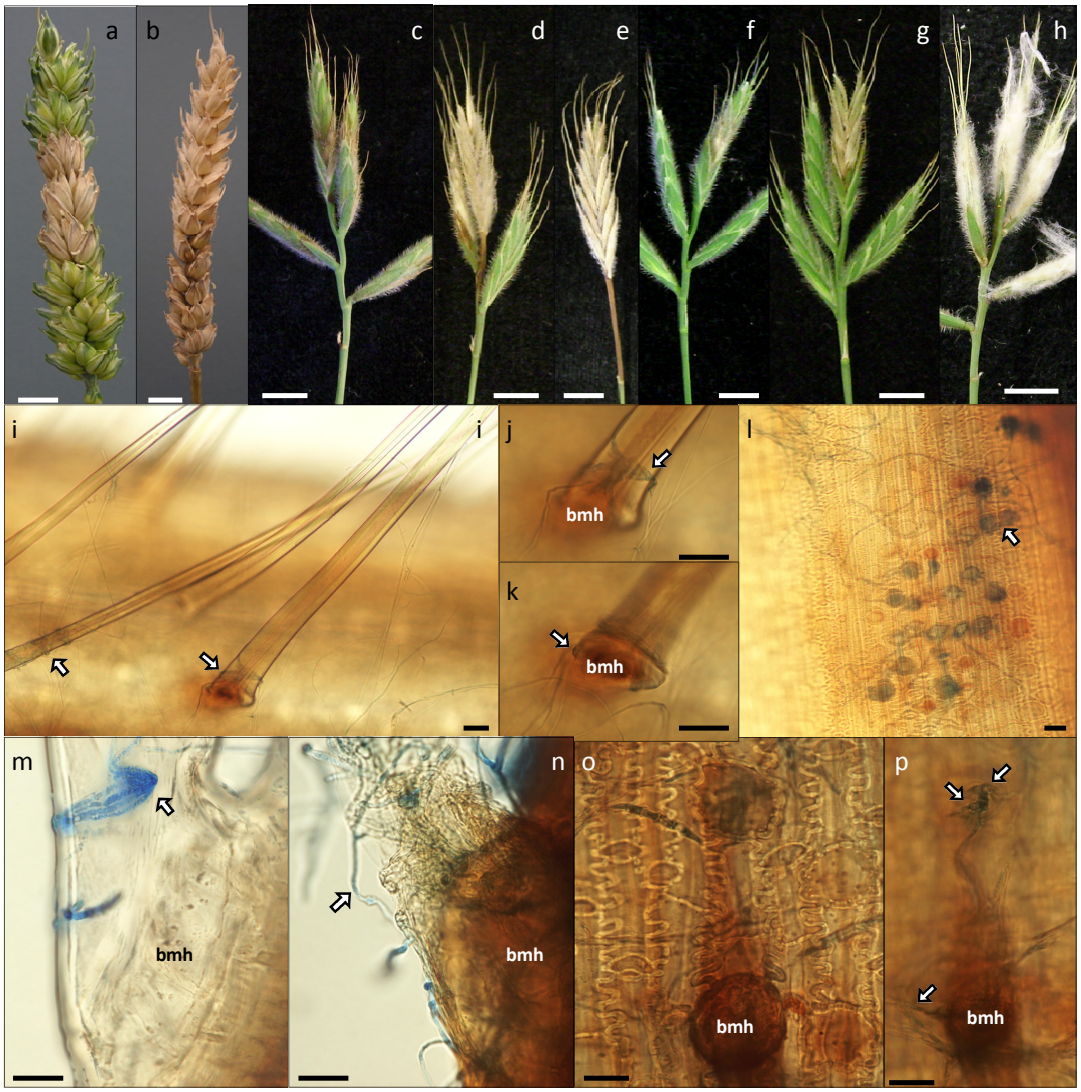

Figure 3.1: Fusarium head blight symptoms and penetration sites on Bd spikes. a) Typical early FHB symptoms on point inoculated wheat spike. b) Typical late FHB symptoms on point inoculated wheat spike displaying bleaching. c - e) FgUK1 spray inoculation symptoms: 3, 7 and 14 dpi, respectively. f & g) FgUK1 point inoculation, same spike 2 and 4 dpi, respectively. h) FgUK1 symptoms following spray inoculation with maintained high humidity. Scale bars a-h = 1 cm. i-p) Light microscope images of detached Bd21 florets, 3dpi with Fg, cleared and stained with aniline blue. i) External surface of lemma showing hyphal contact on macro-hairs (arrows). j & k) are close ups of picture i) taken at different focal planes. j) shows hyphal strands enveloping the macro-hair and k) shows a globose fungal structure formed at the base of the macro-hair (bmh). l) Internal surface of the palea showing hyphal colonization, necrosis and accumulation of phenolic compounds in corrugated circular cells (arrow). m & n) Macro-hair base of lemma at early stage of fungal colonization showing aggregated hyphal structure, n) Macro-hair base of lemma at late stage of fungal colonization showing extensive hyphal strands enveloping the base of the macro-hair, intense phenolic compound accumulation and collapse of the macro-hair. o-p) External surface of the palea showing the base of a macro-hair and neighbouring corrugated circular cell (arrow head) accumulating phenolic compounds (o) in response to hyphal contact (p), Upper arrow points at globose structure located above the corrugated circular cell and lower arrow pointing at hyphal strands in contact with the base of the macro-hair. Scale bars i-p = 20 µm.

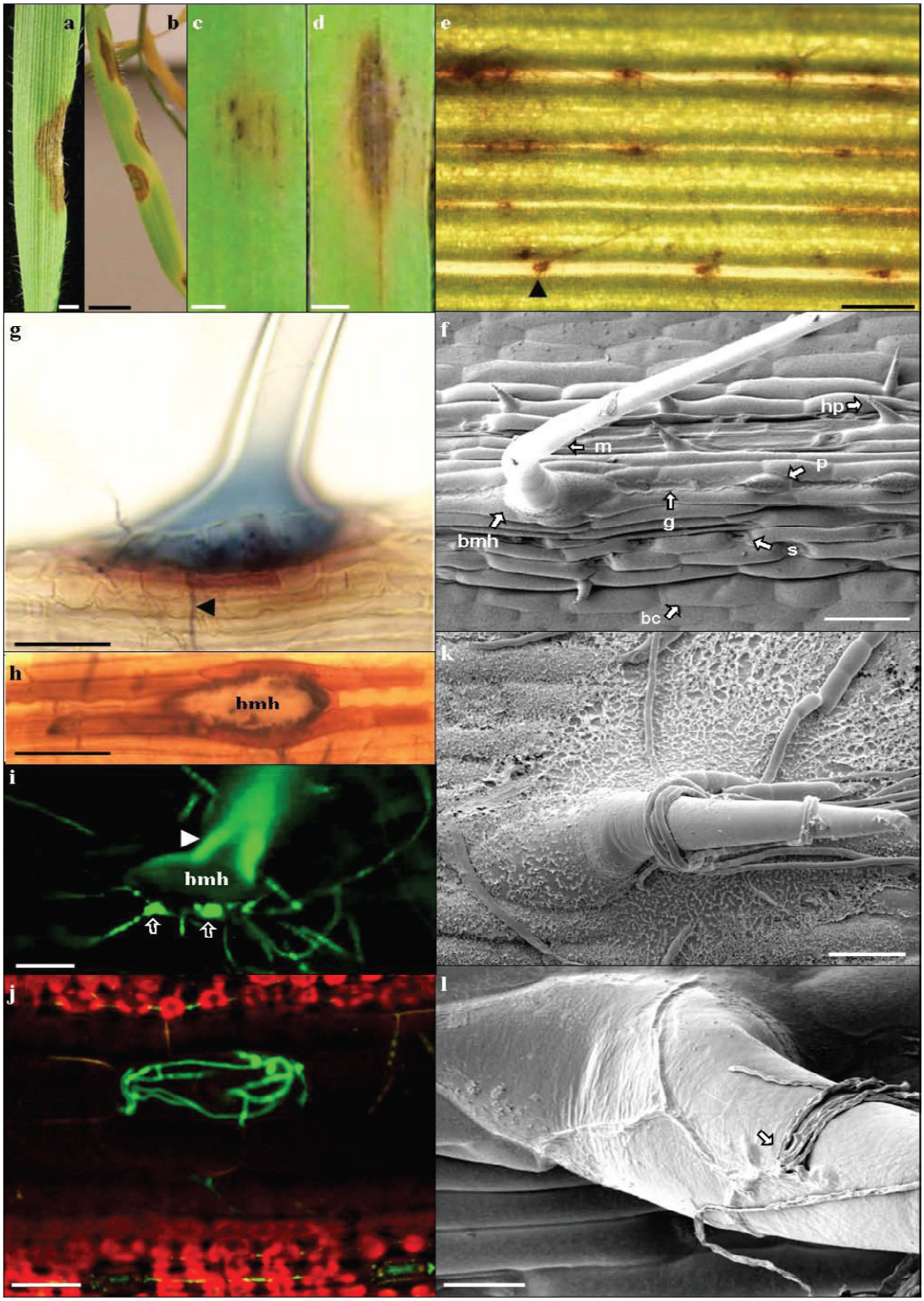

Figure 3.2: Fusarium symptoms and penetration sites on Bd21 foliar tissue. a & b) FgUK1symptoms on Bd21 leaves after whole plant spray. Scale bars: k = 0.5 cm, m = 1 cm: early and late symptoms, respectively. c-e) Fg symptoms on intact Bd21 detached leaf: c & e) 96hpi, and d) 144hpi. Scale bars: c & d = 0.25 cm, e = 250 µm. f) SEM image of Bd21 intact leaf surface showing Bd epidermis cell types (bc: bulliform cell, mh: macro-hair, bmh: base of macro-hair, g: girder, p: prickle cell, hp: hooked prickle, s: stomata). Scale bar = 50 µm. g and h) Light microscope images of chlorophyll cleared Bd21 leaves infected with Fg UK1, 120 hpi stained with trypan blue. Scale bars g & h = 50 µm. i) Fluorescent microscope image of Bd21 foliar macro-hair base 96hpi with GFP1-Fc.

Figure 3.2 continued: Arrow head shows macro hair endogenous fluorescence. Arrows show GFP1-Fc fluorescent hyphae forming globose structures at the bmh. Scale bar = 50 µm. j) Confocal laser scanning microscope (CLSM) image of GFP1-Fc infection on intact Bd21 detached leaf, 72 hpi, showing chlorophyll-less cells above the vascular bundles and GFP1-Fc hyphae in the cell directly beneath the bmh (bmh not in focal plane). Scale bar = 20 µm. k & l) SEM images of intact Bd21 leaf infection with FgS1, 48hpi. k) Fg hyphae enveloping a prickle cell. Scale bar = 20 µm. l) Fg hyphae aggregating near the bmh, penetrating (arrow) and growing underneath the cuticle. Scale bar = 10 µm.

3.3.2 *Foliar infection*

Spray inoculation of whole Bd21 plants was first performed to identify tissues compatible with Fusarium infection. Brown, water soaked necrotic lesions developed between 48 and 72hpi on leaves (Figure 3.2a) followed at later stages by a surrounding chlorotic area (Figure 3.2b). Detached leaf assays were also performed to study symptom development on both intact and wounded foliar tissues inoculated with Fg or Fc. Following wound inoculation, dark-brown, water-soaked necrotic lesions appeared initially at the wound site between 24 and 48 hpi and extended primarily along the vascular bundles towards both the leaf tip and base (see Annexe 2 Supplementary Figure 1). Following inoculation of intact Bd foliar tissues, very small necrotic spots appeared on the leaf beneath the inoculum droplet (Figure 3.2c,e) followed by the appearance of more widespread necrosis. Chlorotic areas subsequently developed around these lesions (Figure 3.2d). Symptoms developed in a similar manner to those on the wound-inoculated leaves although progression was generally retarded by approximately 48 hours. When studying infection processes it is important to consider the structure of the tissues. The foliar epidermis of Bd is characterised by distinct cell types organized in a succession of parallel ribs and furrows (Figure 3.2f). Ribs are voluminous structures which overlay the vascular bundles. They comprise different cell types organised along the longitudinal axis centred on successive wave-edged girder cells intercalated by prickle cells and voluminous macro-hairs (Figure 3.2f). On each side of this axis are between two and four rows of elongated cells between which lie stomata (towards the line of girder cells) and prickle cells (towards the furrow). Furrows are formed by bulliform cells. Following inoculation onto intact leaf surfaces, Fg conidia generally aggregated in furrows. Conidia germinated between 12 and 36 hpi and hyphae grew in all directions across the leaf surface from the inoculation site. Hyphae were observed to grow towards and over stomatal apertures (results not shown) but evidence for direct penetration was not obtained. Hyphae were frequently observed to coil around prickle cells (Figure 3.2k) and macro-hairs. Association with the base of macro-hairs was frequently observed (Figure 3.2g) and this correlated with the earliest visible host response: an amber-brown discolouration of the base of the macro-hair being particularly

prominent in the cells lying immediately alongside the macro-hair (Figure 3.2g,h). In many instances hyphal growth was extensive about macro-hairs and globose fungal structures developed at the base of hairs (Figure 3.2i) and hyphae were observed with CLSM within the cell directly beneath the base of a macro-hair (Figure 3.2j). SEM revealed that hyphae growing on the macro-hairs could penetrate the cuticle and continue to grow beneath the cuticle towards the base of the macro-hair (Figure 3.2l) at which point it appears that infection proceeds, possibly via the globose structures that formed at the base of hairs (Figure 3.2i).

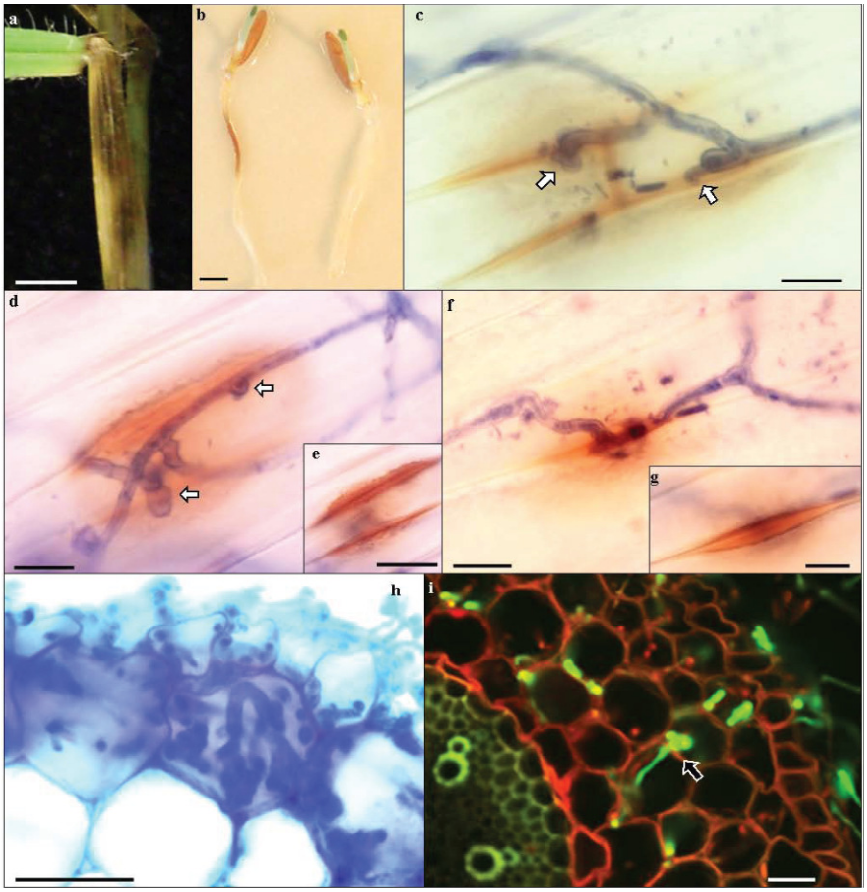

Figure 3.3: Analysis of Fusarium infection on Bd coleoptile and root. a) FgUK1 symptoms on leaf sheath. Scale bar = 1 cm. b) FgUK1 symptoms on Bd21 roots (left) and mock inoculation control (right), 48 hpi. Scale bar = 0.5 cm. c-g) Light microscope images of Fg UK1 infection on Bd21 coleoptiles, 6 dpi, stained with trypan blue. c) Fg hyphae penetration attempt via infection pegs (arrows) at the junction between adjacent cells showing associated deposition of phenolic compounds. d) Unsuccessful penetration attempt via infection pegs (arrows) at the junction between adjacent cells which, at lower focal plane (e), display intense deposition of phenolic compounds beneath the attempted infection point. f) Successful penetration attempt via infection pegs (arrows) at the junction between adjacent cells which, at lower focal plane (g) appear to be prised apart. Scale bars: c = 10 µm, d = 10 µm; e = 20 µm, f & g = 10 µm. h) Light microscope image of Fg UK1 at disease front of Bd21 root infection, 48 hpi stained with trypan blue. Scale bar = 20 µm. i) CLSM image of GFP-expressing Fc at infection site of Bd21 root, 48 hpi. Arrow shows hyphal translocation between two adjacent cortical cells. Scale bar = 10 µm.

3.3.3 *Infection on other Bd tissues*

Additional assays were used to investigate the ability of Fg and Fc to infect other tissues and assess the potential of Bd as a model for other cereal diseases caused by Fusarium species. Brown, water-soaked necrotic lesions developed between 48 and 72 hpi on virtually all aboveground plant parts including stems, stem nodes, leaf sheaths and leaves. Infected stems and stem nodes displayed only dark necrotic lesions even at late stages of the interaction (between 5 and 7 dpi) whereas necrotic areas on leaf sheaths became surrounded by chlorosis (Figure 3.3a). Symptoms developed rapidly on roots of Bd21 with amber-brown discolouration present at the site of contact with the inoculum by 24 hpi (Figure 3.3b). Discolouration of roots continued and, from 48 hpi onwards, lesions became dark brown. Root symptoms spread in both directions along the root from the infection site until the whole root was necrotic between 96 and 120 hpi. The outermost cell layer in the primary root of Bd is the rhizodermis, a single cell layer under which is located the cortex, made of multiple cell layers. Internal to the cortex and separated from it by the single cell layer endodermis is the stele within which lie the central metaxylem vessel and xylem vessels. Amber-brown discolouration of the roots was observed at the site of infection by 24 hpi, at which time intercellular and intracellular presence of the fungus could only be observed in the rhizodermis and the most external cortical cell layer (Figure 3.3h). By 48 hpi, hyphae were colonising, by both inter- and intracellular growth (Figure 3.3i), cortical cell layers and this was associated with the amber-brown colouration of cortical cells. Confocal microscopy confirmed that the fungus invaded most internal layers of cortical cells by 48 hpi (Figure 3.3i) but hyphae were excluded from the stele even after 96 hpi (results not shown). No symptoms developed on roots following spray inoculation with Fg conidia. However, mycelium grew externally to reach the coleoptile where attempted penetration was frequently observed at the junction between adjacent cells and appeared to proceed via infection pegs (Figure 3.3c,d). Attempted penetration was associated with localised production of an amber-brown deposit within contacted host cells at the site of contact/attempted penetration (Figure 3.3d,e). In most instances fungal ingress was effectively prevented while in some cases the cells appeared to be prised apart allowing growth of the hypha between them (Figure 3.3f,g).

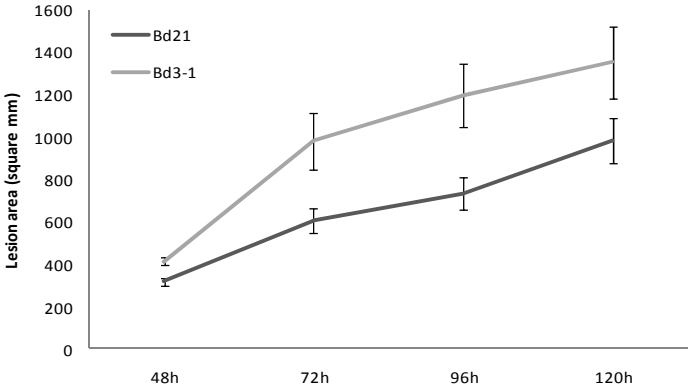

Figure 3.4: Comparison of Fusarium symptoms development on Bd21 and Bd3-1 leaves inoculated with Fg. Development of necrotic lesion area induced by Fg UK1 on wound-inoculated leaves of Bd21 and Bd3-1 at 48, 72, 96 and 120 hpi. Means ± s.e. were each calculated from measurements of twelve experimental replicates. The data shown is representative of six independent experiments.

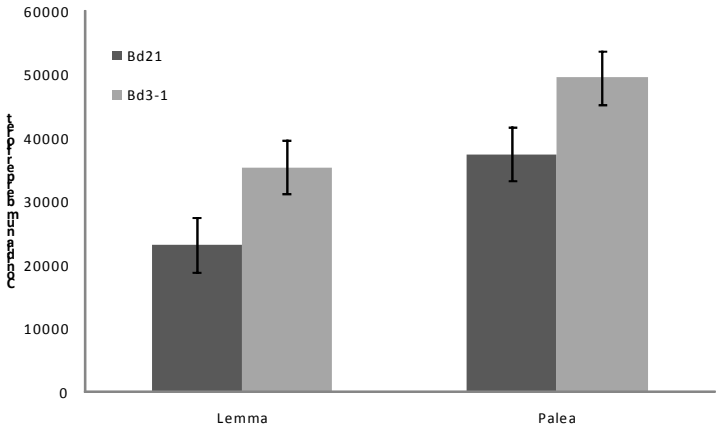

Figure 3.5: Comparison of Fg conidial production on lemma and palea of Bd21 and Bd3-1 detached spikelets. Conidial production following inoculation of Fg UK1 onto palea or lemma surface of Bd21 and Bd3-1 detached florets, 144 hpi. Means ± s.e. were each calculated from measurements of twenty experimental replicates. The data shown is representative of three independent experiments.

3.3.4 *Differential responses of Bd21 and Bd3-1 to Fg and DON*

Two Bd ecotypes, parents to a mapping population (modelcrop.org), were examined as a first step to determine the potential for natural variation for resistance to Fusarium within Bd. Leaves of lines Bd21 and Bd3-1 were compared for their response to wound-inoculation with Fg. Symptom development was significantly more rapid on Bd3-1 than on Bd21 ($P = 0.016$) (Figure 3.4). Most strikingly, lesions on Bd3-1 were surrounded by large areas of chlorosis whereas those on Bd21 retained their green colouration (Appendix 2 Supplementary Figure 1). Conidial production on Bd3-1 leaves was observed to be

significantly (P = 0.001) higher when compared to Bd21 leaves, 7dpi (Appendix 2 Supplementary Figure 2). Bd21 and Bd3-1 were also compared to assess whether they differed in type II resistance following single floret point inoculation with Fg. Disease progress as determined by AUDPC was significantly (P < 0.05) greater in Bd3-1 (31.92) than in Bd21 (20.16) (Annexe 2 Supplementary Figure 3), although there was no significant difference in conidial production at 13 dpi, when the experiment was terminated (data not shown). In complementary experiments, single florets of Bd21 and Bd3-1 were detached, placed on moist filter paper in Petri dishes and inoculated with conidial suspension onto either the palea or lemma surface in order to study infection of these tissues and to identify potential differences in susceptibility between the Bd lines and between the tissues. Conidial production on infected florets was significantly greater (P < 0.001) when conidia were inoculated onto the palea than onto the lemma, in both Bd21 and Bd3-1 ecotypes. In addition, conidial production on both palea and lemma was higher in Bd3-1 (49,556 and 35,400 conidia/floret, respectively) than in Bd21 (37,533 and 23,200 conidia/floret, respectively) (Figure 3.5). Lines Bd21 and Bd3-1 were also assessed for susceptibility to DON. Detached leaves were wound-inoculated with a range of DON concentrations (15, 75 and 150 μM). At the highest DON concentration, an amber-brown discolouration appeared around the wound site of both Bd 21 and Bd3-1 from 72 hpi. Lesions spread along the vascular bundles, becoming necrotic around 96 hpi. Lower DON concentrations did not result in the spread of necrotic lesions (data not shown). The size of the necrotic areas on Bd21 and Bd3-1 were not statistically different. However, chlorosis developed on Bd3-1 at all DON concentrations, whilst none was observed on Bd21 (Figure 3.6). DON has been demonstrated to be a virulence factor for FHB and crown rot infection of wheat by Fg. The influence of DON on Fusarium infection of Brachypodium was examined on wound-inoculated detached leaves to determine whether it enhanced virulence for Fg and Fc. Amendment of conidial inoculum with DON (75 μM) significantly increased (P < 0.001) average lesion area for both Fg and Fc (Figure 3.7a) and conidial production (Figure 3.7b) when compared with infections using the conidia alone. These results were strikingly similar to the effect of DON amendment on lesion development on wheat leaves (Annexe 2 Supplementary Figure 4). As shown above, symptom development on floral tissues was greater in Bd3-1 than in Bd21 and additional experiments were carried out to determine whether this was also reflected in differences in accumulation of DON. Spikes of Bd21 and Bd3-1 were spray inoculated with conidia of Fg and the DON content was assessed 21 dpi. No significant difference (P = 0.971) in

DON content was observed between Bd21 and Bd3-1 (620 mg/kg and 625 mg/kg of fresh tissue, respectively).

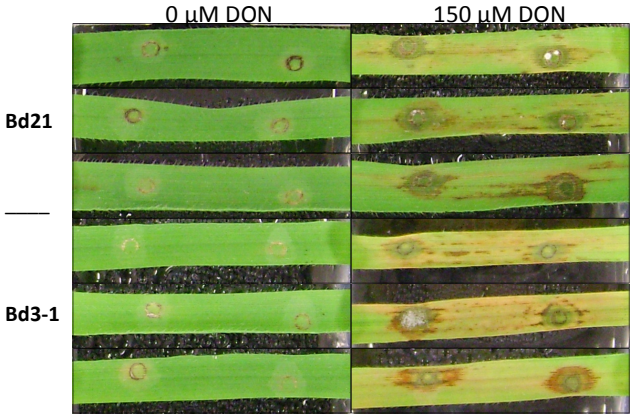

Figure 3.6: Comparison of DON-induced lesions of Bd21 and Bd3-1 detached leaves. Symptoms on leaves of Bd21 and Bd3-1, 120 hpi following wound-inoculation with water or DON (150 µM). Means ± s.e. were each calculated from measurements of eight experimental replicates. The data shown is representative of three independent experiments.

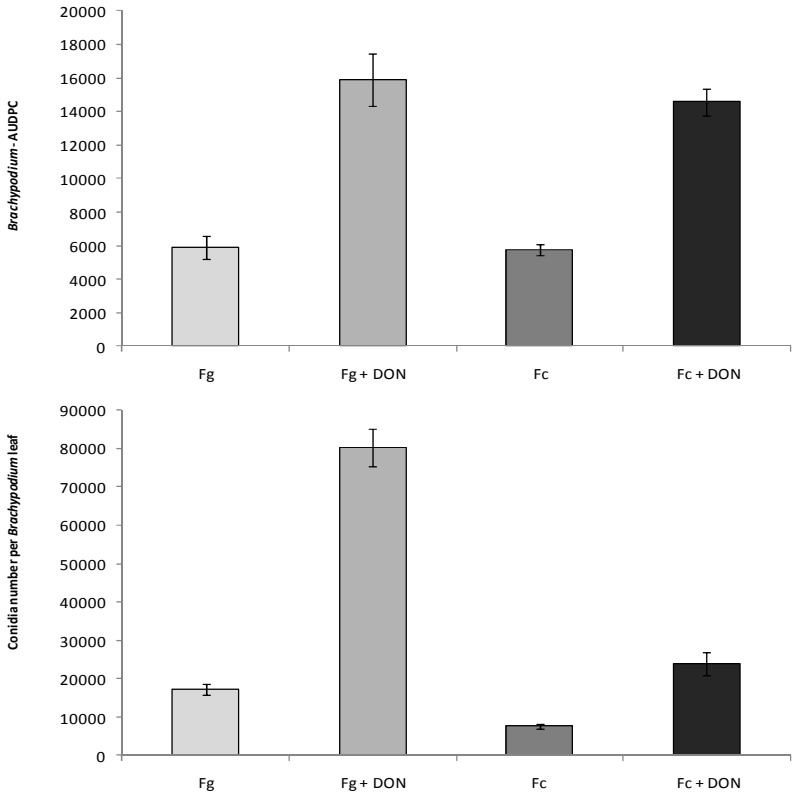

Figure 3.7: Effect of DON treatment on Bd21 detached leaves infected with Fg or Fc. a) Area under disease progress curve (AUDPC, 6dpi) for lesions following wound-inoculation of leaves of Bd21 with Fg UK1 or Fc GFP1 with or without amendment with DON (75 µM). b) Conidial production (6dpi) on leaves of Bd21 following wound-inoculation with Fg UK1 or Fc GFP1 with or without amendment with DON (75 µM). Means ± s.e. were each calculated from measurements of three experimental replicates. The data shown is representative of two independent experiments.

3.3.6 *Assessment of the compatibility of interaction between Bd and other fungal diseases of small-grain cereals*

Interaction between *Gaeumannomyces graminis* var. *tritici* and Bd

Root infection tests using mycelium plugs of the Gg T5 isolate were performed to assess the ability of the soil-borne pathogen to infect and colonise Bd tissues. Dark black, necrotic lesions generally appeared 3 days following inoculation of roots of one week old Bd21 seedlings (see Figure 3.8a) and necrosis later spread in both directions from the point of infection (see Figure 3.8b and c). At a later stage, disease symptoms were observed at the base of the coleoptiles (see Figure 3.8d). Also, seedlings infected for 9 to 10 days with Gg displayed signs of accelerated senescence in their first and second leaves (results not shown). Observation under a light microscope of Gg infected roots, stained with aniline blue, revealed the presence of macrohyphal structures, also named runner hyphae, on the external surface of the roots 5 days following inoculation (see Figure 3.8e). Closer examination of the runner hyphae revealed a close association with thinner hyphae growing towards the surface of the root epithelium. Swelling structures resembling hyphopodial infection pegs, characteristic of infections on wheat, were observed branching from these thin hyphae and contacting the epithelium (see Figure 3.8f). The presence of Gg hyphae within the host cortical cells was verified by observation under a confocal microscope of Bd21 root samples stained with a fluorescent dye specific to chitin (Uvitex), 5 days following infection (see Figure 3.8g-h). Also, cell-to-cell invasion by Gg hyphae was observed within the outer cortical cell layers of Bd21 roots (see Figure 3.8j), and was correlated, at this site of observation, with intercellular penetration from the outer surface of the root (see Figure 3.8i). Finally, comparison of symptom development on roots of the two Bd accessions revealed that lesion extension was significantly more rapid (p-value < 0.001) in Bd3-1 compared to Bd21, 7 days following infection with Gg mycelium plugs. Lesions in Bd3-1 extended an average of 9.1 cm while those in Bd21 extended 5.1 cm 7 days post inoculation.

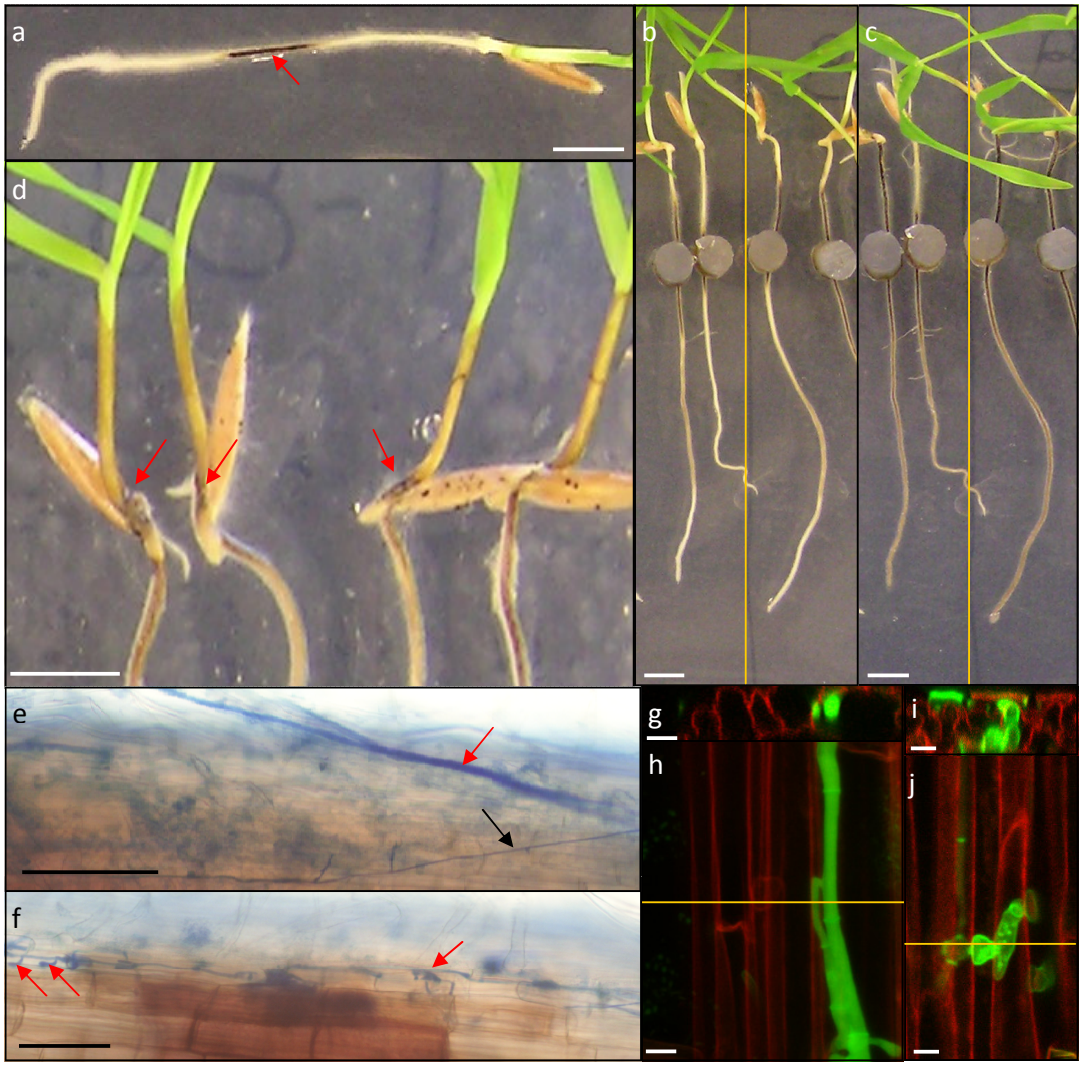

Figure 3.8: Take-all symptoms development on Bd seedlings following mycelium plug infection with Gg (T5 isolate). a) First visible lesion developed on Bd21 root, 3 days following infection. Red arrow indicates mycelium plug site. b) Comparison of Gg symptom development on the roots of Bd21 (left) and Bd3-1 (right), 6 days following mycelium plug infection with Gg T5 isolate. c) Comparison of Gg symptom development on the roots of Bd21 (left) and Bd3-1 (right), 10 days following mycelium plug infection with Gg T5 isolate. d) Symptoms expression on Bd3-1 coleoptiles, 9 days following Gg root infection using T5 isolate mycelium plugs. Arrows indicate blackening of the base of coleoptiles. a-d) Scale bar = 0.5 cm. b-c) Yellow line indicate separation between Bd21 and Bd3-1 seedlings. e) Bd21 roots stained with 0.1% aniline blue, 5 days following mycelium plug infection with Gg T5 isolate. Red arrow indicates runner hyphae. Black arrow indicates branching hyphae. Scale bar = 100 µm. f) Bd21 roots stained with 0.1% aniline blue, 5 days following mycelium pluf infection with Gg T5 isolate. Arrows indicate hyphopodia structures formed from infection hyphae. Scale bar = 50 µm. g-j) Confocal microscope images of Uvitex-stained Bd21 roots, 5 days following mycelium plug infection with Gg T5 isolate. h) Composite confocal image showing intracellular growth of Gg hyphae within Bd21 cortical cell. Yellow line indicates horizontal view showed in g). j) Composite confocal image showing Bd21 cortical cell invasion by Gg hyphae. Yellow line indicates horizontal view showed in i). Scale bars = 10 µm.

Bd21 and Bd3-1 plants were grown under two light intensity regimes prior to spray inoculation with Rcc to compare host response of the two accessions following the different pre-treatment conditions. The two light pre-treatments resulted in plants with strikingly different plant morphologies. Bd plants grown for three weeks under the low light regime (150-200 $\mu mol.m^{-2}.s^{-1}$) produced a lower number of long and soft leaves and only just begun to tiller at the time of inoculation compared to plants grown under high light regime regardless of the Bd accession (see Figure 3.9a). Bd plants grown under high light regime (400-450 $\mu mol.m^{-2}.s^{-1}$) produced a greater number of shorter and thicker leaves, and produced a greater number of tillers compared to the low light regime, regardless of the Bd accession (see Figure 3.9b). Leaves of Bd plants of both accessions developed brown necrotic spots surrounded by chlorotic areas 21 days following spray inoculation with Rcc (see Figure 3.9c-f). Although no attempt was made to quantify disease, clear differences in symptom development were observed between the two Bd accessions as well as between the two light intensity pre-treatments. Regardless of the light intensity regime, it was observed that Bd3-1 plants developed relatively larger necrotic lesions as well as larger surrounding chlorotic area compared to those observed on Bd21 plants (see Figure 3.9c and e compared to d and f). In addition, it was observed that both Bd21 and Bd3-1 plants developed larger and more numerous necrotic lesions when grown under the high light regime compared to when grown under the low light regime (see Figure 3.9c and d compared to e and f). Observation under a light microscope of the abaxial surface of aniline blue stained Bd3-1 leaves revealed amber-brown colouration of adjacent cells were centred around necrotic lesions, but that those brown lesions were not always obviously associated with the presence of Rcc hyphae (see Figure 3.9g). Areas of dense hyphal colonization were observed on both sides of the leaf blade and, on the abaxial surface, were associated with hyphal structures emerging from stomata (see Figure 3.9h). Most importantly, diagnostic swan's neck shaped conidiophores baring conidia were observed emerging from the interstitial space between adjacent epidermal cells on the abaxial surface of the leaf blade (see Figure 3.9i).

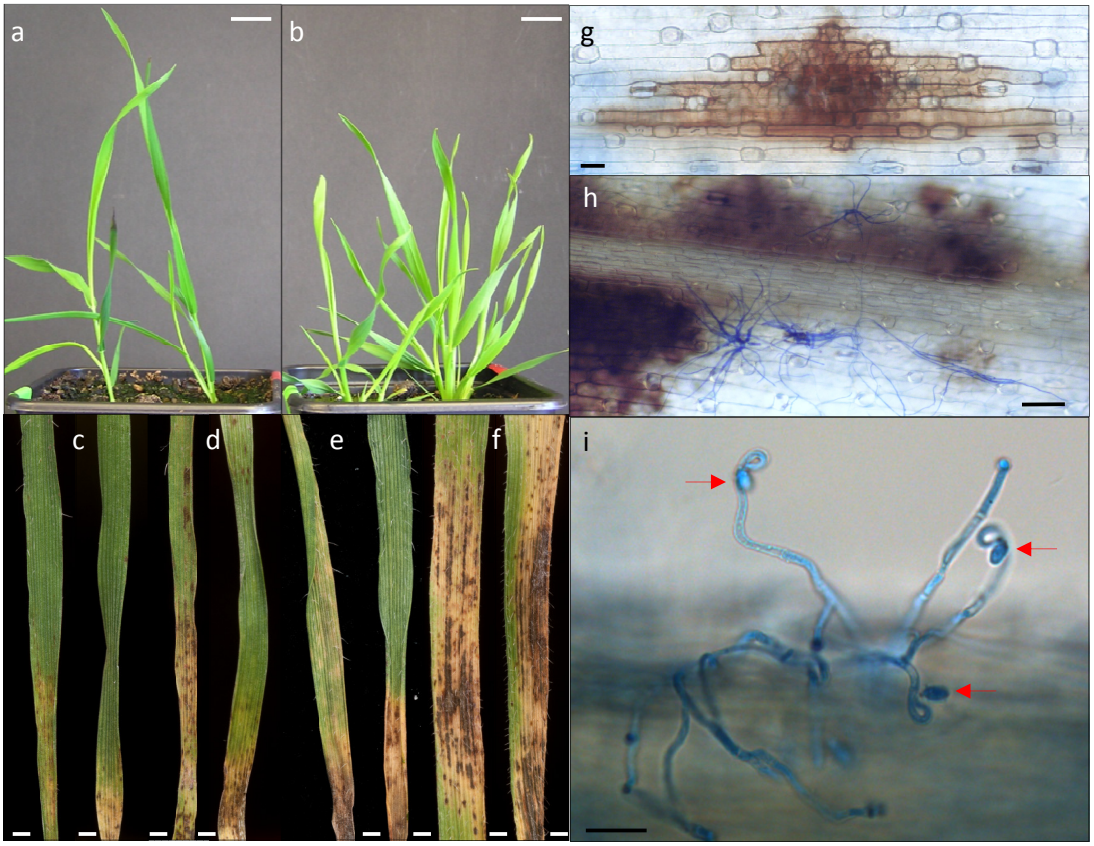

Figure 3.9: Analysis of Ramularia symptoms development following spray inoculation on low and high light-treated *Brachypodium* plants. a-b) Comparison of the effect of low light intensity (a) compared to high light intensity (b) pre-treatment onto the growth of Bd21 (left-hand side plant) and Bd3-1 (right-hand side plant) plants. Scale bars = 1 cm. c-f) Comparison of the Ramularia symptoms developed on the leaves of Bd21 (c) and Bd3-1 (d) plants exposed to low light pre-treatment and leaves of Bd21 (e) and Bd3-1 (f) plants exposed to high light pre-treatment, 21 days following spray inoculation with Rcc094B conidia. Scale bars = 0.1 cm. g) Light microscope image of a necrosis lesion developed on the abaxial side of a leaf of Bd3-1 plant exposed to high light pre-treatment, stained with 0.1% aniline blue, 21 days following spray infection with Rcc094B conidia. Scale bar = 20 µm. h) Hyphal structures extruding from a stomata on the abaxial side of a Bd3-1 leaf blade exposed to high light pre-treatment, stained with 0.1% aniline blue, 21 days following spray inoculation with Rcc094B conidia. Scale bars = 10 µm, i) Light microscope image of swan's neck shaped Ramularia conidiophores , produced on the abaxial side of a Bd3-1 leaf blade exposed to high light treatment, stained with 0.1% aniline blue, 21 days following spray inoculation with Rcc094B conidia. Arrows indicate Ramularia conidia. Scale bar = 20 µm.

Interaction between *Oculimacula* species (*O. yallundae, O. acuformis*) and Bd

Stem base infection of Bd21 and Bd3-1 accessions with Oa and Oy resulted in development of honey-brown to amber-brown lesions on the leaf sheath immediately above the lower nodes. Eye-shaped lesions were observed on the leaf sheath of Bd3-1 plants 28 days following infection with Oy (see Figure 3.10a). However, colouration and shape of the lesions observed varied greatly depending on the fungus-Bd accession

combination (see Figure 3.10b-g). Visual differences in the intensity of symptoms as well as in the incidence of infected leaf sheaths were observed. Leaf sheaths of Bd21 plants developed relatively fewer and less intensely coloured disease symptoms than those on Bd3-1 plants, regardless of the fungal species inoculated (see Figure 3.10c and f compared to d and g). Also, disease symptoms induced by Oa were generally relatively darker and affected a greater number of leaf sheaths than those induced by Oy, regardless of the Bd accession. Observation under a light microscope of Bd3-1 leaf sheath displaying eye-shaped lesions 28 days following Oy infection, revealed the presence of multicellular hyphal aggregates of on the host epidermal surface (see Figure 3.10h). Localized amber-brown colouration of single cells near these aggregates was observed, although discolouration was not always associated with the presence of these fungal structures (results not shown). A transverse view through these multicellular aggregates revealed a semi-ovoid shape, tightly attached to the host epidermal cells and appeared to be formed below the cuticle (see Figure 3.10i). Tissue samples of Bd3-1 leaf sheath were stained with Uvitex, 44 days following infection with Oy and observed under a confocal microscope. Multicellular aggregates were observed tightly anchored to the host epidermis from which adventitious hyphae grew outward (see Figure 3.10j). In some instances, adventitious hyphae were observed in close contact with open stomata apparently revealing fungal attempts to invade the stomatal cavities (see arrows in Figure 3.10j). Lateral reconstruction of the confocal images at this site revealed a chitin-associated signal projecting downward the multicellular aggregates, although intensity of the fluorescent signal was rapidly lost in the cell layers situated underneath (see Figure 3.10k). Also, other sites displaying multicellular aggregates revealed a loss of autofluorescence in the epidermal cell walls directly beneath the fungal structure when separating the two fluorescent channels (see Figure 3.10l compared to m). Finally, visual disease scoring of Oa and Oy stem base infection of Bd21 and Bd3-1 plants was undertaken. Results obtained were calculated from two independent experiments, as no significant difference in the three types of disease scores was observed between tests run at 10°C and 15°C. No significant difference (p-value = 0.084) was observed for the incidence score of eyespot symptoms when comparing Oa infected Bd21 (0.5066, s.e. = 0.05297) and Bd3-1 (0.6137, s.e. = 0.0521) plants or when comparing Oy infected Bd21 (0.4726, s.e. = 0.05479) and Bd3-1 (0.5797, s.e. = 0.0521) plants (see Figure 3.11). A significant difference (p-value = 0.004) was observed with the severity score of eyespot symptoms when comparing Oa infected Bd21 (1.132, s.e. = 0.1106) and Bd3-1 (1.517, s.e. = 0.1088) plants, as well as when comparing Oy infected Bd21 (0.949, s.e. = 0.1144) and Bd3-1 (1.333, s.e. = 0.1088) plants (see Figure

3.11). However, no significant difference (p-value = 0.114) was observed for the disease index when comparing Oa infected Bd21 (0.7558, s.e. = 0.1024) and Bd3-1 (0.9453, s.e. = 1.007) plants or when comparing Oy infected Bd21 (0.6022, s.e. = 0.106) and Bd3-1 (0.7917, s.e. = 0.1007) plants (see Figure 3.11).

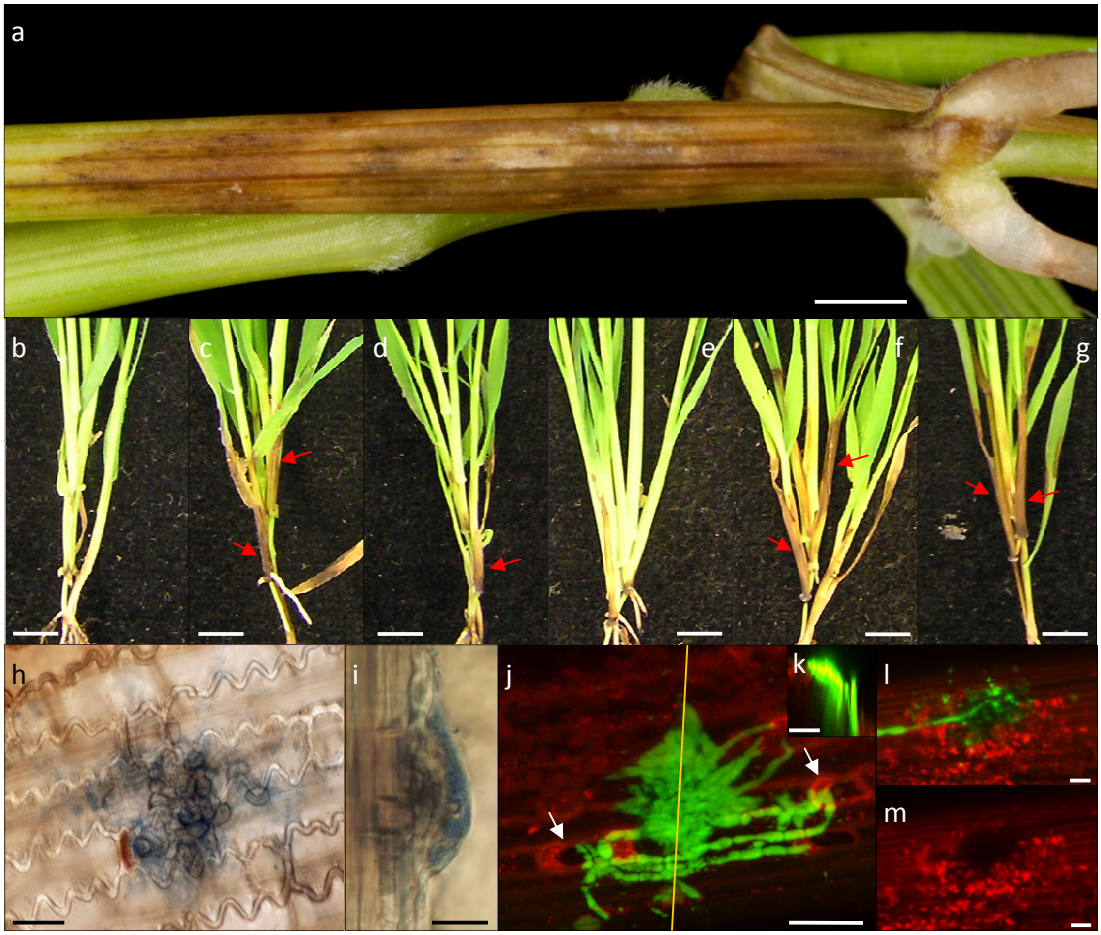

Figure 3.10: Eyespot disease symptoms expressed on Brachypodium Bd21 and Bd3-1 plants following stem base infection with Oy and Oa. a) Eye shape lesion formed on Bd3-1 stem base, 28 days following infection with Oy. Scale bar = 0.1 cm. b-d) Disease symptom expressed on Bd21 plants, 44 days following b) mock inoculation, c) Oa inoculation, d) Oy inoculation. e-g) Disease symptom expressed on Bd3-1 plants, 44 days following e) mock inoculation, f) Oa inoculation, g) Oy inoculation. b-g) Arrows indicate eyespot symptoms. Scale bars = 1 cm. h) Light microscope image of fungal multicellular aggregate formed on Bd3-1 leaf sheath epidermis, stained with 0.1% aniline blue, 28 days following Oy infection. i) Light microscope image of eyespot infection plaque formed on Bd3-1 leaf sheath epidermis, stained with 0.1% aniline blue, 28 days following Oy infection. h-i) Scale bar = 10 µm. j) Composite confocal microscope image of Uvitex-stained infection plaque formed on Bd3-1 leaf sheath epidermis, 44 days following Oy infection. Arrows indicate fungal attempt to invade stomatal cavity. k) Lateral view of j) showing hyphal projections underneath Oy infection plaque. l) Composite confocal microscope image of Uvitex-stained infection plaque connected to hyphae, formed on Bd3-1 leaf sheath epidermis, 44 days following Oy infection. m) Composite confocal microscope image of l) displaying red channel to show loss of autofluorescence of epidermal cells underneath infection plaque. j-m) Scale bars = 20 µm.

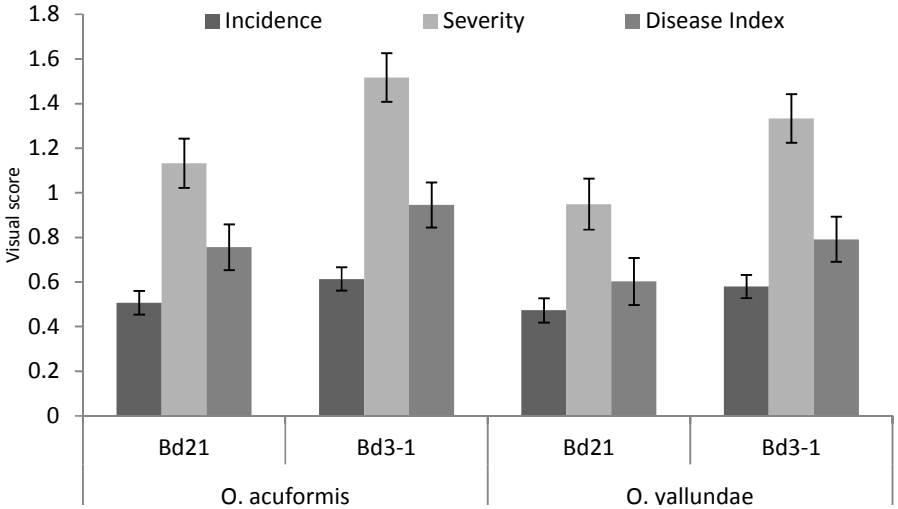

Figure 3.11: Comparison of the visual disease scores of Bd21 and Bd3-1 plants, 44 days following Oa and Oy infection.

3.4 Discussion

The present study aimed to determine the potential for Bd to act as a host to Fg and Fc and ascertain whether this interaction might serve as a model of that between Fusarium species and wheat. The results clearly demonstrated the compatibility of interaction between Bd and the two Fusarium species of greatest relevance to FHB, the major Fusarium-associated disease of wheat. Moreover, the development of disease symptoms closely resembled those reported in wheat. With respect to FHB, after a short asymptomatic period, Bd spikes spray inoculated with Fg conidia displayed small brown spots, which first appeared at the middle or base of the lemma, highly reminiscent of the initial symptoms in wheat (Parry *et al.*, 1995). Lesions spread to infect adjacent florets, often provoking the bleaching of the upper part of the spikelet in a manner similar to that observed in wheat (Weise, 1987; Lemmens *et al.*, 2005) and infection extended down the rachis to adjacent spikelets and even colonised peduncles as seen during infection of wheat. Overall, Fusarium infection of Bd spikes results in the development of symptoms that strikingly resemble those described in wheat heads infected with Fg and Fc (Parry *et al.*, 1995). Microscope analysis of floral tissues highlighted the potential role played by specific epidermal cell types during the early stages of infection. Fusarium hyphae were repeatedly observed entwined about voluminous macro-hairs that displayed a characteristic amber-brown discolouration. Globose fungal structures were repeatedly observed at the base of these hairs, suggesting that these cell types are favoured targets for penetration. Two components of resistance to FHB are widely recognised; resistance to initial infection (type I) and resistance to spread within the head (type II; Schroeder and Christensen, 1963). The palea and lemma tissues of

barley have been shown to express different levels of type I resistance with the former being more susceptible than the latter (Lewandowski *et al.*, 2006). Similar differential type I susceptibility of the palea and lemma tissues of Bd was observed in the present study along with differences in type I susceptibility of the two tested inbred lines. Type II resistance is assessed by point inoculation of individual florets in wheat heads (Parry *et al.*, 1995). Following point inoculation of Bd florets, both Fg and Fc successfully colonised Bd spikelet tissues and spread through the rachis into neighbouring spikelets and down the peduncle, closely resembling the pattern of colonization in heads of susceptible wheat cultivars (Parry *et al.*, 1995). The bleaching of spikelets above the inoculation site in wheat heads is another characteristic symptom of FHB (Lemmens *et al.*, 2005). Bleaching has been correlated with the production of DON by the fungus within infected wheat heads and is also induced following injection of DON into wheat heads (Lemmens *et al.*, 2005). Our observation of bleaching of infected spikes of Bd thus resembles the situation in FHB of wheat more closely than does barley, which has an inherent type II resistance restricting Fusarium symptoms to the area of initial infection (Foroud and Eudes, 2009). DON has been shown to function as a virulence factor in wheat, inhibiting the development of cell wall fortification within the rachis during FHB development (Jansen *et al.*, 2005) and aiding stem colonisation during development of crown rot (Mudge *et al.*, 2006). In contrast DON appears to play no discernable role in disease development in heads of barley (Jansen *et al.*, 2005; Maier *et al.*, 2006) or floral tissues of Arabidopsis (Cuzick *et al.*, 2008). Amendment of the conidial inoculum with DON significantly enhanced both disease symptoms and conidial production by Fg and Fc on wounded detached leaves of Bd. DON amendment similarly influenced symptom development and conidial production in detached wheat leaves following inoculation with Fg and Fc (Additional file 4). This strongly suggests that DON functions in Bd as it does in wheat, where it is understood to act as a virulence factor (Jansen *et al.*, 2005; Mudge *et al.*, 2006). The detection of high concentrations of DON in Bd21 and Bd3-1 flowers following inoculation with Fg indicates that these tissues support DON production in Fusarium species. The levels of DON in Bd spray inoculated spikes were similar to those reported previously following inoculation of wheat under controlled conditions (Savard *et al.*, 2000; Gosman *et al.*, 2005). The high levels of DON observed in floral tissues of Bd differs markedly from the situation with Arabidopsis where the reported levels are generally extremely low (Cuzick *et al.*, 2008; Urban *et al.*, 2002). Trichothecene production has been shown not to be uniformly induced during infection of wheat but, rather, is tissue specific with induction in developing kernels and the rachis node (Ilgen *et al.*, 2009). It is probable that the necessary components to

induce trichothecene production are present in Bd and wheat whereas they are absent in Arabidopsis, making Bd an attractive model for wheat. The current experiment could not provide information on kernel resistance as whole floral tissues were sampled because the high infection pressure resulted in extremely shrivelled seeds. However, reducing infection pressure and dissection of floral parts could provide insight onto resistance to kernel infection in future experiments.

Following spray inoculation of whole Bd plants, symptoms developed on virtually all above-ground plant parts (stems, leaf sheaths and leaves). Unexpectedly, intact leaves from spray inoculated plants also developed necrotic and chlorotic symptoms as did inoculated unwounded detached leaf sections. The presence of Fusarium within Bd tissues was confirmed by CLSM observation of GFP-expressing fungus. This is, to our knowledge, the first report to date of a successful infection on intact foliar tissue by a Fusarium species. Detached leaf assays have been used previously to identify components of resistance related to FHB but these experiments, although using unwounded inoculation, were carried out using *Microdochium majus*, a nontoxin producing FHB species (Browne *et al.*, 2006). We have determined that Fg and Fc can infect floral and foliar tissues of Bd allowing the mycotoxin-producing species to be used in comparative assays on these tissues. The susceptibility of intact Bd leaves therefore provides the first opportunity to establish the relationship between foliar and floral components of resistance to Fusarium species and identify those foliar components of relevance to FHB resistance. The unique susceptibility of Bd to foliar penetration by Fusarium spp. also provides the potential to undertake high throughput genetic screening of Bd mutant collections to identify lines altered in susceptibility to penetration. Having observed disease symptoms on all tested Bd tissues, histological examination was undertaken to determine how Fg and Fc gain entry into this host. Direct stomatal penetration of wheat head tissues by Fg and Fc has been previously reported (Beccari *et al.*, 2011; Pritsch *et al.*, 2000; Kang and Buchenhauer, 2000). Despite observing multiple instances of direct contacts between Fg and Fc germination hyphae and stomatal apertures, we did not obtain evidence for entry into Bd via stomata. Overall, our results suggest that, although penetration may occur through stomatal apertures, it is not likely to be the main mode of entry. In numerous instances, hyphal contact with stomata resulted in guard cells becoming very dark brown, indicating the possible deposition of phenolic compounds. Interestingly, phenolic compounds have been previously shown to play a role in FHB disease resistance in wheat (Boutigny *et al.*, 2009) and a similar situation may occur in the guard cells of Bd. Light microscopy images of the first visible symptoms developing on leaves revealed a characteristic amber-brown discolouration

(distinct from the colour of contacted guard cells), of the macro-hair base and directly adjacent cells that was correlated with the presence of the fungus and attempted penetration of the host. Although this amber-brown colour is also indicative of phenolic compounds, the results from coleoptile infection studies showed that its accumulation at the site of attempted fungal penetration is not effective in preventing infection. Similar appositions have been observed during infection of wheat by Fg and were more pronounced in resistant than in susceptible cultivars (Kang *et al.*, 2008). Recently, Wagasha and co-workers (2012) demonstrated for the first time that Fg and Fc are able to colonize foliar tissues of wheat seedlings and cause necrotic lesions. This report supports our findings from Bd that Fg and Fc can colonise foliar tissues and provides an instance where the new model informs on the situation in wheat.

During infection of Bd coleoptiles Fg appeared to produce infection pegs and gain entry via growth between cells. Again, this is similar to infection observed on wheat (Kang and Buchenhauer, 2000). SEM analysis of intact Bd leaf surface indicated that penetration of hair cells may be the preferred route of entry for the pathogen. We observed penetration of the cuticle, growth and branching at the base of the macro-hair. Macro-hairs are located above the vascular bundles, and targeting their base for initial penetration provides the pathogen almost direct access to the vascular bundles enabling rapid spread to adjacent tissues (Kang and Buchenhauer, 1999). This is an interesting finding in relation to previous studies made on detached wheat glumes where Fg was observed to penetrate and invade host tissue through short hair cells (termed prickle hairs; Rittenour and Harris, 2010). Association between Fg hyphae and prickle hairs (also referred to as papilla cells) on wheat was also noted by Pritch and colleagues (Pritsch *et al.*, 2000), although they did not undertake detailed investigation of the interaction. The comparison of microscope images of infected floral and foliar Bd tissues revealed striking similarities. Fusarium hyphae were observed to specifically target hairs in both tissues, where globose hyphal structures developed about BMH. Accumulation of phenolic compounds of unknown composition occurred in both floral and foliar tissues as a host response to penetration attempts. These similarities support the idea that investigating the mechanisms of Fusarium infection on foliar tissues may have direct relevance to the mechanisms of resistance of the floral tissues to FHB.

Root tissues were also successfully infected following inoculation by contact with mycelial plugs. The infection pressure generated by conidia, however, failed to induce infection and it remains to be determined whether infection can proceed directly from conidia or whether infection requires hyphae. Infection was indicated by discolouration and confirmed by

observation of inter and intracellular fungal hyphae in the cortex at an early stage of infection. Even at late stages of infection fungal hyphae were excluded from the stele, a situation similar to that recently reported in wheat (Beccari *et al.*, 2011). Together with observation of symptoms developing on the stem base, these results suggest that Bd can also be used for modelling crown rot and root rot. Differential responses among Bd accessions to biotic and abiotic stresses have been observed by others indicating that naturally occurring allelic variation in Bd accessions may provide insights into mechanisms underlying responses to agronomically important traits (Routledge *et al.*, 2004; Luo *et al.*, 2010). Inoculation of Fg conidia on detached Bd florets revealed quantitative differences in fungal development between Bd21 and Bd3-1 lines. Interestingly, the two lines also differed in susceptibility in the detached leaf assay with the most notable difference between them being the extensive chlorosis that developed in Bd3-1. Interestingly, DON application to wounded Bd21 and Bd3-1 leaves also resulted in a difference in response with respect to the development of chlorosis indicating that the differential response of the two lines to Fg is, at least in part, a result of differential susceptibility to DON.

Bd roots were successfully infected by Gg growing from mycelium plugs and the symptoms that developed on both Bd21 and Bd3-1 accessions were highly reminiscent of those described in wheat (Cook, 2003). Hence, black necrotic lesions developed underneath the infection site as early as 3 dpi, and spread in all directions, eventually reaching the coleoptile. Root infection of barley seedlings with Gg can result in accelerated senescence of the young leaves and is used as part of the disease scoring system for take-all (Mrs M Corbitt, personal communication). Microscope observation of large runner hyphae, from which thinner hyphae grew to form infection peg-like structures on the root epidermis, mirrors the situation in wheat. Finally, confirmation by confocal microscopy of fungal intracellular presence and cell-to-cell invasion are strongly suggesting the compatibility of interaction between Gg and Bd. The disease assay could be completed in a remarkably short period of time, providing the potential for a very rapid screening of host materials for expression of differential levels of resistance. However, due to the short time-scale of the interaction, sporulation could not be documented. This is a critical aspect of the pathogen's life cycle and more study is required to establish whether Bd is able to support completion of the entire life-cycle of Gg. This study revealed the first finding of potential differences in resistance to take all in Bd. Necrotic lesions formed more rapidly on Bd3-1 roots than on the roots of Bd21.

Inoculation of Bd with hyphal fragments of Rcc tests resulted in the development of foliar symptoms closely similar to those observed on the natural host, barley (Walters *et al.*, 2007). Plants grown under high light conditions displayed necrotic and chlorotic symptoms covering a larger leaf area, regardless of the Bd accession than plants grown under low light conditions. High light intensity as a pre-treatment prior to Rcc infection was also previously reported as a factor increasing disease symptoms in barley (Makepeace *et al.*, 2008). In addition, lesions on Bd3-1 leaves were observed to develop larger symptomatic areas than those on Bd21 leaves. No attempt was made to quantify symptoms and the development of a visual disease assessment scoring method is required in order to assess difference in symptom development between Bd accessions. The observation of hyphae emerging from stomatal cavities on the abaxial surface of the leaf epidermis is a specific feature of the biology of Ramularia disease (Dr James Fountaine, personal communication). Most importantly, characteristic swan's neck shaped conidiophores baring conidia were observed. This represents a result of critical importance in demonstrating that Rcc is fully compatible with Bd. Formation of such conidiophores is rarely observed even on barley under laboratory conditions (Prof. JKM Brown, personal communication). Rcc is generally described as a specific pathogen of spring and winter barley. However, Walters and colleagues (2007) mentioned reports of Ramularia infection observed on oats and barley (Huss, 2005). Therefore, observation of a compatible interaction between Rcc and Bd suggests that the pathogen may have evolved a wider range of compatible hosts than previously suspected.

Stem base infection of Bd21 and Bd3-1 plants with both eyespot-causing species resulted, in many instances, in the development of eye-shaped, honey-brown to darker brown lesions resembling those observed in wheat. Multicellular aggregation of hyphal structures resembled the infection plaques that form on wheat as described by Daniels and collegues (1991). Observation of these infection plaques under the confocal microscope suggested attempted penetration through stomatal cavities by adventitious hyphae. Also, hyphal projections growing through or between epidermal cells were observed underneath the infection plaques, although a rapid loss of the fluorescent signal in the lower cell layers was observed. The use of a different technique for chitin-specific fluorescent staining would be needed to confirm the successful penetration of the fungus into deeper layers of the leaf sheath.

Throughout the disease bioassays performed herein comparing the relative resistance of the two Bd accessions, Bd3-1 plants displayed consistently enhanced disease symptoms

compared to Bd21 in the detached leaf and detached floret tests with Fg, and in the root infection test with Gg. Visual differences were also observed in Ramularia infection test, with symptom development appearing greater in Bd3-1 compared to Bd21, regardless of the light intensity pre-treatment. Finally, visual scoring of the eyespot infection test revealed that Bd3-1 plants displayed more severe symptoms compared to Bd21 plants in response to both Oa and Oy infection. Taken together, these results suggest that Bd3-1 is relatively more susceptible than Bd21 to a range of necrotrophic pathogens. It remains to be determined whether these differences in resistance are due to a common mechanism. Interestingly, Cui and co-workers (2012) recently characterized a high level of resistance to the Barley Stripe Mosaic Virus (BSMV) in Bd3-1 plants compared to the susceptible Bd21 accession. Researchers investigated a recombinant inbred line (RIL) population from the cross between Bd3-1 and Bd21 to fine map the resistance gene to BSMV to a 23kb interval containing five putative genes.

The availability of the population derived from a cross between Bd21 and Bd3-1 (http://www.modelcrop.org), will permit genetic mapping of the differential susceptibility displayed by Bd21 and Bd3-1 lines to DON, infection with Fusarium and take-all. The, Ramularia and eyespot pathosystems could also be investigated, but both pathosystems require optimising to allow high throughput assessment of differences in disease resistance. The observation of differences in resistance to a range of necrotrophic pathogens between accessions of Bd provides encouragement to examine the available natural variation for lines differeing more markedly in resistance. Investigating the wide range of di-, tetra and hexaploid Bd accessions would be expected to reveal different levels and mechanisms of resistance to *Fusarium* and other necrotrophic pathogens of small-grain cereals. Bd was previously reported as a model for rice in order to study resistance to *Magnaporthe grisea* (Routledge *et al.*, 2004) and studies on Bd interaction with different types of cereal rusts have been undertaken (Mur *et al.*, 2011 and references therein).

The current study provides the first detailed report of Bd as a potential model for wheat diseases caused by the two main FHB-causing species of *Fusarium.* This study also documented potential compatibility of interaction with three other economically important necrotrophic pathogens of small-grain cereals and greatly expanded the scope of fungal pathogens which can be studied in Bd. Overall, the current work presents strong evidence to support the central role that can be played by Bd as a model pathosystem in future research on the genetic basis of cereal disease resistance.

Chapter 4

Exploiting T-DNA tagged genetic resources to identify new mechanisms conferring resistance to *Fusarium* infection

Data from this chapter has been included in the publication:

Thole V, Peraldi A, Worland B, Nicholson P, Doonan JH, Vain P: T-DNA mutagenesis in *Brachypodium distachyon*. *Journal of experimental botany* 2012, 63:567-576.

4.1 Introduction

Brachypodium distachyon was first suggested as a model system for functional genomics in grasses over a decade ago (Draper *et al.*, 2001). Since the publication of the entire genome sequence for the Bd21 accession in 2010 (IBI, 2010), other key resources have been developed: high efficiency transformation methods, large collections of natural accessions, and essential techniques like efficient crossing and chemical mutagenesis (Brkljacic *et al.*, 2011). Therefore, Bd has emerged as a valuable model system for temperate cereals and forage grasses, offering desirable physiological and genetic features with which to conduct functional genetic analysis relevant to small-grain cereals (Brkljacic *et al.*, 2011, Mur *et al.*, 2011).

4.1.1 *Brachy-TAG collection*

Several laboratories around the world have developed efficient transformation methods to develop Bd insertional mutant collections (Păcurar *et al.*, 2008, Vogel and Hill, 2008). However, the Brachy-TAG collection, developed at the John Innes Centre by Drs P. Vain and V. Thole, is the only T-DNA collection to report a successful transformation of the Bd21 accession (others using the Bd21-3 accession) using the Agrobacterium-mediated transformation system (Vain *et al.*, 2008). Researchers have used compact embryogenic calli derived from immature Bd21 embryos for efficient transformation (Thole *et al.*, 2009). The Agrobacterium strain AGL1, harbouring the pVec8-GFP binary vector (Murray *et al.*, 2004) was used to deliver a T-DNA containing the hygromycin resistance gene (HPT) and green fluorescent gene (GFP) into the Bd 21 genome. Importantly, the presence of the GFP gene alongside the HPT gene in each T-DNA insert enables researchers to quickly monitor the inheritance of the insertion within mutant line progenies using a conventional fluorescent microscope. A simple procedure was developed to enable retrieval and mapping of the regions flanking both right and left border of the T-DNA

inserts. The Brachy-TAG project currently lists 5000 T-DNA lines, mainly consisting of T-DNA insertion lines but also containing several hundred promoter trap lines (Thole *et al.*, 2012). Analysis of the first 741 fertile tagged lines has led to the first profiling of T-DNA insertions in the nuclear genome of Brachypodium (Thole *et al.*, 2010). The first Brachypodium T-DNA mutant characterization to be published was that of the RNA helicase elF4A gene tagged in the BdAA115 line from the BrachyTAG collection (Vain *et al.*, 2011). Also, detailed information on the mutant collection, protocols, vectors, T-DNA lines and predicted/putative function of the tagged genes are available (BrachyTAG.org). This collection is an extremely valuable genetic resource to exploit for functional genetic studies because the genome of the Bd21 accession has been sequenced and is publically available (IBI, 2010).

4.1.2 *Method for the selection of T-DNA mutant candidate lines*

T-DNA insertions in genes of interest can be searched in the Modelcrop genome browser (http://www.modelcrop.org/cgi-bin/gbrowse/brachyv1/) which provides gene links to the EnsemblPlants database (http://plants.ensembl.org/index.html) and Flanking Sequence Tags (FST) links to the BrachyTAG.org website (Thole *et al.*, 2012). Therefore, it is possible to search among the list of known or putative genes containing a T-DNA insert from the BrachyTAG website to select mutant candidate lines. In the current study, the predicted gene function of a given tagged T-DNA insertion line was deduced on the basis of sequence homology shared with molecular components involved in hormonal-signalling pathways previously characterized to influence disease resistance. To do so, orthologous gene predictions displayed by the EnsemblPlants website (http://plants.ensembl.org) were used as a basis to identify the putative gene function of a given Bd gene tagged in the BrachyTAG collection. Then, protein domain prediction using the Pfam application (http://pfam.sanger.ac.uk) was used to confirm the presence of protein motifs associated with the function of the gene of interest, based on the available literature. Finally, multiple sequence alignment (www.ebi.ac.uk/Tools/msa/clustalw2) analysis was carried out to compare the sequence homology of the Bd gene with all available predicted orthologous sequences from small-grain cereal species and/or Arabidopsis to confirm the relationships to candidate Bd gene. Using this method, a short list of six T-DNA mutant candidate lines containing a single FST were selected and analysed to investigate potential alteration of the resistance to Fusarium infection. These were:

4.1.3 *Brassionosteroid Insensitive 1* (*BRI1*)

Brassinosteroids are plant steroid hormones regulating a wide range of developmental and physiological processes, such as cell elongation, vascular differentiation, root growth, responses to light, resistance to stresses, and senescence (Kim and Wang, 2010). The first mutant allele of a receptor to brassinosteroids, brassinosteroid insensitive 1 (*BRI1*) was identified in Arabidopsis (Clouse *et al.*, 1996). The *bri1* mutant displayed multiple developmental deficiencies such as severely dwarfed stature, dark green and thickened leaves, male sterility, reduced apical dominance, and de-etiolation of dark-grown seedlings. Subsequently, monocot homologues to BRI1 were characterized in rice (d61 antisense transgenic line; Yamamuro *et al.*, 2000) and barley ('uzu' semi-dwarf variety; Chono *et al.*, 2003). BRI1 is a leucine-rich repeat (LRR) receptor protein kinase (RPK) belonging to the family of serine/threonine kinases. This family of plant receptors is characterized by a single transmembrane domain, separating an extracellular N-terminal domain bearing multiple LRRs where the binding site is located, and an intracellular C-terminal domain bearing a phosphorylation domain responsible for transducing the relevant signal. Emerging evidence suggests that BRs are involved in the regulation of plant defence responses (Bari and Jones, 2009). It was shown by Nakashita and co-workers (2003) that epi-brassinosteroid (eBL) treatments enhanced resistance to tobacco mosaic virus, *Pseudomonas syringae* pv. *tabaci* and *Oidium* sp. in tobacco and also induced resistance to *Magnaporthe grisea* and *Xanthomonas oryzae* pv. *oryzae* in rice. However, no evidence suggests to date that BR-signalling plays a role in the resistance to Fusarium.

4.1.4 *Auxin response factor* (*ARF) 2*

Auxin plays a central role in vegetative, reproductive and root development in Arabidopsis (McSteen, 2010). Modern genetic and molecular techniques have enabled the discovery of key proteins involved in the biosynthesis, transport, perception and transduction of the auxin signal in plants, which is now well characterized in Arabidopsis (Teale *et al.*, 2006, Finet *et al.*, 2012). The auxin response factor (ARF) gene family, together with the Auxin/Indole-3-acetic (Aux/IAA) acid proteins, encode proteins that regulate auxin-mediated transcriptional activation/repression (Okushima *et al.*, 2005). The ARF gene family contains 23 members in *Arabidopsis thaliana* and 25 members have been described in rice (Okushima *et al.*, 2005, Wang *et al.*, 2007). ARFs are transcription factors containing an amino-terminal B3-like DNA-binding domain, which binds to auxin-responsive elements (ARE; TGTCTC) found in the promoter of auxin-responsive genes

(Teale *et al.*, 2006). The carboxy-terminal domain is similar to the carboxy-terminal region found in Aux/IAA proteins and is understood to promote direct interaction between both group of proteins (Ulmasov *et al.*, 1997). Aux/IAA proteins are early auxin-responsive genes which bind ARF proteins to prevent activation of auxin-responsive gene expression (Teale *et al.*, 2006). Upon activation of the auxin signal through perception of the hormone by the auxin receptor TIR1, Aux/IAA proteins are degraded by the proteasome (Dharmasiri *et al.*, 2005, Kepinski and Leyser, 2005). The ARF2 protein has been shown to be a major player in the auxin-mediated control of leaf longevity in Arabidopsis (Lim *et al.*, 2010). It was demonstrated that mutation of *AtARF2* induced a significant delay in leaf senescence as measured by chlorophyll content, photochemical efficiency of photosystem II, membrane ion leakage, and expression of senescence-associated genes. Interestingly, numerous examples have been reported where mutations in genes associated with auxin-signalling influenced disease resistance (Kazan and Manners, 2009). Also, several aspects of the auxin-signalling pathway are involved in crosstalk with SA and JA-signalling pathways, leading to either increased resistance or susceptibility to different pathogens. It has been proposed that the developmental defects exhibited by most of the auxin-signalling mutants, such as defects in lateral root, root hair and vascular tissue development, could restrict pathogen access into the roots or its movements within the host (Kazan and Manners, 2009). However, the molecular mechanisms by which auxin influences plant defence is not currently understood.

4.1.5 *Lipoxygenase and JA-biosynthesis related gene*

Jasmonic acid (JA) and its derivatives (i.e. methylesterJA –MeJA–, JA-isoleucine conjugate –JA-Ile–) are potent regulators of genes involved in cell growth and biotic and abiotic stress responses (Kazan and Manners, 2008). In the past decade, both forward and reverse genetic approaches, particularly in Arabidopsis, have greatly expanded our understanding of the biosynthesis, perception and signalling pathway, as well as the potential roles of JAs in plants (Wasternack, 2007, Kazan and Manners, 2008, Fonseca *et al.*, 2009). Lipoxygenases (LOXs) are enzymes catalysing the oxygenation of polyunsaturated fatty acids, mainly α-linolenic acid and linoleic acid, which is recognized as the first step in the biosynthesis of a large group of biologically active metabolites named oxylipins, among which is JA (Bannenberg *et al.*, 2009). In plants, the N-terminal domain of LOX proteins can contain the PLAT (Polycystin-1, Lipoxygenase, Alpha Toxin) protein domain (Batman and Sandford, 1999).

Although JAs are involved in diverse physiological processes such as seed germination, root growth, leaf senescence and stomatal opening, they play crucial roles in plant defence responses against pathogens (Bari and Jones, 2009). Together with the phytohormone ethylene (ET), JAs are generally understood to be involved in defence mechanisms effective against necrotrophic pathogens and herbivorous insects (Glazebrook, 2005, Bari and Jones, 2009). Numerous studies have shown that concentrations of JAs increase locally in response to pathogen infection or tissue membrane damage and that exogenous application of JA induced the expression of defence related genes (Lorenzo and Solano 2005, Wasternack 2007). The JA/ET defence pathways mainly function in a mutually antagonistic fashion with the salicylic acid (SA) pathway, which is classically understood to trigger resistance against biotrophic and hemi-biotrophic pathogens (Glazebrook, 2005). However, evidence for synergistic interactions between SA and JA/ET pathways have also been reported (Bari and Jones, 2009 and references therein).

The phytohormones SA and JA have been shown to play a critical role in the resistance to Fusarium infection in both Arabidopsis and wheat (Makandar *et al.*, 2006, Makandar *et al.*, 2010, Makandar *et al.*, 2012). Initially, Makandar and co-workers showed that expressing the Arabidopsis Non-expressor of Pathogenesis-related Protein (NPR) 1 gene, which regulates the activation of systemic acquired resistance, in a susceptible wheat background, confers a type II resistance to FHB disease caused by Fg (Makandar *et al.*, 2006). However, other work suggested that JA was involved in the induction of resistance to FHB in wheat, as point application of MeJA into the spikelets of an FHB-susceptible wheat variety increased resistance against FHB (Li and Yen, 2008). Desmond and co-workers (2006) also showed that application of MeJA was able to delay symptom development by the crown rot pathogen *Fusarium pseudograminearum* in wheat, thereby implicating JA signalling in resistance to crown rot. Makandar and co-workers (2010) later demonstrated that JA might play contrasting roles in the resistance to Fusarium. These authors reported that mutation of some of the core signalling components of the JA pathway (*opr3*, *coi1* and *jar1*) induced a hyper-resistance phenotype in Arabidopsis plants challenged with Fg. Observation of a greater induction of PR1 transcripts and SA accumulation in *opr3* and *jar1* mutants compared to the WT plants, led the authors to conclude that JA-induced susceptibility may function via attenuation of SA-induced defence mechanisms. However, they also observed a faster progression of Fusarium disease symptoms in the *jar1 npr1* double mutant compared to the single *npr1* mutant, suggesting that JA-regulated mechanisms of defence may be effective against Fusarium infection, at least during the

later stages of infection (Makandar *et al.*, 2010). However, the role of JA signalling in wheat interactions with Fg has yet to be genetically validated.

4.1.6 *Ethylene response factor (ERF)-like*

Ethylene (ET) is a low molecular weight gaseous phytohormone playing important roles in seed germination, seedling growth, fruit ripening, leaf and flower senescence and adaptative responses to stresses (Zhu and Guo, 2008, and references therein). Extensive literature on the biosynthesis, perception, transduction and activation of ET-responsive gene expression, as well as cross-talk with other phytohormones is currently available (Zhu and Guo, 2008, Stepanova and Alonso, 2009, Robert-Seilaniantz *et al.*, 2011). Involvment of ET in the activation of plant defence mechanisms against different biotic stresses through its participation in a complex signalling network with other phytohormones has been extensively reviewed (Adie et al., 2007, Robert-Seilaniantz *et al.*, 2011). Members of the ethylene response factors (ERF) gene family belong to the APETALA2 (AP2) class of transcription factors (Grennan, 2008). ERFs contain a single DNA-binding domain which targets the GCC box found in the promoter of several pathogenesis-related genes, ET- and JA-inducible genes (Gutterson and Reuber, 2004). Berrocal-Lobo and co-workers (2002) showed that overexpression of *ERF1* in *Arabidopsis* enhanced resistance against several necrotrophic pathogens such as i.e. *Botrytis cinerea* and *Plectosphaerella cucumerina* but induced susceptibility to the hemibiotroph *Pseudomonas syringae tomato* DC3000, exemplifying the contrasting role that ET-signalling plays in plant defence mechanisms. Also, these authors later showed the involvement of AtERF1 in the resistance to the soilborne pathogen *Fusarium oxysporum*, concomitantly with JA and SA-related defence mechanisms (Berrocal-Lobo *et al.*, 2004). Interestingly, ET-signalling has recently been proposed to be a critical modulator of the NPR1-dependent antagonism of SA and JA pathways (Leon-Reyes et al., 2009). Of particular relevance to the current study, Chen and co-workers (2009) provided the first demonstration of an involvement of ET signalling in the modulation of resistance to Fg in both Arabidopsis and Wheat. These authors showed, using a genetic and chemical genetic approach, that mutants displaying enhanced production of ET were more susceptible to Fg while mutants with reduced ET signalling or perception of the hormone were more resistant. Attenuation of *EIN2* expression, a core component of ET-signal transduction, in wheat reduced both disease symptoms and DON contamination of grain. They concluded that Fg may exploit ET-signalling in both

monocotyledonous and dicotyledonous plants to favour host colonization (Chen *et al*., 2009).

In this chapter, a short list of Bd21 T-DNA mutant candidate lines were selected for study on the basis of the T-DNA tag being associated with genes whose products shared significant sequence homology with characterised genes functioning as components of hormone-signalling pathways known to influence disease resistance. Six mutant candidate lines were investigated for a potential alteration of Fusarium disease resistance and provide the first example of functional genetic study in *Brachypodium distachyon* as a stepping stone for model-to-crop translation of a cereal pathosytem.

4.2 Materials and methods

4.2.1 *Brachypdodium lines and growth conditions*

Mutant Bd21 lines BdAA466, BdAA615, BdAA688, BdAA700, BdAA724 and BdAA900 were obtained from the BrachyTAG collection (John Innes Centre) as a kind gift from Dr. P. Vain. The six candidates are shown in Figs. 4.1, 4.5 and 4.6 including the insertion site and flanking sequence information for each (Table 4.1). Bd mutant seeds were germinated and grown in the same conditions as described in Peraldi *et al.*, 2011.

Table 4.1: Summary of T-DNA line, associated tagged gene, closest identified ortholog, percentage of protein sequence homology shared with ortholog and putative protein function.

T-DNA line	Brachypodium gene ID	Closest ortholog	Sequence homology	Putative function
BdAA900	Bradi2g48280	HvBRI1 (AB088206)	90%	Brassinosteroid receptor
BdAA724	Bradi4g07470	OsARF24 (LOC_Os12g29520)	75%	Auxin-response factor
BdAA466	Bradi2g32190	AtDDB1A (AT4G05420)	55%	DNA-damage binding protein
BdAA615	Bradi1g11680	AtLOX1 (AT1G55020)	57%	Lipoxygenase
BdAA700	Bradi4g35336	Acyl-CoA thioesterase 10 (LOC_Os09g34190)	83%	Acyl-CoA thioesterase
BdAA688	Bradi5g17490	AtERF5 (AT5G47230)	43%	Ethylene-response factor

4.2.2 *Multiple sequence alignment and protein domain prediction*

All Brachypodium, Arabidopsis, rice and barley gene sequences were obtained from the EnsemblPlants website (http://plants.ensembl.org). Multiple sequence alignments were performed using the ClustalW2 application (www.ebi.ac.uk/Tools/msa/clustalw2). Protein domain prediction was performed using the Pfam sequence analysis tool (http://pfam.sanger.ac.uk).

4.2.3 *Characterization of T-DNA insertions*

DNA from 2–4-week-old wild-type and T0, T1 and T2 plants, was extracted using a DNeasy plant mini kit (Qiagen, http://www.qiagen.com/) according to the manufacturer's instructions. For validation of the BdAA900 T-DNA insertion, and assessment of zygocity level, PCRs were performed with 15 ng genomic DNA and Taq DNA polymerase (New England Biolabs, http://www.neb.com/). PCR reactions consisting of 50 µl volumes containing 70 ng of DNA were performed according to Bryan *et al*. (1997). Reactions consisted of 2.5 µl of 2 mM of the appropriate primer pair, 2.5 mM each of dATP, dCTP, dGTP and dTTP, and 0.75 µl of *Taq* DNA polymerase (Boehringer Mannheim Ltd., Germany) in 10 mM Tris-HCL (pH 8.3), 1.5 mM $Mgcl_2$, 50 Mm KCl, 100 mg ml^{-1} gelatine, 0.05 % (w/v) Tween 20 and Nonidet 40. The identity of the PCR fragments was verified by sequencing. The T-DNA insertion in Bradi2g48280 (*BRI1*) was validated using primers BdAA900LBR3 and TDNA4, amplifying a 380 nt T-DNA:Bradi2g48280 junction sequence (Appendix 3 Supplementary Table 1). The BdAA900LBR3 and BdAA900LBV2 primers amplify a 410 nt promoter:Bradi2g48280 fragment that does not contain the T-DNA insertion. The size of the T-DNA insertion prevents amplification from primers BdAA900LBR3 and BdAA900LBV2 in the mutant alleles. In homozygous BdAA900 T-DNA lines, only the 380 nt fragment is detected, while in hemizygous T-DNA lines both the 380 and 410 nt fragments are found. Wild-type Bd21 plants and BdAA900 NIL segregants only produce the 410 nt fragment. The cycling conditions used for both primer combinations were denaturation at 94°C for 1.5 min, followed by 35 cycles of denaturation at 94°C for 30 sec, annealing at 58°C for 30 sec and extension at 72°C for 30 sec, and a final extension at 72°C for 10 min. The T-DNA insertion in Bradi4g07470 (*ARF2*) in the BdAA724 T-DNA line was validated using primers Bdfa and TDNA4 (Appendix 3 Supplementary Table 1), amplifying a 320 nt T-DNA: Bradi4g07470 junction sequence. The primers Bdfa and Bdra2 (Appendix 3 Supplementary Table 1) amplify a 771 nt Bradi4g07470 fragment that does not contain the T-DNA insertion. The cycling conditions

used for both primer combinations were denaturation at 94°C for 5 min, followed by 35 cycles of denaturation at 94°C for 30 sec, annealing at 64°C for 1 min and extension at 72°C for 1 min, and a final extension at 72°C for 10 min.

4.2.4 *Maintenance and preparation of Fusarium inoculum*

DON-producing isolates of Fg (UK1 and S1) and Fc (Fu42) from the culture collection of the John Innes Centre were used. Conidial inoculum was produced as described in Peraldi *et al.*, 2011.

4.2.5 *Fusarium spray inoculation, detached leaf and root infection tests*

Whole Bd T-DNA mutant NIL and Ho plants were sprayed with Fc Fu42 conidial suspension (1 x 10^5 conidia ml^{-1}), amended with 0.01% Tween 20, using a handheld mister until run off. Sprayed plants were placed under a plastic cover and misted periodically with SDW to increase relative RH to about 90%, until 3 days post inoculation (dpi) when covers were removed and misting ceased. Disease symptoms were photographed using a Samsung NV7 digital camera. Visual disease scores were performed by assessment of the percentage of disease symptoms observed on individual spikelets, and averaged for each flower.

For the detached leaf tests on wounds, the Fg UK1 isolate was used and the method used was the same as described in Peraldi *et al.*, 2011. Each box contained a total of six leaf sections from different plants, including two leaves from each genotype (NIL, He and Ho). Root infection tests were carried out on Bd T-DNA mutant seedlings germinated as described above. Six seedlings of each genotype, Ho and NIL fixed lines, were grown on the surface of 10 × 10 cm square plastic boxes containing 0.8% agar-agar media for 2 days at 20°C under a 16 h/8 h light-dark cycle. Each T-DNA mutant lines was tested with four replicates. Each root was inoculated using a mycelium plug (5 mm dia) from the growing edge of a 14 day old colony grown on potato dextrose agar (PDA) at 20°C. Care was taken to inoculate NIL and their respective Ho seedlings with plugs from the same agar plate. Different plates were generally used for different T-DNA tagged lines.

4.2.6 *Light microscopy*

Leaf sections from BdAA900 Ho and NIL plants were cleared in 70% ethanol at 70°C for one hour to remove chlorophyll. Samples were mounted in 40% glycerol, viewed with a Nikon Eclipse 800 microscope and photographed with a Pixera Pro ES 600 digital camera.

4.2.7 *Leaf unrolling assay*

Brachypodium seeds of Bd21 ("wt", wild-type), BdAA900 "Ho" mutant plants (homozygous for the T-DNA insertion in the *BRI1* gene, Bradi2g48280) and BdAA900 "nil" plants (not containing a T-DNA insertion) were germinated in the dark at 5°C on damp filter paper for 5 days. Seedlings were then transferred onto 0.8% (w/v H2O) agar plates and grown at 20°C in the dark for 7 days. Under these growth conditions the resulting seedlings were etiolated with rolled leaves. Under green light (500-550 nm wave length), 4mm (±1mm) sections were cut from the central portion of the first emerging etiolated leaf of each seedling and incubated in the dark for 48 hours in solutions containing 0, 0. 1, 1, 10, 100 and 1000 nM eBL (epibrassinolide, Sigma-Aldrich, CAS number: 78821-43-9) supplemented with 0.01% (v/v H_2O) ethanol. Leaf sections were photographed after 48-h incubation and the extent of leaf unrolling was assessed using Image-J software.

4.2.8 *Statistical analysis*

Disease severity, conidial production, root lesion sizes and foliar lesion area data were analysed by generalised linear modelling (GLM) using the software package GENSTAT version 11.1 (Lawes Agricultural Trust, Rothamsted Experimental Station, UK). Individual treatments and/or genotypes were compared with the appropriate control using the unpaired *t*-tests within GLMs.

4.3 Results

Eight to twelve T_1 seeds of each Bd21 T-DNA mutant line were obtained from the Brachy-TAG collection. All T_1 seeds were germinated, the presence of a GFP signal was determined and each GFP positive and negative plant was bulked. T_2 seeds were also germinated and characterized for presence or absence of GFP signal. The putative genotype was inferred from the segregation of seedlings expressing GFP signal by comparing parental GFP signal with the proportion of GFP positive plants within the progeny. Therefore, based on the GFP signal of parents, 100% non-GFP expressing progeny lines and 100% GFP-expressing progeny lines were fixed in T_3 generation and termed respectively NIL and Ho fixed lines.

4.3.1 *Brassinosteroid insensitive-1 (BRI1) T-DNA mutant candidate*

A mutant exhibiting reduced plant height and altered architecture identified a gene previously known from *Arabidopsis* to affect the brassinosteroid pathway. The mutant Bd21 line (BdAA900) from the Brachy-TAG collection contained a T-DNA insertion in the 5'-untranslated region of the Bradi2g48280 gene, 9 nt upstream of the translation start signal (Figure 4.1A). The T-DNA insertion was characterized by the JIC00665_900 FST (http://www.modelcrop.org/). The Bradi2g48280 gene is predicted to encode an 1122 amino acid long protein composed of one transmembrane domain, a serine/threonine kinase domain, 15 LRRs, and a signal peptide (see Appendix 3 Supplementary Table 2). The predicted Bradi2g48280 protein shares 84% amino acid identity with the D61 rice receptor and 90% with the barley BRI1 protein (GenBank accession no. AB088206) [...]; Table 4.1). Approximately 28% (20/71) of the BdAA900 plants segregating for the T-DNA insert exhibited a severe dwarf and contorted plant phenotype, suggesting the presence of a single T-DNA locus (χ^2-test, P=0.79). Genotyping of T1 plants with PCR primers specific to the T-DNA:Bd21 junction sequence or to the wild-type allele of Bradi2g48280 (primers spanning the insertion site) demonstrated that the mutant phenotype only occurred in the plants homozygous (Ho) for the T-DNA insert, while hemizygous (He) plants and nontransgenic segregants (nil) exhibited a regular wild-type phenotype (Figure 4.1D and Figure 4.2). Overall plant height in Ho individuals was reduced by 50–60%, with leaves, sheaths, and stems affected to a similar extent. Most organs exhibited a contorted phenotype from the earliest stages of development (Figure 4.1B-C). Branching was increased in Ho individuals (Figure 4.1e). Ho inflorescence height was also reduced by half, and the number of spikelets averaged 2.7 compared with 3.5 in the nil plants (Figure 4.1F). Seed size and shape were also altered (6.46 mm long in Ho versus 5.46 mm in nil plants, t-test, $P < 0.001$; Figure 4.1F). Interestingly, a gene dosage effect was observed for GFP (present in the T-DNA) in Brachypodium plants segregating for the T-DNA mutation which enabled Ho genotypes (with intense fluorescence) to be accurately distinguished from He (with moderate fluorescence) genotypes. Ho individuals exhibited an altered epidermal cell shape and architecture (Figure 4.1G). Using a leaf-unrolling assay (Takesuo, 1994), Ho plants were shown to be significantly less sensitive to brassinosteroid application when compared with nil and wild-type plants (Figure 4.3).

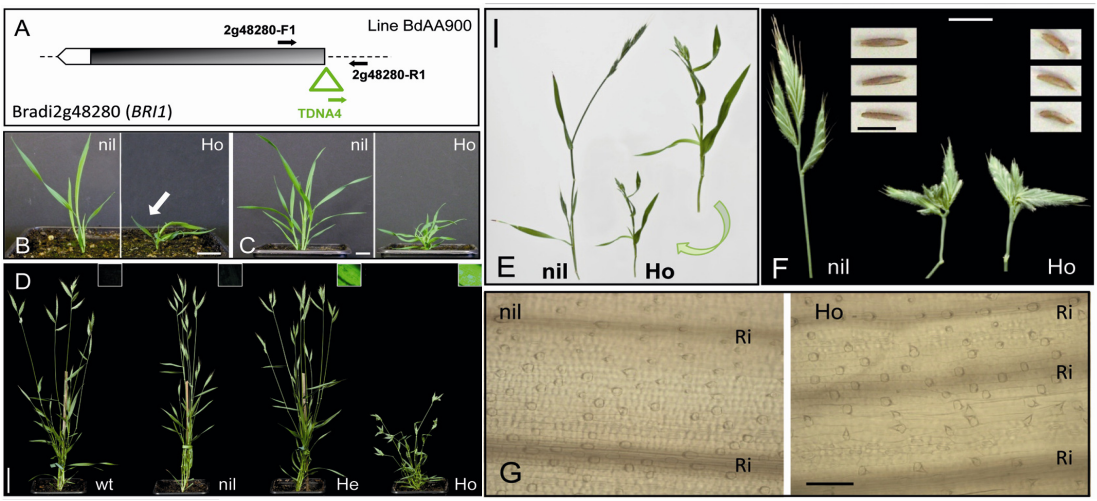

Figure 4.1: Brachypodium bri1 T-DNA mutant from the BrachyTAG collection (line BdAA900). (A) Schematic representation of T-DNA insertion in the 5#-untranslated region of the Bradi2g48280 gene (BRI1). The exon (grey box) and untranslated region (white box) of the Bradi2g48280 transcript as well as the T-DNA (green triangle) insertion site are represented. Dotted lines represent surrounding Bd21 genomic regions. PCR primers TDNA4 (5'-CGGCCGCATGCATAAGCTTA), 2g48280-R1 (5'-GCCTCGACGTAAGTAAAGGATAA) and 2g48280-F1 (5'-GCGACAAACAGTGCCGCCGCTAT) were used to genotype homozygous (Ho), hemizygous (He), and nil plants containing two, one, or no T-DNA insertion in Bradi2g48280, respectively. (B) Two-week-old Ho and nil plants. The white arrow indicates that the first leaf from Ho mutant plants often does not display a contorted phenotype. Bar=1 cm. (C) Three-week-old Ho and nil plants. Bar=1 cm. (D) Six-week-old Brachypodium wild-type (Bd21), nil, Ho, and He plants. GFP fluorescence of leaves is presented in the top right corner of each plant. Bar=3 cm. (E) Tiller architecture of nil and Ho T-DNA mutant plants. Bar=2 cm. (F) Inflorescence and seeds from nil and Ho plants. White bar=1 cm. Black bar=0.5 cm. (G) Light microscopic observation of the abaxial epidermis of cleared leaves (Vain *et al.*, 2011) from 3.5-week-old plants. Ri, rib; Bar=100 µm.

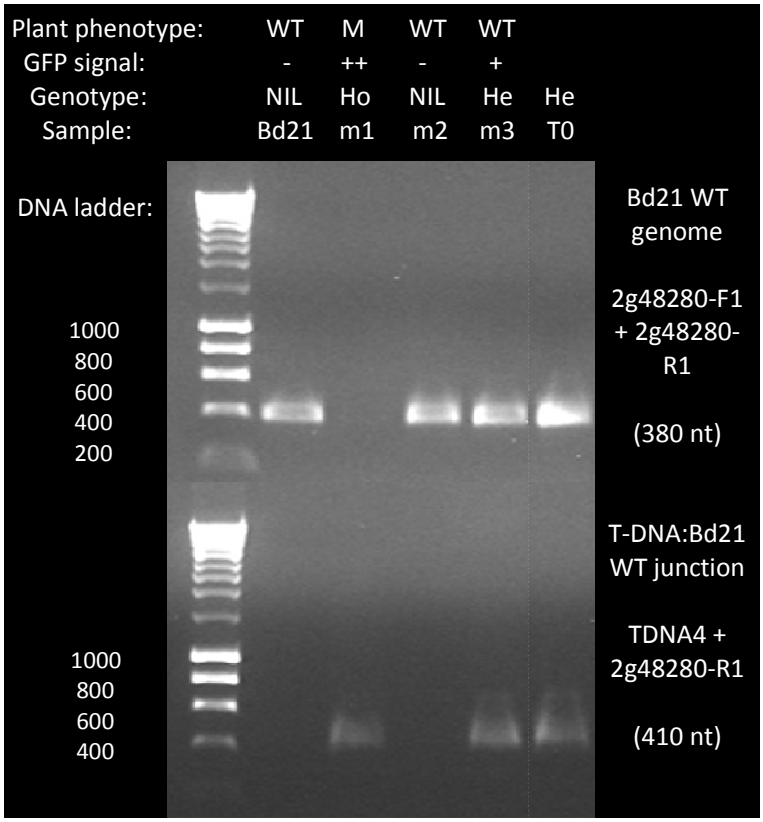

Figure 4.2: PCR genotyping of BdAA900 plants and correlation with GFP signal and plant phenotype segregation. Plant phenotype: WT = wild-type phenotype, M = mutant phenotype. GFP signal: - = no GFP fluorescence, + = GFP fluorescence, ++ = GFP fluorescence double intensity. Genotype: NIL = near isogenic line, Ho = Homozygous mutant, He = Hemizygous mutant. Sample: Bd21 = DNA extracted from Bd21 wild-type plant, m1, m2, m3= DNA extracted from BdAA900 plants 1, 2 and 3, T0 = DNA extracted from Agrobacterium-transformed callus. DNA ladder sizes are expressed in number of nucleotides. Bd21 WT genome = Amplicon specific to the Bradi2g48280 gene of Bd21 wild-type genome using 2g48280-F1 and 2g48280-R1 primers, 380 nucleotide (nt) long. T-DNA:Bd21 WT junction = Amplicon specific to the junction of Bradi2g48280 gene and T-DNA insert, 410 nt long.

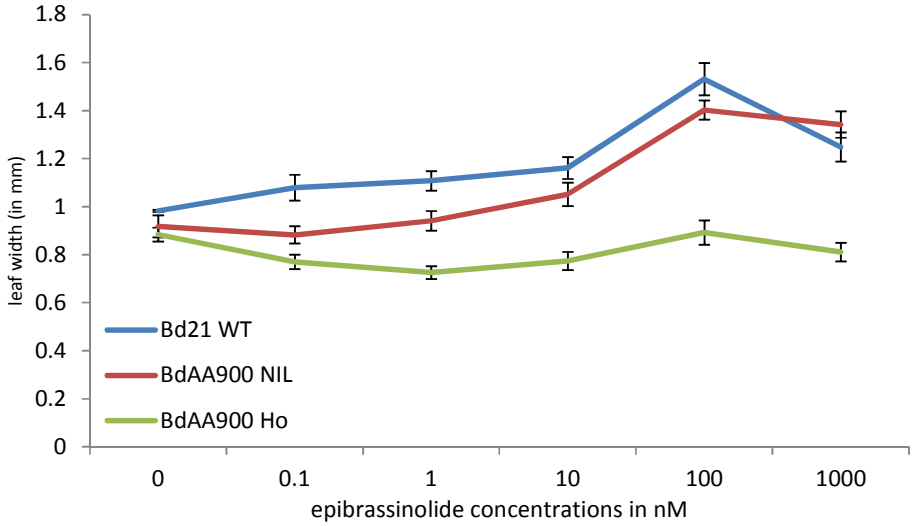

Figure 4.3: Leaf unrolling assay to characterize the relative sensitivity of Bd21 WT, BdAA900 (Bdbri1) NIL and BdAA900 (Bdbri1) Ho plants to brassinosteroids, 48 hours following incubation of etiolated leaf sections with increasing concentrations of epibrassinolide. Error bars indicate standard errors.

Spray inoculation tests on flowers of NIL and Ho plants was performed to assess the effect of Bradi2g48280 mutation on the resistance to *Fusarium* infection. Visual disease scoring, measuring the percentage of diseased spikelet, was recorded 5, 10 and 15 days following spray inoculation with Fc conidial suspension. No significant difference (p-value = 0.347) in visual symptoms between NIL (22.71%, s.e. = 2.14%) (Figure 4.4b) and Ho (18.61%, s.e. = 2.41%) (Figure 4.4c) plants was observed 5 days following spray inoculation (Figure 4.4A). However, some flowers from younger tillers found on Ho plants that were not recorded for disease assessment showed severe symptoms developed 5 days following spray inoculation (see Figure 4.4C, arrow). Visual scores, 10 and 15 days following spray inoculation, revealed that flowers of the Ho plants developed significantly reduced (p-value = 0.003 and 0.002, respectively) symptoms (26.74%, s.e. = 2.64% and 40.28%, s.e. = 3.29%, respectively) compared to those observed on the flowers of NIL plants (41.9%, s.e. = 2.29% and 55.08%, s.e. = 2.86%, respectively. See Supplementary Table 4). Detached leaf tests were also performed to characterize the effect of Bradi2g48280 mutation on the resistance to *Fusarium* infection in a different tissue than the flowers (Figure 4.4d). The necrotic lesion area that developed on the leaves of NIL plants reached an average of 7.746 mm^2 (s.e. = 1.155), 7 days following infection with Fg UK1 on wounds (see Figure 4.4d). No significant difference (p-value = 0.345) was observed with the necrotic lesion area developed on the leaves of He plants (9.275 mm^2, s.e. = 1.129) when compared to the NIL. However, a significant difference, at 95%C.I., (p-value = 0.038) was observed when comparing the mean necrotic lesion area developed on the Ho leaves (4.284 mm^2, s.e. =

1.18) with that on the NIL (See Supplementary Table 5). Results of the detached leaf test were further analysed by estimating the secondary conidial production per leaf. An average of 1597 conidia (s.e. = 424.7) were produced on the leaves of NIL plants, 7 days following infection (see Figure 4.4e). No significant difference was observed with the secondary conidia produced on the leaves of He plants (1123 conidia, s.e. = 424.7, p-value = 0.44) and Ho plants (1696 conidia, s.e. = 424.7, p-value = 0.872) when compared to the production on the NIL leaves (See Supplementary Table 6).

In addition, a spray inoculation test was performed on entire BdAA900 Ho and NIL seedlings. Despite spray inoculation with Fu42 conidial suspension ($1x10^5$ conidia.mL^{-1}) each week for three weeks, little disease symptoms developed on the leaves, stems or leaf sheaths of either BdAA900 NIL or Ho plants (see Figure 4.4h). Interestingly, however, it was noted that both NIL and Ho plants sprayed with mock treatment (water amended with 0.01% tween) developed numerous flowers and reached mid-anthesis, 30 days following the first spray inoculation whereas plants sprayed with *Fusarium* inoculum had not produced any flowers at that time (see Figure 4.4g-h, arrows). Flowering in sprayed plants of both NIL and Ho plants was delayed by at least 10-12 days relative to mock treated plants.

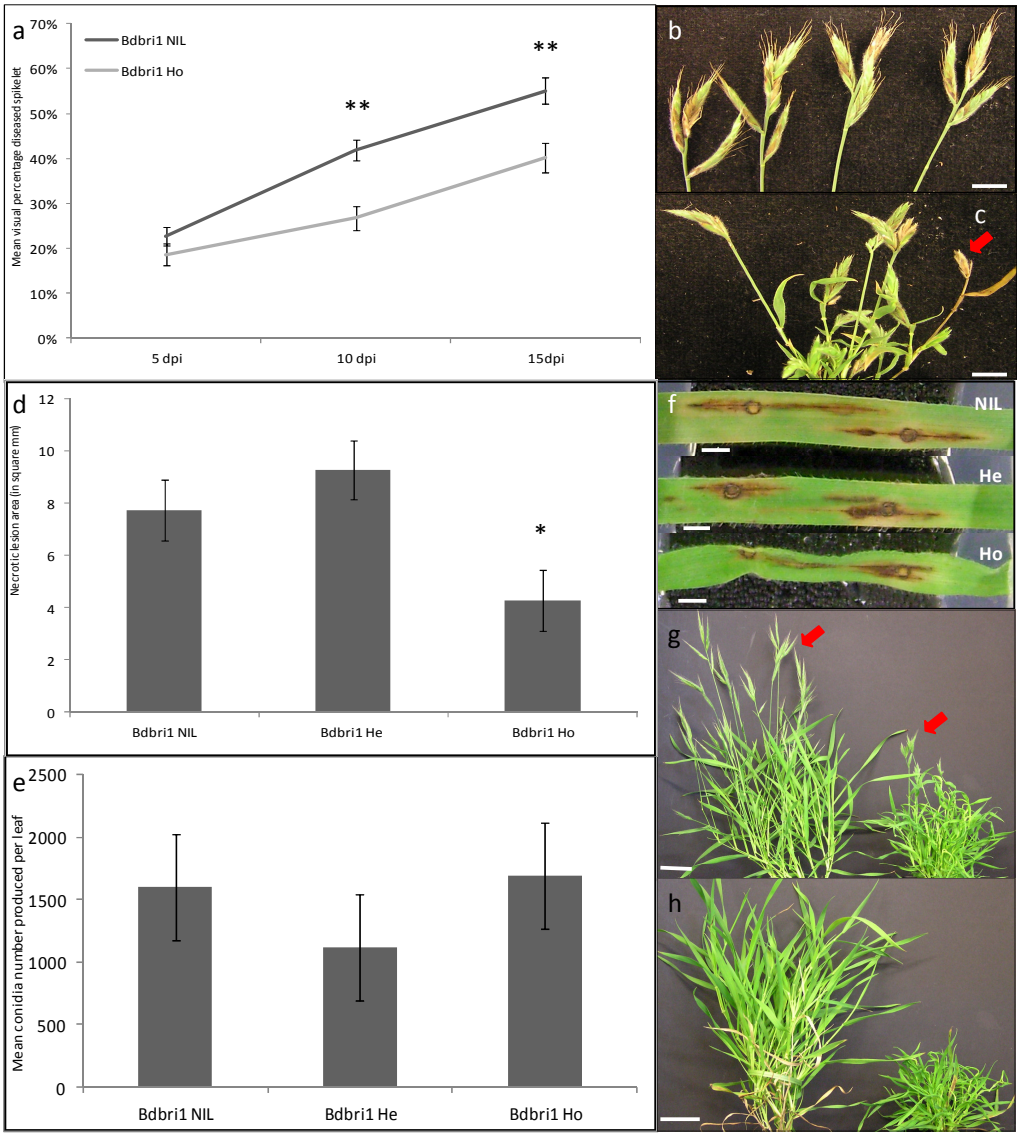

Figure 4.4: Characterization of the impact of BdBRI1 mutation on the resistance to Fusarium infection. a) Comparison of the mean percentage diseased spikelet of Bdbri1 NIL and Bdbri1 Ho plants, 5, 10 and 15 days following spray inoculation with Fc Fu42 isolate. b) Representative images of Bdbri1 NIL flowers, 5 days following spray inoculation with Fc. c) Representative images of Bdbri1 Ho flowers, 5 days following spray inoculation with Fc. Arrow indicates severely infected flower. Scale bars = 1 cm. d) Mean necrotic lesion area developed on the leaves of Bdbri1 NIL, Bdbri1 He and Bdbri1 Ho plants, 7 days following infection on wound with Fg UK1 conidial suspension e) Mean secondary conidial production on the leaves of Bdbri1 NIL, Bdbri1 He and Bdbri1 Ho plants, 7 days following infection on wound with Fg UK1 conidial suspension. f) Representative images of the detached leaf assay on Bd21 WT, Bdbri1 NIL, Bdbri1 He and Bdbri1 Ho leaf sections, 7 days following infection on wound with Fg UK1 conidial suspension. Scale bars = 0.2 cm. g) Images of Bdri1 NIL (left) and Bdbri1 Ho (right) control plants, 30 days following mock spray inoculation. Arrows shows flowers. h) Images of Bdri1 NIL (left) and Bdbri1 Ho (right) control plants, 30 days following Fc Fu42 isolate spray inoculation. Scale bars = 4 cm. Statistically significant differences observed between NIL and Ho results are indicated by: ** at 99 % C.I. and * at 95% C.I.

4.3.2 *Putative auxin-response factor (ARF) 2 T-DNA mutant candidate*

Unpublished results produced by Dr Xinwei Chen screened 6000 Arabidopsis T-DNA mutant lines for altered resistance to Fg foliar infection on wounding. One T-DNA line, named fgr1, was identified as highly resistant to Fg infection. The fgr1 mutant was identified as a new allele of ARF2, caused by a single nucleotide (adenine) insertion into exon 12, after codon N639 at position 2896 from the translational start site (Figure 4.5a). Leaves of the fgr1 Ho mutant retained green colouration following Fg infection on wound whereas leaves of the NIL line developed extended chlorotic area surrounding the inoculation point (see Figure 4.5b-c). Also, Fg infected leaves of fgr1 Ho plants produced significantly (p-value < 0.001) fewer secondary conidia (3.8×10^4 conidia per leaf, s.e. = 1.6×10^4) compared to the secondary conidia produced on the leaves of fgr1 NIL plants (14.9×10^4 conidia per leaf, s.e. = 1.6×10^4; see Figure 4.5d).

The mutant Bd21 line (BdAA724) from the Brachy-TAG collection was predicted to contain a T-DNA insertion in the 5'-untranslated region of the Bradi4g07470 gene, 394 nt upstream of the translation start signal (Figure 4.5e). Analysis of the putative protein sequence of the Bradi4g07470 gene by Pfam (http://pfam.sanger.ac.uk) identified a B3 DNA-binding, an auxin-response and an Aux/IAA domain signature (see Figure 4.5f). Also, multiple sequence alignment of the putative protein sequence of Bradi4g07470 gene by ClustalW (www.ebi.ac.uk/Tools/msa/clustalw2) revealed that the two most likely orthologs were members of the rice ARF gene family related to Arabidopsis ARF2: 75% protein sequence homology is shared with OsARF24 (LOC_Os12g29520), 65% homology with OsARF23 (LOC_Os11g32110) and 49% homology with AtARF2 (At5g62000; see Table 4.1).

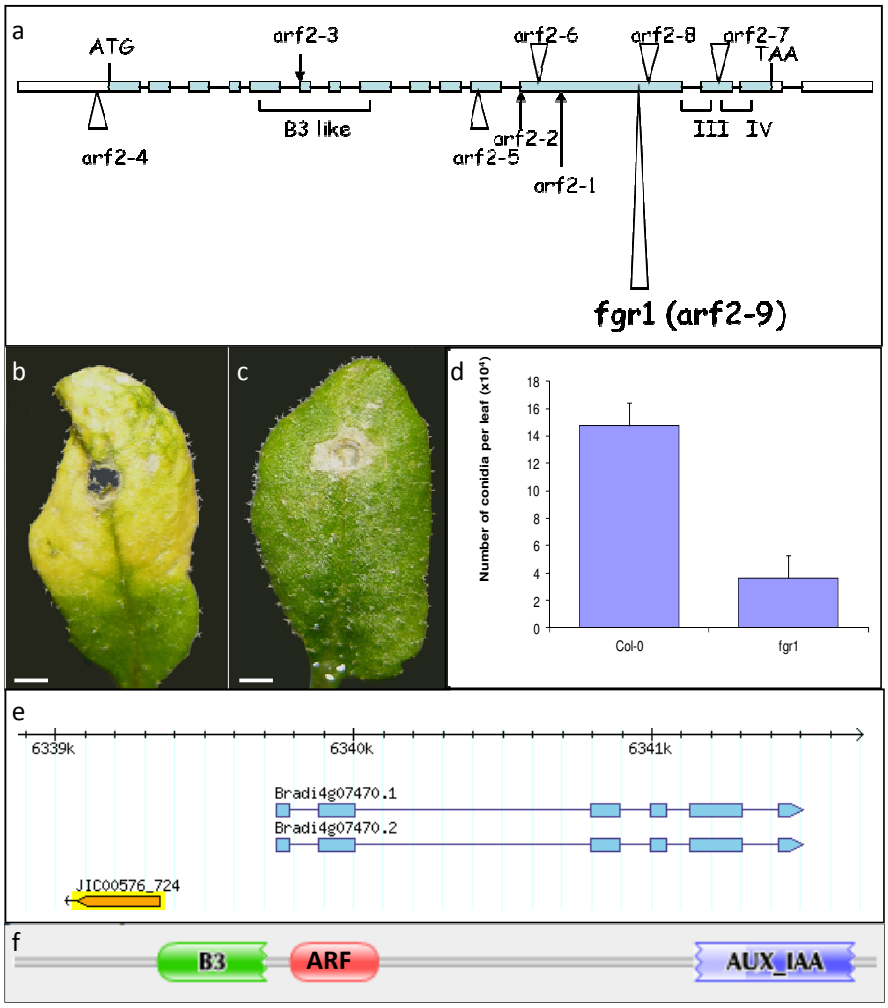

Figure 4.5: Enhanced resistance to *Fusarium graminearum* infection in fgr1, induced by mutation of Arabidopsis *ARF2* gene. a) The *fgr1* mutation occurs due to a single nucleotide 'A' insertion in exon 12 after codon N639 at position 2896 (C) from the translational start site. b-c) Mutation of *ARF2* confers enhanced resistance to *Fusarium graminearum* foliar infection (b) compared to Col-0 control (c). Scale bars = 0.5 mm. d) Mutation of *AtARF2* also reduces secondary conidial production following *Fusarium graminearum* foliar infection. e) The mutant Bd21 line (BdAA724) from the Brachy-TAG collection contains a T-DNA insertion in the 5'-untranslated region of the Bradi4g07470 gene, 394 nt upstream of the translation start signal. f) Pfam protein domain prediction of Bradi4g04740 predicted protein sequence showing B3 DNA-binding (green), Auxin-response (red) and Aux/IAA (blue) motives.

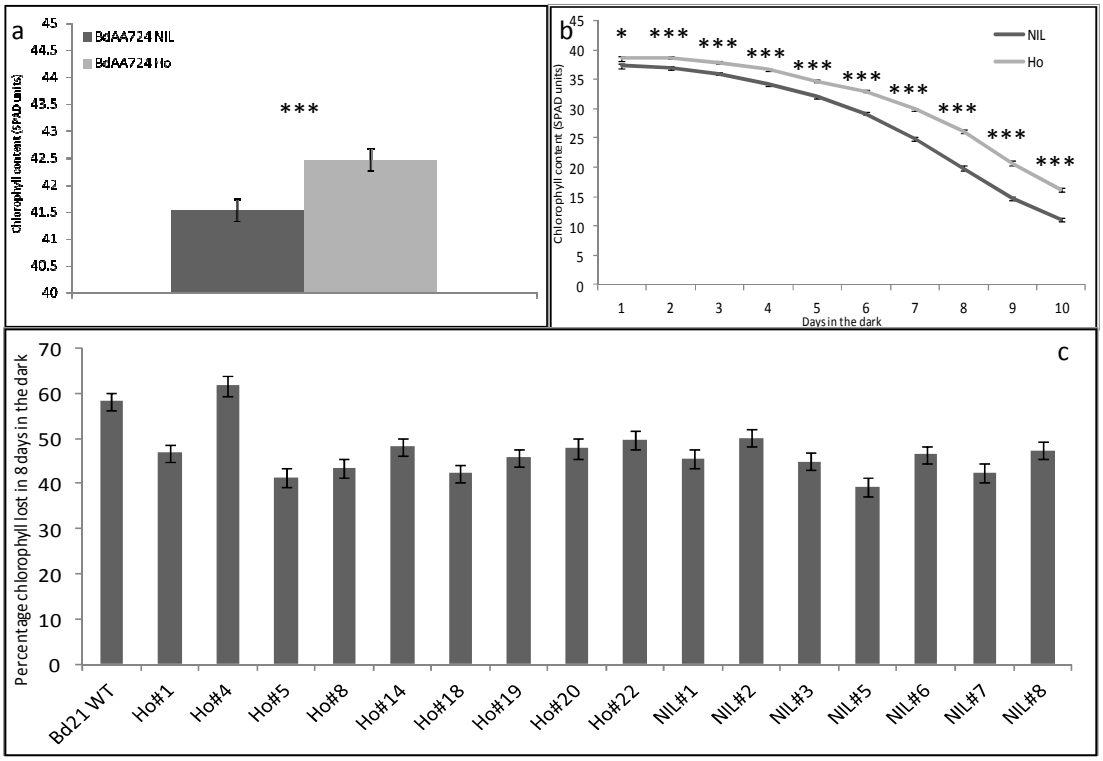

Figure 4.6: Comparison of the senescence characteristics and resistance to *Fusarium graminearum* infection of BdAA724 NIL and BdAA724 Ho plants. a) Mean chlorophyll contents in leaf 5, as measured *In Planta,* of BdAA724 NIL and BdAA724 Ho plants. b) Mean chlorophyll content, measured every day, on leaf 5 of BdAA724 NIL and BdAA724 Ho plants exposed to darkness for 10 days. c) Average percentage chlorophyll lost during 8 days of exposure to darkness in the leaves of T_4 fixed BdAA724 NIL and Ho lines. Bars show standard errors.

Foliar chlorophyll contents *In Planta* and in detached leaves exposed to darkness for ten days were measured to compare BdAA724 NIL and BdAA724 Ho plants. Leaf 5 of BdAA724 NIL plants contained an average of 41.53 S.U. (s.e. = 0.2). A significantly higher (p-value <0.001) chlorophyll content was measured in leaf 5 of BdAA724 Ho plants, which displayed an average of 42.46 S.U. (s.e. = 0.2; see Figure 4.6a). Measurements in the leaf 5 of BdAA724 NIL and BdAA724 Ho plants exposed to darkness showed a significantly (p-value = 0.013), higher chlorophyll content in the leaves of Ho plants when compared to the leaves of NIL plants, 1 day following exposure to darkness (see Figure 4.6b). All subsequent measurements, between 2 and 10 days following exposure to darkness, showed that leaves of Ho plants had significantly (p-value <0.001) higher chlorophyll content when compared to leaves of NIL plants (see Figure 4.6b). A repeat DIS experiment was performed on leaves of all the different T_4 lines of

BdAA724 NIL (seven lines) and Ho (nine lines) fixed on the basis of GFP signal segregation. Leaves from the Ho plants lost between 41.39% (s.e. = 2.057) of chlorophyll as displayed by Ho line 5 and 61.71% (s.e. = 2.187) as displayed by the Ho line 4, in eight days of exposure to darkness. Leaves from the NIL plants lost between 39.27% (s.e. = 1.945) of chlorophyll as displayed by the NIL line 5 and 50.16% (s.e. = 1.945) as displayed by the NIL line 2, following eight days of exposure to darkness (see Figure 4.6c). Results displayed by individual Ho and NIL lines were merged to calculate the overall percentage of chlorophyll lost by the NIL and Ho genotypes and compared to the Bd21 WT result. Overall, Bd21 WT leaves lost an average of 58.23% (s.e. = 2.052) chlorophyll while the overall percentage of chlorophyll lost by the NIL genotypes was 45.16% (s.e. = 0.787) and 47.16% (s.e. = 0.71) for the Ho genotypes. The percentage of chlorophyll lost by the Bd21 WT leaves were significantly (p-value < 0.001) higher when compared to the NIL, but no significant difference, at 95% C.I., was observed between the percentage of chlorophyll lost by NIL and Ho leaves (p-value = 0.06; results not shown).

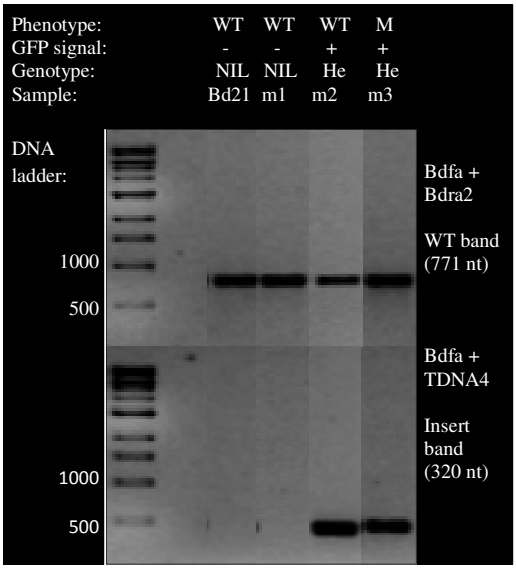

Figure 4.7: Genotyping of BdAA724 NIL and BdAA724 Ho plants. Plant phenotype: WT = wild-type phenotype, M = mutant phenotype. GFP signal: - = no GFP fluorescence, + = GFP fluorescence, ++ = GFP fluorescence double intensity. Genotype: NIL = near isogenic line, Ho = Homozygous mutant, He = Hemizygous mutant. Sample: Bd21 = DNA extracted from Bd21 wild-type plant, m1, m2, m3= DNA extracted from BdAA724 plants 1, 2 and 3. PCR primers TDNA4 (5'-CGGCCGCATGCATAAGCTTA), Bdfa (5'-ACATGTTAGCCACATCAACGAGC) and BdRa2 (5'-AGAAGAGACACTCACCTCCGGC) were used to genotype homozygous (Ho), hemizygous (He), and NIL plants predicted to contain two, one, or no T-DNA insertion in Bradi4g07470, respectively. nt = nucleotide.

Genotyping of T_4 plants with PCR primers specific to the T-DNA:Bd21 junction sequence or to the wild-type allele of Bradi4g07470 (primers spanning the insertion site) was performed. It was demonstrated that only wild-type specific amplification was observed in NIL plants, which exhibited a regular wild-type phenotype. However, genotyping of He and Ho plants, fixed on the basis of GFP signal segregation, could not be distinguished from one another as both wild-type and T-DNA:Bd21 junction specific bands were amplified in every plant (see Figure 4.7). All T_4 NIL and Ho sister lines fixed on the basis of GFP signal segregation were then genotyped to investigate if the presence of a wild-type specific band in the Ho fixed line was due to a single genetic event or was reminiscent of the BdAA724 transformation event. All NIL and Ho fixed lines investigated in the DIS test presented in Figure 4.6C were genotyped. Only wild-type specific amplification was observed in the NIL lines, however, all nine Ho lines resulted in amplification of both wild-type specific and T-DNA:Bd21 junction specific bands (results not shown). A new batch of BdAA724 T_1 seeds was germinated to generate a new lineage from T_1 to T_3 generation. New BdAA724 NIL and Ho lines were fixed on the basis of GFP signal segregation and genotyped. Again, however, all NIL fixed lines resulted in the sole detection of a wild-type specific band while all Ho fixed lines resulted in the detection of both WT-specific and DNA:Bd21 junction specific bands as had been observed for the original NIL and Ho selected plants as shown in Fig 4.7. These results indicated that, although BdAA724 contained a T-DNA with an FST identical to the region adjacent to Bradi4g07470, the wild-type gene itself and the upstream region were not altered. For this reason, this line was not investigated further.

4.3.3 *Putative JA-biosynthesis related and ERF-like T-DNA mutant candidates*

Among all Bd21 lines available from the Brachy-TAG collection, four candidate lines (BdAA466, BdAA615, BdAA700 and BdAA688) were selected on the basis of putative protein function prediction from sequence alignment. The mutant line BdAA466 was predicted to contain a T-DNA insertion in the 3'-untranslated region of the Bradi2g32190 gene, 1241 nt downstream of the translation stop signal (Figure 4.8a). Originally, BdAA466 was selected for study because the Bradi2g32190 gene, predicted to encode an 816 amino acid long protein, was suggested to share homology with the lipoxygenase gene family (Dr. L. Mur, pers. comm.). However, subsequent analysis of the putative protein sequence of the Bradi2g32190 gene by Pfam (http://pfam.sanger.ac.uk) identified a mon-functional DNA-alkylating methyl methanesulfonate N-terminal (MMS1 N) domain from amino acids 182 to 387 and a cleavage and polyadenylation specificity factor (CPSF) A

domain from amino acids 682 to 784. Also, a revised version of the putative protein function displayed by EnsemblPlants (http://plants.ensembl.org) identified 55% sequence homology with the DDB1A and DDB1B Arabidopsis genes, which are DNA-damage binding proteins (Table 4.1).

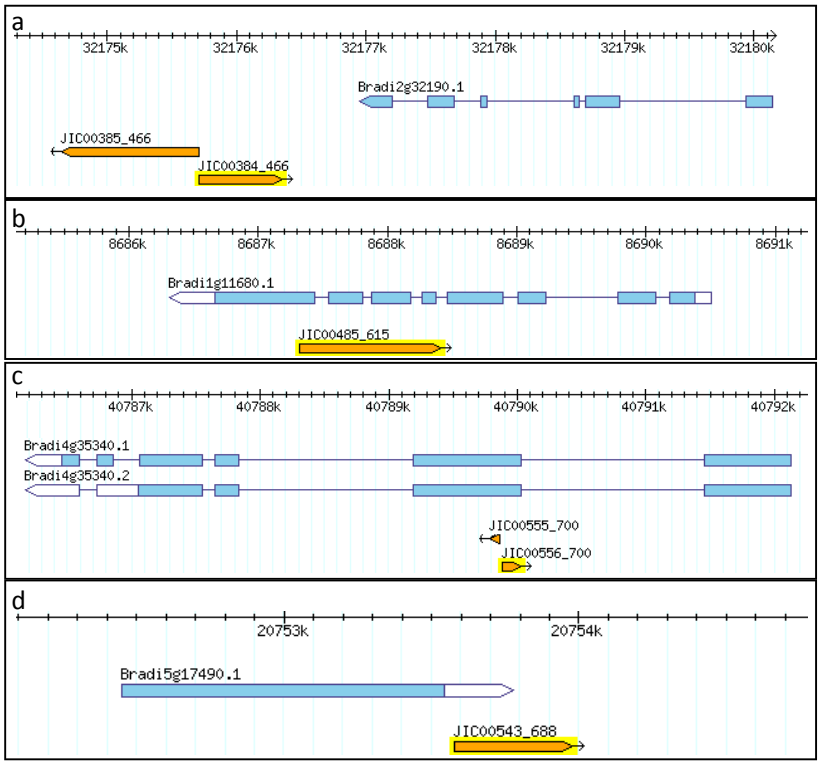

Figure 4.8: Bd21 T-DNA mutant candidates to test for potential alteration of *Fusarium* resistance. a) The mutant Bd21 line (BdAA466) from the Brachy-TAG collection contains a T-DNA insertion in the 3'-untranslated region of the Bradi2g32190 gene, 1241 nt upstream of the translation stop signal. b) The mutant Bd21 line (BdAA615) from the Brachy-TAG collection contains a T-DNA insertion in the eight exon of the Bradi1g11680 gene, 3110 nt upstream of the translation start signal. c) The mutant Bd21 line (BdAA700) from the Brachy-TAG collection contains a T-DNA insertion in the second exon of the Bradi4g35336 gene (former Bradi4g35340 in Bd21 Assembly v.1), 3612 nt upstream of the translation start signal. d) The mutant Bd21 line (BdAA688) from the Brachy-TAG collection contains a T-DNA insertion in the 3'-untranslated region of the Bradi54g17490 gene, 1 nt downstream of the translation stop signal.

The mutant line BdAA615 was predicted to contain a T-DNA insertion in the eighth exon of the Bradi1g11680 gene, 1011 nt upstream of the translation stop signal (see Figure 4.8b). The Bradi1g11680 gene is predicted to encode an 860 amino acid long protein composed of a PLAT/LH2 (found in a variety of membrane or lipid-associated proteins, including lipoxygenases) domain from amino acids 61 to 158 and a lipoxygenase domain

from amino acids 171 to 837 (http://pfam.sanger.ac.uk). The Bradi1g11680 predicted gene product shares 57% of sequence homology with AtLOX1 (Table 4.1).

The mutant line BdAA700 was predicted to contain a T-DNA insertion in the second exon of the Bradi4g35340 gene, 3612 nt downstream of the translation start signal, according to the v1.0 of the Brachypodium Bd21 genome sequence (see Figure 4.8c). It was observed that the v1.2 assembly of the Brachypodium Bd21 genome sequence changed the gene code associated to the insertion characterised in the BdAA700 line to Bradi4g35336. The Bradi4g35336 gene is predicted to encode a 500 amino acid long protein composed of two thioesterase superfamily (4HBT) domains from amino acids 178 to 247 and 369 to 426 (http://pfam.sanger.ac.uk). Also, the v2.0 BrachyCyc pathway database found in Gramene platform (www.gramene.org/pathway) predicted the Bradi4g35336 gene to encode an enzyme involved in the conversion of jasmonyl-CoA into (+)-7-iso-jasmonate, precursor of the bioactive form of JA in Arabidopsis; (+)-7-iso-jasmonate-isoleucine (Staswick *et al*., 2004). The Bradi4g35336 predicted gene product shares 83% of sequence homology with the rice Acyl-CoA thioesterase 10 (Table 4.1).

The mutant line BdAA688 was predicted to contain a T-DNA insertion in the 3'-untranslated region of the Bradi5g17490 gene, 199 nt downstream of the translation stop signal (see Figure 4.8d). The Bradi5g17490 gene is predicted to encode a 364 amino acid long protein composed of an AP2 domain from amino acids 174 to 225, characteristic of the AP2/ethylene-responsive element binding protein (EREBP) family of transcription factors (http://pfam.sanger.ac.uk). The Bradi5g17490 predicted gene product shares 43% of sequence homology with AtERF5 (Table 4.1).

Spray inoculation tests on flowers of BdAA466, BdAA615, BdAA700 and BdAA688 NIL and Ho plants, fixed on the basis of the GFP signal segregation in progeny, were performed to test for altered resistance to Fusarium infection, using the Fc Fu42 isolate. Flowers of the BdAA466 NIL plants displayed an average of 55% (s.e. = 5.87) diseased spikelets, 5 days following spray inoculation whereas flowers of the Ho plants displayed an average of 69% (s.e. = 5.084) diseased spikelets (see Figure 4.9a). Ten days following spray inoculation, flowers of the NIL plants displayed an average of 80.33% (s.e. = 5.564) diseased spikelets whereas flowers of the Ho plants displayed an average of 86.25% (s.e. = 4.819) diseased spikelets (see Figure 4.9a). No significant difference was observed between the average percentage diseased spikelets of NIL and Ho plants at 5 (p-value = 0.0072) and 10 days (p-value = 0.422) following spray inoculation (see Appendix 3 Supplementary Table 7).

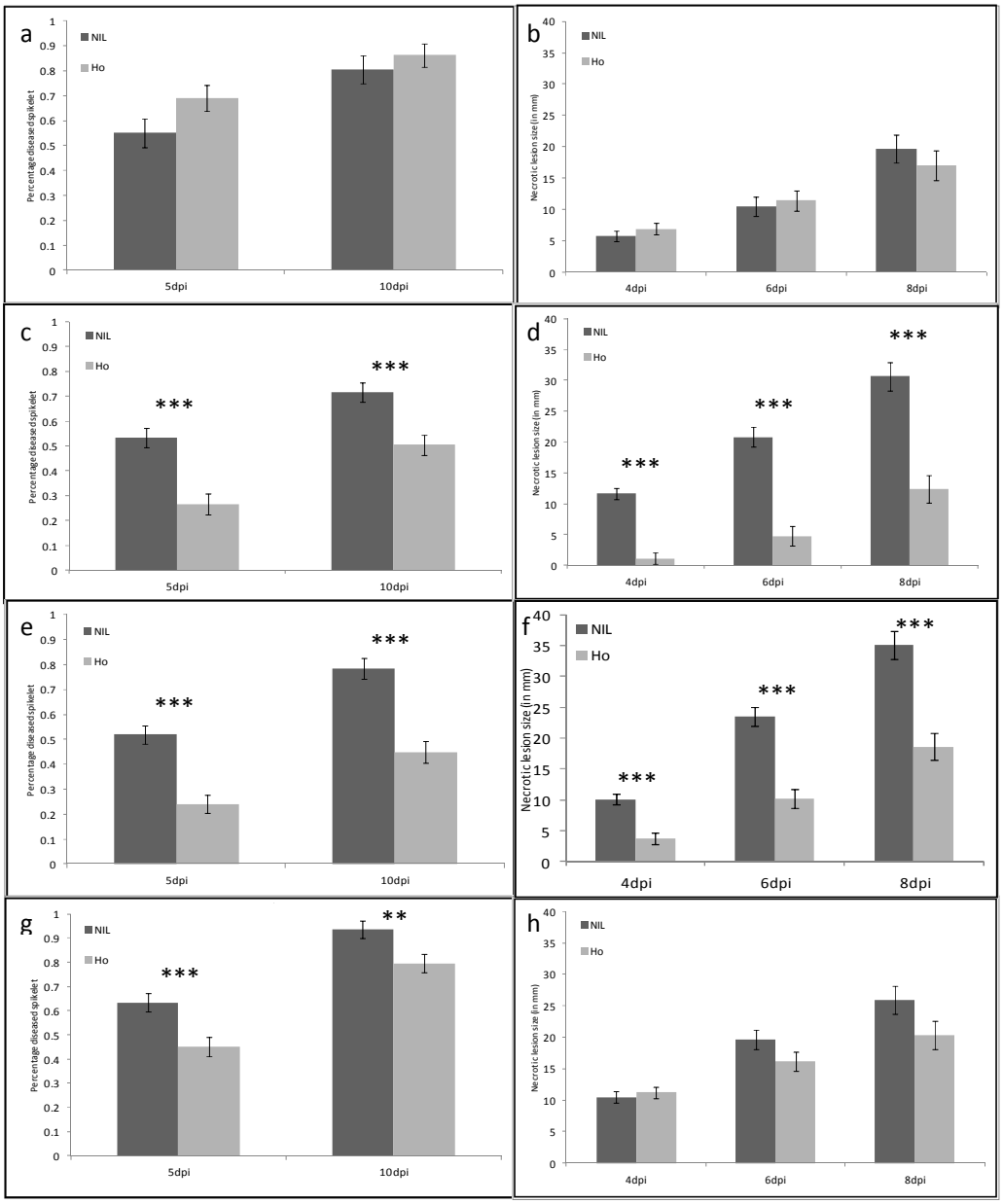

Figure 4.9: Fusarium resistance disease tests on Bd21 T-DNA mutant candidates BdAA466, BdAA615, BdAA700 and BdAA688. a) Average percentage diseased spikelet of BdAA466 NIL and Ho plants, 5 and 10 days following spray inoculation with Fu42. b) Average necrotic lesion size developed on the roots of BdAA466 NIL and Ho seedlings, 4, 6 and 8 days following Fu42 mycelium plug infection. c) Average percentage diseased spikelet of BdAA615 NIL and Ho plants, 5 and 10 days following spray inoculation with Fu42. d) Average necrotic lesion size developed on the roots of BdAA615 NIL and Ho seedlings, 4, 6 and 8 days following Fu42 mycelium plug infection. e) Average percentage diseased spikelet of BdAA700 NIL and Ho plants, 5 and 10 days following spray inoculation with Fu42. f) Average necrotic lesion size developed on the roots of BdAA700 NIL and Ho seedlings, 4, 6 and 8 days following Fu42 mycelium plug infection. g) Average percentage diseased spikelet of BdAA688 NIL and Ho plants, 5 and 10 days following spray inoculation with Fu42. h) Average necrotic lesion size developed on the roots of BdAA688 NIL and Ho seedlings, 4, 6 and 8 days following Fu42 mycelium plug infection. Bars show standard errors. Statistically significant differences observed between NIL and Ho results are indicated by: *** at 99.9% C.I. and ** at 99% C.I.

Flowers of the BdAA615 NIL plants displayed an average of 53.33% (s.e. = 3.789) diseased spikelets whereas flowers of the Ho plants displayed an average of 26.61% (s.e. = 4.083), 5 days following spray inoculation (see Figure 4.9c). Ten days following spray inoculation, flowers of the NIL plants displayed an average of 71.56% (s.e.3.81) diseased spikelets whereas flowers of the Ho plants displayed an average of 50.36% (s.e. = 4.073) diseased spikelet (see Figure 4.9c). Flowers of the BdAA615 Ho plants displayed a significantly (p-value < 0.001) reduced percentage of diseased spikelets when compared to the flowers of NIL plants, both at 5 and 10 days following spray inoculation (see Appendix 3 Supplementary Table 7).

Flowers of the BdAA700 NIL plants displayed an average of 51.97% (s.e. = 3.688) diseased spikelets whereas flowers of the Ho plants displayed an average of 24.05% (s.e. = 3.737) diseased spikelets, 5 days following spray inoculation (see Figure 4.9e). Ten days following spray inoculation, flowers of the NIL plants displayed an average of 78.33% (s.e. = 4.147) diseased spikelets whereas flowers of the Ho plants displayed an average of 44.8% (s.e. 4.31) diseased spikelets (see Figure 4.9e). Flowers of the BdAA700 Ho plants displayed a significantly (p-value < 0.001) reduced percentage of diseased spikelets when compared to the flowers of NIL plants, both at 5 and 10 days following spray inoculation (see Appendix 3 Supplementary Table 7).

Flowers of the BdAA688 NIL plants displayed an average of 63.38% (s.e. = 3.737) diseased spikelet whereas flowers of the Ho plants displayed an average of 45.15% (s.e. = 3.899) diseased spikelets, 5 days following spray inoculation (see Figure 4.9g). Ten days following spray inoculation, flowers of the NIL plants displayed an average of 93.68% (s.e. = 3.696) diseased spikelets whereas flowers of the Ho plants displayed an average of 79.68% (s.e. 3.871) diseased spikelet (see Figure 4.9g). Flowers of the BdAA688 Ho plants displayed a significantly reduced percentage of diseased spikelet when compared to the flowers of NIL plants, both at 5 and 10 days following spray inoculation (p-value = 0.001 and 0.009, respectively; see Appendix 3 Supplementary Table 7).

Root infection tests were also performed onto seedlings of BdAA466, BdAA615, BdAA700 and BdAA688 NIL and Ho fixed lines, using mycelium plugs of the Fc Fu42 isolate, to characterise Fusarium resistance in a different tissue than the flowers. Roots of the BdAA466 NIL seedlings displayed an average necrotic lesion size of 5.685 mm (s.e = 0.871) 4 dpi, 10.5 mm (s.e. = 1.54) at 6 dpi and 19.66 mm (s.e. = 2.18) at 8dpi (see Figure 4.9b). Roots of the BdAA466 Ho seedlings displayed an average necrotic lesion size of 6.902 mm (s.e. = 0.932) at 4dpi, 11.38 mm (s.e. = 1.64) at 6 dpi and 17.03 (s.e. = 2.34) at 8 dpi (see Figure 4.9b). No significant difference was observed between the average necrotic

lesion size displayed by BdAA466 Ho seedlings when compared to the NIL seedlings, at 4, 6 and 8 dpi (p-value = 0.342, 0.698 and 0.412, respectively; see Appendix 3 Supplementary Table 8).

Roots of the BdAA615 NIL seedlings displayed an average necrotic lesion size of 11.669 mm (s.e = 0.91) 4 dpi, 20.79 mm (s.e. = 1.6) at 6 dpi and 30.63 mm (s.e. = 2.28) at 8dpi (see Figure 4.9d). Roots of the BdAA615 Ho seedlings displayed an average necrotic lesion size of 1.119 mm (s.e. = 0.932) at 4dpi, 4.75 mm (s.e. = 1.57) at 6 dpi and 12.45 (s.e. = 2.23) at 8 dpi (see Figure 4.9d). The average necrotic lesion size displayed by BdAA615 Ho seedlings were significantly (p-value < 0.001) reduced compared to the necrotic lesions developed on NIL seedlings, at 4, 6 and 8 dpi (see Appendix 3 Supplementary Table 8).

Roots of the BdAA700 NIL seedlings displayed an average necrotic lesion size of 10.107 mm (s.e = 0.89) 4 dpi, 23.52 mm (s.e. = 1.57) at 6 dpi and 35.1 mm (s.e. = 2.23) at 8dpi (see Figure 4.9f). Roots of the BdAA700 Ho seedlings displayed an average necrotic lesion size of 3.737 mm (s.e. = 0.871) at 4dpi, 10.17 mm (s.e. = 1.54) at 6 dpi and 18.6 (s.e. = 2.18) at 8 dpi (see Figure 4.9F). The average necrotic lesion size displayed by BdAA700 Ho seedlings were significantly (p-value < 0.001) reduced compared to the necrotic lesions developed on NIL seedlings, at 4, 6 and 8 dpi (see Table 4.16). Roots of the BdAA688 NIL seedlings displayed an average necrotic lesion size of 10.496 mm (s.e = 0.89) 4 dpi, 19.63 mm (s.e. = 1.57) at 6 dpi and 25.97 mm (s.e. = 2.23) at 8dpi (see Figure 4.9h). Roots of the BdAA688 Ho seedlings displayed an average necrotic lesion size of 11.217 mm (s.e. = 0.871) at 4dpi, 16.12 mm (s.e. = 1.54) at 6 dpi and 20.34 (s.e. = 2.18) at 8 dpi (see Figure 4.9h). No significant difference was observed between the average necrotic lesion sizes displayed by BdAA688 Ho seedlings when compared to the NIL seedlings, at 4, 6 and 8 dpi (p-value = 0.564, 0.112 and 0.073, respectively; see Appendix 3 Supplementary Table 8).

4.4 Discussion

4.4.1 *Characterisation of BRI1 mutation in Bd*

Bd21 mutant line BdAA900 was originally selected from the T-DNA mutant candidate list as a proof of concept because its Arabidopsis counterpart displayed a severely dwarfed phenotype (Clouse *et al.*, 1996) which was expected to be easily observable in the first segregating generation of mutants. The high level of sequence homology shared between Bradi2g48280 and the rice and barley brassinosteroid receptors, as well as the prediction of

protein domains essential to the function of BRI1 strongly suggested that Bradi2g48280 was a BRI1 homologue. The severe phenotype displayed by BdAA900 Ho plants, correlated with the GFP signal segregation and genotyping, affecting all above-ground plant parts exhibiting severely contorted and dwarfed tissues. The BdAA900 Ho phenotype appeared intermediate to the Barley 'uzu' mutants, displaying semi-dwarfism but otherwise normal tissue development, and the severe phenotype observed in Arabidopsis bri1 mutant which is extremely dwarfed and also affects leaf and stem development (Chono *et al.*, 2003, Clouse *et al.*, 1996). Observation of a dwarfism and contorted leaf phenotype as early as two weeks post germination but not in leaf 1 suggests that the influence of BR on early seedling stages of development in Bd may be relatively minor. Comparison of the microscope images of the leaf epidermis of BdAA900 Ho and NIL suggests that the BR signal controls, at least partially, the foliar developmental plan. Interestingly, loss of function of the rice BRI1 homolog prevents internode elongation (Yamamuro *et al.*, 2000) and BR signalling has been shown to be involved in the promotion of cell expansion rather than cell division (Clouse *et al.*, 2011). The reduction in size observed in seeds produced from Ho plants was not observed among the seeds produced by He plants, suggesting it is the result of a maternal effect induced by the architecture of the parental flower. Barley 'uzu' mutants are also fertile (Chono *et al.*, 2003), unlike Arabidopsis where bri1 mutants are male sterile (Clouse *et al.*, 1996). Hence, the reduction in size and spikelet number observed in the flowers of BdAA900 Ho plants suggests that BR-mediated control of flower development does not impact on male fecundity in moncotyledonous species. Taken together, these results suggest that Bradi2g48280 is most probably the gene coding for the main brassinosteroid receptor in Brachypodium. As a final step to validate Bradi2g48280 as functional homologue of BRI1, BdAA900 Ho mutant plants could be complemented with the functional Bradi2g48280 gene or with the BRI1 Arabidopsis gene, which would be expected to restore, at least partially, the wild-type phenotype. This validation step, if confirmed, could enable researchers to develop site-targeted mutagenesis approaches, by complementing BdAA900 Ho plants with truncated version of the Bradi2g48280 gene, to study the impact of particular protein domain deletion and/or single amino acid changes on the plant architecture and development. This strategy could potentially shed light on the developmental mechanisms controlled by BR signalling, and their specificity in monocotyledonous plants.

Despite recent evidence indicating the influence that BRs can exert onto plant defence mechanisms, no evidence has been published to date suggesting that BR signalling can

modulate resistance mechanisms effective against *Fusarium* spp. It was noted that the visual floral symptoms observed on the BdAA900 Ho plants were reduced compared to the NIL plants for the latter two scores but not for the first, suggesting a greater resistance to the colonisation/spread of the fungus (type II) rather than the initial penetration (type I) of the fungus. BdAA900 Ho leaves inoculated with Fusarium conidia on wounds also showed reduced symptoms compared to the NIL, 7 days following infection but secondary conidial production appeared to be unaffected. It is possible that these contrasting results reflect an alteration in tolerance rather than resistance as has been observed in several studies of bacterial infection of Arabidopsis (Bent *et al*., 1992) and tomato (Lund *et al*., 1998). The reduced symptoms observed in the bacterial studies often reflect tolerance rather than resistance because the levels of bacterial growth in the mutants were similar to those in the wild-type controls. However, it is also possible that the apparent reduction in lesion size is an artefact caused by the severe distortion of the leaves of the Ho plants. The size of lesions may have been underestimated when taking measurements from photographic images which could not accurately reflect the lesion areas. No such effect was expected to impact on the assessment of floral infection although the severe contortion of floral architecture could impact the ability of the fungus to spread to nearby floral units. In barley, morphological attributes such as the inflorescence architecture and plant height have been reported to correlate with several QTLs conferring FHB resistance (Zhu *et al.*, 1999). It is therefore important to hypothesise that the reduction of FHB symptoms displayed by the Bdbri1 Ho plants compared to the NILs may be due to the severe contorsion of the floral architecture. Nontheless, the phenotype of Bdbri1 Ho plants, in particular the shorter, contorted and compact spikelets with reduced number of florets, was expected to increase relative humidity in the floral cavities and allow faster spread of the fungus to the adjacent tissues, conditions which are understood to be factors of susceptibility. Interestingly, recent report by De Vleesschauwer and co-workers (2012) showed that *Pythium graminicola*, an oomycete pathogen of rice roots, exploits BRs as a virulence factor for host colonization. These authors demonstrated that the immune-suppressive effect of BRs is, at least partially, due to negative cross-talk with SA and GA pathways. Also, studies conducted in Arabidopsis showed that activation of the BRI1 pathway inhibits pathogen-triggered immunity (PTI) signalling mediated by several pattern-recognition receptors (PRRs) (Albrecht *et al.*, 2012). As a concluding remark, they proposed that BR signalling may play an important role in the modulation of plant immunity and so provides a potential target for manipulation by pathogens during infection. The reduction in symptom development on floral tissues of the *Bdbri1* plants

relative to the NIL suggests that Fg may also exploit BR signalling to aid colonisation of Bd.

On a side note, spray inoculation of BdAA900 Ho and NIL plants with Fusarium at the seedling stage resulted in a severe delay in flower emergence in the inoculated plants compared with the mock controls, regardless of the *BRI1* mutation. This finding, although based on relatively few plants, merits further investigation. Challenge with Fusarium appears to influence plant development. Some of the traits associated with resistance to pathogens and herbivores are known to reduce plant fitness, mostly resistance genes associated with yield penalty (Brown, 2002, Tian *et al.*, 2003). However, little is known about the effect pathogen-triggered defences may exert on plant developmental mechanisms. Additional work is required to confirm this finding and to establish whether treatment with other biotic agents might have similar effects.

4.4.2 *Putative arf2 mutant candidate*

A strong reduction in Fusarium symptom development and secondary conidial production was observed in a novel T-DNA mutant allele of Arabidopsis ARF2 (Chen X, unpublished results). However, further investigation of the effect of ARF2 mutation on the resistance to Fusarium was not carried out due to the poor relevance of the Arabidopsis model system for model-to-crop translation in wheat. This situation supported the choice of investigating a putative T-DNA insertion mutant in Bd21 predicted to be inserted nearby a Bd gene sharing sequence homology with members of the ARF gene family. Analysis of the putative protein domains suggests the Bradi4g07470 gene product contains essential DNA-binding and Auxin-responsive motifs common to members of the ARF gene family that have been described. Also, multiple sequence alignment with the AtARF2 and members of the rice ARF gene family sharing close phylogenetic relationship with AtARF2 sequence shows that the Bradi4g07470 gene product shares highest sequence homology with those gene products. Together, these results suggested that the Bradi4g07470 gene is a likely ortholog of AtARF2. ARF2 has been showed to be a repressor of auxin signalling in Arabidopsis (Lim *et al.*, 2010). Lim and co-workers showed that mutation of AtARF2 causes a highly significant delay in several senescence parameters such as chlorophyll content, photochemical efficiency of photosystem II, membrane ion leakage and expression of senescence-associated genes. Hence, ARF2 mutant leaves exposed to darkness retained over 70% of chlorophyll content while the wild-type plants lost 90% of their chlorophyll after 6 days. The first set of experiments studying the impact of

Bradi4g07470 (putative) gene insertion on the chlorophyll content of leaves *In Planta* and in the DIS test suggested that leaves of the Ho plants retained significantly higher levels of chlorophyll compared to the NIL. However, the repeat DIS experiment investigating all T_3 lines produced during the segregation did not correlate this effect with the Ho lineage. It is interesting to note that, despite statistical significance at 99.9% C.I. from day 3 to day 10 of the experiment, leaves of the NIL plants lost an average of 69.96% chlorophyll compared to 58.06% chlorophyll lost in the leaves of Ho plants. This effect of chlorophyll retention observed in the leaves of BdAA724 Ho plants was relatively marginal compared to the situation reported in Arabidopsis ARF2 mutant. Also, the same effect was not confirmed when investigating all Ho and NIL sister lines in a repeat DIS experiment. Furthermore, every single BdAA724 Ho fixed line investigated showed both Bd21:T-DNA junction specific and wild-type specific bands amplification. Also, despite further attempts to fix Ho and NIL lines from a new batch of T_1 seeds from the Brachy-TAG collection, the same pattern of genotype segregation was observed. The amplification of a wild-type specific band in lines fixed to result in a 100% of GFP-expressing progeny is a difficult result to explain. Hence, lines were fixed on the basis of GFP signal segregation but appeared to retain a functional copy of Bradi2g07470. It appeared that the transformation event resulted in lines containing both a functional copy of Bradi2g07470 and a (possibly truncated) segment of wild-type DNA relating to this locus linked to the T-DNA tag.

4.4.3 *Putative JA-biosynthesis mutant candidates*

Both mutant lines BdAA615 and BdAA700, displayed highly significant reduction in Fusarium symptoms developed on the Ho plants compared to the NIL, in both flower spray inoculation and root infection tests, at all time points. The protein function predicted for the Bd genes Bradi1g11680 (BdAA615) and Bradi4g35336 (BdAA700) relate to different enzymes involved in the early and late steps, respectively, of the biosynthesis pathway involved in the production of the phytohormone JA. Therefore, observation of an enhanced resistance phenotype in the Ho mutants, predicted to be impaired in the production of bioactive form of JA, suggests that JA-signalling may act as a factor of susceptibility to Fusarium infection. Interestingly, the data suggests that JA-induced susceptibility to Fusarium infection is tissue-independent. In the classic understanding of plant-pathogen interactions, JA-mediated defence mechanisms, often coupled with ET-signalling, promote resistance to necrotrophic pathogens, and generally acts antagonistically with the SA-mediated defence mechanisms, which promote resistance to biotrophic and hemi-

biotrophic pathogens (Glazebrook, 2005; Kazan and Manners, 2008). A detailed microscopic study of the infection process of Fg spikelet to spikelet colonisation in wheat heads did not observe evidence that Fg displays a necrotrophic mode of nutrition at the initial stage of infection (Brown *et al.*, 2010). This would support the view that the short asymptomatic phase observed during infection of wheat, Arabidopsis and also Bd, suggests that Fg exhibits a hemi-biotrophic rather than classic necrotrophic life-style (Brown *et al.*, 2010, Peraldi *et al.*, 2011, Kazan *et al.*, 2012).

Interestingly, it was previously shown in Arabidopsis that resistance to Fusarium infection is compromised in mutants impaired in the production or signalling of SA, while resistance was enhanced in mutants impaired in JA-signalling (Makandar *et al.*, 2010). Disruption of SA accumulation in the *sid2* mutant and NahG transgenic plants, as well as disruption of SA signalling in the *npr1* and *wrky18* mutants resulted in increased susceptibility to Fg. Conversely, Makandar and co-workers observed an enhanced resistance in Arabidopsis *opr3*, *coi1* and *jar1* mutants, indicating that the JA-signalling pathway contributes to susceptibility to Fg infection. However, hypersusceptibility to Fusarium infection was observed in the double mutant *jar1 npr1*, suggesting that *JAR1* also contributes to defence, enlightening the contrasting role of JA in this interaction (Makandar *et al.*, 2010). It was recently demonstrated in wheat, that SA accumulation in infected heads contributes to basal resistance to FHB and that simultaneous or prior activation of JA signalling can compromise resistance (Makandar *et al.*, 2012). However, authors also observed that MeJA vapors applied for 24 hours starting two days post-inoculation and later enhanced resistance to FHB in Bobwhite plants. Therefore, authors concluded that JA signalling can also contribute to defence against Fusarium infection. Overall, Makandar and co-workers have compiled a data set that suggests a contrasting role of JA-signalling in resistance to Fusarium infection, playing the role of a susceptibility factor during early stages of infection by mainly antagonizing SA-mediated defence mechanism and promoting resistance at later stages.

Validation of the BdAA615 and BdAA700 mutant lines will be necessary. This will be achieved by genotyping of the NIL and Ho fixed lines using wild-type specific and Bd21:T-DNA junction specific primers adapted to the gene of interest, Bradi1g11680 and Bradi4g35336, respectively. Provided that the protein function of Bradi1g11680 and Bradi4g35336 genes correlates with impaired JA production in the Ho plants compared to the NIL plants of BdAA615 and BdAA700 lines, and that the mutant genotypes are validated by PCR, the Brachypodium-Fusarium pathosystem could provide new insights

on the subtle role played by JA-signalling pathway in resistance to Fusarium. Also, gene expression analysis using quantitative PCR is required to prove that the gene product is expressed in the NIL but not in the Ho fixed line. Finally, quantification of the endogenous JA production by mass spectroscopy should be also performed to demonstrate that Ho plants have reduced JA levels compared to their NIL counterparts, or differ in JA production following challenge with Fg.

The mutant line BdAA466, with the insert lying in the 3' untranslated region of the Bradi2g32190 gene, was originally included in the list of mutant candidates because it had been assessed to share homology with members of the lipoxygenase gene family. However, protein domain prediction and peptide sequence alignment with the five members of the Arabidopsis LOX gene family revealed a poor sequence homology. Rather, EnsemblPlants sequence alignment suggested that the Bradi2g32190 gene product shared homology to the DNA-damage binding protein (DDB1), involved in nucleotide excision repair. No difference was observed between BdAA466 NIL and Ho plants in the flower spray inoculation or the root infection tests indicating that the Bradi2g32190 gene plays no discernible role in resistance to Fg.

4.4.4 *ERF-like mutant candidate*

The flower spray inoculation test performed on BdAA688 NIL and Ho fixed lines resulted in reduced disease severity in the Ho fixed lines compared to the NIL, but no significant difference in necrotic lesion sizes was observed in the root infection test. The difference observed in percentage diseased spikelets on the flowers of NIL compared to Ho plants reduced over time when comparing the disease scores at 5 and 10dpi. Interestingly, the difference in necrotic lesion size developed on the roots of Ho seedlings was slightly higher at 4dpi compared to the roots of NIL seedlings, but was smaller at 6dpi and 8dpi. These results suggest that ET-responsive genes may promote susceptibility to Fusarium in flowers at early stages of infection, whereas playing no significant role at early stages of Fusarium infection the roots. ET-signalling has been demonstrated to play an important role in the regulation of plant's defence response against pathogen and insect attack (Van Loon *et al.*, 2006). Also, it was demonstrated that ET-signalling is exploited by Fg, in both dicotyledonous and monocotyledonous plants, to favour host colonization (Chen *et al.*, 2009). Hence, Chen and co-workers observed that Arabidopsis mutants impaired in ET-signalling or perception were more resistant to Fg infection compared to the wild-type, while mutants with enhanced ET production were more susceptible. The data obtained in

the current study would support the view that ET-signalling plays a role as a susceptibility factor to Fusarium at early stages of floral infection in Bd. However, validation of the BdAA688 candidate line will be necessary to conclude on the effect of Bradi5g17490 on resistance to Fusarium. To do that, genotyping of Ho and NIL fixed lines will be performed to correlate the resistance phenotype observed to the absence of Bradi5g17490 gene transcript due to the T-DNA insertion. Also, it will be necessary to further characterise the Bradi5g17490 gene. This could be achieved in part by monitoring changes in gene expression in response to exogenous ET treatments and determining whether the Ho plants are altered in ET responses like senescence or root/shoot growth.

The data presented and discussed in this chapter provides the first example of functional genetic study using Bd as a model pathosystem to investigate the genetic basis for resistance to Fusarium infection in monocotyledonous plants. A preliminary bioinformatic screen of the Brachy-TAG collection revealed the potential presence of T-DNA insertions disrupting predicted genes homologous to major components of hormonal signalling pathways known to influence disease resistance. The most likely main receptor to BR in Bd, encoded by the Bradi2g48280 gene, was characterised as a proof of concept for T-DNA mutant validation. A short list of mutant candidates relating to Auxin, ET and JA signalling pathways were tested for altered resistance to Fusarium infection in different tissues. Mutant candidate lines BdAA615 and BdAA700, relating to JA-biosynthesis, as well as BdAA688, relating to ET-signalling, showed reduced susceptibility in the Ho mutants compared to their respective NIL control. Further validation of these candidate genes will be needed to confirm the first evidence, to date, of a T-DNA mutation altering Fusarium resistance in Bd. This should be achieved by genotyping of NIL and Ho plants, measurements of endogenous JA levels (for lines BdAA615 and BdAA700), or ET-responsiveness (for line BdAA688) and analysis of corresponding transcript expression.

Chapter 5

Exploiting the *Brachypodium distachyon* root system to study the mechanisms of deoxynivalenol phytotoxicity

5.1 Introduction

Deoxynivalenol (DON) is a polar organic compound belonging to the type B trichothecenes with the chemical name 12,13-epoxy-3α,7α,15-trihydroxytrichothec-9-en-8-on (Nagy *et al.*, 2005). DON is one of the most common contaminants of grains and is also referred to as vomitoxin because of its emetic effects when consumed by animals and humans (Foroud and Eudes, 2008). Among the numerous *Fusarium* species associated with FHB, DON is produced only by *Fc* and some members of the *Fg* species complex (Foroud and Eudes, 2008).

5.1.1 *Cytotoxic effects of deoxynivalenol and related trichothecenes*

Toxic effects of DON have been extensively studied in animal and human systems and can induce a large spectrum of effects, depending on the dosage of toxin used (Rocha *et al.*, 2005, Sobrova *et al.*, 2010). Short-term and sub-chronic exposure to DON cause decrease in body weight, reduced weight gain and feed consumption in mice, rats and pigs, whereas acute exposure can cause shock-like death of mice and ducklings (Rotter *et al.*, 1996, Sobrova *et al.*, 2010). Trichothecenes, including DON, have been shown to produce a diverse range of cytotoxic effects on eukaryotic cells, including inhibition of protein, DNA amd RNA synthesis, inhibition of mitochondrial function, and effects on cell division and membranes (Rocha *et al.*, 2005). The primary toxic effects of DON and other trichothecenes is thought to be mediated via inhibition of protein synthesis in eukaryotes (McLaughlin *et al.*, 1977). DON is understood to inhibit the elongation-termination step of protein synthesis by non-competitive binding of the 60S subunit of eukaryotic ribosomes (Ueno *et al.*, 1985). This process is also known to rapidly activate mitogen-activated protein kinases (MAPKs) and induce apoptosis and is commonly referred to as the "ribotoxic stress response" (Pestka *et al.*, 2004). Trichothecene-producing fungi have an altered ribosomal protein L3 (Rpl3) as a protective mean against the primary effects of trichothecenes on protein synthesis. Harris and Gleddie (2001) showed that modification of the Rpl3 gene conferred tolerance to DON in the cells, tissues and protoplasts of rice.

Similar approaches in wheat and maize showed that expression of an altered Rpl3 increased resistance to FHB and ear rot, respectively (Rocha *et al.*, 2005). Cloning of the *RPL3* gene family in wheat was achieved by Lucyshyn and collegues in 2007 and revealed that the genetic location of the 5A homoeologue of TaRPL3A mapped close to one of the most repeatable QTL conferring resistance to FHB (Qhs.ifa-5A). In addition, DON has been shown to affect mammalian macrophages, T cells and B cells, inducing an immunostimulatory or immunosuppressive effect depending on dose, exposure frequency and timing of functional immune assays (Pestka *et al.*, 2004). Exposure to low concentrations of trichothecenes is able to upregulate expression of cytokines, chemokines and inflammatory genes with concurrent immune stimulation. In contrast, exposure to high concentrations of trichothecenes induces leukocyte apoptosis with concomitant immune suppression (Pestka *et al.*, 2004). Although cytotoxic effects of DON and other trichothecenes have been well characterized using different eukaryotic systems, most studies were performed *in vitro* and relevant studies on the phytotoxic effects of DON are more limited.

5.1.2 *Phytotoxic effects of deoxynivalenol and related trichothecenes*

The toxic effects of DON and other trichothecenes on plant are chlorosis, necrosis and wilting and are usually associated with inhibition of protein synthesis (Lemmens *et al.*, 2005). However, few studies have investigated the mechanisms underlying phytotoxicity of DON *In Planta*. Masuda and co-workers (2007) investigated the effect of DON and other trichothecenes such as T-2 toxin and diacetoxyscirpenol (DAS) in comparison to cycloheximide (CHX), a potent inhibitor of protein synthesis in eukaryotes, on the growth and morphology of *Arabidopsis* seedlings. The authors observed that, although all compounds investigated decreased seed germination in a concentration-dependent manner, CHX was the most potent and DON the least potent inhibitor of Arabidopsis seed germination. Also, all compounds investigated reduced the fresh weight of shoots and inhibited root growth compared to the control treatment. Additionally, they observed inhibition of root growth with concomitant decrease of root hair length induced by DON which could also be induced by T-2. DON alone, however, induced morphological abnormalities in the roots, as observed by a reduction of root cell organization, which were not induced by other compounds (Masuda *et al.*, 2007). DON has been shown to induce the production of hydrogen peroxide (H_2O_2) six hours following infiltration of wheat leaves with 100 mg/L of mycotoxin (Desmond *et al.*, 2008). Authors also showed that H_2O_2

production was later followed by the induction of cell death, 24 hours following DON infiltration, which was associated with DNA laddering, a hallmark of programmed cell death (PCD) in plants and other eukaryotes (Tada *et al.,* 2001). DON infiltration also induced a defence response characterized by the up-regulation of pathogenesis-related (PR) genes 24h following DON treatment. Co-infiltration of DON with ascorbic acid, an anti-oxidant capable of scavenging reactive oxygen species (ROS), was able to reduce both the production of H_2O_2 and the induction of cell death, suggesting that the DON response was at least partially mediated by ROS, known to be signalling molecules in plants (Desmond *et al.,* 2008). However, expression of PR genes following infection of wheat stems with a *tri5* Fg strain was not significantly different from the situation observed with a DON-producing Fg strain suggesting that DON may not be a primary determinant of host defence response during early stages of infection. Treatment of barley leaf segments, stripped of epidermis, with 30 to 90 parts per million (corresponding to approximately 100 and 300 μM, respectively) was able to induce bleaching of the segments incubated in light within 48 to 96h as well as a loss of electrolytes, reduction in chlorophyll a and b and carotenoid contents (Bushnell *et al.*, 2010). However, when leaf segments were incubated with DON in the dark, they remained green but continued to lose electrolytes, indicating that the loss of chlorophyll was due to photobleaching and was a secondary effect of DON, not required for toxicity. In contrast, treatment with low concentrations of DON prevented the gradual reduction in chlorophyll content of detached leaf segments, indicating that DON delayed the senescence induced by detachment of the leaves (Bushnell *et al.,* 2010). It was suggested that DON may play multiple roles during infection, delaying senescence at low concentrations early in infection but inducing bleaching and cell death at higher concentrations later in infection (Bushnell *et al*., 2010).This study provided evidence that DON can induce opposing effects on plant metabolism, potentially relevant to its role in FHB.

5.1.3 *DON is a non-protein effector of Fusarium fungi promoting fungal colonization and spread within host tissues*

Bai and co-workers (2002) first reported that *tri5* mutation in Fg restricts disease symptoms to inoculated spikelets as the fungus did not spread to uninoculated spikelets. It was suggested that DON plays a role in the spread of infection rather than a role in the initial infection. Jansen and co-workers (2005) confirmed using of a Fg *tri5* knockout mutant strain that disruption of trichothecene biosynthesis does not prevent infection but

prevented later movements of the fungus into the rachis because, in the absence of DON, the wheat host developed substantial cell-wall fortifications, preventing the spread of Fg through the rachis into adjacent tissues. Interestingly, the situation in barley differs substantially as *Fusarium* hyphal growth is inhibited at the rachis node and rachilla, irrespective of the ability of the fungus to produce trichothecenes (Jansen *et al.*, 2005). This observation was not associated with development of cell wall thickenings, possibly indicating that the inherent type II resistance displayed by barley relies on a different mechanism. It is now commonly accepted that DON acts as a virulence factor promoting Fg aggressiveness in wheat (Kazan *et al.*, 2012). Understanding that DON has the ability to alter host-cell structure and function to facilitate infection complies with the modern definition of a non-protein effector (Hogenhout *et al.*, 2009).

Significantly, almost all studies to date investigating the mechanisms by which DON may function as a virulence factor, or pathogen effector, employed very high concentrations of mycotoxin mirroring toxin concentrations detected in contaminated grain, at a very late stage of FHB infection rather than the low concentrations that must occur early in infection. Some evidence suggested an active form of transport of DON within host tissues. Snijders and co-workers (1992) were the first to detect the presence of DON ahead of fungal colonization. They observed that DON was transported from the chaff to the young kernel prior to pathogen colonization of the kernel. In the resistant line DON translocation from chaff to kernel was inhibited and little fungal colonization occurred (Snijders et al., 1992). Kang and Buchenauer (1999) studied immunocytochemical localization of DON and 3-acetyl-DON (3-ADON) in Fc infected wheat spikes using two antisera specific to these mycotoxin chemotypes. Authors detected toxins in the cytoplasm, chloroplasts, plasmalemma, cell wall and vacuoles of the host cells, and only sometimes associated with endoplasmic reticulum and ribosomes in the host cytoplasm. Interestingly, ten days following infection, DON was also detected in the tissues of spikelets situated above and below the point of inoculation, in the absence of fungal hyphae. These results led the authors to suggest that DON can be translocated through xylem vessels and phloem sieve tubes (Kang and Buchenauer, 1999). Interestingly, although they were able to detect DON in a variety of sub-cellular compartments, DON was only occasionally associated with cytoplasmic ribosomes. This suggests that inhibition of protein synthesis, via binding of the 60S ribosomal sub-unit, is one but, perhaps, not the only molecular target of DON in plant cells, and would support the hypothesis that DON may have other influences on host metabolism. A recent study investigating the colonization of soft wheat following stem base infection by Fc also provided evidence suggesting a translocation of DON into the

host. Covarelli and co-workers (2012) observed that, although fungal growth was not detected beyond the third node, DON was detected in the last internode and the heads. Authors also observed that the rachis contained higher concentrations of DON than the chaff (lemma and palea tissues) and grain tissues, suggesting that DON may be restricted in its ability to be transported into the heads from the stem. An active form of DON transport within its host would also suggest that the host cellular machinery is able to recognize the molecule and process it through its metabolism. In addition, new evidence suggests that some of the effects induced by DON may involve additional mechanisms of action rather than relying solely on inhibition of protein synthesis.

5.1.4 *A new emerging paradigm: evidence suggesting that DON influences BR homeostasis*

One of the most effective QTL conferring resistance to FHB in wheat, originally termed *Qfhs.ndsu-3BS* and later renamed *fhb1*, was recently associated with the ability to detoxify DON (Lemmens *et al.*, 2005). Lemmens and co-workers (2005) observed that resistant wheat lines carrying the FHB resistance QTL *Qfhs.ndsu-3BS* were able to convert DON into DON-3-O-glucoside as the detoxification product. Poppenberger and co-workers (2003) first demonstrated glycosylation of DON in Arabidopsis where they showed that the UDP-glycosyltransferase UGT73C5 catalysed the transfer of glucose to the hydroxyl group at carbon 3 of DON and by doing so induce tolerance to the toxin. Further investigation of the physiological role of Arabidopsis UGT73C5 revealed that this enzyme also catalyses 23-*O*-glucosylation of the BR hormone brassinolide (BL) and castasterone, a precursor of BL, is involved in the regulation of BR homeostasis (Poppenberger *et al.*, 2005). However, these authors commented that plant UGTs are thought to recognize a wide range of substrates and mammalian UGTs involved in steroid hormone glucuronylation are also known to function in detoxification processes. As, the nature of the endogenous substrate or substrates of UGT73C5 in plants is currently unknown, it is justified to question the role UGT73C5 may play regarding BR homeostasis. Nevertheless, this series of studies established the first link between mechanisms of DON detoxification and BR homeostasis in plants. An additional study of the effect of trichothecenes on Arabidopsis by Masuda and co-workers (2007) showed that T-2 toxin, which is closely related to DON, was able to induce a defence response and up-regulated *AtST1* gene which is a homolog of *Brassica napus* BR sulfotransferase 3 gene (*BnST3*) involved in the inactivation of BR activity. These authors also observed that the AtHB5 gene, a homeodomain-leucine zipper (HDZip) transcription factor that is a positive regulator of ABA-responsiveness, was up-regulated

by T-2 treatment whereas it was down-regulated in BR-treated wild-type plants and *det2* mutants (Goda *et al.*, 2002). The phenotype displayed by Arabidopsis plants treated with T-2 toxin resembles that of BR-deficient mutants which display similar morphological and growth defects, suggesting that T2 may interfere with BR biosynthesis or signalling. Interestingly, Gardiner and co-workers (2010) found that injection of DON into barley spikes induced an up-regulation of Contig7290_at which was annotated as brassinosteroid insensitive 1-associated receptor based on analysis of sequence homology.

Unpublished results produced by Steed A. (JIC) characterized the effect of low concentrations of DON on the growth of Arabidopsis roots. Root growth of Columbia-0 seedlings incubated on 6.75 μM DON containing media were slightly shorter than the control seedlings but the difference was not significant (p-value = 0.087). Seedlings incubated on 10.125 μM DON containing media were only 37.84% (s.e. = 1.891) of the control length, a significant reduction in growth (p-value < 0.001, Figure 5.1).

Interestingly, the roots of seedlings grown on 6.75 μM DON, although not significantly differing for length, displayed waving roots, interpreted as an alteration of the gravitropic response, which will be referred to as "root waving" (Figure 5.1c compared to 5.1b), this effect was also observed on roots grown on 10.125 μM DON (results not shown). Steed A. then observed that treatment with 0.25 μM epibrassinolide (eBL) was able to significantly reduce root growth (results not shown) and induce an alteration of root gravitropism reminiscent of the "root waving" effect induced by DON (Figure 5.1c compared to 5.1b). Inhibition of root growth by DON was previously reported in Arabidopsis (Masuda *et al.*, 2007), although alteration of the root gravitropism was not. Interestingly, the "root waving" phenotype was observed at DON concentrations lower than the levels of mycotoxin inducing inhibition of root growth.

The At root waving phenotype has been extensively described in the literature and, although the mechanisms underlying this phenomenon remain elusive, gravitropism is considered a major driving force behind this phenotype (Santner and Wateson, 2006). The work by Santner and Wateson (2006) on the WAG1 and WAG2 protein kinases suggested a link between root waving and auxin distribution in the roots of At. Authors observed that both *wag1* and *wag2* mutants displayed an enhanced root waving phenotype when grown on solid agar, further enhanced in the double knock-out mutant. When grown on media containing the inhibitor of auxin transport N-1-naphthylphthalamic acid (NPA), the double mutants were observed more resistant to the inhibitory effect of NPA on root curling. This

result, together with the fact that the *WAG* promoters are most active in the root tips, led authors to suggest that auxin transport may be affected in the *wag* mutants.

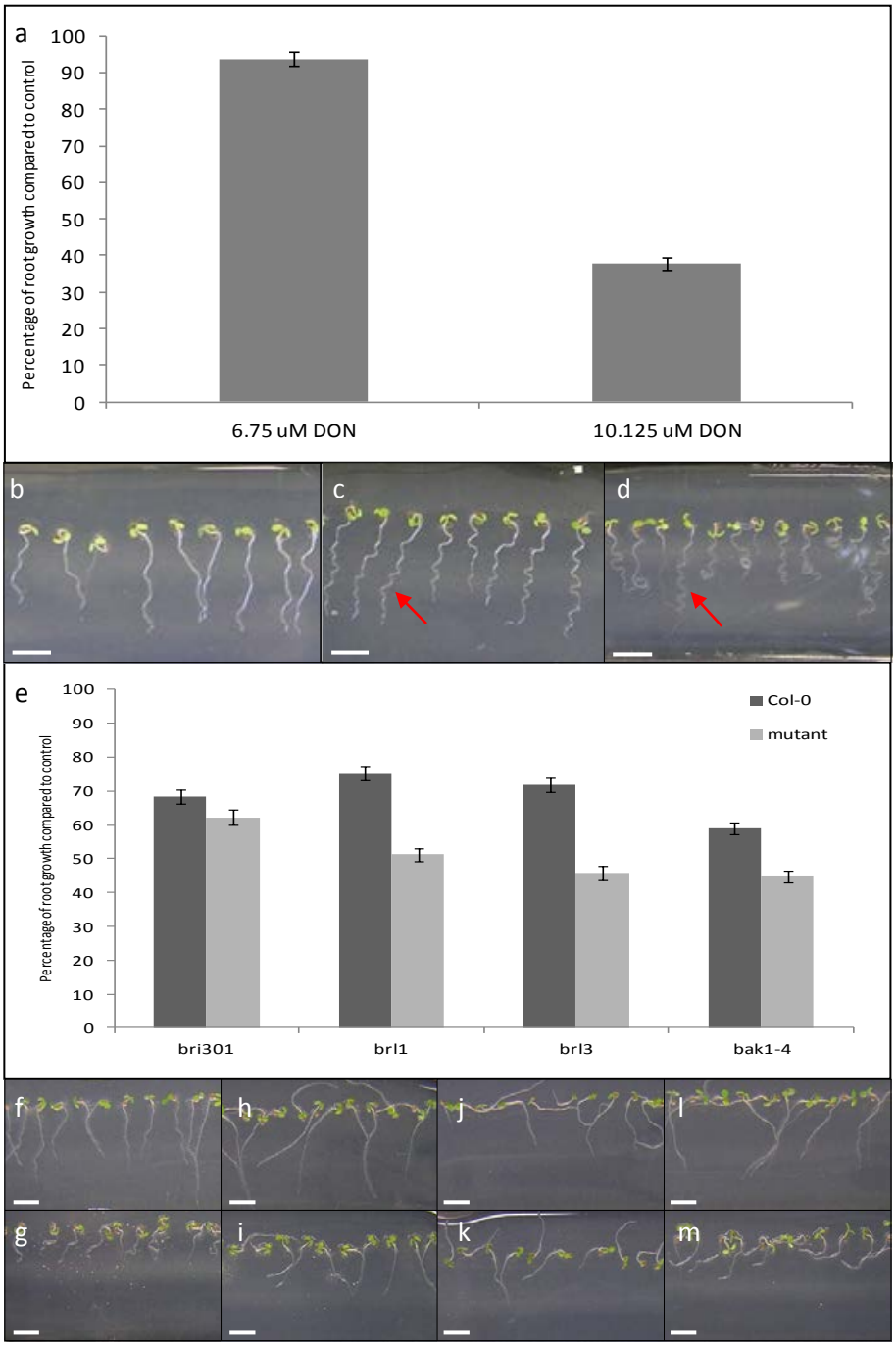

Figure 5.1: Effect of deoxynivalenol (DON) and epibrassinolide (eBL) treatments on the growth of Arabidopsis roots. a) Columbia-0 (Col-0) percentage of primary root growth induced by 6.75 and 10.125 µM DON treatment, 7 days post-germination (dpg). b) Col-0 control roots. c) 6.75 µM DON. d) Col-0 roots grown on 0.25 µM eBL. b-d) Arrow indicates "root waving". e) Comparison of 6.75 µM DON treatment compared to the control treatment, of *Arabidopsis* Col-0, *brassinosteroid-insensitive (bri) 1*, *bri1-associated kinase (bak) 1-4*, *bri1-like (brl) 1* and *brl3* seedlings, 7 dpg. f-m) Effect of DON on the gravitropism of Col-0, *aux1-1*, *axr2-1* and *axr4-1* mutants, 4dpg. f) Col-0 control, g) Col-0 response to DON, h) *aux1-1* control, i) *aux1-1* response to DON, j) *axr2*-1 control, k) *axr2*-1 response to DON, l) *axr4-1* control, m) *axr4-1* response to DON.

Arabidopsis mutants defective in one of the three BR-receptors characterized *bri301*, *brl1* and *brl3*(BRI1, BRL1 (BRI-1-like) and BRL3, respectively), as well as *bak1-4*,the BRI1-associated kinase (BAK) 1, were characterized for their response to DON treatment. Roots of *bri301* seedlings grown on 6.75 μM DON reached 62.23% (s.e. = 2.174) of the control compared to the 68.24% (s.e. = 2.134) of root growth inhibition displayed by Col-0 (Figure 5.1e). DON-induced inhibition of root growth of *bri301* seedlings was not significantly different (p-value = 0.051) from the root growth inhibition displayed by Col-0 seedlings, although this difference was very close from statistical significance at 95% C.I.. Roots of the *brl1* seedlings grown on 6.75 μM DON reached 51.2% (s.e. = 2.018) of the control compared to the 75.33% (s.e. = 2.117) of root growth inhibition displayed by Col-0 (Figure 5.1e). DON-induced inhibition of root growth displayed by *brl1* seedlings was significantly greater (p-value < 0.001) than that of Col-0 seedlings. Roots of the *brl3* seedlings grown on 6.75 μM DON reached 45.77% (s.e. = 2.014) of the control compared to the 71.87% (s.e. = 1.988) of root growth inhibition displayed by Col-0 (Figure 5.1e). DON-induced inhibition of root growth displayed by *brl3* seedlings was significantly greater (p-value < 0.001) than that of Col-0 seedlings. Roots of the *bak1-4* seedlings grown on 6.75 μM DON reached 44.74% (s.e. = 1.71) of the control compared to the 58.99% (s.e. = 1.727) of root growth inhibition displayed by Col-0 (Figure 5.1e). DON-induced inhibition of root growth displayed by *bak1-4* seedlings was significantly greater (p-value < 0.001) than that of Col-0 seedlings. Interestingly, all *bri301*, *brl1*, *brl3* and *bak1-4* seedlings also displayed a DON-induced "root waving" phenotype (A. Steed personal communication).

A. Steed further tested Arabidopsis mutants defective in molecular components involved in other phytohormone-signalling pathways, such as abscisic acid (ABA), ET, cytokinin (CK), JA, SA, BR and gibberellic acid (GA), to test whether the DON-induced "root waving" could be altered. Three mutants defective in auxin transport and or signal transduction were characterized for their inability to display the DON-induced "root waving" phenotype. Arabidopsis *aux1-1* mutant, impaired in auxin influx transport, *axr2*,impaired in the repression of auxin-inducible gene expression and playing a role in the control of gravitropic growth, and *axr4-1*, an auxin resistant mutant defective in appropriate localisation of AUX1, were all unable to develop the "root waving" phenotype (Figure 5.1f-m). A similar level of DON-induced inhibition of root growth was observed in all four auxin mutants compared to the situation observed in the control, although marginal differences were observed across different experiments (A. Steed personal

communication). These results imply that alteration of Arabidopsis root gravitropism caused by DON is probably mediated via perturbations of auxin distribution in the roots.

This chapter aimed to investigate the mechanisms of action of DON *In Planta* The hypothesis that DON may function as a non-protein effector manipulating the host hormonal signalling and/or homeostasis to promote fungal colonisation has been tested using a chemical and genetic approach. This approach is inspired from the At root system, which has been used to characterise which hormonal signals were in control of the root growth and developmental programs as well as identifying the key genetic elements involved in those regulations. The effects induced by DON treatment on Bd were investigated using the root system and the influences of the mycotoxin on well characterized hormonal responses were characterized. This approach enables dissection of the different hormone-signalling pathways influenced by the mycotoxin, focusing especially on the involvement of BRs, in order to decipher the mechanisms of DON phytoxicity.

5.2 Material and Methods

5.2.1 *Brachypodium lines and growth conditions*

Brachypodium distachyon inbred lines Bd21 (Vogel *et al.*, 2006) were used throughout. Bd seeds were germinated and incubated for 5 days in Petri dishes on damp filter paper in the dark at 5°C. Seed were then incubated at 20°C for 24 h exposed to a 16 h/8 h light-dark cycle for 24 h prior incubation with treatments.

5.2.2 *Brachypodium root growth assays*

Sixteen to twenty Bd21 WT seedlings were placed in 150 x 45 mm in diameter opened top plastic tubes containing 0.5 % agar-agar media, amended with the different treatments used, and incubated in a tray with a plastic cover at 22°C for 3 to 5 days, depending on the experiment, under a 16 h/8 h light-dark cycle (300 µmol m^{-2} s^{-1}). On the day experiment was terminated, seedlings were delicately removed with tweezers, laid flat and photographed (Olympus digital camera 4-15C, Olympus Tokyo, Japan). A total of seven experiments, each treatment tested in three replicates, investigated the effect of 0, 0.675, 6.75 and 67.5 µM DON (CAS number: 51481-10-8) following 5 days incubation. A single experiment tested the effect of 0.001, 0.01, 0.1 and 1 µM epibrassinolide (eBL) and indole-

3-acetic acid (IAA, Sigma-Aldrich, CAS number: 78821-43-9 and 6505-45-9, respectively) treatments, amended with 0.01% (1:1 H_2O) ethanol, after 5 days incubation. The effect of long term storage at -20°C of an eBL stock, repeatedly thawed over the course of two years, was tested in comparison with a freshly purchased stock of eBL. The experiment investigated the effect of 0, 0.001, 0.01, 0.1, 1 and 10 μM of 'old' compared to 'fresh' eBL stocks, amended with 0.26% ethanol, after 3 days incubation. Two independent experiments compared the effect of 0, 0.675, 6.75 and 67.5 μM DON, 0.001 and 0.01μMeBL treatments with combination treatments of 0.001 μM eBL with 0.675 and 6.75 μM DON and 0.01 μM eBL with 0.675, 6.75 and 67.5 μM DON. Each treatment was amended with 0.001% ethanol and tested in three replicates after a period of 5 days incubation. A single experiment investigated the effect of 0, 0.01, 0.1, 1, 10 and 100 μM brassinazole (BRZ, Tokyo Chemical Industry Co. LTD, Tokyo, Japan; CAS number: 224047-41-0), an inhibitor of brassinosteroids biosynthesis in plants, amended with 0.016% dimethyl sulfoxide (DMSO, Sigma-Aldrich, CAS number: 67-68-5) after 4 days incubation. A single experiment investigated the effect of 0, 0.005, 0.05, 0.5, 5 and 50 μM BIK (Sigma-Aldrich, CAS number: 188011-69-0), a nonsteroidal molecule able to activate the BR-signalling pathway down-stream of the BRI1 receptor in Arabidopsis (De Rybel *et al.*, 2009), amended with 0.273% DMSO, after 5 days incubation. Two repeat experiments which compared the effect of 0.05, 0.5, 5 and 50 μM DON with similar concentrations of cycloheximide (CHX, Sigma-Aldrich, CAS number: 66-81-9), a potent inhibitor of protein synthesis in eukaryotes, and T-2 toxin (Sigma-Aldrich, CAS number: 21259-20-1) after 4 days incubation. A single experiment compared the effect of 0.01 μM eBL and 1 μM CHX treatments with a combination of 0.01 μM eBL plus 1 μM CHX, each amended with 0.001% ethanol, after 4 days incubation. A repeat experiment compared the effect of 0.5, 5 and 50 μM treatment with DON or CHX after 5 days incubation, all treatments tested in three replicates. A single experiment investigated the interaction between 5 μM BIK and 6.75 and 67.5 μM DON treatments alone and in combination, after 3 days incubation. A similar experiment was performed to compare the effect of 5 μM BIK and 5 and 50 μM DON alone and in combination with 5 and 50 μM CHX alone and in combination with 5 μM BIK.

5.2.3 *Leaf unrolling assay*

Brachypodium seeds of Bd21 ("wt", wild-type), BdAA900 "Ho" mutant plants (homozygous for the T-DNA insertion in the *BRI1* gene, Bradi2g48280) and BdAA900

"nil" plants (not containing a T-DNA insertion) were germinated in the dark at 5°C on damp filter paper for 5 days. Seedlings were then transferred onto 0.8% (w/v H2O) agar plates and grown at 20°C in the dark for 7 days. Under these growth conditions the resulting seedlings were etiolated with rolled leaves. Under green light (500-550 nm wave length), 4mm (±1mm) sections were cut from the central portion of the first emerging etiolated leaf of each seedling and incubated in the dark for 48 to 72h in the different solutions. In a first experiment, etiolated leaf sections of Bd21 WT, BdAA900 NIL and BdAA900 Ho plants were incubated in solutions containing 0, 0.00675, 0.0675, 0.675, 6.75 and 67.5 μM DON (CAS number: 51481-10-8) for 48 hours. In a second experiment, etiolated leaf sections of Bd21 WT were incubated in solutions containing 0, 0.1 μMeBL, 6.75 μM DON, 67.5 μM DON, 6.75 μM DON with 0.1 μMeBL and 67.5 μM DON with 0.1 μMeBL for 72h . All solutions not containing eBL were amended with 0.001% (v/v H_2O) ethanol. In a third experiment, etiolated leaf sections of Bd21 WT were incubated in solutions containing 0, 0.1 μMeBL, 1 μM CHX, 10 μM CHX, 1 μM CHX with 0.1 μMeBL and 10 μM CHX with 0.1 μMeBL for 72h. All solutions not containing eBL were amended with 0.001% (v/v H_2O) ethanol. Leaf sections were photographed after 48 to 72h incubation and the extent of leaf unrolling was assessed using Image-J software.

5.2.4 *Light microscopy*

Root sections from Bd21 WT plants were stored in lactoglycerol (1:1:1) solutions. Samples were mounted in 40% glycerol, viewed with a Nikon Eclipse 800 microscope and photographed with a Pixera Pro ES 600 digital camera.

5.2.5 *Confocal microscopy*

Bd21 WT root sections, mounted in 40% glycerol, were analysed under a Leica SP5 (II) confocal microscope excited by a 405 nm laser diode and autofluorescence of cell walls was detected at 600-700 nm.

5.2.6 *Statistical analysis*

The length of primary roots, percentage of root growth compared to control and etiolated leaf width data were analysed by generalised linear modelling (GLM) using the software

package GENSTAT version 11.1 (Lawes Agricultural Trust, Rothamsted Experimental Station, UK). Individual treatments were compared with the appropriate controls using the unpaired t-tests within the GLMs.

5.3 Results

5.3.1 *The effect of differing concentrations of DON on root growth of Bd*

A total of seven independent experiments investigated the effect of low DON concentration treatments on the primary root growth of Bd21 WT seedlings. Bd roots grown on media containing DON concentrations less than 0.675 μM DON appeared to be unaffected and grow in a manner similar to the un-treated control seedlings (results not shown). Roots grown on concentrations between 0.67 and 6.75 μM DON, however, exhibited a stimulation of root growth. Roots grown on 0.675 μM DON reached 110% (s.e. = 1.715) of the growth of control seedlings, displaying a significant (p-value = 0.005) increase in primary root growth (Figure 5.2a). Roots grown on 6.75 μM DON reached 139% (s.e. = 1.536) of the control growth, displaying a significant (p-value < 0.001) increase in primary root growth. At higher concentrations of DON, root growth was generally inhibited. Roots grown on 67.5 μM DON reached 70.1% (s.e. = 1.658) of the growth of control seedlings, displaying a significant (p-value < 0.001) reduction in primary root growth. Interestingly, the shape of Bd roots grown on 6.75 and 67.5 μM DON was straighter than those grown on control medium (Figure 5.2d-e compared to 5.2b-c). Additionally, the production of root hairs on the roots of DON-treated seedlings was compared to the controls under a normal light microscope (Figure 5.2f-i). Increasing concentrations of DON (Figure 5.2g,h and i) reduced both the length and density of root hairs compared to the untreated roots (Figure 5.2f).Also, cortical cells of roots grown on 6.75 and 67.5 μM DON appeared to be longer than those observed on the roots of controls and seedlings grown on 0.675 μM DON (Figure 5.2h-i compared to 5.2f-g). Alteration of cortical cells length appeared correlated with a reduction in the root diameter at 6.75 and 67.5μM DON compared to the control roots (Figure 5.2h-i compared to 5.2f-g). However, measurements of the root hair length and frequency, length of cortical cells and root diameter was not undertaken.

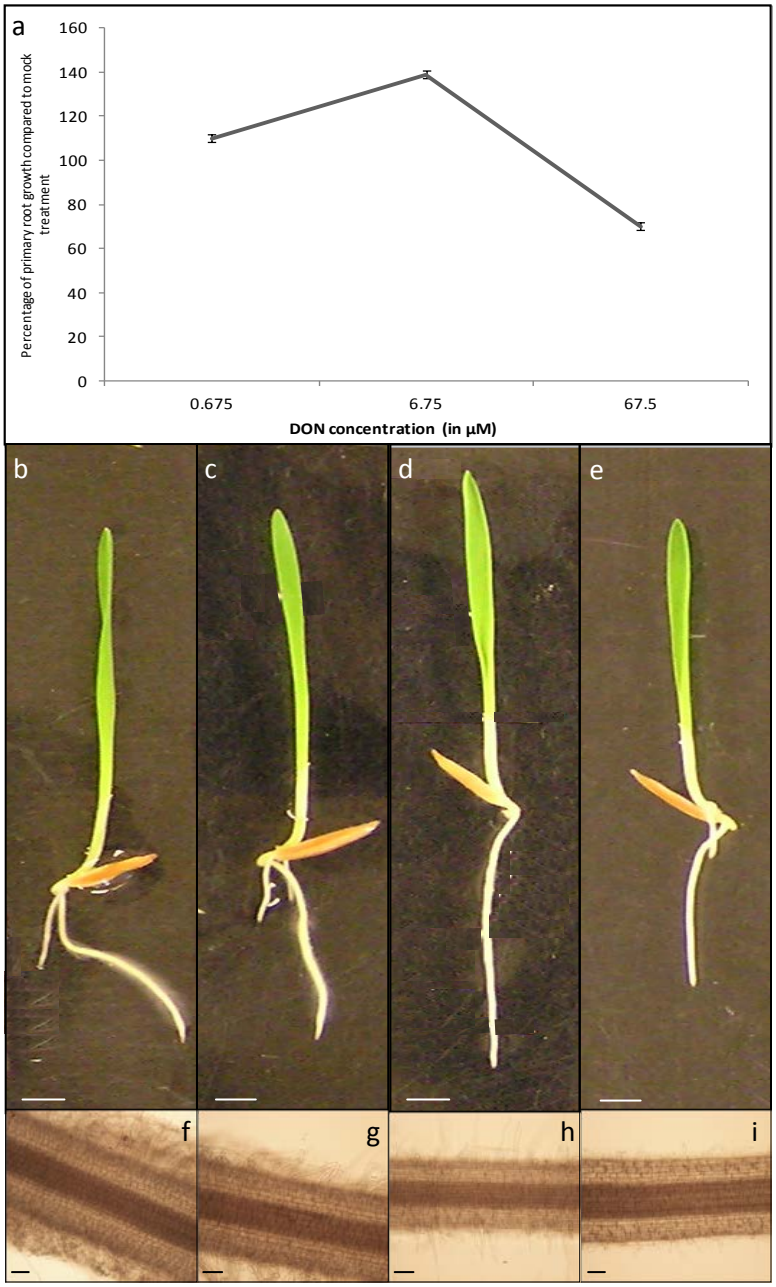

Figure 5.2: DON treatment effects on the primary root growth, gravitropism and root hair elongation of *Brachyodium* seedlings, 5 days following incubation (dpi). a) primary root growth of Bd21 seedlings, compared to the control treatment. Bars indicate standard errors. b-e) Representative images showing the effect of DON treatments on the gravitropism of Bd21 seedling. b) control c) 0.675 µM DON. d) 6.75 µM DON. e) 67.5 µM DON. b-e) Scale bars = 2.5 mm. f-i) Light microscope images showing the effect of DON treatments on the elongation of *Brachypodium* root hairs. f) control. g) 0.675 µM DON. h) 6.75 µM DON. i) 67.5 µM DON. f-i) Scale bars = 100 µm.

5.3.2 *Effect of epibrassinolide and auxin (IAA) on root growth of Bd*

The unpublished work of A. Steed had indicated that the altered root growth induced by DON mimicked that induced by eBL. Furthermore, the findings relating to the auxin transport mutants suggested that auxin distribution might be involved in this phenomenon.

For these reasons it was decided to examine how eBL and auxin (IAA) influenced root growth of Bd. Bd 21 WT seedlings were grown on increasing concentrations of eBL and IAA to characterize their response to these phytohormones. The primary root growth of Bd21 seedlings grown on eBL was significantly increased (p-value < 0.001) compared to that of controls at all concentrations tested. The roots of Bd21 seedlings grown on 0.001 μM eBL reached 129.2% (s.e. = 4.129) of the control root growth, 159.2% (s.e = 4.129) when grown on 0.01 μM eBL, 165.6% (s.e. = 4.129) on 0.1 μM eBL and 178.9% (s.e. = 4.478) on 1 μM eBL (Figure 5.3a). Stimulation of the primary root growth induced by eBL treatment was accompanied with a "root waving" phenotype compared to the controls, interpreted as an inhibition of the root gravitropism (results not shown). Interestingly, a decrease in the length and density of root hairs was observed on roots grown on 0.1 and 1 μM eBL compared to the control roots and those grown on 0.001 and 0.01 μM eBL (Figure 5.3d-e compared to 5.3b-c). Also, the diameter of roots grown on 1 μM eBL appeared to be reduced in comparison of the diameter of the controls, and appeared correlated with an increase in the length of cortical cells.

No significant difference with the controls was observed in the root growth of seedlings grown on 0.001 and 0.01 μM IAA (p-value = 0.421 and 0.932, respectively), but treatments with 0.1 and 1 μM IAA significantly reduced primary root growth compared to the controls (p-value < 0.001). The roots of Bd21 seedlings grown on 0.001 μM IAA reached 102.9% (s.e. = 4.129) of the control root growth, 96.4% (s.e.= 4.129) when grown on 0.01 μM IAA, 69.6% (s.e.= 4.129) on 0.1 μM IAA and 42.3% (s.e.= 4.129) on μM IAA (Figure 5.3a). The length and density of root hairs on IAA-treated roots appeared to be increased at 0.01, 0.1 and 1 μM IAA compared to the situation observed on the control roots and 0.001 μM IAA (Figure 5.2g-i compared to 5.2f). Also, the diameter of IAA treated roots appeared to increase and the length of cortical cells to decrease with increased IAA concentration (Figure 5.2h-i compared to 5.2f-g). No alteration of the gravitropism of roots was observed in response to IAA treatments (results not shown).

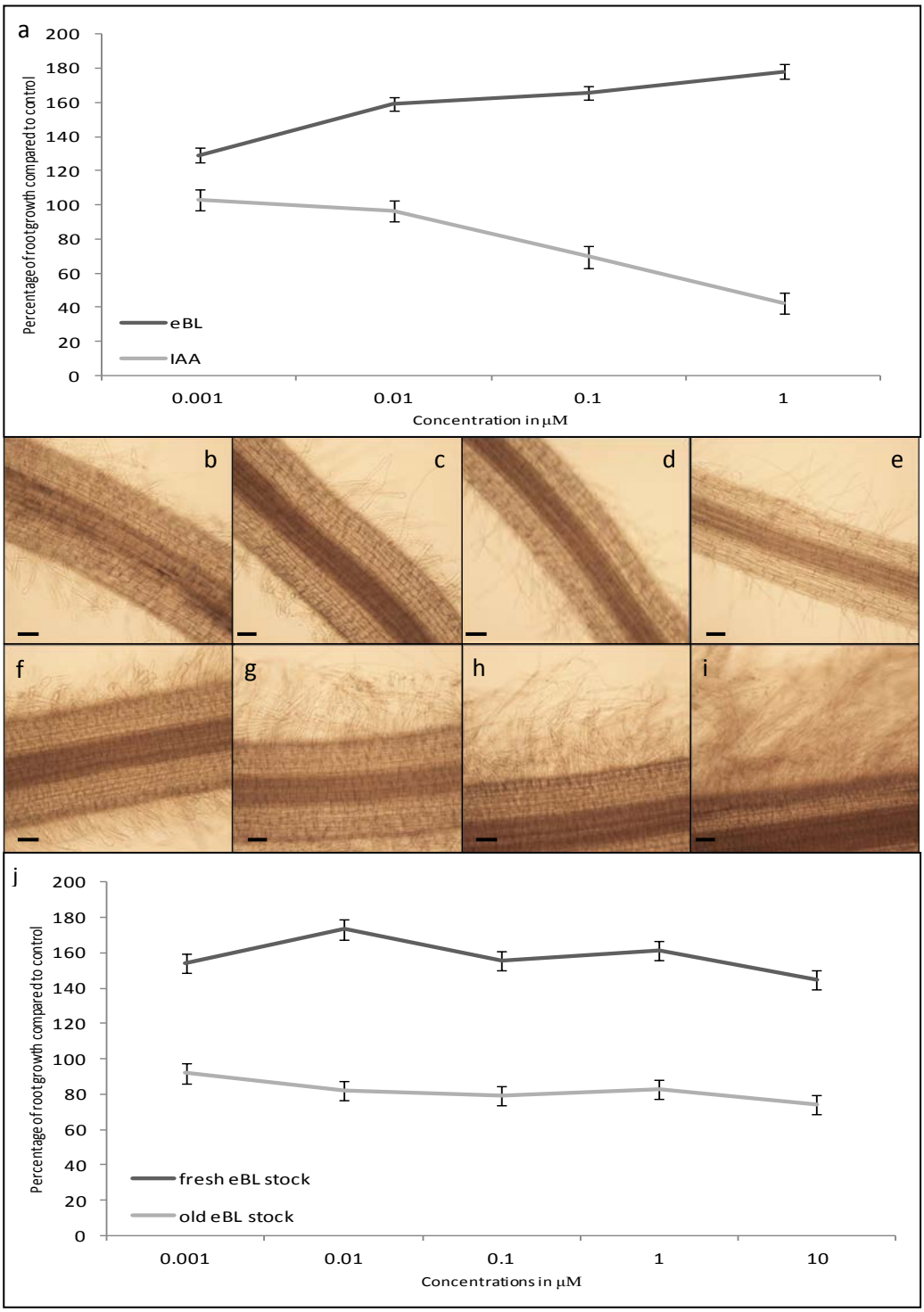

Figure 5.3: eBL and indole-3-acetic acid (IAA) treatments effects on the primary root growth and root hair elongation of *Brachyodium*. a) Effects of 0.001, 0.01, 0.1 and 1 µM eBL and IAA treatments on Bd21 seedlings, 5 dpi. b-e) Inhibitory effect of eBL treatment on the root hair elongation of Bd21: b) 0.001 µM eBL, c) 0.01 µM eBL, d) 0.1 µM eBL and e) 1 µM eBL. f-i) Stimulatory effect of IAA treatment on the root hair elongation of Bd21: i) 0.001 µM IAA, g) 0.01 µM IAA, h) 0.1 µM IAA and i) 1 µM IAA. b-i) Scale bars = 100 µm. j) Comparison of fresh and old stocks of eBL on the percentage of primary root growth of Bd21, 3dpi. Bars indicate standard errors.

5.3.3 *The influence of storage on the effects of epibrassinolide on root growth of Bd*

It was noted, however, that the extent of the response of primary root growth treated with similar concentrations of eBL differed across independent experiments (results not shown). Therefore, a freshly purchased stock of eBL was tested in comparison to an older eBL stock, which had been previously used and thawed several times over the course of two years. In addition, the effect of high concentration of eBL, beyond 1 μM, was investigated. Primary root growth of Bd21 seedlings treated with a fresh stock of eBL was significantly increased relative to that of untreated seedlings (p-value < 0.001) at all concentrations investigated. The roots of Bd21 seedlings grown on 0.001μM of fresh eBL stock reached 153.9% (s.e. = 5.535) of the control root growth, 173.2% (s.e. = 5.535) when grown on 0.01 μM of fresh eBL, 155.3% (s.e. = 5.535) on 0.1 μM, 161.1% (s.e. = 5.535) when grown on 1 μM and 144.8% (s.e. = 5.535) when grown on 10 μM of fresh eBL stock (Figure 5.3j). In contrast, roots grown on 0.001 μM of 'old' eBL stock were reduced in length compared to controls (91.9%, s.e. = 5.535) although this was not significantly different (p-value = 0.52).When grown on higher concentrations of the 'old' eBL stock, root growth was increasingly inhibited with increasing concentrations: 82% (s.e = 5.535) on 0.01 μM (s.e. = 5.535), 79.1% (s.e. = 5.535) on 0.1 μM, 82.6% (s.e. = 5.535) on 1 μM and 74.2% (s.e. = 5.251) when grown on 10 μM an old eBL stock (Figure 5.3j). The primary root growth of seedlings grown on 0.01, 0.1, 1 and 10 μM of old eBL stock was significantly reduced (p-value = 0.027, 0.008, 0.035 and < 0.001, respectively) compared to the controls. Noticeably, the roots grown on fresh stock of eBL displayed the "root waving" effect, but this phenotype was not observed on the roots grown on 'old' stock of eBL, which appeared straighter compared to the controls (results not shown).

5.3.4 *The effect of combinations of brassinosteroids and DON on root growth of Bd*

The similarity in aspects of root growth induced by DON and eBL led to conduct experiments in which roots of Bd21 were exposed to combinations of these two compounds. The effect on Bd21 root growth induced by DON and eBL treatment alone was compared with treatments of DON and eBL in combination. As for previous experiments, DON stimulated root growth at concentrations up to 6.75 μM but inhibited growth at higher concentration (67.5 μM). The roots of Bd21 seedlings grown on 0.675 μM DON reached 105.9% (s.e. = 1.442) of the control root growth, 141.5% (s.e. = 1.378) on 6.75 μM DON and 85.6% (s.e. = 1.719) when grown on 67.5 μM DON (Figure 5.4). Both 0.001 and 0.01 μM eBL stimulated root growth. Root growth of seedlings grown on 0.001 μM eBL reached 119.1% (s.e. 2.255) of the control root growth and 210.4% (s.e. =

6.093) when grown on 0.01 µM eBL (Figure 5.4). The combination of 0.001 µM eBL with 0.675 µM DON (119.2%; s.e. = 2.198) was not significantly different (p-value = 0.98) from that induced by 0.001 µM eBL treatment alone. Roots grown on 0.001 µM eBL combined with 6.75 µM DON were significantly (p-value < 0.001) longer than those grown on either compound alone. Roots reached 147.9% (s.e. = 1.289) of the control root growth (Figure 5.4). Roots of seedlings grown on combinations of 0.01 µM eBL combined with either 0.675 or 6.75 µM DON were significantly reduced in length compared to those treated with 0.01 µM eBL alone. Roots grown on 0.01 µM eBL combined with 0.675 µM DON reached 187% (s.e. = 4.289) of the control root growth, a significant (p-value < 0.001) reduction in stimulation of the root growth induced by 0.01 µM eBL treatment alone, but a significant (p-value < 0.001) increase in stimulation of the root growth induced by 0.675 µM DON treatment alone. Roots grown on 0.01 µM eBL combined with 6.75 µM DON reached 186.7% (s.e. = 3.561) of the control root growth, a significant (p-value < 0.001) reduction in stimulation of the root growth induced by 0.01 µM eBL treatment alone, but a significant (p-value < 0.001) increase in stimulation of the root growth induced by 0.675 µM DON treatment alone. The combination of 0.01 µM eBL plus the highest concentration of DON (67.5µM) inhibited root growth more than DON alone. The roots of seedlings grown on 0.01 µM eBL combined with 67.5 µM DON reached 72% (s.e. = 1.8) of the control root growth, a significantly greater (p-value < 0.001) reduction in root growth than that induced by 67.5 µM DON treatment alone.

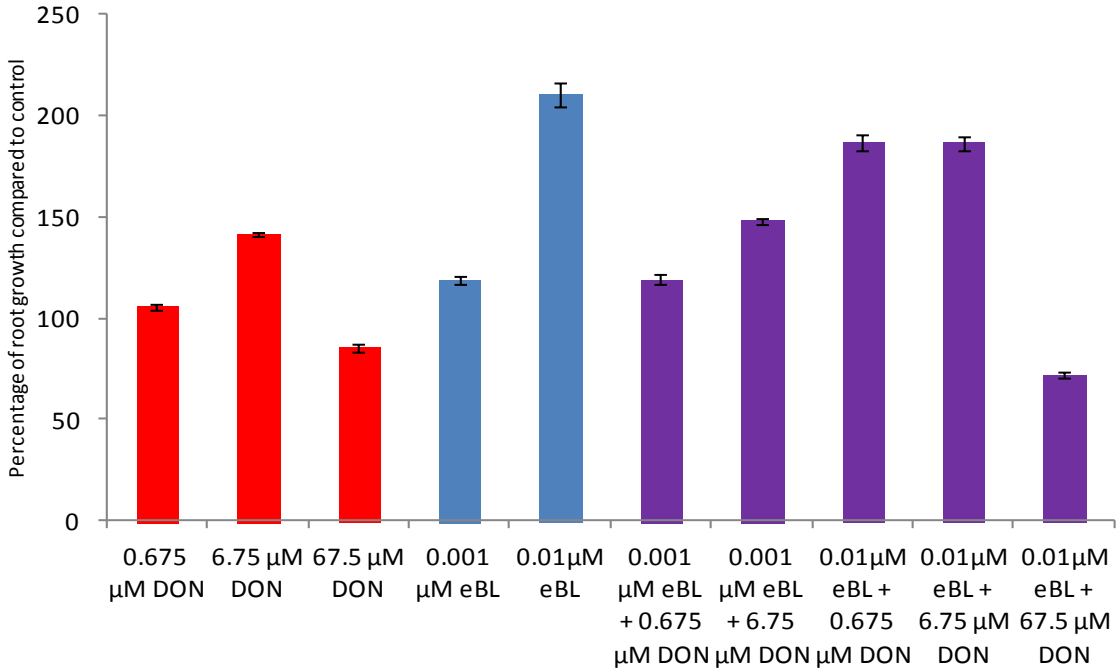

Figure 5.4: Effect of 0.675, 6.75 and 67.5 µM DON, 0.001 and 0.01 µM eBL and combination of DON and eBL treatments on the percentage of primary root growth of Bd21 seedlings, compared to the control treatment, 4dpi. Bars indicate standard errors.

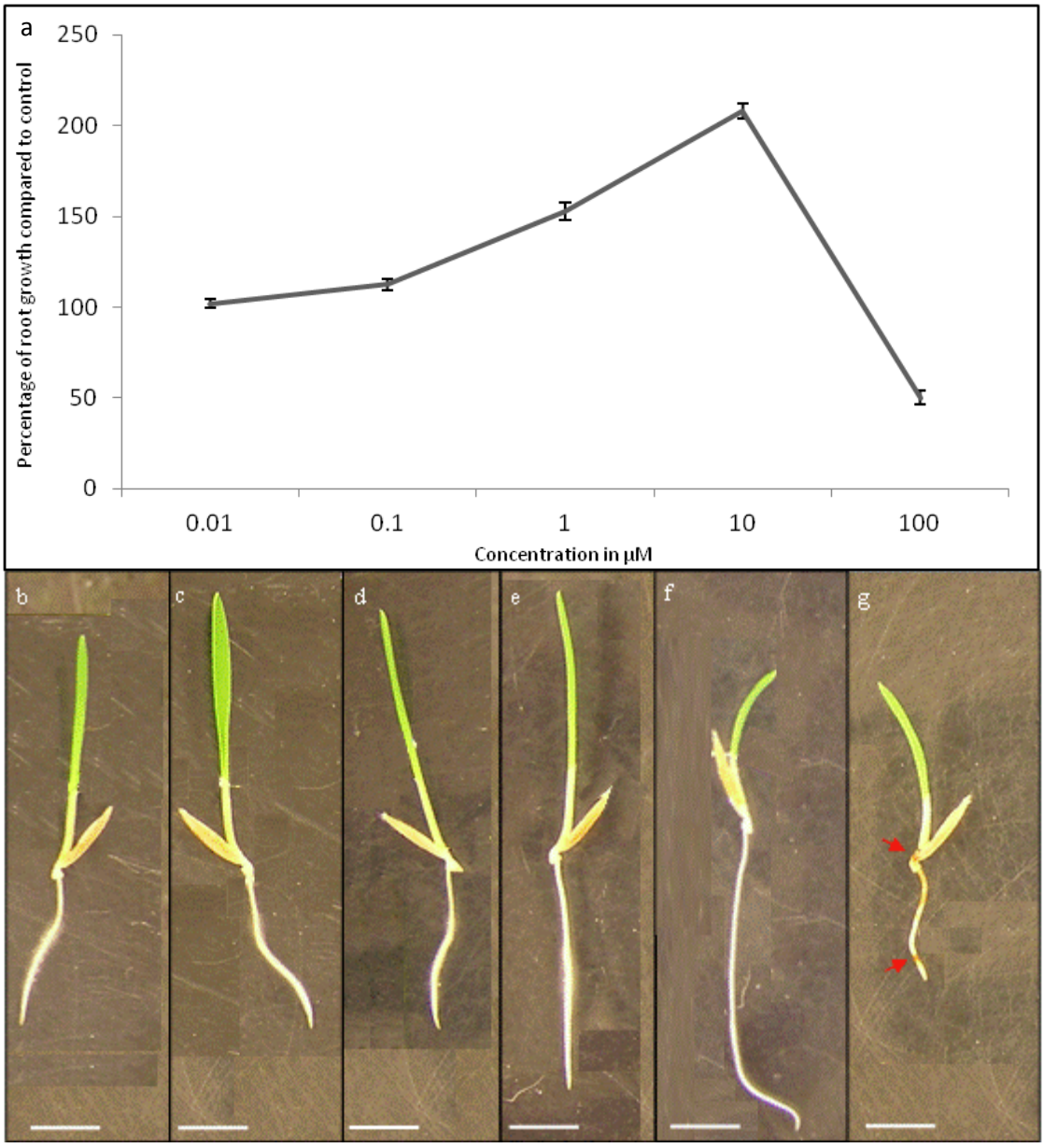

Figure 5.5: Brassinazole (BRZ) treatments effects on the primary root growth and gravitropism of *Brachypodium*. a) 0.01, 0.1, 1, 10 and 100 µM of BRZ treatments on Bd21, 4 dpi. Bars indicate standard errors. b-g) BRZ treatments on the gravitropism of Bd21, 4dpi. b) Bd21 control. c) 0.01 µM BRZ. d) 0.1 µM BRZ. e) 1 µM BRZ. f) 10 µM BRZ. g) 100 µM BRZ. Arrows indicate amber-brown colouration at the base and tip of the root. Scale bars = 2.5 mm.

5.3.5 *The effect of an inhibitor of brassinosteroids biosynthesis on root growth of Bd*

In the above experiment, the addition of DON generally antagonised the stimulation of root growth induced by eBL suggesting that DON might be inhibiting responses to eBL or

inhibiting BR biosynthesis. To further characterize the response of Bd root growth to BRs, the effect of an inhibitor of BR biosynthesis, brassinazole (BRZ), was investigated. Low concentrations of BRZ (0.01 and 0.1 μM) did not significantly affect root length. The roots of Bd21 seedlings grown on 0.01 or 0.1 μM BRZ reached 101.7% (s.e. = 2.409) and 112.4% (s.e. = 2.868) of the untreated root growth respectively, results which were not significantly different from the control root growth (p-value = 0.825 and 0.19, respectively). Surprisingly, intermediate concentrations of BRZ stimulated root growth rather than inhibiting it as had been anticipated. Roots grown on 1 μM BRZ reached 152.7% (s.e. = 4.57) of the control root growth and 208.1% (s.e. = 4.21) when grown on 10 μM BRZ, a significant (p-values < 0.001) increase in root growth compared to the controls. The highest concentration of BRZ did significantly reduce root growth. Roots grown on 100 μM BRZ were significantly (p-value < 0.001) shorter (50%; s.e. = 3.723) than roots of untreated seedlings (Figure 5.5). Interestingly, Bd21 roots grown on 0.01 and 0.1μM BRZ did not show any noticeable alteration in gravitropism (Figure 5.5c-d compared to b), but 1 and 10 μM BRZ induced a straightening of Bd roots, reminiscent of the effect induced by 6.75 μM DON treatment (Figure 5.5e-f compared to b). Note, the root shown in Figure 5.5f is bent at the end because it reached the bottom of the tube by the 4th day of experimentation. In addition, 10 and 100 μM BRZ treatments appeared to inhibit the formation of root hairs, although this aspect of BRZ treatment was not further investigated. Also, seedlings grown on 100 μM BRZ displayed an amber-brown colouration of their roots behind the root tip, towards the upper part of the root and at the junction with the coleoptiles (Figure 5.5g arrows).

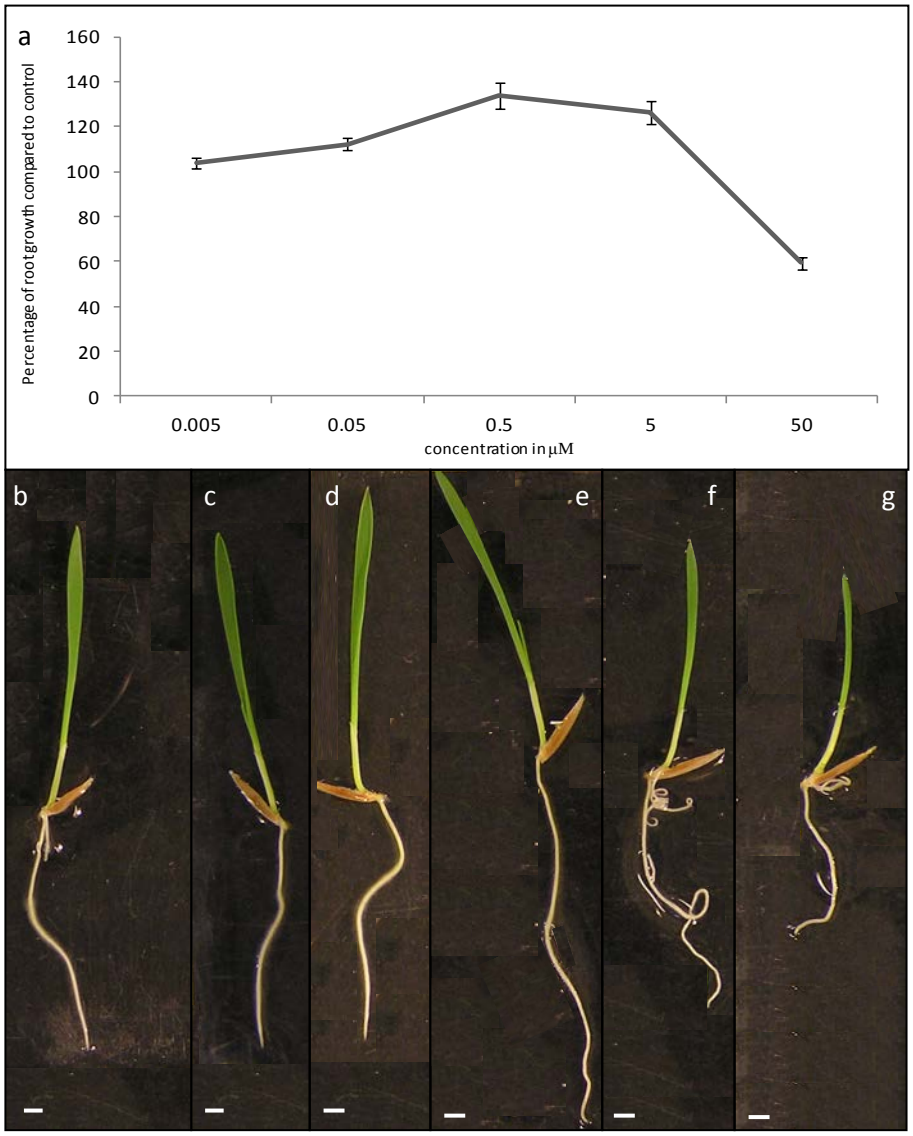

Figure 5.6: Effect of bikinin treatments on the primary root growth and gravitropism of *Brachypodium* seedlings, 5dpi. a) 0.005, 0.05, 0.5, 5 and 50 µM bikinin. b-g) Effect induced by bikinin treatments on Bd21, 5dpi. b) control. c) 0.005 µM bikinin. d) 0.05 µM bikinin. e) 0.5 µM bikinin. f) 5 µM bikinin. g) 50 µM bikinin. b-g) Scale bars = 1 mm.

5.3.6 *The effect of an inducer of brassinosteroid-signalling on root growth of Bd*

As stated above the DON-induced root alterations might reflect altered BR responses or signalling. To finalize the characterization of the response of Bd root growth to BRs, the effect of an activator of BR signalling acting down-stream of the BRI1 receptor, bikinin (BIK), was investigated. De Rybel and co-workers (2009) showed that BIK is a strong activator of BR-signalling in plants. BIK directly binds to BIN2, a member of the Arabidopsis glycogen synthase kinase (GSK) 3 gene family, and inactivates it by acting as an ATP-competitor. BIN2 inactivation was shown to result in the de-repression of BES1 and BZR1, two plant-specific transcription factors regulating the expression of many

known BR-responsive genes (Li and Jin, 2007). The lowest concentrations of BIK had no effect on root length. The roots of Bd21 seedlings grown on 0.005 or 0.05 μM BIK were not found significantly different from the root growth of control seedlings (103.7%; s.e = 2.351 and 112.2%; s.e. = 2.632 of the control root growth respectively; Figure 5.6a). Roots grown on 0.5 μM BIK reached 133.7% (s.e. = 5.861) of the control root growth and roots grown on 5 μM BIK reached 126.5% (s.e. = 5.164) of the control root growth, a significant increase (s.e. = 0.003 and 0.026, respectively) in root growth compared to the controls (Figure 5.6). Roots grown on 50 μM BIK reached 59.4% (s.e. = 2.521) of the control root growth, a significant (p-value < 0.001) reduction in root growth compared to the controls (Figure 5.6). Interestingly, Bd21 roots grown on 0.005 and 0.05 μM BIK did not display an alteration in gravitropism (Figure 5.6c-d compared to b), but at 0.5 μM and higher concentrations of BIK, the roots appeared to wave (Figure 5.6e-g compared to b) and this effect was exacerbated at 5μM BIK as numerous roots were observed to loop around completely (Figure 5.6f). Also, treatments with 0.5μM and higher concentrations of BIK inhibited the formation of root hairs, although this aspect of BIK treatment was not further investigated.

5.3.7 *Comparison of the effects of DON, cycloheximide and T-2 toxin on root growth of Bd*

Although the effects induced on root growth by DON exhibited characteristics similar to those observed by treatments that related to BRs, BR signalling or biosynthesis, DON is generally considered to function primarily as a protein synthesis inhibitor, at least in yeast and animal systems (Pestka *et al.*, 2004). For this reason the effect induced by DON on the root growth of Bd seedlings was compared with an inhibitor of protein synthesis in eukaryotes, cycloheximide (CHX) and another *Fusarium*-produced trichothecene, T-2 toxin (T-2). The roots of Bd21 seedlings grown on 0.05, 0.5 or 5 μM DON were significantly longer than those of the controls (p-values = 0.016, p-value < 0.001 p-value < 0.001 respectively) reaching 109.5% (s.e. = 2.882), 114.76% (s.e. = 2.882) and 128% (s.e. = 2.882) respectively of the control root growth, (Figure 5.7a). Roots grown on 50 μM DON were significantly (p-value < 0.001) shorter than those of the controls, reaching 43.7% (s.e. = 2.809) of the control root growth (Figure 5.7a).

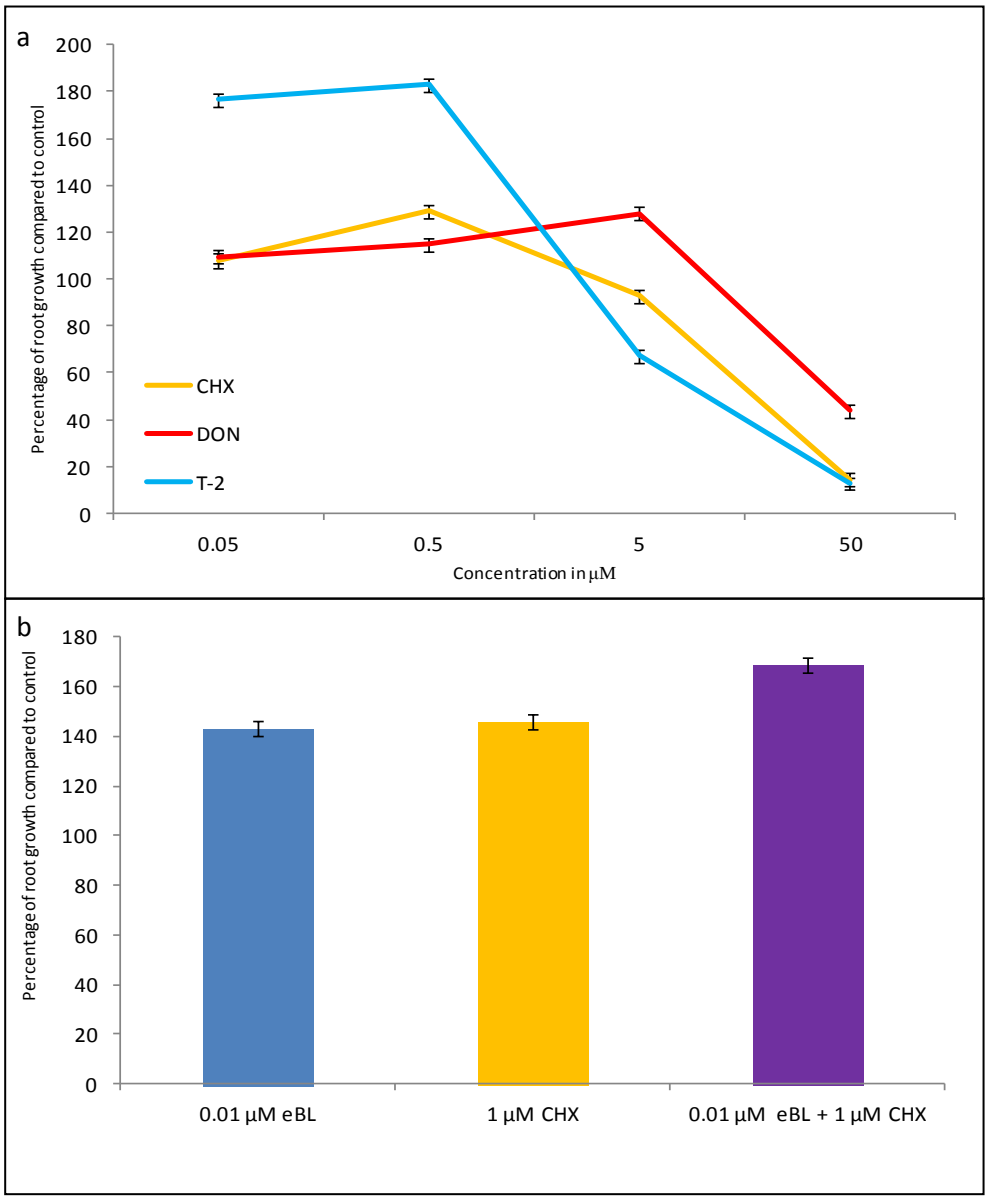

Figure 5.7: Effect of cycloheximide (CHX, DON and T-2 toxin on the primary root growth of *Brachypodium*. a) Effects of 0.5, 5 and 50 µM treatments with T-2 toxin, CHX and DON on Bd21 primary root growth, 4 dpi. b) Effect of 10 nM eBL, 1µM CHX and combination treatments on Bd21 primary root growth, 4dpi. Bars indicate standard errors.

The roots of Bd21 seedlings grown on 0.05 or 0.5 µM CHX were significantly longer (p-value = 0.045 and < 0.001, respectively) than the controls, reaching 108% (s.e. = 2.961) and 128.9% (s.e. = 2.809) of the control root growth respectively (Figure 5.7a). Roots grown on 5 µM CHX were of similar length (p-value = 0.065) to the controls and reached 92.8% (s.e. = 2.882) of the control root growth. Roots grown on 50 µM CHX were severely inhibited and were only 14.3% of the control root length, a significant (p-value < 0.001) reduction (Figure 5.7a). Roots grown on 0.5 µM CHX and higher concentrations were like those treated with DON, straighter compared to the controls and no root hairs

were visible. In addition, 50 μM CHX treatment induced an amber-brown colouration of Bd root tips, similar to that observed with 100 μM BRZ treatment (results not shown).

The roots of Bd21 seedlings grown on 0.05 or 0.5 μM T-2 were almost double the length of the control roots (176.6%; s.e. = 2.882 and 183%; s.e. = 2.962, respectively) , this being highly statistically significant (p-values < 0.001) (Figure 5.7a). In contrast, roots grown on 5 or 50 μM T-2 were significantly (p-values < 0.001) shorter than those of controls, being 67.4% (s.e. = 2.809) and 12.7% (s.e. = 2.809) respectively, to that of the controls (Figure 5.7). Roots grown on 0.05 μM T-2 and higher concentrations were straighter than the control roots and no root hairs were visible (results not shown). Also, 50 μM T-2 treatment induced an amber-brown colouration of the root tips, similar to the situation observed with 50 μM CHX and 100 μM BRZ (results not shown).

5.3.8 *Effect of combinations of brassinosteroid and cycloheximide on root growth of Bd*

The similarity in aspects of root growth induced by DON and CHX led to conduct experiments in which roots of Bd21 were exposed to combinations of eBL and CHX. The effect on Bd21 root growth induced by CHX and eBL treatment alone was compared with treatments of CHX and eBL in combination, in order to test whether inhibition of protein synthesis is able to alter BRs response. As previously observed, the roots of Bd21 seedlings grown on 0.01 μM eBL and 1 μM CHX were significantly longer (p-values < 0.001) than the controls, reaching 143.1% (s.e. = 2.887) and 145.8% (s.e. = 2.924) of the control root growth respectively, although no difference (p-value = 0.932) was observed when comparing the stimulation of root growth induced by both treatments (Figure 5.7b). Roots grown on 0.01 μM eBL combined with 1 μM CHX reached 168.5% (s.e. = 2.887) of the control root growth, a significant (p-values < 0.001) increase in stimulation of the root growth induced by either 0.01 μM eBL treatment alone, or by 1 μM CHX treatment alone. These results suggested that CHX can also have an additive effect on the stimulation of root growth induced by BRs.

5.3.9 *Effect of DON on leaf-unrolling in Bd lines differing in BRI1 function*

The ‘leaf unrolling assay’ (Chono *et al.*, 2003) has been reported to specifically identify BR-associated responses. To investigate further the effect of DON, a range of low DON concentrations was tested in this assay using leaf sections of Bd21 WT, BdAA900 NIL and

BdAA900 (*bri1*) Ho etiolated seedlings. Leaf sections of Bd21 WT etiolated seedlings incubated in the control treatment measured 0.914 mm (s.e. = 0.03419) in width, 48h following incubation. With the exception of a single instance (0.675 μM DON), leaf width increased with increasing DON concentrations. Bd21 WT leaf sections incubated in 0.00675, 0.0675, 0.675, 6.75 or 67.5 μM DON treatment measured 1.023 mm (s.e. = 0.03419), 1.056 mm (s.e. = 0.03419), 0.9581 (s.e. = 0.03419) 1.112 mm (s.e. = 0.03419) and 1.157 mm (s.e. = 0.03419) respectively (Figure 5.8a). Treatments with 0.00675, 0.0675, 6.75 and 67.5 μM DON induced a significant (p-values = 0.025, 0.003, < 0.001 and < 0.001 respectively) increase in the width of etiolated Bd21 WT leaf sections compared to the control treatment. No significant difference (p-value = 0.362) was observed with 0.675μM DON treatment. Leaf sections of BdAA900 NIL etiolated seedlings incubated in the control treatment measured 0.915 mm (s.e. = 0.03176) in width, 48h following incubation (Figure 5.8a). As for the parental line, BdAA900 NIL leaf sections incubated in the presence of DON unfurled more with increasing DON concentration: 0.931 mm (s.e. = 0.03176) in 0.00675 μM DON 1.021 mm (s.e. = 0.03176) in 0.0675 μM DON, 1.091 mm (s.e. = 0.03176) in 0.675 μM DON, 1.017 mm (s.e. = 0.03176) in 6.75 μM DON and 1.077 mm (s.e. = 0.3176) in 67.5 μM DON (Figure 5.8a). The leaf width of leaf sections of BdAA900 NIL etiolated seedlings incubated with 0.00675 μM DON were not significantly (p-value = 0.755) different to those of the control treatment. Treatments with 0.0675, 0.675, 6.75 and 67.5 μM DON induced a significant (p-values = 0.019, < 0.001, 0.024 and < 0.001, respectively) increase in the width of BdAA900 NIL etiolated leaf sections. In contrast leaf sections of BdAA900 Ho etiolated seedlings (disrupted in the brassinosteoid receptor, *BRI1*) were not altered in leaf width at any DON concentration (Figure 5.8a). Sections incubated in the control treatment measured 0.8135 mm (s.e. = 0.3419) in width 48h following incubation while leaf sections incubated in 0.00675, 0.0675, 0.675, 6.75 or 67.5 μM DON measured 0.83 mm (s.e. = 0.0422), 0.7418 mm (s.e. = 0.0376), 0.844 mm (s.e. = 0.04894), 0.891 mm (s.e. = 0.03419) and 0.856 mm (s.e. = 0.0422) respectively (Figure 5.8a). No DON treatment induced a significant change in the width of etiolated BdAA900 Ho leaf sections (p-values = 0.755, 0.159, 0.614, 0.108 and 0.428, respectively). Together, these results indicated that DON was able to partially induce leaf unrolling, in a manner reminiscent of the action of BR and that this was dependent upon the brassinosteroid receptor BRI1.

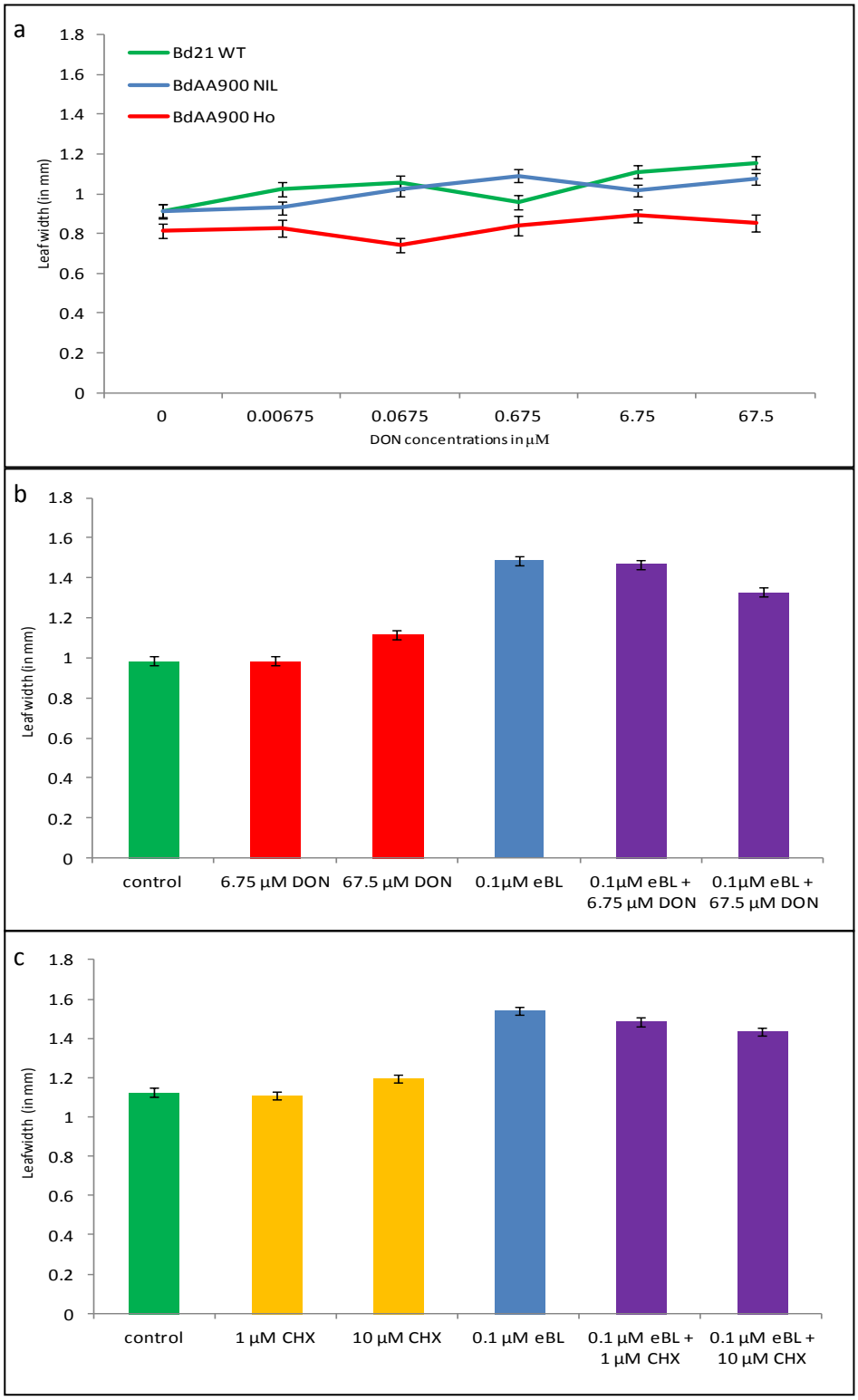

Figure 5.8: Effect of eBL, DON, CHX, and combination treatments on the unrolling of etiolated leaf sections of Bd21. a) 0.00675. 0.0675, 0.675, 6.75 and 67.5 µM DON treatments of Bd21 WT, BdAA900 (*bri1*) NIL and BdAA900 (*bri1*) Ho, 2dpi. b) Effect of eBL, DON and combination treatments on the unrolling of leaf sections of Bd21 etiolated seedlings, 3dpi. c) Effect of eBL, CHX and eBL combination treatments on the unrolling of leaf sections of Bd21 etiolated seedlings, 3dpi. Bars indicate standard errors.

5.3.10 *Effect of combinations of brassinosteroid and DON on leaf unrolling*

The interaction between eBL and DON treatments was further investigated on Bd21 WT with the leaf unrolling assay. Leaf sections of Bd21 WT etiolated seedlings incubated in the control treatment measured 0.985 mm (s.e. = 0.02413) in width, 72h following incubation. Bd21 leaf sections incubated with 6.75 μM DON were similar in width (0.985 mm, s.e. = 0.02328; p-value = 0.985), to untreated sections while incubation with 67.5 μM DON induced a significant (p-value < 0.001) increase in width (1.118 mm, s.e. = 0.02268; Figure 5.8b). Bd21 leaf sections measured 1.487 mm (s.e. = 0.02328) in width when incubated for 72h with 0.1 μM eBL treatment, a significant (p-value < 0.001) increase compared to the control treatment. Bd21 leaf sections incubated with 0.1 μM eBL plus 6.75 μM DON in width, were not significantly (1.467 mm, s.e. = 0.02268; p-value = 0.539) different from the width of leaf sections incubated with 0.1 μM eBL alone (Figure 5.8b). The combination of 0.1 μM eBL plus 67.5 μM DON resulted in an unrolling of leaf sections that was significantly (p-value < 0.001) less than that induced when incubated with 0.1 μM eBL alone (1.328 mm, s.e. = 0.02268; Figure 5.8b).

5.3.11 *Effect of combinations of brassinosteroid and cycloheximide on leaf unrolling*

The interaction between eBL and CHX treatments was investigated on Bd21 WT with the leaf unrolling assay, to compare with that observed for the interaction of eBL and DON treatments. Leaf sections of Bd21 WT etiolated seedlings incubated for 72h in the control treatment measured 1.126 mm (s.e. = 0.02106) in width (Figure 5.8c). Bd21 leaf sections incubated with a 1μM CHX treatment measured 1.111 mm (s.e.= 0.02106), which was not significantly (p-value = 0.623) different from the width of leaf sections in the control treatment. Leaf sections incubated with a 10 μM CHX treatment measured 1.194 mm (s.e. = 0.02106) in width, a significant (p-value = 0.025) increase in leaf width compared to the control. Leaf sections incubated with 0.1 μM eBL measured 1.542 mm (s.e. = 0.02106) in width, a significant (p-value < 0.001) increase compared to the control treatment. The unrolling of leaf sections incubated with 0.1 μM eBL plus 1μM CHX was not significantly different (p-values = 0.058) from that of 0.1 μM eBL alone (1.485 mm, s.e. = 0.02106; Figure 5.8c). The combination of 10μM CHX with 0.1 μM eBL, however, induced a significant (p-value = 0.001) reduction in width (1.436 mm, s.e. = 0.02106) compared to the width of leaves incubated with 0.1 μM eBL treatment alone.

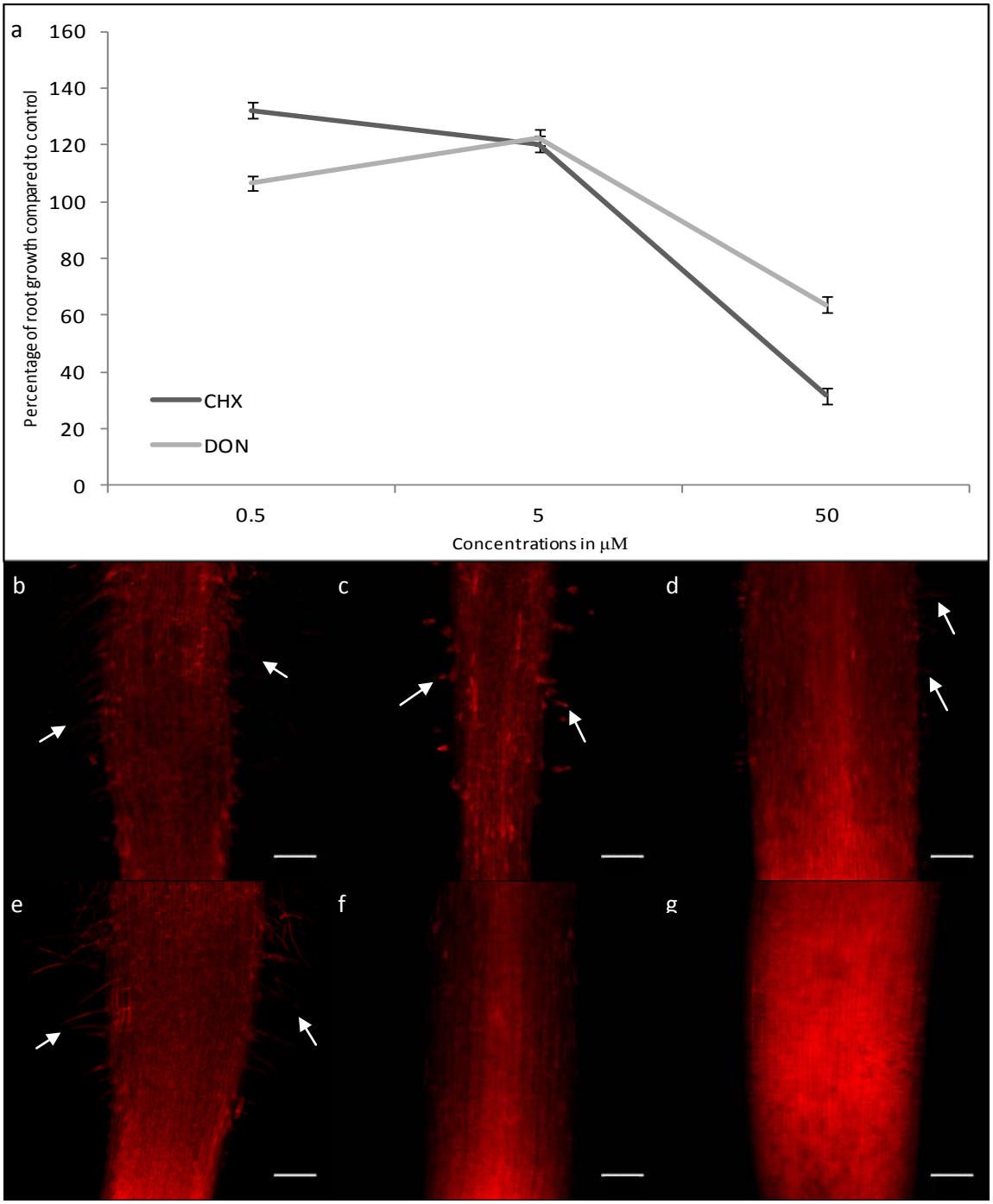

Figure 5.9: Repeat experiment on the effect of DON and CHX treatments on the primary root growth and root hair initiation of *Brachypodium* seedlings. a) Effect of 0.5, 5 and 50 µM CHX and DON treatments on Bd21 primary root growth, 5 dpi. b-f) Confocal microscope images of Bd21 root hairs when grown on: b) control, c) 5 µM DON, d) 50 µM DON, e) control media f) 5 µM CHX g) 50 µM CHX. Arrows indicate root hairs. Scale bars = 100 µm.

5.3.12 *Effect of DON and cyloheximide on primary root growth of Bd*

A repeat experiment aimed to observe and compare, under a confocal microscope, the effect of DON and CHX on the root growth of Bd21 WT seedlings, with special attention paid to the observation of root hairs. In this experiment, Bd21 WT seedlings grown on 0.5μM DON reached 106.4% (s.e. = 2.649) of the control root growth, which was not significantly (p-value = 0.078) different from the control (Figure 5.9a). Roots of seedlings grown on 5 μM DON reached 122.6% (s.e. = 2.649) of the control length, a significant (p-value < 0.001) increase in root growth compared to the control. Roots grown on 50 μM DON reached 63.8% (s.e. = 2.649) of the control root growth, a significant (p-value < 0.001) reduction in growth compared to the control. Roots of seedlings grown on 0.5 or 5 μM CHX were significantly (p-values < 0.001) longer than those of controls. Roots reached 132.3% (s.e. = 2.649) and 120.4% (s.e. = 2.649) of the control when grown on 0.5 and 5 μM CHX respectively (Figure 5.9a). In contrast, roots of seedlings grown on 50μM CHX reached 31.6% (s.e.= 2.649) of the control root growth, displaying a significant (p-values < 0.001) reduction in root growth compared to the control. The amber-brown colouration of the root tips observed in other experiments with high concentrations of some compounds was also observed.

Notably, the stimulation of root growth induced by 5 μM DON was not significantly (p-value = 0.526) different from the effect induced by 5 μM CHX. The roots of seedlings grown on control, 5 and 50 μM DON and CHX treatments were observed under a confocal microscope to compare the effect of these compounds on the initiation and elongation of root hairs. The roots of seedlings grown on 5 and 50 μM DON treatments revealed that these concentrations of mycotoxin inhibited the elongation of root hairs (Figure 5.9c-d compared to b and e). However, root hair initiation was still be observed on the roots of seedlings grown on 5 and 50 μM DON (Figure 5.9c-d). Observation of roots grown on 5 and 50 μM CHX revealed that the initiation of root hairs was completely abolished and no root hair initiation could be observed (Figure 5.9f-g compared to b and e). In addition, roots grown on 50μM CHX produced a more intense autofluorescence signal, detected between 600 and 700 nm, than any other control or treated-root observed (Figure 5.9g).

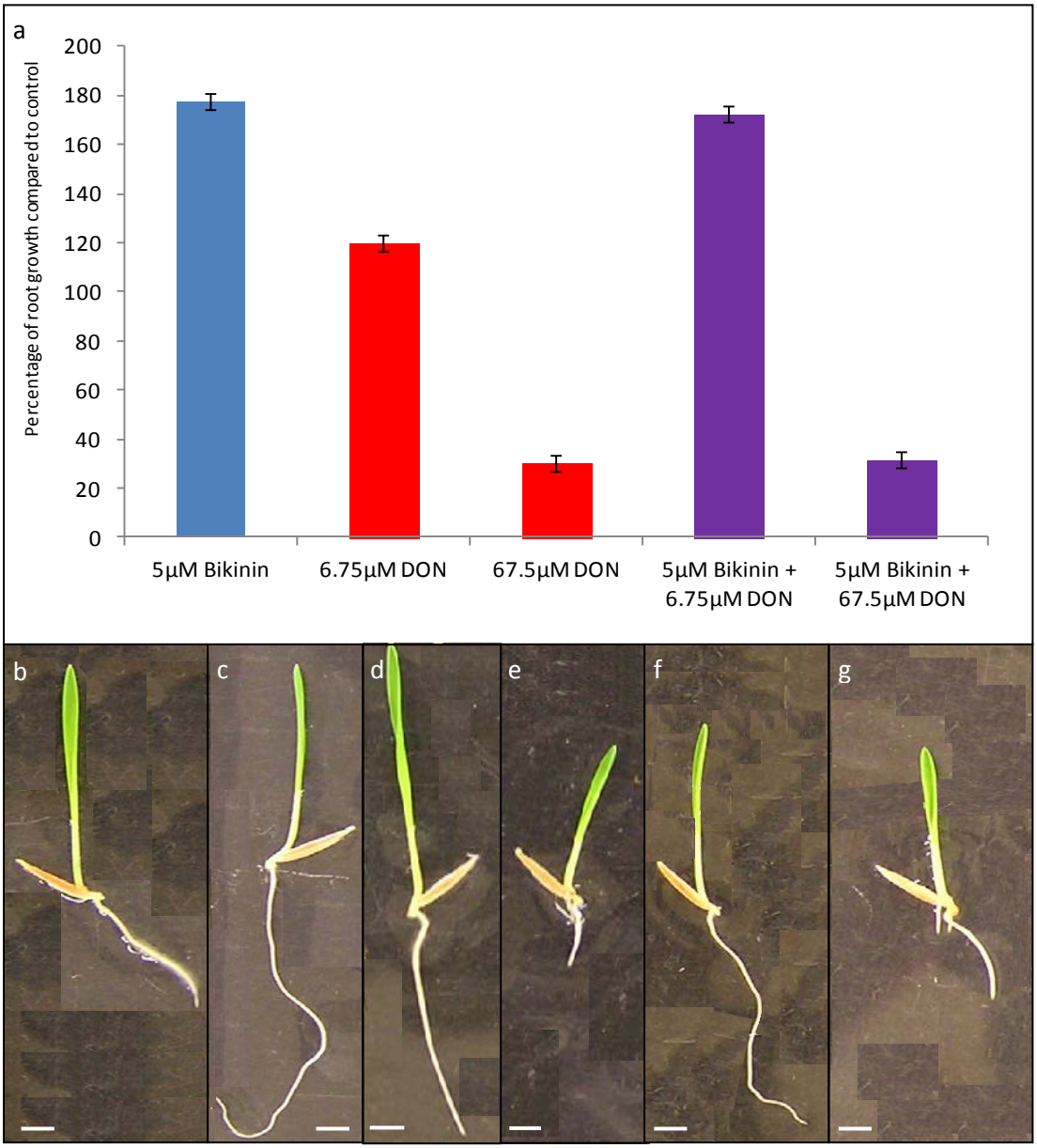

Figure 5.10: Effect of bikinin (BIK) and DON alone and in combination treatments on Bd21 root growth and gravitropism. a) Effect of 5 µM BIK, 6.75 µM DON, 67.5 µM DON and combination treatments, 3 dpi. Bars indicate standard errors. b-g) Effect of BIK, DON alone and in combination treatments on Bd21, 3 dpi. Scale bars = 2.5 mm. b) control. c) 5 µM BIK. d) 6.75 µM DON. e) 67.5 µM DON. f) 5 µM BIK plus 6.75 µM DON,. g) 5 µM BIK plus 67.5 µM DON.

5.3.13 *The effect of combinations of DON or cycloheximide with BIK on root growth of Bd*

The results from the leaf unrolling experiments had indicated that DON could induce partial leaf unrolling and that this was dependent upon BRI1 (see above). BIK functions in BR signalling below the point of BR perception. A small series of experiments were carried out to establish whether the effects of DON on root growth of Bd could be countered by BIK. The effect exerted by stimulatory and inhibitory concentrations of DON, and BIK, alone and in combination treatments on the root growth of Bd seedlings

was investigated. Bd21 WT roots grown on 5 μM BIK reached 177.3% (s.e. = 3.249) of the control root growth, displaying a significant (p-value < 0.001) increase in root growth compared to the control (Figure 5.10a). In addition, treatment with 5 μM BIK disrupted root gravitropism and reduced the appearance of root hairs (Figure 5.10c compared to b). Roots of seedlings grown on 6.75 μM DON reached 119.7% (s.e. = 3.249) of the control root growth, a significant (p-value < 0.001) increase in root growth compared to the control. In contrast, roots of seedlings grown on 67.5μM DON reached 31.6% (s.e. = 3.249) of the control root growth, a significant (p-value < 0.001) reduction in root growth compared to the control. Both 6.75 and 67.5 μM DON produced roots on which no root hairs could be observed. In addition the 6.75 μM DON treatment induced straightening of the roots compared to the controls (Figure 5.10d and e compared to b). Roots grown on 5 μM BIK combined with 6.75μM DON were similar (p-value = 0.31) in length to those treated with 5 μM BIK alone and reached 172.3% (s.e. = 3.29) of the control root growth. This combined treatment induced a significant (p-value< 0.001) increase in root growth compared to effect induced by 6.75 μM DON treatment alone. Roots grown on 5 μM BIK combined with 67.5μM DON reached 31.6% (s.e. = 3.249) of the control root growth, a significant (p-value < 0.001) reduction in root growth compared to the effect induced by treatment with 5 μM BIK alone, but not significantly (p-value = 0.751) different from the effect induced by 67.5 μM DON treatment alone (Figure 5.10a). Interestingly, roots incubated with both 5 μM BIK plus 6.75 μM DON displayed a “waving root” phenotype similar to control roots and roots of seedlings grown on 5 μM BIK alone. This was in marked contrast to the straight roots induced by treatment with 6.75 μM DON alone (Figure 5.10f compared to c and d). Interpretation of the effect on gravitropism induced by 67.5 μM DON treatment alone or in combination with 5 μM BIK was not possible because of the severe inhibition of root growth induced by this concentration of mycotoxin.

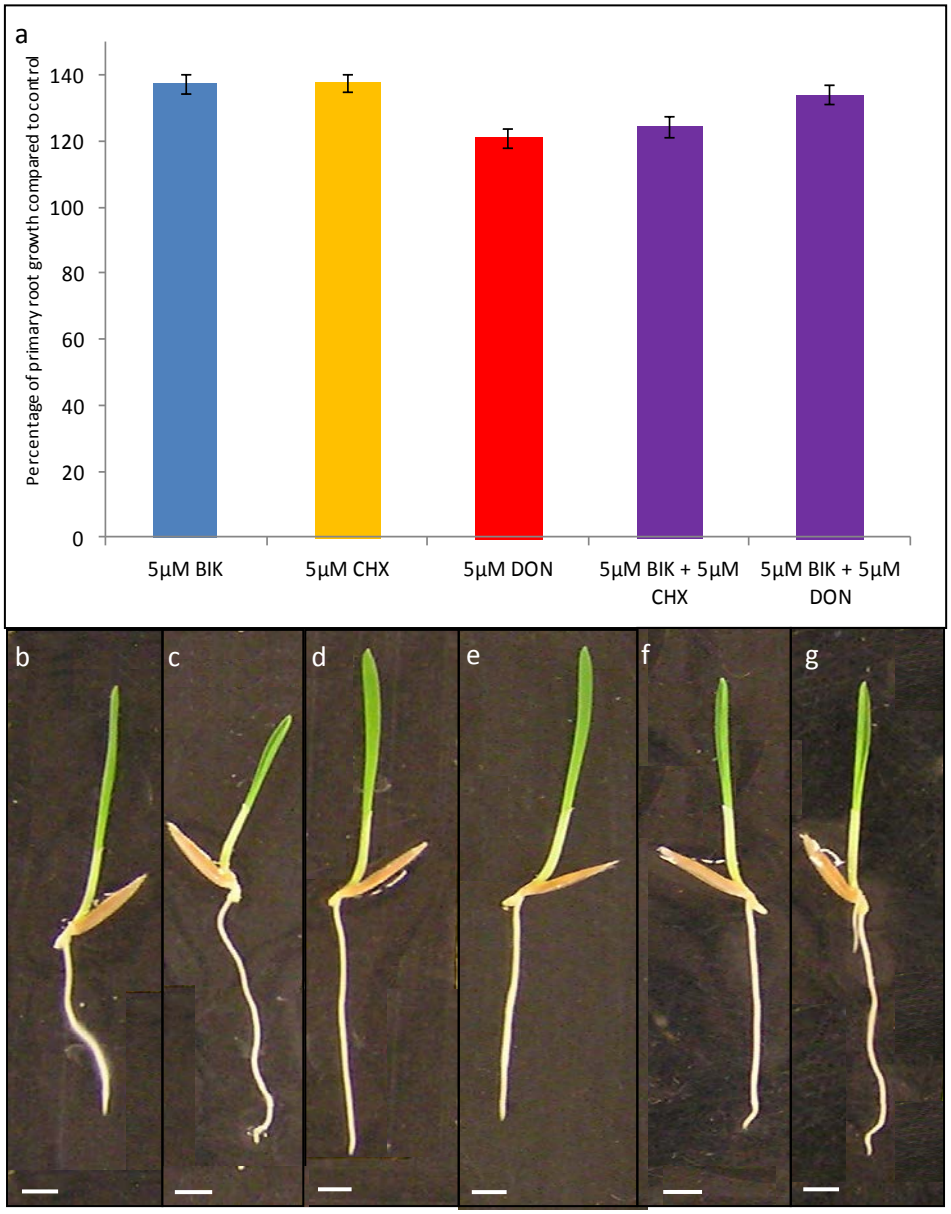

Figure 5.11: Effect of bikinin (BIK), DON and CHX alone and in combination treatments on Bd21 root growth and gravitropism. a) Effect of 5 µM BIK, 5 µM CHX, 5 µM DON and combination treatments, 3 dpi. Bars indicate standard errors. b-g) Effect of BIK, DON and CHX alone and in combination treatments on Bd21 gravitropism, 3 dpi. Scale bars = 2.5 mm. b) control. c) 5 µM BIK. d) 5 µM CHX. e) 5 µM DON. f) 5 µM BIK plus 5 µM CHX. g) 5 µM BIK plus 5 µM DON.

Finally, a repeat experiment compared the effect on root growth of combination treatments of CHX plus BIK with the effect of DON plus BIK. In this experiment, roots grown on 5 µM BIK reached 137.6% (s.e. = 2.848) of the control root growth, roots grown on 5 µM of CHX reached 137.7% (s.e. = 2.848) and roots grown on 5 µM DON reached 121.1% (s.e. = 2.848) of the control root growth (Figure 5.11a). Treatment with 5 µM BIK induced a "root waving" phenotype (Figure 5.11c) while treatments with 5 µM DON and 5 µM CHX induced a straightening of roots compared to the controls (Figure 5.11d and e compared to

b). All three treatments induced a significant (p-values < 0.001) increase in root growth compared to the control. However, 5 μM BIK and CHX treatments did not differ significantly (p-value = 0.966) from one another, while the increase in root growth induced by treatment with 5 μM DON was significantly less than that induced by 5 μM BIK or 5 μM CHX (p-values < 0.001). Roots of seedlings grown on 5 μM BIK plus 5 μM CHX reached 124.6% (s.e. = 3.045) of the control root growth, a significant reduction in the stimulatory effect of root growth induced by either 5 μM BIK or 5 μM CHX treatments alone (p-values = 0.002) (Figure 5.11a). Roots grown on 5 μM BIK combined with 5 μM DON reached 134.2% (s.e. = 2.848) of the control root growth, and the stimulatory effect was similar (p-value 0.402) to that induced by 5 μM BIK treatment alone, but significantly (p-value = 0.001) greater than the stimulation induced by 5 μM DON treatment alone. Interestingly, roots of seedlings treated with 5 μM BIK plus 5 μM CHX exhibited straight roots, similar to the effect induced by 5 μM CHX treatment alone but different from the effect of 5 μM BIK treatment alone (Figure 5.11f compared to c and d). In contrast, roots of seedlings treated with 5 μM BIK plus 5 μM DON exhibited a "root waving" similar to the effect induced by 5 μM BIK treatment alone and markedly different from the root straightening effect induced by 5 μM DON treatment alone (Figure 5.11g compared to c and e).

5.4 Discussion

The results presented in this chapter showed that DON treatment can induce alterations in primary root growth, root gravitropism and root hair development in both At and Bd, suggesting that similar mechanisms are influenced in dicot and monocot species. However, treatment with other compounds such as eBL, BRZ, T-2 toxin and CHX also caused largely similar effects. It is therefore necessary for the current analysis to dissect in detail the effect each compound induced on the different aspects of root growth and development altered by DON.

5.4.1 *DON alters BR and auxin-related growth and developmental processes in both At and Bd*

DON treatment was shown to induce a "root waving" effect and a reduction in root hair elongation in At (A. Steed, personal communication), in addition to the reduction of primary root growth, which was previously characterized (Masuda *et al.*, 2007).

Comparison of the effects induced by eBL and IAA treatments on Bd root growth and morphology compared to those of DON suggests that the mycotoxin does not mimic auxin-induced phenotypes but can mirror, at least at low (stimulatory) concentrations, the effects induced by BRs. Because Arabidopsis mutant *bak1-4*, *brl1* and *brl3*, impaired in the perception or signal transduction of BRs, displayed an enhanced inhibition of root growth in response to DON, it seems that DON influences primary root growth, at least partially, via influencing BR-signalling. The primary root growth response of *bri301*, a mild *BRI1* mutant allele, to DON treatment was not significantly altered when compared to the control response. These results support previous findings in rice indicating that OsBRI1 is not expressed in roots whereas OsBRL1 and OsBRL3 are expressed in root tissues (Nakamura *et al.*, 2006). Analysis of the root growth and morphology of Bd revealed that DON can exert its effects on the same developmental and growth processes as those affected in At. Reminiscent to the situation described in At, DON treatment also induced an alteration of primary root growth, root gravitropism and root hair development in Bd. DON inhibited the primary root growth of Bd at high concentrations. Surprisingly, at lower concentrations, DON was able to induce a significant stimulation of root growth. It is currently unknown whether or not DON is able to stimulate At primary root growth at concentrations lower than those investigated by Steed A. and others. However, DON induced a stimulation of Bd root gravitropism, whereas At roots seemed to be impaired in their gravitropic root response. The effect of DON on root gravitropic responses differed between the two species, apparently reducing gravitropism in At while enhancing it in Bd. However, these differences may reflect differences in the methodologies employed in the two studies. The method used to investigate the effect of DON on Bd root growth and development involved growth of roots through the agar media, being completely embedded within the matrix whereas At roots were grown on the surface of the agar media and grown on plates held at a 60° angle. These differences in experimental setup could possibly explain the differences described above. The influence of DON on root gravitropism seems to be mediated via the redistribution of auxins in the root. Arabidopsis mutants *aux1-1*, *axr2-1* and *axr4-1*, defective in auxin transport or responsiveness, did not display a “root waving” phenotype in response to DON treatment. However, a negative interaction has been reported between the effects of BRs and auxin in the control of Arabidopsis gravitropic root response and growth, and it was proposed that those hormonal pathways influence each other at least partly via modulation of one another’s biosynthesis (Kim *et al.*, 2007). It is currently unknown to what extent the hormonal control and regulation of cross-talk in growth and development are conserved between At and Bd.

Investigation of the effects on root growth and morphology of Bd by combination treatments of eBL and DON, suggest that DON interacts in a dose-dependent manner on BRs, capable of inducing additive or counteracting effects on the response mediated by BR in the roots of Bd. Surprisingly, great differences were observed in the effects induced by a 'fresh' stock of eBL compared to the effects induced by an 'old' stock on the root growth and morphology of Bd. These differences most probably reflect the presence of eBL break-down products resulting from the degradation of the compound at room temperature. These products induced root growth inhibition and stimulation of gravitropism (results not shown) opposite to the effects induced by the 'fresh' stock of eBL. This result is difficult to interpret but one possible explanation could be that alteration of the chemical structure of BRs alters the response mediated by BR-signalling on root growth and development. Interestingly, the effect of the 'old' stock of eBL on root elongation and gravitropism was similar to that of DON. A similar level of root hair inhibition was observed on both 'fresh' and 'old' eBL-treated roots, suggesting that root hair development is similarly affected by both eBL and its degradation products. Further investigation will be necessary to confirm these differences. Overall, the data suggests that the effects induced by DON on Bd and At root growth, gravitropism and hair development result from alteration in BR perception and/or signalling, perhaps via influence on auxin transport.

5.4.2 *Dose-dependent effects of DON is mirrored by T-2, CHX, BRZ and bikinin*

The dose-dependent effects of DON onto the primary root growth; a stimulation at low concentrations followed by an inhibition at higher concentrations, was also observed, surprisingly, in treatments with compounds characterized as protein synthesis inhibitors (PSI), such as T-2 toxin (another trichothecene), and cycloheximide (CHX), an inhibitor of eukaryotic protein synthesis. Similar effects were observed following treatments with compounds known to specifically influence BR-signalling; an inhibitor of BR biosynthesis (BRZ), and a stimulator of BR-signalling pathway (bikinin). Intriguingly, DON, T-2 toxin and CHX have all previously been reported to inhibit the primary root growth of Arabidopsis (Masuda *et al.*, 2007). However, the study of Masuda and co-workers (2007) did not investigate the effect of these compounds at concentrations sufficiently low to mirror the results presented in the current work. It is thus possible that these compounds affect different mechanisms at low concentrations. Noticeably, differences were observed regarding the extent to which the different compounds tested could induce a stimulation of Bd root growth at low concentrations. In this respect, T-2 toxin and BRZ were the most

potent compounds in terms of stimulation of Bd primary root growth, which nearly doubled when treated with concentrations between 0.05 and 0.5 μM of T-2 and 10 μM BRZ.

It was previously described that inhibition of Arabidopsis root elongation seems to be a general effect induced by most hormones tested (Clouse *et al.*, 1996, and references therein). Interestingly though, studies on the hormonal interactions taking place at the root apical meristem of Arabidopsis suggest that the developmental output mediated by a single hormonal pathway is largely modified through a whole network of interactions with other hormonal pathways (Benková and Hejátko, 2009). It was suggested that studies investigating the effects of single hormone treatment by exogenous application are limited to overall effects of a given signal on size and growth of a whole organ and its global impact on cell division and expansion processes (Ubeda-Thomás *et al.*, 2012). Therefore, the current dataset can only provide limited information on the general trends of hormone-mediated control of root growth and the influence that DON can play on these mechanisms. Inhibition of root growth in Arabidopsis has also been observed in response to host recognition of pathogen-associated molecular patterns (PAMPs), which initiates PAMP triggered immunity (PTI) in plants (Zipfel *et al.*, 2004). PTI involves recruitment of the plant receptor kinase BAK1/SERK3 to the receptor complex and, perhaps significantly, BAK1 is also involved in the perception of BRs in plants by functioning as a co-receptor of BRI1 (Nam *et al.*, 2002). This provides another link between the regulation of pathogen defence-related mechanisms and BR-signalling. However, Albrecht and co-workers (2012) showed that BRs were able to inhibit PTI-signalling independently from BAK1, and also suggested BR action on growth mechanisms could directly antagonize plant immunity.

5.4.3 *Is DON acting in plants as a PSI or as a modulator of BR signal?*

Overall, BRZ and CHX showed the closest similarities in effect compared to those induced by DON treatment, in terms of the dose-dependent effect on primary root growth, as well as the stimulation of root gravitropism and inhibition of root hair elongation at all concentrations. However, small qualitative differences in the effects induced by CHX and BRZ with those induced by DON may reflect subtle but significant differences in the myriad of underlying mechanisms influenced by these compounds. For example, both BRZ and CHX induced an amber-brown colouration of treated root tips and root base in the case of BRZ, indicating an accumulation of phenolic-like compounds. This accumulation may indicate that a defence-like response is induced by BRZ and CHX. In contrast, even at high

concentrations DON-treated Bd roots did not display any similar colouration suggesting a difference in effect between DO and the other two compounds. The basis of this differential response requires further study.

The fact that an extremely potent inhibitor of protein synthesis such as CHX was able to stimulate, at low concentrations, a growth process is somewhat surprising. It was previously reported that CHX appears to have a wide range of effects on cellular functions even at low concentrations and that these 'side effects' may not be distinguishable from its effects on protein synthesis (McMahon, 1975). CHX was also reported to enhance polar auxin transport in etiolated pea seedlings (Nam *et al.*, 1999). To explain these results, authors postulated that CHX may exert a stimulatory effect if it is assumed that a protein essential for the system to operate has a rapid turn-over rate whereas another protein involved in the inhibition of auxin transport has a slow turn-over rate. T-2 toxin, originally reported to act as an inhibitor of protein synthesis also induced root elongation at low concentrations. T-2 toxin, in addition to inhibiting protein synthesis, was also shown to induce up-regulation of genes involved in the inactivation of BR bioactivity, thus expected to provoke an attenuation of the BR signal (Masuda *et al.*, 2007). Therefore, it is difficult, with the current data, to differentiate between a PSI mode of action for DON and T-2 and a potential influence of CHX on BR signalling to explain the similar patterns of dose-dependent stimulation of root growth observed. One could hypothesize that protein synthesis inhibition of repressors of root growth, provided that they are turned over more rapidly than the enhancers of growth, could alleviate inhibition of root growth and transiently stimulate growth. On the other hand, the current dataset also provides evidence suggesting that either reducing the pool of bioactive BR (i.e. with BRZ) or activating the BR signal (i.e. with bikinin) can stimulate root growth in Bd.This view could also suggest that the control of root growth mechanisms may integrate BR signals with other growth-related hormone signals (i.e. GA, auxin, ET) to adapt the root growth response to different environmental stimuli.

5.4.4 *DON and CHX act via a different mechanism at low concentrations in plants*

Concentrations which induced a similar level of stimulation on the primary root growth of Bd revealed that CHX was able to prevent the initiation of root hairs whereas DON did not. Also, inhibitory concentrations of these compounds further suggested that DON inhibits the elongation step of root hair development whereas CHX prevents the initiation step. This would suggest that inhibition of root hair development induced by CHX is

mediated by a different mechanism to that exerted by DON.This view was further supported by the result displayed by comparing the effects of combination treatments of DON and bikinin compared to single compound treatments on Bd root growth. As previously mentioned, low concentrations of bikinin induced a stimulation of primary root growth, an inhibition of root gravitropism andinhibition of root hair elongation. Stimulatory concentrations of DON combined with bikinin induced a phenotype reminiscent to the effect induced by bikinin treatment alone. However, inhibitory concentrations of DON combined with bikinin resulted in Bd roots which size and morphology were reminiscent of the effect of inhibitory DON treatment alone. This result suggests that DON-induced stimulation of root gravitropism can be rescued by bikinin, which also restores the full extent of root growth stimulation induced by bikinin treatment alone. This would also suggest that DON-induced modulation of host hormonal signalling may be mediated by targeting a molecular component up-stream of the BIN2 repressor of BR signalling, that is the target of bikinin. However, bikinin was not able to counteract the effect of an inhibitory concentration of DON, suggesting again that DON-induced effects on Bd root growth and morphology is mediated via different mechanisms at different concentrations; via interference with BR signalling at low concentrations and via PSI at high concentrations.

CHX induced a stimulation of root growth, root gravitropism and inhibition of root hair growth. The interaction between CHX and bikinin differed to that between bikinin and DON for both root growth and gravitropism traits. Combining a low, stimulatory concentration of CHX with a stimulatory concentration of bikinin resulted in an antagonistic effect on primary root growth, reducing the stimulatory effect on root growth induced by treatment with CHX or bikinin alone. In addition, bikinin was unable to rescue the CHX-induced gravitropic response. Therefore, these results support the view that whereas bikinin can rescue DON-induced effects on root growth it is unable to rescue CHX-induced effects. This situation indicates that certain components of the DON-induced phenotypes on roots of Bd, although very similar to those induced by CHX, may not solely involve the same mechanisms.

5.4.5 *Evidence suggesting DON alters phytohormone-related processes at low concentrations*

Overall, it is tempting to formulate the hypothesis that, based on the results obtained and discussed in this chapter, DON may have a dual mode of action; at low concentrations

(stimulatory for primary root growth), DON may act as a modulator of BR hormone homeostasis whereas, at high concentrations (inhibitory for primary root growth), it may act as a PSI. The current results suggest that DON may exert its action to modulate BR-signal up-stream of BIN2, as BIK restored the BR-induced effect on root gravitropism disrupted by the mycotoxin. DON may act at (or up-stream of) the BRI1 receptor to BRs, as mutation of *bri1* prevented the DON-induced partial unrolling effect. However, DON may have a direct or indirect influence on BR biosynthesis and/or homeostasis. Interestingly, some reports suggest that DON can act as a hormone and/or can influence a hormonal-response. Unpublished results produced by Dr. N. Gosman (JIC) showed that DON stimulated germination of GA-insensitive barley. A concentration equivalent to 23.5 μMDON actually stimulated the germination of M640 *H. vulgare* cv. Himalaya (carrying a dominant mutation allele of DELLA/SLENDER1 protein conferring a reduced sensitivity to GA, Saville *et al.*, 2012). DON treated M640 seeds germinated at 139% compared to the untreated M640 seed, whereas DON inhibited germination of wild-type Himalaya (72% of seed germination compared to the untreated control). The M640 line is insensitive to GA but responsive to BR. BR has been shown to play a role in tobacco seed germination via a distinct pathway than that of GA (Leubner-Metzger, 2001) and, given the above results, this supports the view that DON may be altering BR homeostasis to stimulate germination. Also, despite a generally accepted inhibitory effect induced by DON treatment on the growth of wheat coleoptiles, Dr. P. Smith (1997) observed that culture filtrates from all tested isolates of Fc and Fg stimulated the growth of *T. aestivum* cv. Mercia coleoptiles. Interestingly, Bruins and co-workers (1993) observed many instances where DON and 3-ADON stimulated the growth of wheat coleoptiles at 10^{-6} M concentrations whereas concentrations of 10^{-5} M DON inhibited coleoptile growth by up to 50%. Measurements of wheat coleoptiles sizes are generally used as a bioassay to assess the potential of new chemicals to mimic auxin but may also reflect BR activity. Additionally, it has been previously reported that DON treatment was able to induce root differentiation of wheat calli treated with a combination of 2,4-D and DON concentrations between 10^{-6} and 10^{-4} M.

The accumulated evidence suggests that DON may function, in part, by interfering with BR homeostasis. DON is widely regarded to act as a virulence factor on wheat but the mechanism behind this is unclear. However, disruption of BR homeostasis may disturb the ability of the plant hot to mount an effective defence. Nakashita and co-workers (2003) provided the first report suggesting that activation of BR-signalling in plants could promote resistance against a variety of biotrophic pathogens. In contrast, recent reports by

De Vleesschauwer and co-workers (2012) suggested that BRs can antagonize GA and SA-mediated root immunity in rice to promote susceptibility to the oomycete *Pythium graminicola*. Finally, Belkhadir and co-workers (2012) provided evidence to suggest a dual role for BRs in Arabidopsis PAMP-triggered immunity. These authors proposed the existence ofa narrow range of BR concentrations that sets the immune responsefor rapid deployment, and that biotrophic pathogens may have evolved virulence mechanisms thatmodulate their host metabolic state which would result in setting BR concentrations optimal forpathogen success. In accordance with the findings mentionedabove, it appears that DON-production by Fusarium species at initial stages of infection could function as a virulence factor via attenuation of the host BR-signalling to inhibit SA and GA-mediated mechanisms of defence, understood to provide effective resistance against Fusarium.

5.4.6 *Hijacking host hormonal-signalling: a common infection strategy in plant pathogens*

It is currently accepted that hormonal treatments of plants result in the reprogramming of the host metabolism, altered gene expression and modulation of plant defence mechanisms and that, depending on the type of plant-pathogen interactions, feed-outs fromdifferent hormone signalling pathways play positive or negative roles against pathogens with different life styles (Bari and Jones, 2009). The best exampleillustrating this situation is the trade-off existing between defence mechanismseffective against biotrophic and necrotrophic pathogens (Glazebrook, 2005). However, it is only recently that evidence is accumulating to support the view that pathogens have evolved efficient virulence mechanisms relying on the perturbation of the host hormonal balance via regulation of hormone-responsive gene expression, secretion of phytohormones, phytohormone-mimics or effectors targeting components of hormone signalling or biosynthesis into the host (Robert-Seilaniantz *et al.*, 2007).

One of the earliest examples of hormone-pathway hijacked by a plant pathogen to favour disease development comes from the study of aphytotoxin produced by various strains of *Pseudomonas syringae* named coronatine (Mittal and Davis, 1995). Coronatine is a compound presenting structural similarities to JA-isoleucine (JA-Ile) and was used as a JA-analog to make essential discoveries in the JA-signalling pathway (Browse, 2009). A recent study showed that production of a chemical analog perceived by the host as a JA signal is able to activate a signalling cascade inhibiting the accumulation of SA, therefore promoting virulence (Zheng *et al.*, 2012). Also, Torres-Zabala and co-workers (2007) provided evidence suggesting that *Pseudomonas syringae* pv. *tomato* secretes effectors

targeting molecular components of the ABA-biosynthesis and signalling pathway to cause disease. These authors showed that genes up-regulated following effector delivery shared a 42%overlap with ABA-responsive genes, among which were key enzymes involved in the biosynthesis (NCED3) and regulation (ABI1) of ABA signalling. Viruses have also been shown to employ similar strategies. Padmanabhan and co-workers (2006) showed that the genome of tobacco mosaic virus encodes for a replicase which can directly interact with At PAP1/IAA26, IAA18 and IAA27 proteins, involved in auxin signalling, through its helicasedomain to promote disease symptoms. Finally, the causal agent of rice 'foolish seedling' disease, *Fusarium fujikuroi,* secretes GA into the host to promote virulence (Brian *et al.*, 1954). As mentioned above, it was recently suggested that BRs were exploited by *P. graminicola* as virulence factors to hijack the rice BR-signalling to induce disease susceptibility (De Vleesschauwer*et al.*, 2012). Finally, it was demonstrated that Fg exploits ET signalling in both dicotyledonous and monocotyledonous plants to promote fungal colonization and disease spread within its host (Chen *et al.*, 2009). Therefore, evidence exist also among the *Fusarium* genera that pathogens have developed virulence strategies relying on the disruption of the host hormonal balance in order to promote metabolic conditions in their host favourable to the establishment and expression of disease.

The results discussed in this chapter provide new evidence suggesting much remains to be learned about the mechanism of action of DON and other trichothecenes in plants. Comparison with classic PSI and BR synthesis inhibitors revealed commonalities but also differences suggesting that DON, although it can act as a weak PSI, also has the capacity to influence BR homeostasis and/or perception to induce growth-promoting mechanisms in its host via a different mode of action. Bd proved itself extremely well suited to investigate these complex aspects of plant-pathogen interactions in the context of phytohormone signals influencing growth, development and plant defence responses.

Chapter 6

General discussion

Genetic research on cereal hosts is tedious, time-consuming and impaired by the complexity inherent to study of polyploid genomes. The aim of this work was to investigate the *Brachypodium distachyon* (Bd) model system to study the genetic components of phytohormone signalling which also control disease resistance in cereals. The compatibility of Bd with four major fungal pathogens of wheat and other small-grain cereals was demonstrated for the first time. Hence, successful infection by the causal agents of Fusarium head blight (FHB) and other Fusarium diseases, Ramularia leaf spot (RLS), eyespot and take-all diseases support this model system as an adequate tool to conduct functional genetic studies of disease resistance mechanisms relevant to cereals. Further, selected Bd T-DNA tagged lines which mutation was predicted to alter specific phytohormonal pathways were investigated. Results provided the first evidence to date of a role for brassinosteroids signalling in the resistance to Fusarium diseases. Also, candidate mutants putatively involved in jasmonic acid (JA) biosynthesis and ethylene (ET) signal transduction suggested an alteration of resistance mechanisms. Finally, the Bd model system was further exploited to study the mode of action of the mycotoxin effector deoxynivalenol (DON) *in planta*. Results presented provide the first evidence that DON disrupts the brassinosteroid (BR) signalling pathway via either interaction with a component of the biosynthetic pathway or a modulator of the BR-signal.

A study of the genetic mechanisms of FHB resistance in wheat was presented in chapter 2 to exemplify the current state of genetic research in disease resistance applied to cereals and identify the limits of conducting research on natural hosts. Chen and colleagues (2009) provided a rare example of model-to-crop translation from the *Arabidopsis thaliana* (At) model to the cereal crop which opened new research prospects onto the hormonal mechanisms pathogens exploit to promote disease in cereals. ET has long been known to hasten leaf senescence (Abeles *et al.*, 1988) and Niu and Guo (2012) recently provided evidence to show that EIN2, the central component in ET signalling, is a critical factor in the regulation of leaf senescence, a mechanism understood to be a form of programmed cell death (PCD) in plants. It is commonly accepted that necrotrophic pathogens, which take up nutrients from dying cells, benefit from the onset of PCD mechanisms (Glazebrook, 2005). This led to the hypothesis formulated in Chapter 2 that some forms of FHB resistance may rely on altered mechanisms of senescence which may be, at least partially, regulated by ET-signalling. In order to test this hypothesis, a wheat EMS mutant

population previously characterized for altered senescence in the field was examined. This population was used to test whether a correlation could be observed between plants exhibiting early senescence and/or hypersensitivity to ET with susceptibility to FHB or, conversely, whether there was a correlation between delayed senescence and/or reduced sensitivity to ET with resistance to FHB. Despite the difficulties of determining resistance levels in lines due to extreme environmental conditions during the 2010 and 2011 growing seasons, two mutant lines displayed a strong and reproducible level of FHB resistance that was either correlated with reduced sensitivity to ET (line 2375A) or correlated with a delay in senescence (line 2939A) associated with a developmental delay. However, no correlation could be established with certainty between the two mechanisms and resistance to FHB neither validating nor invalidating the starting hypothesis. Further analysis of the two FHB resistant mutant lines identified is required to determine whether the differences in reduced ET sensitivity or delayed senescence and FHB resistance is causal or coincidental. These lines need to be crossed to a wild-type line and segregation of the different traits assessed to establish resistance to FHB is linked with an alteration of either senescence or ET-sensitivity, in lines 2339A and 2375A. If linkage is demonstrated then further analysis is warranted to understand the underlying mechanisms involved.

The starting panel of EMS mutant lines was probably too limited to ensure sufficient coverage of the genomic mutations induced by EMS in order to test the scientific hypothesis formulated. A preferable approach would be to characterise the senescence properties of individual lines in the entire set using a high-throughput assay such as the dark-induced senescence (DIS) test. This should allow the selection of a larger panel of EMS mutant candidates for subsequent FHB studies. An alternative strategy to investigate the genetic mechanisms of FHB resistance in wheat would be to exploit TILLING mutant resources. However, it seems that this approach would be similarly hindered by the complexity of polyploidy genomes, as most mutations are masked by homoeologous functional alleles. Therefore, this situation justifies the use of an alternative model system, relevant to cereals, with simplified genomics. The availability of both diploid and polyploid accessions in Bd natural accessions allows future research to investigate the mechanisms underlying the complex regulation of homoeologous gene expression in polyploid organisms. Brachypodium exhibits all the desirable traits expected for a functional genetic model system: a sequenced genome, available EST libraries, genomic markers allowing forward genetic screens, a high level of synteny with major cereals, T-DNA tagged and EMS mutant populations, microarrays and bioinformatic resources (Mur *et al.*, 2011 and references therein). This situation led to the investigation of the potential

compatibility of interaction between Bd and the main causal agents of FHB to assess the potential of Bd for conducting model-to-crop translation studies.

Evidence presented in Chapter 3 demonstrates for the first time that two accessions of Bd, Bd21 whose genome is sequenced and Bd3-1, are compatible with the two major Fusarium species causing FHB (*F. graminearum* and *F. culmorum*). Critically, it was demonstrated that, Bd displays a high level of type II susceptibility to FHB which mirrors closely the situation in wheat. Bd also provided evidence to suggest a novel route for initial infection by *Fusarium* species at the base of macro-hairs. A direct penetration of intact foliar tissues by Fg was never observed prior to the current study, and a recent report validated this phenomenon in wheat (Wagacha *et al.*, 2012). Natural variation in resistance to FHB and susceptibility to the DON virulence factor was observed between the two accessions tested. These lines were chosen for study because of the availability of a segregating population generated from these as parental lines. This population was used to fine-map the *Bsr1* resistance gene to the barley stripe mosaic virus (BSMV; Cui *et al.*, 2012). A similar approach could therefore be employed to test the segregation of resistance to Fusarium and/or to DON toxicity and further investigate the genetic loci conferring resistance within the Bd21/Bd3-1 segregating population. This work also provided evidence supporting the potential to use Bd as a functional model for other diseases of small-grain cereals. A compatible interaction was demonstrated for the emerging barley disease Ramularia caused by *Ramularia collo-cygni* and for all the pathotypes of the causal agent of Take-all disease, *Gaeumannomyces graminis*. Little is known about the genetic basis of resistance mechanisms effective against either Ramularia or Take-all disease and furthermore, Take-all is currently a major target for breeders as no source of resistance exist to the author's knowledge (Dr. P. Nicholson, personal communication). The Bd pathosystem model offers therefore the opportunity to undertake novel investigations to identify approaches to enhance resistance to Take-all and Ramularia diseases. In addition, evidence to support a compatible interaction with *Oculimacula yallundae* and *O. Acuformis*, the two causal agents of eyespot disease of wheat, was obtained. The current work has therefore greatly expanded the scope of Bd to serve as a model for economically important cereal diseases. At the outset of the project, pathosystem studies using Bd as a host were only reported in the scientific literature for the rice pathogen *Magnaporthe grisea* (Routledge *et al.*, 2004) and rust pathogens (Draper *et al.*, 2001). The interaction with the latter produces symptoms that do not mirror those observed on cereal hosts (unpublished observations). Since then, a compatible arbuscular-mycorrhizal symbiosis has been described (Hong *et al.*, 2012), compatibility of interaction with BSMV has led to the fine-mapping of a resistance gene

(Cui *et al.*, 2012) and discovery of QTLs conferring resistance to the Bd adapted rust pathogen *Puccina brachypodii* were reported (Barbieri *et al.*, 2012). The research carried out herein provides additional evidence to support the view that Bd is an excellent pathosystem model with which to conduct model-to-crop translation studies and gain insight into resistance to a wide range of pathogens of cereals.

This work provides a basis for future work aiming at characterising variation in disease resistance for Fusarium, RLS, eyespot or take-all diseases in the entire collection of Bd natural accessions currently available. This approach could lead to the characterisation of strong resistant or susceptible phenotypes to one or several of these pathogens and allow the discovery of new sources of resistance, whether specific or broad-range, directly transferable to cereals, using a QTL detection method as exemplified by Cui *et al.* (2012) and Barbieri *et al.* (2012). Also, together with recently published studies, our results suggest that Bd allow successful infection mainly with necrotrophic and/or hemibiotrophic pathogens, organisms which have evolved infection strategies compatible to different plant host species. However, the situation seems different for obligate biotrophic fungal pathogens. Compatibility tests with *Blumeria graminis* f.sp. *hordei*, the adapted species causing powdery mildew in barley, showed that the fungus is neither able to infect Bd21 nor Bd3-1 (result not presented), as previously mentioned by Draper and colleagues (2001). Nevertheless, Barbieri and colleagues (2012) have used a Bd adapted species of *Blumeria, B. brachypodii* and characterised a QTL conferring resistance to the disease, demonstrating that the Bd system can also be used to study the mechanisms of resistance rusts. Therefore, the Bd pathosystem provides new opportunities to study fundamental aspects of plant-pathogen interactions.

A critical condition to the establishment of Bd as a powerful genetic model is the ability to conduct functional genetic studies in this system to study pathogen resistance mechanisms. Therefore, chapter 4 investigated a small number of T-DNA mutant line candidates from the BrachyTAG collection (Vain *et al.*, 2008) selected by bioinformatic analysis and prediction of the putative function of tagged genes implicated in host resistance/susceptibility. Characterization of the functional homolog of At brassinosteroid-insensitive 1 (BRI1) in Bd was described. Preliminary investigations of the effect of *bri1* mutation in Bd revealed a potential role in resistance to Fusarium infection, although the severely altered morphology of *Bdbri1* plants hindered assessment of disease resistance. New evidence obtained as a result of studies in Chapter 5 (see below) suggests a mechanistic relationship between DON and BR homeostasis. These results, together with

other findings suggesting that BR-signalling can influence plant defence mechanisms (Balkhadir *et al.*, 2012; De Vleesschauwer *et al.*, 2012), provide a framework for future research using the Bd model system to study the mechanisms of trichothecene toxicity in plants. Such studies will be greatly facilitated by the fact that the number of tagged mutants in Bd will rapidly increase in the various T-DNA collections currently available or being established (see collections available and list of initiated projects in Thole *et al.*, 2012). Analysis of five other T-DNA mutant candidate lines was also described in Chapter 4. T-DNA candidates predicted to disrupt genes homologous to a lipoxygenase (in line BdAA615) and an acyl-CoA thioesterase (in line BdAA700) involved in jasmonic acid (JA) biosynthesis were tested for altered resistance to Fusarium infection. Preliminary results suggest that these mutations increase resistance to FHB and root infection by Fc, supporting previous reports that JA-signalling may be a factor of susceptibility during the initial stage of Fusarium infection of wheat heads (Makandar *et al.*, 2012). Subsequent investigation of these two mutant candidates in bioassays testing the resistance to Take-all infection in Bd roots suggested that disruption of JA-biosynthesis also increases resistance to *G. graminis* and suggests that JA-signalling may also be a susceptibility factor for Take-all disease. These results require further validation of the mutation in each candidate line by genotyping and expression analysis to confirm that the gene is 'knocked-out', as well as characterization of the gene function. Provided a correlation can be established between phenotype and genotype segregation, this could lead to the first report of a genetic mutation altering resistance to *G. graminis* and reinforce the utility and advantages of using the Bd pathosystem. A mutation predicted to disrupt a Bd gene displaying homology to ethylene response factors (ERF) was also shown to confer resistance to FHB but not to Fusarium infection in the roots. This result echoes findings by Chen and co-workers (2009) who previously proposed that Fg might exploit ET-signalling to favour host colonization. These authors, however, did not carry out experiments on roots and this aspect warrants further investigation. Further validation of the tagged gene and characterization of its function will also be required to continue the investigation on the involvement of ET-signalling in the mechanisms of resistance to FHB. Unfortunately, characterization of a Bd T-DNA tagged gene in the line BdAA724, sharing high sequence homology with the At auxin response factor ARF2, revealed that a non-tagged mutation was responsible for the phenotype originally observed. Thus, although results from work on At indicate that homozygous *arf2* lines are more resistant to Fg than wild-type, the available Bd-T-DNA tagged line is not suitable for testing this in a grass species.

Recent transcriptomics analysis by Gottwald and colleagues (2012) reported contradicting results concerning the role played by JA and ET signalling pathways in the resistance to FHB in a study comparing differential gene expression between resistant (Dream and Sumai-3) and susceptible (Lynx and Florence-Aurore) wheat cultivars. Authors observed the up-regulation of several genes sharing sequence homology with ET-biosynthesis (ACC oxidase) or ET-response (GDSL-like lipase) as well as an up-regulation of genes associated with JA-biosynthesis (lipoxygenases) and JA-response genes (lipid-transfer proteins, thionins and defensins). The results of Gottwald and colleagues (2012) echoed another transcriptomics analysis reported by Li and Yen (2008). The results of these transcriptomics analysis are somehow in contradiction with the work of Makandar and colleagues (2010, 2012) who studied the role of JA- and SA-signalling pathways in the resistance to FHB in Arabidopsis and wheat. Authors reported that resistance to FHB was enhanced in the susceptible Bobwhite cultivar by constitutive expression of the AtNPR1 (a key regulator of the SA-signalling pathway) and that this could be counteracted by application of MeJA. Authors concluded that JA suppressed SA-activated defence effective against FHB, at least during the early phase of infection. The results reported by Gottwald *et al.* (2012) and Ji and Yen (2008) are also contradicting those of Chen *et al.* (2009). It is important to note that Makandar and Chen both used a reverse genetic approach using the model system Arabidopsis which was translated to wheat, whereas Gottwald and Li and Yen report a transcriptomics approach relying on gene function predictions by analysis of sequence homology shared with previously characterised genes from different species. These two contradicting series works are an example of the diverging reports and opinions argued among the scientific community with respect to the control exerted by the core phytohormone pathways (JA, SA and ET) on disease resistance mechanisms. Makandar and collegues (2012) hypothesised that the method of hormonal application, whether directly spraid or supplied as soil drench, could explain the diverging conclusions on the role of JA-signalling in FHB resistance. Also, it is important to note that the work of Makandar and Chen was conducted using the Bobwhite cultivar wheareas studies by Gottwald and Li and Yen only had the super resistant Sumai-3 cultivar in common. In addition, Gottwald and Li and Yen investigated plant-pathogen interactions between 24 and 72 hours post infection, which coincide with the switch in the nutrition mode of Fusarium species whereas Chen and Makandar investigated longer temporal interactions. The diametrically opposing results disscussed here may rely on the genetic background utilised, the temporal interaction as well as the genetic background studied. If true, this would suggest that the control and cross-regulation of FHB resistance

mechanisms by SA-, JA- and ET-signalling are not only dependent upon the method of investigation and the time-scale of plant-pathogen interaction, but also the allelic variation found among different genotypes. Hence, the results presented in this study, provided further validation is carried out where necessary, support the conclusions of Makandar and colleagues (2010, 2012) on the role of JA-signalling as a factor of susceptibility to FHB. Our results also tend to suggest thatET-signalling may be exploited by Fusarium species to favour fungal colonisation and spread, as reported by Chen and colleagues (2009).

Finally, chapter 5 investigated a novel approach to research on FHB resistance, centred on the mode of action of the characterised virulence factor DON. Investigation of the various effects induced by low concentrations of the mycotoxin on the growth and morphology of Bd roots suggests that the DON may not function solely as a protein synthesis inhibitor (PSI), as characterized in the scientific literature (McLaughlin *et al.*, 1977, Rocha *et al.*, 2005), at low concentrations. Results presented suggested that DON may disrupt, directly or indirectly, the host hormonal balance, as it was shown to influence greatly BR homeostasis. These results were analyzed in the light of recent reports on the complexity of interactions taking place between the different growth and defence-related phytohormones in the regulation of plant defence mechanisms (Robert-Seilaniantz *et al.*, 2007 and 2011, Bari and Jones 2009). These findings potentially provide a framework to study the currently unknown molecular targets of trichothecenes in plants and decipher the mechanisms of DON toxicity in plants. To achieve this however, will require the availability of a substantial number of mutants involved in major components involved in hormonal regulation and biosynthesis. In addition, more bioassays could be developed to enable the study of the complex effects induced by the mycotoxins to reveal the underlying molecular mechanisms involved. One way to identify those mechanisms would be to use a RNA sequencing and/or microarray analysis approach to examine the various changes in gene expression induced by DON treatment.Investigation on the complex interactions existing between phytohormone signalling and their impact on the mechanisms of disease resistance are at the forefront of molecular genetic research in plants. This is an extremely important aspect of biological research due to potential application for crop protection. However, it has proven extremely difficult in the best known plant genetic model At, due to the numerous levels of interactions existing among the plant hormone signalling network. Disruption of one hormonal signalling pathway often impacts on several others, and the outcome on the regulation of disease resistance is generally also dependent upon the environmental conditions. Nevertheless, the field is rapidly expanding and those processes are starting to be unravelled. But findings from the At system has limited

relevance to the situation in monocotyledons and cereals. This situation further justifies the exploitation of Bd as a model system able to bridge the gap between other model systems and cereal crops. Future work utilizing the Bd pathosystem as a model for cereal diseases should help in the development of more durable sources of disease resistance for improved cereal quality and production. The increasing availability of pathogen genomic sequences also provides new opportunities to study in Bd the host mechanisms exploited by protein effectors. Libraries of pathogen protein effectors could be screened using high throughput methods of analysis of Bd transgenic plants expressing designed vector systems.

In conclusion, the current work using Bd as a novel genetic tool to study disease resistance in cereals provided novel findings and additional evidence expanding an emerging view where the resistance to Fusarium infection can be modulated by alteration of numerous phytohormone-signalling pathways and/or homeostasis including: GA (Saville *et al.*, 2012), ET (Chen *et al.*, 2009), SA and JA (Makandar *et al.*, 2012), auxin (Steed A., unpublished results) and BR-signalling (the current study). A positive role in the resistance to Fusarium has been suggested for SA and, in the initial stages of infection, GA-signalling pathways (Saville *et al.*, 2012; Makandar *et al.*, 2012). Disruption of ET, JA, auxin and BR-signalling seem to reduce the ability of the fungus to infect its host (Chen *et al.*, 2009; Makandar *et al.*, 2012; Steed A. unpublished results; the current study). Therefore these results suggest that the pathogen's virulence is impaired in a situation where a whole range of phytohormone pathways are disrupted. However, further work is required to know whether these hormonal signalling pathways are antagonistic to the SA-signalling pathway or whether knocking down these pathways renders plants less susceptible to Fusarium.

During the course of nearly four years of experimental research, the investigation strategy engaged two approaches: i) exploiting a currently available genetic resource in the natural host system to investigate resistance mechanisms to FHB, and ii) investigate the potential of developing a programme with a new compatible pathosystem model and test the tools currently available to study the genetic components of disease resistance in cereals also involved in phytohormonal signalling. Research done on the spring wheat mutant population was tedious and slowed down by the relatively long life-cycle of the host and impaired because experiments were vulnerable to extreme environmental conditions that could not be controlled in field, glasshouse or polytunnel experiments. In contrast, research conducted in parallel on the Bd model system has proven extremely powerful and provided convincing arguments to continue its use for research in functional genetics applied to disease resistance relevant to cereals. Bd has enabled the discovery of important aspects of

Fusarium infection relevant to its natural host, provided new candidate genes with apparent roles in resistance to FHB and shed light onto the mechanisms of DON action in plants. Furthermore, studies of the natural variation in pathogen resistance among Bd accessions could provide knowledge directly translatable to crops as one can exploit the high synteny Bd shares with other cereals to search for allelic variants in cereal germplasms or TILLING populations. The collection of TILLING mutants, generated by sodium azide mutagenesis, held at the INRA institute of Versailles (Dr Richard Sibout) provides the first opportunity to investigate new alleles conferring disease resistance and allow model-to-crop translation via introgression or MAS in cereals. It is therefore very likely that Bd will establish itself in a near future as a fundamental pathosystem model for cereal diseases and enable major discoveries related to efforts to improve crop protection and production.

References

Abeles FB, Dunn LJ, Morgens P, Callahan A, Dinterman RE, Schmidt J: Induction of 33-kD and 60-kD peroxidises during ethylene-induced senescence of cucumber cotyledons. *Plant Physiology* 1988, 87:609-615.

Abramoff MD, Magelhaes PJ, Ram SJ: Image processing with ImageJ. *Biophotonics International* 2004, 11:36-42.

Adie B, Chico JM, Rubio-Somoza I, Solano R: Modulation of plant defences by ethylene. *Journal of Plant Growth Regulation* 2007, 26:160-177.

Albrecht C, Boutrot F, Segonzac C, Schwessinger B, Gimenez-Ibanez S, Chinchilla D, Rathjen JP, De Vries SC, Zipfel C: Brassinosteroids inhibit pathogen-associated molecular pattern-triggered immune signalling independent of the receptor kinase BAK1. *Proceedings of the National Academy of Sciences of the United States of America* 2012, 109:303-308.

Amatulli MT, Spadaro D, Gullino ML, Garibaldi A: Molecular identification of *Fusarium* spp. associated with bakanae disease of rice in italy and assessment of their pathogenicity. *Plant Pathology* 2010, 59:839-844.

Anderson JA: Marker-assisted selection for Fusarium head blight resistance in wheat. *International Journal for Food Microbiology* 2007, 119:51-53.

Aoki T, O'Donnell K: Morphological and molecular characterization of *Fusarium pseudograminearum* sp nov., formerly recognized as the group 1 population of *F. graminearum*. *Mycologia* 1999, 91:597-609.

Bai GH, Desjardins AE, Plattner RD: Deoxynivalenol-nonproducing Fusarium graminearum causes initial infection, but does not cause disease spread in wheat spikes. *Mycopathologia* 2002, 153:91098.

Ban T: Analysis of quantitative trait loci associated with resistance to Fusarium head blight caused by *Fusarium graminearum* Scwabe and of resistance mechanisms in wheat (*Triticum aestivum* L.). *Breeding Science* 2000, 50:131-137.

Bannenberg G, Martínez M, Hamberg M, Castresana C: Diversity of the enzymatic activity in the lipoxygenase gene family of *Arabidopsis thaliana*. *Lipids* 2009, 44:85-95.

Barbieri M, Marcel TC, Niks RE: Host status of false brome grass to the leaf rust fungus *Puccinia brachypodii* and the stripe rust fungus *P. striiformis*. *Plant Disease* 2011, 95:1339-1345.

Barbieri M, Marcel TC, Niks REFrancia E, Pasquariello M, Mazzamurro V, Garvin DF, Pecchioni N: QTLs for resistance to the false brome rust *Puccinia brachypodii* in the model grass *Brachypodium distachyon* L. *Genome* 2012, 55:152-163.

Bari R, Jones DGJ: Role of plant hormones in plant defence responses. *Plant Molecular Biology* 2009, 69:473-488.

Bateman A, Sandford R: The PLAT domain: a new piece in the PKD1 puzzle. *Current Biology* 1999, 9:R588–R590.

Beccari G, Covarelli L, Nicholson P: Infection processes and soft wheat response to root rot and crown rot caused by *Fusarium culmorum*. *Plant Pathology* 2011, 60: 671-684.

Belkhadir Y, Jailais Y, Epple P, Balsemão-Pires E, Dangl JL, Chory J: Brassinosteroids modulate the efficiency of plant immune response to microbe-associated molecular patterns. *Proceedings of the National Academy of Science of the United States of America* 2012, 109:297-302.

Beltrano J, Carbone A, Montaldi ER, Guiamet JJ: Ethylene as promoter of wheat-grain maturation and ear senescence. *Plant Growth Regulation* 1994, 15:107-112.

Benková E, Hejátko J: Hormone interactions at the root apical meristem. *Plant Molecular Biology* 2009, 69:383-396.

Bent AF, Innes RW, Ecker JR, Staskawicz BJ: Disease development in ethylene-insensitive *Arabidopsis thaliana* infected with virulent and avirulent *Pseudomonas* and *Xanthomonas* pathogens. *Molecular Plant–Microbe Interactions* 1992, 5:372-378.

Berrocal-Lobo M, Molina A, Solano R: Consitutive expression of ETHYLENE RESPONSE FACTOR 1 in Arabidopsis confers resistance to several necrotrophic fungi. *The Plant Journal* 2002, 29:23-32.

Berrocal-Lobo M, Molina A: Ethylene response factor 1 mediates Arabidopsis resistance to the soilborne fungus *Fusarium oxysporum*. *Molecular Plant-Microbe Interactions* 2004, 17:763-770.

Boddu J, Cho S, Kruger WM, Muehlbauer GJ: Transcriptome analysis of the barley-*Fusarium graminearum* interaction. *Molecular Plant-Microbe Interactions* 2006, 19:407-417.

Boenisch MJ, Schäfer: *Fusarium graminearum* forms mycotoxin producing infection structures on wheat. *BMC Plant Biology* 2011, 11:110.

Bottalico A: *Fusarium* diseases of cereals: Species complex and related mycotoxin profiles, in Europe. *Journal of Plant Pathology* 1998, 80:85-103.

Boutigny AL, Richard-Forget F, Barreau C: Natural mechanisms for cereal resistance to the accumulation of Fusarium trichothecenes. *European Journal Plant Pathology* 2008, 121:411-423.

Boutigny AL, Barreau C, Atanasova-Penichon V, Verdal-Bonnin MN, Pinson-Gadais L, Richard-Forget F: Ferulic acid, an efficient inhibitor of type B trichothecene biosynthesis and Tri gene expression in *Fusarium* liquid culture. *Fungal Biology* 2009, 113:746-753.

Brian PW, Elson HG, Hemming MR: The plant-growth-promoting properties of gibberellic acid, a metabolic product of the fungus Gibberella fujikuroi. *Journal of the Science of Food and Agriculture* 1954, 5:602-612.

Brkljacic J, Grotewold E, Scholl R, Mockler T, Garvin DF, Vain P, Brutnell T, Sibout R, Bevan M, Budak H, Caicedo AL, Gao C, Gu Y, Hazen SP, Holt III BH, Hong SY, Jordan M, Manzaneda AJ, Mitchell-Olds T, Mochida K, Mur LAJ, Park CM, Sedbrook J, Watt M, Zheng SJ, Vogel JP: Brachypodium as a model for the grasses: Today and the future. *Plant Physiology* 2011, 157:3-13.

Brown JKM: Yield penalties of disease resistance in crops. *Current Opinion in Plant Biology* 2002, 5:1-6.

Brown NA, Urban M, Van de Meene AML, Hammond-Kosack KE: The infection biology of *Fusarium graminearum*: defining the pathways of spikelet to spikelet colonisation in wheat ears. *Fungal Biology* 2010, 114:555-571.

Browne RA, Mascher F, Golebiowska G, Hofgaard IS: Components of partial disease resistance in wheat detected in a detached leaf assay inoculated with *Microdochium majus* using first, second and third expanding seedling leaves. *Journal of Phytopathology* 2006, 154:204-208.

Browse J: Jasmonate passes muster: A receptor and targets for the defense hormone. *Annual Review of Plant Biology* 2009, 60:183-205.

Bruins MBM, Karsaï I, Schepers J, Snijders CHA: Phytotoxicity of deoxynivalenol to wheat tissue with regard to in vitro selection for Fusarium head blight resistance. *Plant Science* 1993, 94:195-206.

Buerstmayr H, Steiner B, Lemmens M, Ruckenbauer P: Resistance to Fusarium head blight in winter wheat: heritability and trait associations. *Crop Science* 2000, 40:1012-1018.

Buerstmayr H, Ban T, Anderson JA: QTL mapping and marker-assisted selection for Fusarium head blight resistance in wheat: a review. *Plant breeding* 2009, 128:1-26.

Burgess LW, Dodman RL, Pont W, Mayers P: Fusarium diseases of wheat, maize and grain sorghum in Eastern Australia. In, Fusarium: Diseases, Biology and Taxonomy. University Park: Pennsylvania State University Press, pp. 64-76.

Burt C, Hollins TW, Nicholson P: Identification of a QTL conferring seedling and adult plant resistance to eyespot on chromosome 5A of Capelle Desprez. *Theoretical and Applied Genetics* 2011, 122:119-128.

Bushnell WR, Hazen BE, Pritsch C: Fusarium head blight of wheat and barley. St Paul, USA: *American Phytopathological Society Press* 2003, p44.

Bushnell WR, Perkins-Veazie P, Russo VM, Collins J, Seeland TM: Effects of Deoxynivalenol on content of chloroplasts pigments in barley leaf tissues. *Biochemistry and Cell Biology* 2010, 100:33-41.

Cao J, Jiang F, Sodmergen, Cui K: Time-course of programmed cell death during leaf senescence in Eucommia ulmoides. *Journal of Plant Research* 2003, 116:7-12.

Chapman NH, Burt C, Dong H, Nicholson P: The development of PCR based markers for the selection of eyespot resistance genes *Pch1* and *Pch2*. *Theoretical and Applied Genetics* 2008, 117:425-433.

Chen C, Bauske EM, Musson G, Rodriguez-kabana R, Kloepper JW: Biological control of Fusarium wilt on cotton by use of endophytic bacteria. *Biological Control* 1995, 5:83-91.

Chen X, Steed A, Harden C, Nicholson P: Characterization of *Arabidopsis thaliana-Fusarium graminearum* interactions and identification of variation in resistance among ecotypes. *Molecular Plant Pathology* 2006, 7:391-403.

Chen X, Steed A, Travella S, Keller B, Nicholson P: *Fusarium graminearum* exploits ethylene signalling to colonize dicotyledonous and monocotyledonous plants. *New Phytologist* 2009, 182:975-983.

Chen Y, Zhou MG: Characterization of *Fusarium graminearum* isolates resistant to both carbendazim and a new fungicide JS399-19. *Phytopathology* 2009, 99:441-446.

Chono M, Honda I, Zeniya H, Yoneyama K, Saisho D, Takeda K, Takatsuto S, Hoshino T, Watanabe Y.: A semidwarf phenotype of barley uzu results from a nucleotide substitution

in the gene encoding a putative brassinosteroid receptor. *Plant Physiology* 2003, 133:1209–1219.

Clouse SD, Langford M, McMorris TC.: A brassinosteroid insensitive mutant in *Arabidopsis thaliana* exhibits multiple defects in growth and development. *Plant Physiology* 1996, 111:671–678.

Clouse SD: Brassinosteroid signal transduction: from receptor kinase activation to transcriptional networks regulating plant development. *The Plant Cell* 2011, 23:1219-1230.

Cook JR: Fusarium diseases of wheat and other small grained cereals in North America. In: Fusarium diseases, Biology and Taxonomy (PE Nelson, TA Toussoun, JR Cook) Eds., The Pennsylvania State University Press, University Park and London, UK, p39-52.

Cook JR: Fusarium root rot and foot rot of cereals in the Pacific Northwest. *Phytopathology* 1968, 58:127-131.

Cook RJ: *Fusarium* foot rot of wheat and its control in the Pacific Northwest. *Plant Disease* 1980, 64:1061-1066.

Cook RJ: Take-all of wheat. *Physiological and Molecular Plant Pathology* 2003, 62:73-86.

Covarelli L, Beccari G, Steed A, Nicholson P: Colonization of soft wheat following infection of the stem base by *Fusarium culmorum* and translocation of deoxynivalenol to the head. *Plant Pathology* 2012, Doi: 10.1111/j.1365-3059.2012.02600.x.

Cui Y, Lee MY, Huo N, Bragg J, Yan L, Yuan C, Li C, Holditch SJ, Xie J, Luo MC, Li D, Yu J, Martin J, Schackwitz W, Gu YQ, Vogel JP, Jackson AO, Liu Z, Garvin DF: Fine mapping of the *Bsr1* Barley Stripe Mosaic Virus resistance gene in the model grass *Brachypodium distachyon. Plos One* 2012, 7:e38333.

Cuthbert PA, Somers DJ, Thomas J, Cloutier S, Brulé-Babel A: Fine mapping Fhb1, a major gene controlling Fusarium head blight resistance in bread wheat. *Theoretical and Applied Genetics* 2006, 112:1465-1472.

Cuthbert PA, Somers DJ, Brulé-Babel A: Mapping of Fhb2 on chromosome 6BS: a gene controlling Fusarium head blight field resistance in bread wheat (*Triticum aestivum* L.). *Theoretical and Applied Genetics* 2007, 114:429-437.

Cuzick A, Lee S, Gezan S, Hammond-Kosack KE: NPR1 and EDS11 contribute to host resistance against *Fusarium culmorum* in Arabidopsis buds and flowers. *Molecular Plant Pathology* 2008, 9:697-704.

Cuzick A, Urban M, Hammond-Kosack K: *Fusarium graminearum* gene deletion mutants map1 and tri5 reveal similarities and differences in the pathogenicity requirements to cause disease on Arabidopsis and wheat floral tissue. *New Phytologist* 2008, 177:990-1000.

Daniels A, Lucas JA, Peberdy JF: Morphology and ultrastructure of W and R pathotypes of Pseudocercosporella herpotrichoides on wheat seedlings. *Mycological Research* 1991, 95:385-397.

De Vleesschauwer D, Van Buyten E, Satoh K, Balidion J, Mauleon R, Choi IR, Vera-Cruz C, Kikuchi S, Höfte M: Brassinosteroids antagonize gibberellins- and salicylate-mediated root immunity in rice. *Plant Physiology* 2012, 158:1833-1846.

Derkx AP, Orford S, Griffiths S, Foulkes MJ, Hawesford MJ: Identification of differentially senescing mutants of wheat and impacts on yield, biomass and nitrogen partitioning. *Journal of Integrative Plant Biology* 2012, 54:555-566.

Desmond OJ, Edgar CI, Manners JM, Maclean DJ, Schenk PM, Kazan K: Methyl jasmonate induced gene expression in wheat delays symptom development by the crown rot pathogen *Fusarium pseudograminearum*. *Physiological and Molecular Plant Physiology* 2006, 67:171-179.

Desmond OJ, Manners JM, Stephens AE, Maclean DJ, Schenk PM, Gardiner DM, Munn AL, Kazan K: The *Fusarium* mycotoxin deoxynivalenol elicits hydrogen peroxide production, programmed cell death and defence responses in wheat. *Molecular Plant Pathology* 2008, 9:435-445.

Dharmasiri N, Dharmasiri S, Estelle M: The F-box protein TIR1 is an auxin receptor. *Nature* 2005, 435:441–445.

Díaz J, ten Have A, van Kan JAL: The role of ethylene and wound signalling in resistance of Tomato to *Botrytis cinerea*. *Plant Physiology* 2002, 129:1341-1351.

Dignani MC, Anaissie E: Human fusariosis. *Clinical Microbiology and Infection* 2004, 10 (Suppl.1):67-75.

Dill-Macky R, Jones RK: The effect of previous crop residues and tillage on Fusarium head blight of wheat. *Plant Disease* 2000, 84:71-76.

Draper J, Mur LAJ, Jenkins G, Ghosh-Biswas GC, Bablak P, Hasterok R, Routledge APM: Brachypodium distachyon. A new model system for functional genomics in grasses. *Plant Physiology* 2001, 127:1539-1555.

Eckardt NA: Foolish seedlings and DELLA regulators: The functions of rice SLR1 and Arabidopsis RGL1 in GA signal transduction. *The Plant Cell* 2002, 14:1-5.

Ecker JR: The ethylene signal-transduction pathway in plants. *Science* 1995, 268:667-675.

Finet C, Jaillais Y: Auxology: When auxin meets plant evo-devo. *Developmental Biology* 2012, 369:19-31.

Fonseca S, Chico JM, Solano R: The jasmonate pathway: the ligand, the receptor and the core signalling module. *Current Opinion in Plant Biology* 2009, 12:539-547.

Foroud NA, Eudes F: Trichothecenes in cereal grains. *International Journal of Molecular Sciences* 2009, 10:147-173.

Fujita M, Fujita Y, Noutoshi Y, Takahashi F, Narusaka Y, Yamaguchi-Shinozaki K, Shinozaki K: Crosstalk between abiotic and biotic stress responses: a current view from the points of convergence in the stress signalling networks. *Current Opinion in Plant Biology* 2006, 9:436-442.

Gale MD, Law CN: The identification and explotation of Norin 10 semidwarfing genes. *UK, Plant Breeding Institute: Annual report* 1976, 21-35.

Gale MD, Marshall GA: Chromosomal location of *Gai1* and *Rht1*, genes for gibberellins insensitivity and semi-dwarfism, in a derivative of Norin-10 wheat. *Heredity* 1976, 37:283-289.

Gale MD, Youssefian S: Dwarfing genes in wheat. In: *Progress in Plant Breeding* 1985 (ed. Russel G.E.) pp. 1-35 (Butterworths, London, UK).

Gardiner D, Kazan K, Praud S, Torney FJ, Rusu A, Manners JM: Early activation of wheat polyamine biosynthesis during Fusarium head blight implicates putrescine as an inducer of trichothecene mycotoxin production. *BMC Plant Biology* 2010, 10:289.

Glazebrook J: Contrasting mechanisms of defense against biotrophic and necrotrophic pathogens. *Annual Review of Phytopathology* 2005, 43:205-227.

Goda H, Shimada Y, Asami T, Fujioka S, Yoshida S: Microarray analysis of brassinosteroid-regulated genes in Arabidopsis. *Plant Physiology* 2002, 130:1319–1334.

Gosman N, Srinivasachary, Steed A, Chandler E, Thomsett M, Nicholson P: Evaluation of type I Fusarium head blight resistance of wheat using non-deoxynivalenol-producing fungi. *Plant Pathology* 2010, 59:147-157.

Gottwald S, Samans B, Luck S, Friedt W: Jasmonate and ethylene dependent defence gene expression and suppression of fungal virulence factors: Two essential mechanisms of Fusarium head blight resistance in wheat? *BMC Genomics* 2012, 13:369.

Gorvin EM, Levine A: The hypersensitive response facilitates plant infection by the necrotrophic pathogen *Botrytis cinerea*. *Current Biology* 2000, 10:751-757.

Gosman N, Chandler E, thomsett M, Draeger R, Nicholson P: Analysis of the relationship between parameters of resistance to Fusarium head blight and in vitro tolerance to deoxynivalenol of the winter wheat cultivar WEK0609®. *European Journal of Plant Pathology* 2005, 111:57-66.

Gosman NE: Analysis of the genetic basis of resistance to *Fusarium culmorum* in wheat. PhD Thesis 2001. University of East Anglia: UK.

Goswami RS, Kistler HC: Heading for disaster: Fusarium graminearum on cereal crops. *Molecular Plant Pathology* 2004, 5:515-525.

Gregersen PL, Holm PB, Krupinska K: Leaf senescence and nutrient remobilisation in barley and wheat. *Plant Biology* 2008, 10 (Suppl.1):37-49.

Grennan AK: Ethylene response factors in jasmonate signalling and defence response. *Plant Physiology* 2008, 146:1457-1458.

Griffiths S, Sharp R, Foote TN, Bertin I, Wanous M, Reader S, Colas I, Moore G: Molecular characterization of Ph1 as a major chromosome pairing locus in polyploid wheat. *Nature* 2006, 439:749-752.

Guenther JC, Trail F: The development and differentiation of Gibberella zeae (anamorph: Fusarium graminearum) during colonization of wheat. *Mycologia* 2005, 97:229-237.

Guilleroux M, Osborn A: Gene expression during infection of wheat roots by the “take-all” fungus *Gaeumannomyces graminis. Molecular Plant Pathology* 2004, 5:203-216.

Guo H, Ecker JR: The ethylene signalling pathway: new insights. *Current Opinion in Plant Biology* 2004, 7:40-49.

Guo Y, Cai Z, Gan S: Transcriptome of *Arabidopsis* leaf senescence. *Plant Cell and Environment* 2004, 27:521–549.

Gutterson N, Reuber TL: Regulation of disease resistance pathways by AP2/ERF transcription factors. *Current Opinion in Plant Biology* 2004, 7:465-471.

Guzman P, Ecker J R: Exploiting the triple response of Arabidopsis to identify ethylene-related mutants. *Plant Cell* 1990,2:513-523.

Handa H, Namiki N, Xu D, Ban T: Dissecting of the FHB resistance QTL on the short arm of wheat chromosome 2D using a comparative genomic approach: from QTL to candidate gene. *Molecular Breeding* 2008, 27:71-84.

Hao DY, Ohme-Takagi M, Sarai A: Unique mode of GCC box recognition by the DNA-binding domain of ethylene-responsive element-binding factor (ERF domain) in plant. *Journal of Biological Chemistry* 1998, 273:26857-26861.

Hare MC, Parry DW: Observations on the maintenance and measurement of soil water in simple pot experiments and its effects on seed-borne *Fusarium culmorum* seedlilng blight of winter wheat. *Annals of Applied Biology* 1996, 129:227-235.

Harris LJ, Gleddie SC: A modified Rpl3 gene from rice confers tolerance of the *Fusarium graminearum* mycotoxin deoxynivalenol to transgenic tobacco. *Physiological and Molecular Plant Pathology* 2001, 58:173–181.

Henkes GJ, Jousset A, Bonkowski M, Thorpe MR, Scheu S, Lanoue A, Schurr U, Röse US: *Pseudomonas fluorescens* CH0 maintains carbon delivery to *Fusarium graminearum*-infected roots and prevents reduction in biomass of barley shoots through systemic interactions. *Journal of Experimental Botany* 2011, 62, 4337–4344.

Hogenhout SA, Renier AL, Van der Hoorn, Terauchi R, Kamoun S: Emerging concepts in effector biology of plant-associated organism. *Molecular Plant-Microbe Interactions* 2009, 22:115-122.

Hogg AC, Johnston RH, Dyer AT: Applying real-time quantitative PCR to fusarium crown rot of wheat. *Plant Disease* 2007, 91:1021–1028.

Hong JJ, Park YS, Bravo A, Bhattarai KH, Daniels DA, Harrison MJ: Diversity of morphology and function in arbuscular mycorrhizal symbiosis in *Brachypodium distachyon*. *Planta* 2012, 236:851-865.

Hörtensteiner S, Feller U: Nitrogen metabolism and remobilization during senescence. *Journal of Experimental Botany* 2002, 53:927–937.

Hua J, Meyerowitz EM: Ethylene responses are negatively regulated by a receptor gene family in *Arabidopsis thaliana*. *Cell* 1998, 94:261-271.

Hua J, Sakai H, Nourizadeh S, Chen QHG, Bleecker AB, Ecker JR, Meyerowitz EM: EIN4 and ERS2 are members of the putative ethylene receptor gene family in Arabidopsis. *Plant Cell* 1998, 10:1321-1332.

Huala E, Dickerman AW, Garcia-Hernandez M, Weems D, Reiser L, LaFond F, Hanley D, Kiphart D, Zhuang M, Huang W, Mueller LA, Bhattacharyya D, Bhaya D, Sobral BW, Beavis W, Meinke DW, Town CD, Somerville C, Rhee SY: The Arabidopsis Information Resource (TAIR): a comprehensive database and web-based information retrieval, analysis, and visualization system for a model plant. *Nucleic Acids Research* 2001, 29:102-105.

Huo N, Vogel JP, Lazo GR, You FM, Ma Y, McMahon S, Dvorak J, Anderson OD, Luo MC, GuYQ : Structural characterization of *Brachypodium* genome and its syntenic relationship with rice and wheat. *Plant Molecular Biology* 2009, 70:47-61.

Huss H: The biology of Ramularia collo-cygni. Meeting the Challenges of Barley Blights 2004 (Yahyaoui AH, Brader L, Tekauz A, Wallwork H & Steffenson B, eds), pp. 321–328. Proceedings of the Second International Workshop on Barley Leaf Blights, (ICARDA), Aleppo, Syria, April 2002. http://www.icarda.org/Publications/Price_List/book3/Book3.html.

Hussein A, Peng J: DELLA proteins and GA signalling in *Arabidopsis*. *Journal of Plant Growth Regulation* 2003, 22:134-140.

Ilgen P, Hadeler B, Maier FJ, Schäfer W: Developing kernel and rachis node induce the trichothecene pathway of *Fusarium graminearum* during wheat head infection. *Molecular Plant Microbe Interaction* 2009, 8:899-908.

International Rice Genome Sequencing Project: The map-based sequence of the rice genome. *Nature* 2005, 436:793-800.

Jansen C, von Wettstein D, Schafer W, Kogel KH, Felck A, Maier FJ: Infection patterns in barley and wheat spikes inoculated with wild-type and trichodiene synthase gene disrupted *Fusarium graminearum*. *Proceedings of the National Academy of Sciences*, USA 2005, 102:16892-16897.

Kang K, Buchenauer H: Immunocytochemical localization of Fusarium toxins in infected wheat spikes by *Fusarium culmorum*. *Physiological and Molecular Plant Pathology* 1999, 55:275-288.

Kang K, Buchenhauer H: Cytology and ultrastructure of the infection of wheat spikes by *Fusarium culmorum*. *Mycological Research* 2000, 104:1083-1093.

Kang Z, Buchenauer H: Ultrastructure and immunocytochemical investigation of pathogen development and host responses in resistant and susceptible wheat spikes infected by *Fusarium culmorum*. *Physiological and Molecular Plant Pathology 2000*, 57:255-268.

Kang Z, Buchenhauer H, Huang L, Han Q, Zhang H: Cytological and immunocytochemical studies on responses of wheat spikes of the resistant Chinese cv. Sumai 3 and the susceptible cv. Xiaoyan 22 to infection by *Fusarium graminearum*. *European Journal of Plant Pathology* 2008, 120:383-396.

Kazan K, Manners JM: Jasmonate signalling: Towards an integrated view. *Plant Physiology* 2008, 146:1459-1468.

Kazan K, Manners JM: Linking development to defense: auxin in plant-pathogen interactions. *Trends in Plant Science* 2009, 14:373-382.

Kazan K, Gardiner DM, Manners JM: On the trail of a celreal killer: recent advances in *Fusarium graminearum* pathogenomics and host resistance. *Molecular Plant Pathology* 2012, 13:399-413.

Kende H: Ethylene biosynthesis. *Annual Review of Plant Physiology and Plant Molecular Biology* 1993, 44:283-307.

Kepinski S, Leyser O: The *Arabidopsis* F-box protein TIR1 is an auxin receptor. *Nature* 2005, 435:446–451.

Kieber JJ, Rothenberg M, Roman G, Feldmann KA, Ecker JR: CTR1, a negative regulator of the ethylene response pathway in Arabidopsis, encodes a member of the RAF family of protein-kinase. *Cell* 1993, 72:427-441.

Kim TW, Lee SM, Joo SH, Yun HS, Lee Y, Kaufman PB, Kirakosyan A, Kim SH, Nam KH, Lee JS, Chang SC, Kim SK: Elongation and gravitropism response of Arabidopsis roots are regulated by brassinolide and IAA. *Plant , Cell and Environment* 2007, 30:679-689.

Kim TW, Wang ZY.: Brassinosteroid signal transduction from receptor kinases to transcription factors. *Annual Review of Plant Biology* 2010, 61:681–704.

Kimura M, Tokai T, Takahashi-Ando N, Ohsato S, Fujimura M: Molecular and genetic studies of Fusarium trichothecene biosynthesis: pathways, genes and evolution. *Bioscience Biotechnology and Biochemistry* 2007, 71:2105-2123.

Knusden IMB, Hockenhull J, Jensen DF: Biocontrol of seedling diseases of barley and wheat caused by *Fusarium culmorum* and *Bipolaris sorokiniana* – effects of selected fungal antagonists on growth and yield components. *Plant Pathology*, 44:467-477.

Kruger WM, Pritsch C, Chao S, Muehlbauer GJ: Functional and comparative bioinformatic analysis of expressed genes from wheat spikes infected with Fusarium graminearum. *Molecular Plant–Microbe Interactions* 2002, 15:445-455.

Langevin, F.; Eudes, F.; Comeau, A. Effect of trichothecenes produced by *Fusarium graminearum* during fusarium head blight development in six cereal species. *European Journal of Plant Pathology* 2004, *110*, 735-746.

Langridge P, Paltridge N, Fincher G: Functional genomics of abiotic stress tolerance in cereals. *Briefings in Functional Genomics &Proteomics* 2006, 4:343–354.

Lanoue A, Burlat V, Henkes GJ, Koch I, Schurr U, Röse US: De novo biosynthesis of defense root exudates in response to Fusarium attack in barley. *New Phytologist* 2010, 185:577–588.

Lemmens M, Scholz U, Berthiller F, Dall'Asta C, Koutnik A, Schuhmacher R, Adam G, Buerstmayr H, Mesterházy A, Krska R, Ruckenbauer P: The ability to detoxify the mycotoxin deoxynivalenol colocalizes with a major quantitative trait locus for Fusarium head blight resistance in wheat. *Molecular Plant-Microbe Interactions* 2005, 18:1318-1324.

Leon-Reyes A, Spoel SH, De Lange ES, Abe H, Kobayashi M, Tsuda S, Millenaar FF, Welschen RAM, Ritsema T, Pieterse CMJ : Ethylene modulates the role of NONEXPRESSOR OF PATHOGENESIS-RELATED GENES1 in cross talk between salicylate and jasmonate signaling. *Plant Physiology* 2009, 149:1797–809.

Leubner-Metzger G: Brassinosteroids and gibberellins promote tobacco seed germination by distinct pathways. *Planta* 2001, 213:758-763.

Lewandowski SM, Bushnell WR, Evans CK: Distribution of mycelial colonies and lesions in field-grown barley inoculated with *Fusarium graminearum*. *Phytopathology* 2006, 96:567-581.

Li G., Yen Y: Jasmonate and ethylene signaling pathway may mediate *Fusarium* head blight resistance in wheat. *Crop Science*. 2008, 48:1888-1896.

Lim PO, Kim HJ, Nam HG: Leaf senescence. *Annual Review of Plant Biology* 2007, 58:115-136.

Lim PO, Lee IC, Kim J, Kim HJ, Ryu JS, Woo HR, Nam HG: Auxin response factor 2 (ARF2) plays a major role in regulating auxin-mediated leaf longevity. *Journal of Experimental Botany* 2010, 61:1419-1430.

Liu S, Zhang X, Pumphrey MO, Stack RW, Gill BS, Anderson JA: Complex microcolinearity among wheat, rice and barley revealed by fine mapping of the genomic region harbouring a major QTL for resistance to *Fusarium* head blight in wheat. *Functional and Integrative Genomics* 2006, 6:83-89.

Lorenzo O, Piqueras R, Sanchez-Serrano JJ, Solano R: ETHYLENE RESPONSE FACTOR1 integrates signals from ethylene and jasmonate pathways in plant defense. *Plant Cell* 2003, 15:165-178.

Lorenzo O, Solano R: Molecular players regulating the jasmonate signaling network. *Current Opinion in Plant Biology* 2005, 8:532–540.

Lucas JA, Dyer PS, Murray TD: Pathogenicity, host-specificity, and population biology of *Tapesia* spp., causal agents of eyespot disease of cereals. *Advances in Botanical Research* 2000, 33:225-258.

Lucyshyn D, Busch BL, Abolmaali S, Steiner B, Chandler E, Sanjarian F, Mousavi A, Nicholson P, Buerstmayr H, Adam G: Cloning and characterization of the ribosomal protein L3 (*RPL3*) gene family from *Triticum aestivum*. *Molecular Genetics and Genomics* 2007, 277:507-517.

Lund ST, Stall RE, Klee HJ: Ethylene regulates the susceptible response to pathogen infection in tomato. *Plant Cell* 1998, 10:371-382.

Luo N, Liu J, Yu X, Jiang Y: Natural variation of drought response in *Brachypodium distachyon*. Physiologia Plantarum 2010, 141:19-29.

Maier FJ, Miedaner T, Hadeler B, Felk A, Salomon S, Lemmens M, Kassner H, Schäfer : Involvement of trichothecenes in fusarioses of wheat, barley and maize evaluated by gene disruption of the trichodiene synthase (Tri5) gene in three field isolates of different chemotype and virulence. *Molecular Plant Pathology* 2006, 7:449-461.

Makandar R, Essig JS, Schapaugh MA, Trick HN, Shah J: Genetically engineered resistance to Fusarium head blight in wheat by expression of Arabidopsis NPR1. *Molecular Plant-Microbe Interactions* 2006, 19:123-129.

Makandar R, Nalam V, Chaturvedi R, Jeannotte R, Sparks AA, Shah J: Involvement of salicylate and jasmonate signalling pathways in Arabidopsis interaction with Fusarium graminearum. *Molecular Plant-Microbe Interactions* 2010, 23:961-970.

Makandar R, Nalam VJ, Lee H, Trick HN, Dong Y, Shah J: Salicylic acid regulates basal resistance to Fusarium head blight in wheat. *Molecular Plant-Microbe Interactions* 2012, 25:431-439.

Makepeace JC, Havis ND, Burke JI, Oxley SJP, Brown JKM: A method of inoculating barley seedlings with *Ramularia collo-cygni*. *Plant Pathology* 2008, 57:991-999.

Malalasekera RAP, Sanderson FR, Colhoun J: Fusarium diseases of cereals: IX. Penetration and invasion of wheat seedlings by *Fusarium culmorum* and *F. nivale*. *Transactions of the British Mycological Society* 1973, 60:453-462.

Masuda D, Ishida M, Yamaguchi K, Yamaguchi I, Kimura M, Nishiuchi T: Phytotoxic effects of trichothecenes on the growth and morphology of Arabidopsis thaliana. *Journal of Experimtental Botany* 2007, 58:1617-1626.

Mathre DE: Compendium of Barley Diseases. St Paul, USA: *American Phytopathological Society Press* 1982, p78.

Mayer AM, Staples RC, Gil-ad NL: Mechanisms of survival of necrotrophic fungal plant pathogens in hosts expressing the hypersensitive response. *Phytochemistry* 2001, 58:33-41.

McLaughlin CS, Vaughan MH, Campbell IM, Wei CM, Stafford ME, Hansen BS: Inhibition of protein synthesis by trichothecenes. In: Rodericks JV, Hesseltine CW, Mehlman MA, editors. Mycotoxins in human and health 1977. Park Forest South, IL: Pathotoxicity. pp 263–275.

McMahon: Cycloheximide is not a specific inhibitor of protein synthesis *in Vivo*. *Plant Physiology* 1975, 55:815-821.

McSteen P: Auxin and monocot development. *Cold Spring Harbor Perspectives in Biology* 2010, 2:a001479.

Mengiste T: Plant immunity to necrotrophs. *Annual Review of Phytopathology* 2012, 50:13.1-13.28.

Mergoum M, Hill JP, Quick JS: Evaluation of resistance of winter wheat to *Fusarium acuminatum* by inoculation of seedling roots with single, germinated macroconidia. *Plant Disease* 1998, 98:300-302.

Mesterházy A: Types and components of resistance to Fusarium head blight of wheat. *Plant Breeding* 1995, 114:377-386.

Miedaner T: Breeding wheat and rye for resistance to *Fusarium* diseases. *Plant Breeding* 1997, 116:201-220.

Miller JD, Young JC, Sampson DR: Deoxynivalenol and Fusarium head blight resistance in spring cereals. *Journal of Phytopathology* 1985, 113:359-367.

Mittal S, Davis KR: Role of the phytotoxin coronatine in the infection of Arabidopsis thaliana by *Pseudomonas syringae* pv. tomato. *Molecular Plant-Microbe Interactions* 1995, 8:165-171.

Morgavi DP, Riley RT: An historical overview of field disease outbreaks known or suspected to be caused by consumption of feeds contaminated with Fusarium toxins. *Animal Feed Science and Technology* 2007, 137:201-212.

Mudge AM, Dill-Macky R, Dong Y, Gardiner DM, White RG, Manners JM: A role for the mycotoxin deoxynivalenol during crown rot disease of wheat caused by *Fusarium graminearum* and *Fusarium pseudograminearum*. *Physiological and Molecular Plant Pathology* 2006, 69:73-85.

Mur LAJ, Allainguillaum J, Catalàn p, Hasterok R, Jenkins G, Lesniewska K, Thomas I, Vogel J: Exploiting the Brachypodium tool box in cereal and grass research. *New Phytologist* 2011, 191:334-347.

Mur LAJ, Allainguillaume J, Catalán P, Hasterok R, Jenkins G, Lesniewska K, Thomas I, Vogel J: Exploiting the Brachypodium tool box in cereal and grass research. *New Phytologist* 2011, 191:334-347.

Mur LAJ, Kenton P, Atzorn R, Miersch O, Wasternack C: The outcomes of concentration-specific interactions between salicylate and jasmonate signalling include synergy, antagonism, and oxidative stress leading to cell death. *Plant Physiology* 2006, 140:249-262.

Murray F, Brettell R, Matthews P, Bishop D, Jacobsen J: Comparison of Agrobacterium-mediated transformation of four barley cultivars using the GFP and GUS reporter genes. *Plant Cell Reports* 2004, 22:397–402.

Nagy CM, Fejer SN, Berek L, Molnar J, Viskolcz B: Hydrogen bondings in deoxynivalenol (DON) conformations – A density functional study. *Journal of Molecular Structure – Theoretical Chemistry* 2005, 726:55-59.

Nakashita H, Yasuda M, Nitta T, Asami T, Fujioka S, Arai Y, Sekimata K, Takatsuto S, Yamaguchi I, Yoshida S: Brassinosteroid functions in a broad range of disease resistance in tobacco and rice. *The Plant Journal* 2003, 33:887-898.

Nam KH, Li J: BRI1/BAK1, a receptor kinase pair mediating brassinosteroid signalling. *Cell* 2002, 110:203-212.

Nganje WE, Kaitibie S, Wilson WW, Leistritz FL, Bangsund DA: Economic impacts of Fusarium head blight in wheat and barley: 1993-2001. *Applied Economic Perspectives and Policy* 2004, 26:332-347.

Niu YH, Guo FQ: Nitric oxide regulates dark-induced leaf senescence through *EIN2* in *Arabidopsis*. *Journal of Integrative Plant Biology* 2012, 54:516-525.

Nooden LD: Whole plant senescence. In: Nooden LD, Leopold AC Eds: Senescence and Aging in Plants. Academic Press Inc. 1988, San Diego, CA: 392–439.

Okushima Y, Overvoorde PJ, Arima K, Alonso JM, Chan A, Chang C, Ecker JR, Hughes B, Lui A, Nguyen D, Onodera C, Quach H, Smith A, Yu GX, Theologis A: Functional genomic analysis of the AUXIN RESPONSE FACTOR gene family members in Arabidopsis thaliana: Unique and overlapping functions of ARF7 and ARF19. *Plant Cell* 2005, 17:444-463.

Păcurar DI, Thordel-Christensen H, Nielsen KK, Lenk I: A high-throughput Agrobacterium-mediated transformation system for the grass model species Brachypodium distachyon L. *Transgenic Research* 2008, 17:965-975.

Padmanabhan MS, Shiferaw H, Culver JN: The tobacco mosaic virus replicase protein disrupts the localization and function of interacting Aux/IAA proteins. *Molecular Plant Microbe-Interactions* 2006, 19:864-873.

Parry DW, Jenkinson P, McLeod L: Fusarium ear blight (scab) in small grain cereals - a review. *Plant Pathology* 1995, 44:207-238.

Paul PA, El-Allaf SM, Lipps PE, Madden LV: Rain splash dispersal of *Gibberella zeae* within wheat canopies in Ohio. *Phytopathology* 2004, 97:1342–1349.

Peng JR, Richards DE, Hartley NM, Murphy GP, Devos KM, Flintham JE, Beales J, Fish LJ, Worland AJ, Pelica F, Sudhakar D, Christou P, Snape JW, Gale MD, Harberd NP: 'Green revolution' genes encode mutant gibberellins response modulators. *Nature* 1999, 400:256-261.

Peoples M, Dalling M.: The Interplay Between Proteolysis and Amino Acid Metabolism During Senescence and Nitrogen Reallocation. Academic Press, San Diego, CA.1988.

Peraldi A, Beccari G, Steed A, Nicholson P: *Brachypodium distachyon*: a new pathosystem to study Fusarium head blight and other *Fusarium* diseases of wheat. *BMC Plant Biology* 2011, 11:100.

Percival GC, Keary IP, Noviss K: The potential of a chlorophyll content SPAD meter toquantify nutrient stress in foliar tissue of sycamore (*Acer pseudoplatanus*), English oak (*Quercus robur*), and European beech (*Fagus sylvatica*). *Arboriculture & Urban Forestry* 2008, 34:89.

Pestka JJ, Zhou HR, Moon Y, Chung YJ: Cellular and molecular mechanisms for immune modulation by deoxynivalenol and other trichothecenes: unravelling a paradox. *Toxicology Letters* 2004, 153:61-73.

Pieterse CMJ, Ton J, van Loon LC: Cross-talk between plant defence signalling pathways: boost or burden? *AgBiotechNet* 2001, 3:1-8.

Placinta CM, D'Mello JPF, Macdonald AMC: A review of worldwide contamination of cereal grains and animal feed with *Fusarium* mycotoxins. *Animal Feed Science and Technology* 1999, 78:21-37.

Poppenberger B, Berthiller F, Lucyshyn D, Sieberer T, Schuhmacher R, Krska R, Kuchler K, Glössl J, Luschnig C, Adam G: Detoxification of the Fusarium mycotoxin deoxynivalenol by a UDP-glucosyltransferase from *Arabidopsis thaliana*. *The Journal of Biological Chemistry* 2003, 278:47905-47914.

Poppenberger B, Fujioka S, Soeno K, George GL, Vaistij FE, Hiranuma S, Seto H, Takatsuto S, Adam G, Yoshida S, Bowles D: The UGT73C5 of Arabidopsis thaliana glucosylates brassinosteroids. *Proceedings of the National Academy of Sciences of the United States of America* 2005, 102:15253-15258.

Pritsch C, Muehlbauer GJ, Bushnell WR, Somers DA, Vance CP: Fungal development and induction of defense response genes during early infection of wheat spikes by *Fusarium graminearum*. *Molecular Plant-Microbe Interactions* 2000, 13:159-169.

Qi LL, Pumphrey MO, Friebe B, Gill BS: Molecular cytogenetic characterization of alien introgressions with gene Fhb3 for resistance to Fusarium head blight disease of wheat. *Theoretical and Applied Genetics* 2008, 117:1155-1166.

Richards DE, King KE, Ait-ali T, Harberd NP: How gibberellin regulates plant growth and development: a molecular genetic analysis of gibberellin signalling. *Annual Review of Plant Physiology and Plant Molecular Biology* 2001, 52:67-88.

Rittenour WR, Harris SD: An In Vitro method for the analysis of infection related morphogenesis in *Fusarium graminearum*. *Molecular Plant Pathology* 2010, 11:361-369.

Robert-Seilaniantz A, Grant M, Jones JDG: Hormone crosstalk in plant disease and defense: More than just Jasmonate-Salicylate antagonism. *Annual Review of Phytopathology* 2011, 49:317-343.

Robert-Seilaniantz A, Navarro L, Bari R, Jones JDG: Pathological hormone imbalance. *Current Opinion in Plant Biology* 2007, 10:372-379.

Rocha O, Ansari K, Doohan FM: Effects of trichothecene mycotoxins on eukaryotic cells: a review. *Food Additives and Contaminants* 2005, 22:369-378.

Routledge APM, Shelley G, Smith JV, Talbot NJ, Draper J, Mur LAJ: *Magnaporthe grisea* interactions with the model grass *Brachypodium distachyon* closely resemble those with rice (Oryza sativa). *Molecular Plant Pathology* 2004, 5:253-265.

Sachs E, Amelung D, Greif P: Ramularia leaf spot (*Ramularia collo-cygni* Sutton et Waller) on barley in Franconia (Bavaria). *Nachrichtenblatt des Deutschen Pflanzenschutzdienstes* 1998, 50:307-309.

Sachs E, Greil P, Amelung D, Huss H: *Ramularia collo-cygni* – a re-discovered barley pathogen in Europe. Mitt BBA 1998, 357: 96–97.

Santner AA, Wateson JC: The WGA1 and WAG2 protein kinase negatively regulate root waving in Arabidopsis. *The Plant Journal* 2006, 45:752-764.

Savard ME, Sinha RC, Seaman WL, Fedak G: Sequential distribution of the mycotoxin deoxynivalenol in wheat spikes after inoculation with *Fusarium graminearum*. *Canadian Journal of Plant Pathology* 2000, 22:280-285.

Saville RJ, Gosman N, Burt CJ, Makepeace J, Steed A, Corbitt M, Chandler E, Brown JKM, Boulton MI, Nicholson P: The 'Green Revolution' dwarfing genes play a role in disease resistance in *Triticum aestivum* and *Hordeum vulgare*. *Journal of Experimental Botany* 2012, 63:1271-1283.

Savitch LV, Subramaniam R, Allard GC, Singh J: The GLK1 'regulon' encodes disease defense related proteins and confers resistance to *Fusarium graminearum* in Arabidopsis. *Biochemical and biophysical research communications* 2007, 359:234-238.

Schisler DA, Khan NL, Boehm MJ: Greenhouse and field evaluation of biological control of Fusarium head blight on durum wheat. *Plant Disease* 2002, 86:1350-1356.

Schroeder HW, Christensen JJ: Factors affecting resistance of wheat to scab caused by Gibberella zeae. *Phytopathology* 1963, 53:831-838.

Scott PR, Hollins TW: Effects of eyespot on yield of winter-wheat. *Annals of Applied Biology* 1974, 78:269-279.

Simopoulos AP (ed): Evolutionary Aspects of Nutrition and Health.Diet, Exercise, Genetics and Chronic Disease. World Rev Nutr Diet. Basel, Karger, 1999, vol 84, pp 19–73.

Smith PH: Trichodiene synthase and the role of trichothecenes in *Fusarium* spp.. PhD Thesis 1997. University of East Anglia: UK.

Snijders CHA, Krechting CF: Inhibition of deoxynivalenol translocation and fungal colonization in Fusarium head blight resistant wheat. *Canadian Journal of Botany* 1992, 70:1570-1576.

Sobrova P, Adam V, Vasatkova A, Beklova M, Zeman L, Kizek Rene: Deoxynivalenol and its toxicity. *Interdisciplinary Toxicology* 2010, 3:94-99.

Solano R, Stepanova A, Chao QM, Ecker JR: Nuclear events in ethylene signalling: a transcriptional cascade mediated by ETHYLENE-INSENSITIVE 3 and ETHYLENE-RESPONSE-FACTOR 1. *Genes & Development 1998*, 12:3703-3714.

Srinivasachary, Gosman N, Steed A, Hollins TW, Bayles R, Jennings P, Nicholson P: Semi-dwarfing *Rht-B1* and *Rht-D1* loci of wheat differ significantly in their influence on resistance to *Fusarium* head blight. *Theoretical and Applied Genetics* 2009, 118: 695-702.

Staswick PE, Tiryaki I: The oxylipin signal jasmonic acid is activated by an enzyme that conjugates it to isoleucine in Arabidopsis. *The Plant Cell* 2004, 16:2117-2127.

Stepanova AN, Alonso JM: Ethylene signalling and response: where different regulatory modules meet. *Current Opinion in Plant Biology* 2009, 12:548-555.

Stephens AE, Gardiner DM, White RG, Munn AL, Manners JM: Phases of infection and gene expression of *Fusarium graminearum* during crown rot disease of wheat. *Molecular Plant–Microbe Interactions* 2008, 21:1571–1581.

Sutton JC: Epidemiology of wheat head blight and maize ear rot caused by *Fusarium graminearum*. *Canadian Journal of Plant Pathology* 1982, 4:195-209.

Tada Y, Hata S, Takata Y, Nakayashiki H, Tosa Y, Mayama S: Induction and signaling of an apoptotic response typified by DNA laddering in the defence response of oats to infection and elicitors. *Molecular Plant-Microbe Interactions* 2001, 14:477–486.

Takesuo S.: Brassinosteroids: distribution in plants, bioassays and microanalysts by gas chromatography–mass spectrometry. *Journal of Chromatography* 1994, 658:3–15.

Teale WD, Paponov IA, Palme K: Auxin in action: signalling, transport and the control of plant growth and development. *Nature Reviews Molecular Cell Biology* 2006, 7:847-859.

The International Brachypodium Initiative: Genome sequencing and analysis of the model grass *Brachypodium distachyon*. *Nature* 2010, 463:763-768.

The International Rice Genome Sequencing Project: The map-based sequence of the rice genome. *Nature* 2005, 436:793-800.

Thole V, Alves SC, Worland B, Bevan MW, Vain P: A protocol for efficiently retrieving and characterizing flanking sequence tags (FSTs) in *Brachypodium distachyon* T-DNA insertional mutants. *Nature Protocols* 2009, 4:650-661.

Thole V, Worland B, Wright J, Bevan MW, Vain P.: Distribution and characterization of more than 1000 T-DNA tags in the genome of Brachypodium distachyon community standard line Bd21. *Plant Biotechnology Journal* 2010, 8:734–747.

Thole V, Peraldi A, Worland B, Nicholson P, Doonan JH, Vain P: T-DNA mutagenesis in Brachypodium distachyon. *Journal of experimental botany* 2012, 63:567-576.

Tian D, Traw MB, Chen JQ, Kreitman M, Bergelson J: Fitness costs of R-gene-mediated resistance in *Arabidopsis thaliana*. *Nature* 2003, 423: 74-77.

Ton J, Pieterse CMJ, van Loon LC: The relationship between basal and induced resistance in Arabidopsis. In: Tuzan S, Bent E Eds. *Multigenic and Induced Systemic Resistance in Plants*. Dordrecht, The Netherlands: Springer, 197-224.

Torres-Zabala M, Truman W, Bennett MH, Lafforgue G, Mansfield JW, Rodriguez-Egea P, Bögre, Grant M: *Pseudomonas syringae* pv. *tomato* hijacks the Arabidopsis abscisic acid signalling pathway to cause disease. *The EMBO Journal* 2007, 26:1434-1443.

Tóth B, Mesterházy A, Horváth A, Bartók T, Varga M, Varga J: Genetic variability of central European isolates of the *Fusarium graminearum* species complex. *European Journal of Plant Pathology* 2005, 113:35-45.

Trail F: For blighted waves of grain: Fusarium graminearum in postgenomics era. *Plant Physiology* 2009, 149:103-110.

Ubeda-Thomás S, Beemster GTS, Bennett M: Hormonal regulation of root growth: integrating local activities into global behaviour. *Trends in Plant Sciences* 2012, 17:326-331.

Ueno Y: The toxicology of mycotoxins. *Critical Reviews in Toxicology* 1985, 14:99–133.

Ulmasov T, Hagen G, Guilfoyle TJ: ARF1, a transcription factor that binds to auxin response elements. *Science* 1997, 276:1865–1868.

Urban M, Daniels S, Mott E, Hammond-Kosack K: Arabidopsis is susceptible to the cereal ear blight fungal pathogens *Fusarium graminearum* and *Fusarium culmorum*. *The Plant Journal* 2002, 32:961-973.

Vain P, Worland B, Thole V, McKenzie N, Alves SC, Opanowicz M, Fish LJ, Bevan MW, Snape JW: *Agrobacterium*-mediated transformation of the temperate grass *Brachypodium distachyon* (genotype Bd21) for T-DNA insertional mutagenesis. *Plant Biotechnology Journal* 2008, 6:941-941.

Vain P, Thole V, Worland B, Opanoowicz M, Bush MS, Doonan JH: A T-DNA mutation in the RNA helicase elF4A confers a dose-dependent dwarfing phenotype in *Brachypodium distachyon*. *The Plant Journal* 2011, 66:929-940.

Van Der Graaff E, Schwacke R, Schneider A, Desimone M, Flugge UI, Kunze R: Transcription analysis of Arabidopsis membrane transporters and hormones pathways during developmental and induced leaf senescence. *Plant Physiology* 2006, 141:776-792.

Van loon LC, Geraats BPJ, Linthorst HJM: Ethylene as a modulator of disease resistance in plants. Trends in Plant Science 2006, 11:184-191.

Vogel J, Hill T: High-efficiency Agrobacterium-mediated transformation of Brachypodium distachyon inbred line Bd21-3. *Plant Cell Reports* 2008, 27:471-478.

Vogel JP, Gu YQ, Twigg P, Lazo GR, Laudencia-Chingcuanco D, Hayden DM, Donze TJ, Vivian LA, Stamova B, Coleman-Derr D: EST sequencing and phylogenetic analysis of the model grass *Brachypodium distachyon*. *Theoretical and Applied Genetics* 2006, 113:186-195.

Wagacha JM, Oerke EC, Dehne HW, Steiner U: Colonization of wheat seedling leaves by Fusarium species as observed in growth chambers: a role as inoculum for head blight infection?, *Fungal Ecology* 2012, doi:10.1016/j.funeco.2012.02.002.

Walters DR, Havis ND, Oxley SJP: *Ramularia collo-cygni*: the biology of an emerging pathogen of barley. *FEMS Microbiology Letters* 2007, 279:1-7.

Wang D, Pei K, Fu Y, Sun Z, Li S, Liu H, Tang K, Han B, Tao Y: Genome-wide analysis of the *auxin response factors* (ARF) gene family in rice (*Oryza sativa*). *Gene* 2007, 394:13-24.

Wang YZ, Miller JD: Effects of *Fusarium graminearum* metabolites on wheat tissue in relation to Fusarium head blight resistance. *Journal of Phytopathology* 1988, 122:118-125.

Ward TJ, Clear RM, Rooney AP, O'Donnell K, Gaba D, Patrick S, Starkey DE, Gilbert J, Geiser DM, Nowicki TW: An adaptative evolutionary shift in Fusarium head blight pathogen populations is driving the rapid spread of more toxigenic *Fusarium graminearum* in North America. *Fungal Genetics and Biology* 2008, 473-484.

Wasternack C: Jasmonates: an update on biosynthesis, signal transduction and plant stress response, growth and development. *Annals of Botany* 2007, 100:681-697.

Wei L, Muranty H, Zhang H: Advances and prospects in wheat eyespot research: contributions from genetics and molecular tools. *Journal of Phytopathology* 2011, 159:457-470.

Weise MV: Compendium of Wheat Diseases. *The American Phytopathological Society Press*, USA St., Paul, Minn 1987, 112.

Wisnieska H, Busko M: Evaluation of spring wheat resistance to fusarium seedling blight and head blight. *Biologia* (Bratislava) 2005, 60:287–293.

Wisniewska H, Busko M: Evaluation of spring wheat resistance to Fusarium seedling blight and had blight. *Biologia* 2005, 60:287-293.

Xu X, Nicholson P: Community ecology of fungal pathogens causing wheat head blight. *Annual Review of Phytopathology* 2009, 47:83-103.

Xu XM, Monger W, Ritieni A, Nicholson P: Effect of temperature and duration of wetness during initial infection periods on disease development, fungal biomass and mycotoxin concentrations on wheat inoculated with single, or combinations of, Fusarium species. *Plant Pathology* 2007, 56:943-956.

Xu XM, Nicholson P, Thomsett MA, Simpson D, Cooke BM, Doohan FM, Brennan J, Monaghan S, Moretti A, Mule G, Hornok L, Beki J, Tatnell J, Ritieni A, Edwards SG: Relationship between the fungal complex causing Fusarium head blight of wheat and environmental conditions. *Phytopathology* 2008, 98:69-78.

Xue S, Li G, Jia H, Xu F, Lin F, Tang M, Wang Y, An Y, Xu H, Zhang L, Kong Z, Ma Z: Fine mapping Fhb4, a major QTL conditioning resistance to *Fusarium* infection in bread wheat (*Triticum aestivum* L.). *Theoretical and Applied Genetics* 2010, 121:147-156.

Yamamuro C, Ihara Y, Wu X, Noguchi T, Fujioka S, Takatsuto S, Ashikari M, Kitano H, Matsuoka M: Loss of function of a rice brassinosteroid insensitive 1 homolog prevents internode elongation and bending of the lamina joint. *The Plant Cell 2000*, 12:1591-1605.

Yang SF, Hoffman NE: Ethylene biosynthesis and its regulation in higher plants. *Annual Review of Plant Physiology and Plant Molecular Biology* 1984, 35:155-189.

Yi HC, Joo S, Nam KH, Lee JS, Kang BG, Kim WT: Auxin and brassinosteroid differentially regulate the expression of three members of the 1-aminocyclopropane-1-carboxylate synthase gene family in mung bean (*Vigna radiata* L.). *Plant Molecular Biology* 1999, 41:443–454.

Yoo SD, Cho YSJ: Emerging connections in the ethylene signaling network. *Trends in Plant Science 2009*, 14:270-279.

Zadocks JC, Chang TT, Konzak CF: A decimal code for the growth stages of cereals. *Weed Research* 1974, 14:415-421.

Zheng SJ, Vogel JP: Brachypodium as a model for the grasses: today and the future. *Plant Physiology*, 157:3-13.

Zheng XY, Spivey NW, Zeng W, Liu PP, Fu ZQ, Klessig DF, He SY, Dong X: Coronatine promotes *Pseudomonas syringae* virulence in plants by activating a signalling cascade that inhibits salicylic acid accumulation. *Cell Host & Microbe* 2012, 11:587-596.

Zhu H, Gilchrist L, Hayes P, Kleinhofs A, Kudrna D, Liu Z, Prom L, Steffenson B, Toojinda T, Vivar H: Does function follow form? Principal QTLs for Fusarium head blight (FHB) resistance are coincident with QTLs for inflorescence traits and plant height in a double-haploid population of barley, *Theoretical and Applied Genetics* 1999, 99:1221-1232.

Zhu Z, Guo H: Genetic basis of ethylene perception and signal transduction in Arabidopsis. *Journal of Integrative Plant Biology* 2008, 7:808-815.

Zipfel C, Robatzek S, Navarro L, Oakeley EJ, Jones JDG, Felix G, Boller T: Bacterial disease resistance in Arabidopsis through flagellin perception. *Nature* 2004, 428:764-767.

APPENDIX 1

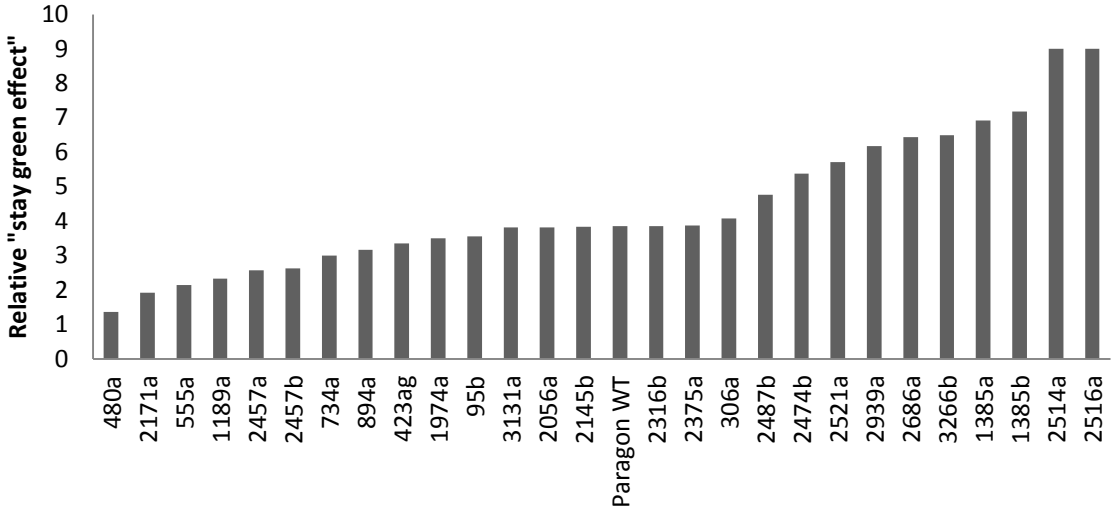

Supplementary Figure 1: Visual ranking of post-anthesis flag-leaf senescence in the field of EMS Paragon mutant lines.

Appendix 2

Supplementary Figure 1**: Comparison of symptoms following Fg infection on Bd21 and Bd3-1 leaves**. Symptoms on leaves of Bd21 and Bd3-1, 120 h following wound inoculation with Fg UK1.

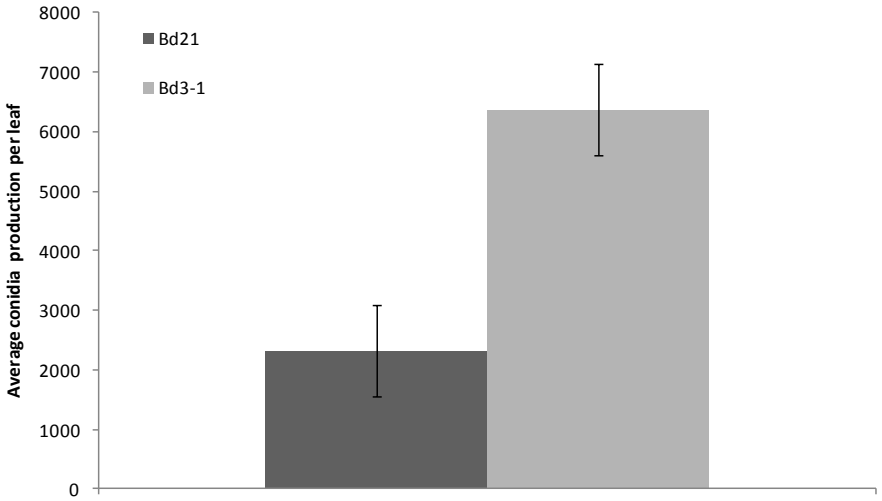

Supplementary Figure 2: **Comparison of Fg conidial production on Bd21 and Bd3-1 detached leaves**. Conidial production following inoculation of Fg UK1 onto Bd21 and Bd3-1 detached leaves, 7 dpi.

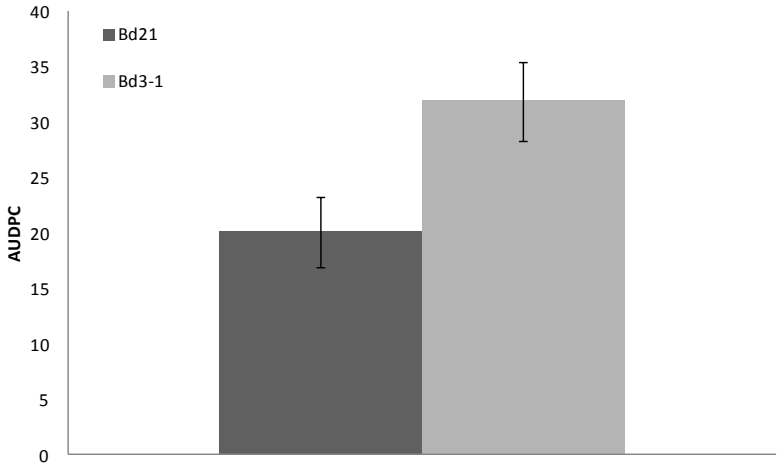

Supplementary Figure 3: **Comparison of necrotic symptoms development following Fg point inoculation on Bd21 and Bd3-1 spikelets**. Area under disease progress curve (AUDPC) for lesions of Bd21 and Bd3-1 spikelets point inoculated with Fg UK1.

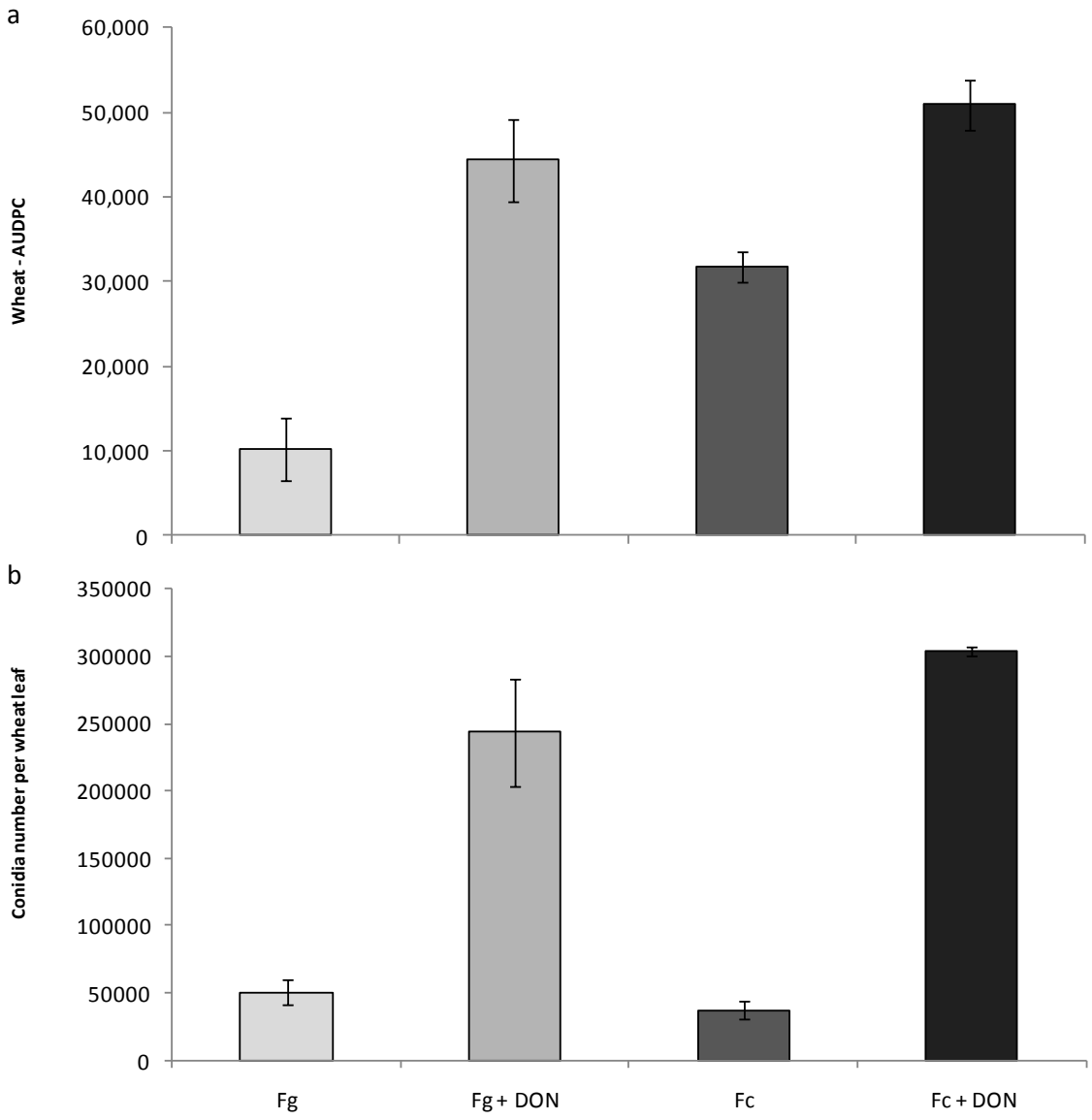

Supplementary Figure 4: **Effect of DON treatment on detached wheat leaves infected with Fg or Fc**. a) Area under disease progress curve (AUDPC) for lesions following wound-inoculation of wheat (cv. Paragon) leaves with Fg UK1 and Fc GFP1 with or without amendment with DON (75 µM). b) Conidial production (6dpi) on leaves of wheat (cv. Paragon) following wound-inoculation with Fg UK1 and Fc GFP1 with or without amendment with DON (75 µM).

Supplementary Table 1: Sequences of the PCR primer used for PCR genotyping of T-DNA mutant lines BdAA900 and BdAA724.

Primer	PCR product	Primer sequence
BDAA900LBR3	T-DNA:Bd21	5'-GCCTCGACGTAAGTAAAGGATAA-3'
TDNA4	T-DNA:Bd21	5'-CGGCCGCATGCATAAGCTTA-3'
BdAA900LBR3	Bd21WT	5'-GCCTCGACGTAAGTAAAGGATAA-3'
BdAA900LBV2	Bd21WT	5'-GCGACAAACAGTGCCGCCGCTAT-3'
Bdfa	T-DNA:Bd21	5'-ACATGTTAGCCACATCAACGAGC-3'
TDNA4	T-DNA:Bd21	5'-CGGCCGCATGCATAAGCTTA-3'
Bdfa	Bd21WT	5'-ACATGTTAGCCACATCAACGAGC-3'
Bdra2	Bd21WT	5'-AGAAGAGACACTCACCTCCGGC-3'

Supplementary Table 2: Multiple alignment of BRI1 (brassinosteroid insensitive-1) protein sequences. The predicted protein sequences of previously characterised BRI1 (brassinosteroid insensitive-1) homologues from *Arabidopsis thaliana* (At4g39400), *Oryza sativa* (Os01g52050) and *Hordeum vulgare* (GenBank accession number BAD01654) were compared to *Brachypodium distachyon* Bradi2g48280 using ClustalW (EMBL-EBI). The percentage of identity between the different sequences as well as the protein alignments are presented below. aa: amino acid, At: *Arabidopsis thaliana*, Os: *Oryza sativa*, Hv: *Hordeum vulgare*, Bd: *Brachypodium distachyon.*

Organism	No. aa	versus	No. aa	%ID
At	1196	Os	1121	55
At	1196	Hv	1118	56
At	1196	Bd	1122	56
Os	1121	Hv	1118	82
Os	1121	Bd	1122	84
Hv	1118	Bd	1122	90

```
Hv      ---MDCLRLAVAAAALLLA---ALAAAAD-----DAQLLDEFRMALPSQAPLEGWTAREG 49
Bd      ---MDSLRVAIAAALFVAAVAVAVAAAAD-----DAQLLEEFRAAVPNQASLSGWKAADG 52
Os      ---MDSLWAAIAALFVAAAVVVRGAAAAD-----DAQLLEEFRQAVPNQAALKGWSGGDG 52
At      MKTFSSFFLSVTTLFFFSFFSLSFQASPSQSLYREIHQLISFKDVLPDKNLLPDWSSNKN 60
           :..:  ::::  .         *:..     : : * .*: .:*.:  * .*.. ..

Hv      ACRFPGAVCRGGRLTSLSLAAVTLNADFRAVANTLLQLSAVERLSLRGANVSGALAAA-- 107
Bd      ACRFPGAACRAGRLTSLSLAGVPLNADFRAVAATLLQLSGVEALSLRGANVSGALAAAGG 112
Os      ACRFPGAGCRNGRLTSLSLAGVPLNAEFRAVAATLLQLGSVEVLSLRGANVSGALSAAGG 112
At      PCTFDGVTCRDDKVTSIDLSSKPLNVGFSAVSSSLLSLTGLESLFLSNSHINGSVSGF-- 118
        .* * *. ** .::**:.*:. .**. * **: :**.* .:* * * .:::.*:::.

Hv      -RCGGKLEELDLSGNAALRGSVADVAALAGSCGALRTLNLSGDAVGAAKPAGGGGGGQGF 166
Bd      ARCGGKLEALDLSGNAALRGSVADVAALADSCAGLKKLNLSGGAVGAAK--AGGGGGAGF 170
Os      ARCGSKLQALDLSGNAALRGSVADVAALASACGGLKTLNLSGDAVGAAK--VGGGGGPGF 170
At      -KCSASLTSLDLSRNS-LSGPVTTLTSLG-SCSGLKFLNVSSNTLDFPG---KVSGGLKL 172
         :*...*  **** *: * *.*: :::*. :*..*: **:*..::. .      .**  :

Hv      AALDALDLSSNKIAGDADLRWMVGAGLGSVRWLDLAWNKISGG---------------- 209
Bd      AALDVLDLSNNKITGDAELRWMVGAGVGSVRWLDLAWNRISGE---------------- 213
Os      AGLDSLDLSNNKITDDSDLRWMVDAGVGAVRWLDLALNRISG----------------- 212
At      NSLEVLDLSANSISGANVVGWVLSDGCGELKHLAISGNKISGDVDVSRCVNLEFLDVSSN 232
         .*: **** *.*:.   : *::. * * :: * :: *:***

Hv      -----LSDFTNCSGLQYLDLSGNLIAGDVAAAALSGCRSLRALNLSSN------------ 252
Bd      -----LPDFTNCSGLQYLDLSGNLIDGDVAREALSGCRSLRALNLSSN------------ 256
Os      -----VPEFTNCSGLQYLDLSGNLIVGEVPGGALSDCRGLKVLNLSFN------------ 255
At      NFSTGIPFLGDCSALQHLDISGNKLSGDFSR-AISTCTELKLLNISSNQFVGPIPPLPLK 291
             :. : :**.**:**:*** : *:..  *:* *  *: **:* *

Hv      ----------------------------------HLAGAFPPNIAGLTSLTALNLSNNN 277
Bd      ----------------------------------HLAGAFPPNIAGLASLTALNLSNNN 281
Os      ----------------------------------HLAGVFPPDIAGLTSLNALNLSNNN 280
At      SLQYLSLAENKFTGEIPDFLSGACDTLTGLDLSGNHFYGAVPPFFGSCSLLESLALSSNN 351
                                          *: *..** :.. : * :* **.**

Hv      FSGEVPADAFTGLQQLQSLSLSFNHFSGSIPDSVAALP-DLEVLDLSSNNFSGSIPDSLC 336
Bd      FSGEVPADAFTGLQQLKSLSLSFNHFTGSIPDSLAALP-ELEVLDLSSNTFTGTIPSSIC 340
Os      FSGELPGEAFAKLQQLTALSLSFNHFNGSIPDTVASLP-ELQQLDLSSNTFSGTIPSSLC 339
At      FSGELPMDTLLKMRGLKVLDLSFNEFSGELPESLTNLSASLLTLDLSSNNFSGPILPNLC 411
        ****:* :::  :: *  *.****.*.*.:*:::: *. .*  ******.*:*.*  .:*
```

```
Hv      QDPNSRLRVLYLQNNYLSGSIPEAVSNCTDLVSLDLSLNYINGSIPESLGELSRLQDLIM 396
Bd      QDPNSSLRVLYLQNNFLDGGIPEAISNCSNLVSLDLSLNYINGSIPESLGELAHLQDLIM 400
Os      QDPNSKLHLLYLQNNYLTGGIPDAVSNCTSLVSLDLSLNYINGSIPASLGDLGNLQDLIL 399
At      QNPKNTLQELYLQNNGFTGKIPPTLSNCSELVSLHLSFNYLSGTIPSSLGSLSKLRDLKL 471
        *:*:. *: ****** : * ** ::***:.****.**:**:.*:** ***.*..*:** :

Hv      WQNLLEGEIPASLSSIPGLEHLILDYNGLTGSIPPELAKCKQLNWISLASNRLSGPIPSW 456
Bd      WQNSLEGEIPASLSRIRGLEHLILDYNGLSGSIPPDLAKCTQLNWISLASNRLSGPIPSW 460
Os      WQNELEGEIPASLSRIQGLEHLILDYNGLTGSIPPELAKCTKLNWISLASNRLSGPIPSW 459
At      WLNMLEGEIPQELMYVKTLETLILDFNDLTGEIPSGLSNCTNLNWISLSNNRLTGEIPKW 531
        * * ****** .*  :  ** ****:*.*:*.**. *::*.:******:.***:* **.*

Hv      LGKLSNLAILKLSNNSFTGKIPAELGDCKSLVWLDLNSNQLNGSIPPELAEQSGKMTVGL 516
Bd      LGKLSNLAILKLSNNSFSGRVPPELGDCKSLVWLDLNNNQLNGSIPPELAEQSGKMSVGL 520
Os      LGKLSYLAILKLSNNSFSGPIPPELGDCQSLVWLDLNSNQLNGSIPKELAKQSGKMNVGL 519
At      IGRLENLAILKLSNNSFSGNIPAELGDCRSLIWLDLNTNLFNGTIPAAMFKQSGKIAANF 591
        :*:*. ***********:* :*.*****:**:*****.* :**:**  : :****: ..:

Hv      IIGRPYVYLRNDELSSQCRGKGSLLEFSSIRSEDLSRMPSKKLCNFT-RMYMGSTEYTFN 575
Bd      IIGRPYVYLRNDELSSQCRGKGSLLEFSSIRSEDLSRMPSKKLCNFT-RVYMGSTEYTFN 579
Os      IVGRPYVYLRNDELSSECRGKGSLLEFTSIRPDDLSRMPSKKLCNFT-RMYVGSTEYTFN 578
At      IAGKRYVYIKNDGMKKECHGAGNLLEFQGIRSEQLNRLSTRNPCNITSRVYGGHTSPTFD 651
        * *: ***::** :..:*:* *.**** .**.::*.*:.:: **:* *:* * *. **:

Hv      KNGSMIFLDLSFNQLDSEIPKELGNMFYLMIMNLGHNLLSGAIPTELAGAKKLAVLDLSH 635
Bd      KNGSMIFLDLSFNQLDSEIPKELGNMFYLMIMNLGHNLLSGPIPLELAGAKKLAVLDLSY 639
Os      KNGSMIFLDLSYNQLDSAIPGELGDMFYLMIMNLGHNLLSGTIPSRLAEAKKLAVLDLSY 638
At      NNGSMMFLDMSYNMLSGYIPKEIGSMPYLFILNLGHNDISGSIPDEVGDLRGLNILDLSS 711
        :****:***:*:* *.. ** *:*.* **:*:***** :**.** .:.  : * :****

Hv      NRLEGQIPSSFSSLS-LSEINLSSNQLNGTIPELGSLATFPKSQYENNSGLCGFPLPPCE 694
Bd      NRLEGPIPSSFSTLS-LSEINLSSNQLNGTIPELGSLATFPKSQYENNSGLCGFPLPPCQ 698
Os      NQLEGPIPNSFSALS-LSEINLSNNQLNGTIPELGSLATFPKSQYENNTGLCGFPLPPCD 697
At      NKLDGRIPQAMSALTMLTEIDLSNNNLSGPIPEMGQFETFPPAKFLNNPGLCGYPLPRCD 771
        *:*:* **.::*:*: *:**:**.*:*.*.***:*.: *** ::: **.****:*** *:

Hv      SHTGQGSSNGGQSN-RRKASLAGSVAMGLLFSLFCIFGLVIIAIESKKRRQKNDEASTSR 753
Bd      AHAGQSASDGHQSH-RRQASLAGSVAMGLLFSLFCIFGLVIIAIESKKRRQKNEEASTSH 757
Os      -HSSPRSSNDHQSH-RRQASMASSIAMGLLFSLFCII-VIIIAIGSKRRRLKNEEASTSR 754
At      PSNADGYAHHQRSHGRRPASLAGSVAMGLLFSFVCIFGLILVGREMRKRRRKKEAELEMY 831
           .   :.  :*: ** **:*.*:*******:.**: ::::.   ::** *::
```

```
Hv      DIYIDSRSHSGTMNSNWR--LSGTNALSINLAAFEKPLQKLTLGDLVEATNGFHNDSLIG 811
Bd      DIYIDSRSHSGTMNSNWR--LSGTNALSINLAAFEKPLQKLTLGDLVEATNGFHNDSLIG 815
Os      DIYIDSRSHSATMNSDWRQNLSGTNLLSINLAAFEKPLQNLTLADLVEATNGFHIACQIG 814
At      AEGHGNSGDRTANNTNWK-LTGVKEALSINLAAFEKPLRKLTFADLLQATNGFHNDSLIG 890
            .. ..  : *::*:   . .: ************::**:.**::******  . **

Hv      SGGFGDVYKAQLKDGRVVAIKKLIHVSGQGDREFTAEMETIGKIKHRNLVPLLGYCKIGE 871
Bd      SGGFGDVYKAQLKDGRIVAIKKLIHVSGQGDREFTAEMETIGKIKHRNLVPLLGYCKIGE 875
Os      SGGFGDVYKAQLKDGKVVAIKKLIHVSGQGDREFTAEMETIGKIKHRNLVPLLGYCKAGE 874
At      SGGFGDVYKAILKDGSAVAIKKLIHVSGQGDREFMAEMETIGKIKHRNLVPLLGYCKVGD 950
        ********** ****  ***************** ********************** *:

Hv      ERLLMYDFMKYGSLEDVLHDRKKIGVRLNWAARRKIAIGAARGLAFLHHNCIPHIIHRDM 931
Bd      ERLLMYDYMQFGSLEDVLHDRKKIGVKLNWPARRKIAIGAARGLAFLHHNCIPHIIHRDM 935
Os      ERLLVYDYMKFGSLEDVLHDRKKIGKKLNWEARRKIAVGAARGLAFLHHNCIPHIIHRDM 934
At      ERLLVYEFMKYGSLEDVLHDPKKAGVKLNWSTRRKIAIGSARGLAFLHHNCSPHIIHRDM 1010
         ****:*::*::********* ** * :*** :*****:*:********** ********

Hv      KSSNVLVDENLEARVSDFGMARMMSVVDTHLSVSTLAGTPGYVPPEYYQSFRCTTKGDVY 991
Bd      KSSNVLVDENLEARVSDFGMARMMSVVDTHLSVSTLAGTPGYVPPEYYQSFRCTTKGDVY 995
Os      KSSNVLIDEQLEARVSDFGMARLMSVVDTHLSVSTLAGTPGYVPPEYYQSFRCTTKGDVY 994
At      KSSNVLLDENLEARVSDFGMARLMSAMDTHLSVSTLAGTPGYVPPEYYQSFRCSTKGDVY 1070
        ******:**:***********:**.:**************************:******

Hv      SYGVVLLELLTGKPPTDSTDFGEDHNLVGWVKMHTKLKITDVFDPELLKDDPTLELELLE 1051
Bd      SYGVVLLELLTGKPPTDSADFGEDNNLVGWVKLHAKLKIIDVFDPELLKDDPSLELELLE 1055
Os      SYGVVLLELLTGKPPTDSADFGEDNNLVGWVKQHTKLKITDVFDPELLKEDPSVELELLE 1054
At      SYGVVLLELLTGKRPTDSPDFG-DNNLVGWVKQHAKLRISDVFDPELMKEDPALEIELLQ 1129
        ************* ****.*** *:******* *:**:* *******:*:**::*:***:

Hv      HLKIACACLDDRPSRRPTMLKVMTMFKEIQAGSTVDSKTSSVATGLSDDPGFGVMDMTLK 1111
Bd      HLKIACACLEDRPTRRPTMLKVMTMFKEIQAGSTVDSKTSSVATGLSDDVGFGVVDMTLK 1115
Os      HLKIACACLDDRPSRRPTMLKVMAMFKEIQAGSTVDSKTSSAAAGSIDEGGYGVLDMPLR 1114
At      HLKVAVACLDDRAWRRPTMVQVMAMFKEIQAGSGIDSQSTIRSIEDGGFSTIEMVDMSIK 1189
        ***:* ***:**. *****:**:********* :**:::  :    .     ::**.::

Hv      EAKEEKD 1118
Bd      EAKEEKD 1122
Os      EAKEEKD 1121
At      EVPEGKL 1196
        *. * *
```

Appendix 3

Peraldi A, Beccari G, Steed A, Nicholson P: *Brachypodium distachyon*: a new pathosystem to study Fusarium head blight and other *Fusarium* diseases of wheat. *BMC Plant Biology* 2011, 11:100.

Appendix 4

Thole V, Peraldi A, Worland B, Nicholson P, Doonan JH, Vain P: T-DNA mutagenesis in *Brachypodium distachyon*. *Journal of experimental botany* 2012, 63:567-576.

	Dark-induced senescence			Flag-leaf senescence				ACC-sensitivity	
EMS lines	0dpi	4dpi	% chl. Loss	mid-anthesis	post-anthesis	%loss41dpi	Late season	(-) M/(-) WT	ACC M/ACC WT
95B	n.s.	n.s.	n.s.	n.s.	n.s.	n.s.	-	n.s.	n.s.
306A	-	-	-	n.s.	n.s.	n.s.	-	hypo.s.	hypo.s.
423AG	FS	SG	SG	FS	n.s.	n.s.	SG	n.s.	n.s.
430A	n.s.	n.s.	n.s.	n.s.	FS	FS	-	n.s.	n.s.
480A	n.s.	n.s.	n.s.	n.s.	n.s.	n.s.	n.s.	n.s.	hyper.s.
555A	n.s.	SG	SG	n.s.	n.s.	n.s.	-	hypo.s.	n.s.
734A	n.s.	SG	SG	n.s.	n.s.	n.s.	-	n.s.	hypo.s.
894A	n.s.	n.s.	n.s.	n.s.	n.s.	n.s.	-	n.s.	n.s.
1189A	n.s.	n.s.	n.s.	n.s.	n.s.	n.s.	SG	n.s.	hyper.s.
1385A	FS	FS	n.s.	FS	FS	Aberrant	-	hypo.s.	hyper.s.
1385B	FS	n.s.	n.s.	n.s.	FS	n.s.	-	n.s.	n.s.
1389A	n.s.	n.s.	n.s.	FS	FS	n.s.	-	n.s.	n.s.
1974A	n.s.	SG	SG	n.s.	n.s.	n.s.	-	n.s.	n.s.
2056A	FS	n.s.	SG	FS	FS	FS	-	n.s.	hypo.s.
2145B	FS	n.s.	SG	n.s.	n.s.	n.s.	n.s.	hypo.s.	n.s.
2150B	n.s.	n.s.	n.s.	n.s.	FS	FS	-	n.s.	n.s.
2171A	n.s.	n.s.	n.s.	n.s.	n.s.	n.s.	-	n.s.	n.s.
2316B	SG	n.s.	n.s.	n.s.	n.s.	n.s.	-	n.s.	hypo.s.
2375A	n.s.	n.s.	n.s.	FS	n.s.	n.s.	-	n.s.	n.s.
2457A	-	-	-	FS	n.s.	n.s.	-	n.s.	hypo.s.
2457B	-	-	-	FS	n.s.	n.s.	-	hyper.s.	hypo.s.
2474B	n.s.	SG	SG	n.s.	n.s.	n.s.	-	n.s.	n.s.
2487B	n.s.	SG	SG	n.s.	n.s.	n.s.	-	n.s.	n.s.
2514A	n.s.	n.s.	n.s.	FS	FS	n.s.	-	n.s.	n.s.
2516A	FS	n.s.	n.s.	FS	FS	FS	-	hypo.s.	hyper.s.
2521A	-	-	-	n.s.	n.s.	n.s.	SG	hypo.s.	hyper.s.
2686A	n.s.	n.s.	n.s.	FS	FS	FS	-	n.s.	n.s.
2939A	SG	SG	SG	n.s.	n.s.	n.s.	SG	n.s.	hypo.s.
3131A	-	-	-	FS	n.s.	n.s.	-	n.s.	n.s.
3266B	-	-	-	FS	FS	FS	-	n.s.	hyper.s.

Supplementary Table 1: Summary of experiments performed on the 30 EMS Paragon mutant lines and associated conclusions respective to the control. SG = stay green, FS = fast senescing, hypo.s. = reduced ET-sensitivity, hyper.s. = enhanced ET-sensitivity, R = resistant, S = susceptible, "–" = data not available, n.s. = non significant result.

	ACC/(-)		Spray inoc. AUDPC		Spray inoc. First score		Point inoc.		Spray inoc. AUDPC	DON	D.L.A.
EMS lines	Exp1	Exp2	Exp 1	Exp2	Exp 1	Exp2	Exp 1	Exp2	field trial	content	Conidia
95B	-	n.s.	-	n.s.	-	n.s.	-	n.s.	n.s.	-	-
306A	n.s.	-	n.s.	-	n.s.	-	n.s.	-	R	-	-
423AG	-	hyper.s.	-	n.s.	-	n.s.	-	n.s.	R	S	n.s.
430A	-	n.s.	-	n.s.	-	n.s.	-	n.s.	n.s.	-	-
480A	-	n.s.	-	n.s.	-	n.s.	-	n.s.	R	n.s.	-
555A	-	n.s.	-	n.s.	-	n.s.	-	n.s.	R	S	-
734A	-	n.s.	-	n.s.	-	n.s.	-	n.s.	n.s.	-	-
894A	-	n.s.	-	n.s.	-	n.s.	-	R	n.s.	-	-
1189A	-	n.s.	-	R	-	R	-	n.s.	R	S	-
1385A	n.s.	-	n.s.	-	n.s.	-	n.s.	-	n.s.	-	-
1385B	-	hypo.s.	n.s.	-	n.s.	-	n.s.	-	n.s.	-	-
1389A	-	n.s.	-	n.s.	-	n.s.	-	n.s.	R	-	-
1974A	-	n.s.	-	n.s.	-	n.s.	-	n.s.	n.s.	-	-
2056A	-	hypo.s.	-	R	-	R	-	n.s.	n.s.	-	-
2145B	hypo.s.	-	n.s.	-	n.s.	-	n.s.	-	R	n.s.	-
2150B	-	n.s.	-	n.s.	-	n.s.	-	n.s.	n.s.	-	-
2171A	-	hypo.s.	-	n.s.	-	n.s.	-	n.s.	n.s.	n.s.	-
2316B	-	hypo.s.	-	n.s.	-	n.s.	-	n.s.	n.s.	-	-
2375A	-	hypo.s.	-	R	-	R	-	n.s.	R	-	-
2457A	hypo.s.	-	S	-	S	-	n.s.	-	R	-	-
2457B	n.s.	-	n.s.	-	S	-	n.s.	-	R	-	-
2474B	-	n.s.	-	n.s.	-	R	-	n.s.	S	n.s.	-
2487B	n.s.	-	R	-	n.s.	-	n.s.	-	R	S	-
2514A	-	n.s.	S	-	S	-	n.s.	-	n.s.	n.s.	-
2516A	n.s.	-	S	-	n.s.	-	n.s.	-	R	-	-
2521A	n.s.	-	n.s.	-	n.s.	-	n.s.	-	R	-	-
2686A	hyper.s.	-	S	-	S	-	n.s.	-	n.s.	-	-
2939A	-	n.s.	-	R	-	R	-	n.s.	R	n.s.	R
3131A	n.s.	-	n.s.	-	n.s.	-	n.s.	-	R	-	-
3266B	n.s.	-	n.s.	-	n.s.	-	n.s.	-	R	-	-

Supplementary Table 1, continued: Summary of experiments performed on the 30 EMS Paragon mutant lines and associated conclusions respective to the control. SG = stay green, FS = fast senescing, hypo.s. = reduced ET-sensitivity, hyper.s. = enhanced ET-sensitivity, R = resistant, S = susceptible, "–" = data not available, n.s. = non significant result.